Engineering Properties, Hydration Kinetics, and Carbon Capture in Sustainable Construction Materials

Thien Q. Tran

Dissertation submitted to the faculty of the Virginia Polytechnic Institute and State University in partial fulfillment of the requirements for the degree of
Doctor of Philosophy
In
Civil Engineering

Alexander S. Brand, Chair
Sherif L. Abdelaziz
Wencai Zhang
Gerardo W. Flintsch

November 21, 2023
Blacksburg, Virginia

Keywords: End-of-life (ELT) tire rubber; Cation Exchange Capacity (CEC); Soil stabilization; Rubberized cementitious materials; Rubberized asphalt concrete; Heat hydration; Carbon capture; Digestion-Titration Method (DTM)

Engineering Properties, Hydration Kinetics, and Carbon Capture in Sustainable Construction Materials

Thien Q. Tran

Academic Abstract

Concrete, the second most consumed material on earth after water, is a source of environmental problems due to global urbanization. The production of this construction material requires a large amount of natural resources, and portland cement (PC) is responsible for around 8 % of planet-warming CO_2 emissions. Producing 1 ton of PC will release roughly 1 ton of CO_2 into the atmosphere. In 2021, around 92 million metric tons of PC were produced in the U.S., and a total of 4.4 billion tons were manufactured worldwide. While there was a yearly increase of around 1.5 % in the direct CO_2 intensity of cement production from 2015 to 2021, urgent annual declines of 3 % until 2030 are necessary to be in line with the Net Zero Emissions by 2050 Scenario. This dissertation presents different approaches and technologies to offset the CO_2 footprint of the production of cement clinker, concrete, and cementitious materials in general.

First, this dissertation investigated the possibility of using end-of-life tire (ELT) rubber powder and its zinc-recovered residual (treated ELT rubber) to partially replace fine aggregates of different construction and infrastructure materials including stabilized soft soil (0 %, 10 %, 30 %, and 50 % ELT rubber added by clay volume), portland cement concrete (0 %, 10 %, 20 %, and 30 % ELT rubber added by sand volume), and asphalt concrete (20 % ELT rubber added by sand volume). This work was discussed through aspects of engineering properties and environmental impacts. The results reveal that the ELT rubber had both negative and positive effects on the engineering properties of the three materials while this waste posed a huge leachability of zinc and total organic carbon (TOC) content when being subjected to aqueous environments. However, the findings indicate that all three materials' matrices could effectively immobilize most leachable zinc from the ELT rubber by more than 90 %. Meanwhile, only stabilized soft soil and asphalt concrete could effectively deal with leachable TOC content from ELT rubber, and portland cement concrete needed the addition of silica fume to reduce TOC concentration in its leachate.

Second, while previous studies have shown that steel furnace slag (SFS) can stabilize clay soils, the evidence is not clear if the stabilization mechanism is chemical and/or mechanical. This dissertation used isothermal calorimetry (IC) to quantify the heat of hydration of the mixture to assess the chemical aspects of the stabilization. Specifically, kaolin and bentonite clays were each blended with 40 % SFS by mass at water-to-binder ratios ranging from 1.0 to 1.5. The hydration properties of stabilized mixtures using lime or PC were also tested for comparison at the same experimental conditions. The obtained thermal power and total heat curves of stabilized mixtures confirmed that, for the specific SFS in this study, there is a hydration process taking place in clay stabilized by SFS. Relative to lime and PC, the SFS performed similarly in terms of heat of

hydration behavior. When blended into clays, SFS provided a more significant heat of hydration behavior than cement, but that was much milder than lime. X-ray diffraction (XRD) and thermogravimetric analysis (TGA) were also employed to qualitatively analyze the mineralogy of the stabilized mixtures.

Finally, this dissertation adopted a Digestion-Titration Method (DTM) for the determination of CO_2 content in cementitious materials that has been mineralized in the form of calcium carbonate ($CaCO_3$). This method was modified based on tests that were originally developed in the early 1900s. The method uses hydrochloric acid to digest $CaCO_3$ under vacuum conditions. The CO_2 released is captured by a barium hydroxide solution, which is then titrated to quantify the amount of CO_2 absorbed. A design of experiments approach was used to optimize the experimental conditions. Samples of known $CaCO_3$ content were first evaluated to establish the baseline test performance, and additional tests were performed on portland cement and various rock samples. The results were also compared to TGA, including a discussion to compare the two test methods. The data suggest that the new test method is feasibly applicable to chemically determine the CO_2 captured in cementitious materials, and it can be an alternative method for TGA with lower experimental cost and easier access.

Overall, it is evident that cement, concrete, and construction materials are essential to the functionality of civilization. Dealing with CO_2 emissions and natural resource depletion induced by the production of these construction materials is urgent for sustainable development. Attempts toward construction materials with lower embodied CO_2 by using low-carbon aggregates (*e.g.*, waste aggregates, recycled aggregates) and alternative cementitious binders while controlling the environmental effects of the utilized waste materials are currently viable sustainable approaches. In addition, tools or new test methods that can support measuring the effectiveness of these reduced carbon cementitious materials are necessary. This dissertation investigates the feasibility of the use of ELT rubber waste in construction materials to reduce the exploitation of natural resources considering engineering properties and environmental impacts. It also provides a deeper understanding of the hydration behavior of stabilized soil using SFS which is expected to partially or fully replace PC in the material. Experimentally, it develops a chemical test model as an alternative method for TGA with lower experimental cost, less interference, and easier access to determine the CO_2 captured in cementitious materials.

Engineering Properties, Hydration Kinetics, and Carbon Capture in Sustainable Construction Materials

Thien Q. Tran

General Audience Abstract

Concrete, the second most consumed material on earth after water, is a source of environmental problems due to global urbanization. The production of this construction material requires a large amount of natural resources, and portland cement (PC) is responsible for around 8 % of planet-warming CO_2 emissions. This dissertation presents different approaches and technologies to offset the CO_2 footprint of the production of construction materials (*i.e.*, cement clinker, concrete, and general cementitious materials).

First, this dissertation investigated the possibility of using end-of-life tire (ELT) rubber powder in different construction materials including stabilized soft soil, portland cement concrete, and asphalt concrete. This work was discussed through aspects of engineering properties and environmental impacts. The results reveal that the ELT rubber had both negative and positive effects on the engineering properties of the three materials. In return, all three materials' matrices could effectively immobilize most leachable zinc and total organic carbon (TOC) from the ELT rubber, which are detrimental to aquatic animals, plants, and humans.

Second, this dissertation used isothermal calorimetry (IC) for the first time to study the heat of hydration of soil stabilized by steel furnace slag (SFS) to assess the chemical aspects of the stabilization. The work compared the hydration behavior of SFS in clayey soil with traditional stabilizers such as lime or portland cement. The results demonstrated that there were chemical reactions taking place during the hydration of stabilized soil using SFS, explaining the improvement in engineering properties of the stabilized soil.

Moreover, this dissertation adopted a Digestion-Titration Method (DTM) for the determination of mineralized CO_2 content in cementitious materials. The method uses hydrochloric acid to digest $CaCO_3$ under vacuum conditions. The CO_2 released is captured by a barium hydroxide solution, which is then titrated to quantify the amount of CO_2 absorbed. The data suggest that the new test method is feasibly applicable to chemically determine the CO_2 mineralized in cementitious materials, and it can be an alternative method for thermogravimetric analysis with lower experimental cost and easier access.

Overall, it is evident that cement, concrete, and construction materials are essential to the functionality of civilization. Dealing with CO_2 emissions and natural resource depletion induced by the production of these construction materials is urgent for sustainable development. This dissertation is expected to fill the knowledge gap in carbon neutral construction materials research, including increasing the use of low-carbon aggregates (*e.g.*, waste aggregates, recycled aggregates) and alternative cementitious binders as well as developing new test methods that can support measuring the effectiveness of these reduced carbon cementitious materials.

ACKNOWLEDGEMENTS

First, I wish to express my great gratitude to my supervisor, Prof. Alexander S. Brand, for giving me the opportunity to be his Ph.D. student, for being lenient during my start at Virginia Tech when I needed to learn many new things while adapting to the new living and working environments, for his boundless support when I needed it, and for his encouragement when I earned achievements or became unmotivated during my studies. I am grateful to Dr. Brand for his stimulating discussions, precious advice, constructive criticisms, and insightful comments to supervise me in obtaining my research goals as well as pave my future career direction. I want to thank him for giving me a lot of freedom in research and time management. His leniency and cheerful personality motivated me to be a better version of myself. It was my biggest privilege to work with him at VT. Needless to say, none of this would have been successful without his outstanding supervision and significant support. And, it would be unfair if I did not say that he changed my life!

I would like to extend appreciation to my committee members, Prof. Sherif L. Abdelaziz, Prof. Wencai Zhang, and Prof. Gerardo W. Flintsch, for their great support, constructive advice, and dedicated reviews on my dissertation.

I would like to extend my gratitude to Dr. David Mokarem, Dr. Bernardo Castellanos, Brett Farmer, Garret Blankenship, Prof. Madeline Schreiber, Dr. Jeffrey Parks, Dr. AJ Prussin, Jody Smiley, Dr. Thomas Staley, Dr. Rituraj Borgohain, Patrick Finley, and all personnel who work at the Civil and Environmental Engineering Department, the Thomas M. Murray Structures and Materials Laboratory, as well as the Materials Science and Engineering Department for providing all needed resources and facilities for completing this research.

I am also grateful to the Center for Tire Research, Economical and Sustainable Materials Stakeholder Committee at Virginia Tech, 4-VA, Luna Innovations, and US Air Force SBIR for generously funding my research at VT. Thank you Lehigh Technologies and Short Mountain Silica for providing the necessary materials for this research.

I greatly appreciate all of the support provided by my research team partners, Dr. Rachel Cook, Dr. Aron Newman, and Paul Stutzman from the National Institute of Standards and Technology and Dr. Bin Ji and Shiyu Li from the Department of Mining and Mineral Engineering. Also, special thanks to my lab members, Dr. Amir Behravan, Dr. Ebenezer Fanijo, Michael Lowry, Xiang Zhao, Md. Hasibul Hasan Rahat, Rashed Alarrak, Tu-Nam Nguyen, and Bao-Chau Le.

Last but not least, to my family: Con xin cảm ơn công ơn nuôi dạy của ông bà ngoại, mẹ, dì Bé (Hoa), chú Linh, dì Vân, cậu Nguyên Khôi, dì Ánh và dì Út (Tuyền). Cảm ơn cô-dì-chú-bác-anh-chị họ hàng hai bên nội ngoại. Một lời cảm ơn chân thành đến những người anh-em đã sát cánh và sẵn lòng giúp đỡ em vô điều kiện để em có được ngày hôm nay. Cuối cùng, con xin gửi tới cha đã khuất – Phước Trần, mẹ – Hương Nguyễn, cùng em trai – Huy Đạt, "*Con trai ba mẹ – Tiến Sĩ Trần, con làm được rồi! Yêu thương ba mẹ rất nhiều*!"

ANNOTATIONS

APA	Asphalt pavement analyzer
CEC	Cation exchange capacity
DTM	Digestion-Titration Method
DOE	Design of experiments
ELT	End-of-life tire
|E*|	Dynamic modulus
IC	Isothermal calorimetry
IDT-CT	Indirect tensile test - cracking tolerance
ITS	Indirect tensile strength
L/S	Liquid-to-solid ratio
LL	Liquid limit
PC	Portland cement
PSE	Pore solution extraction
RCM	Rubberized cementitious materials
RSS	Rubberized stabilized soil
RM	Rubberized mortar
RAC	Rubberized asphalt concrete
RCPT	Rapid chloride penetrability test
RM	Rubberized mortar
SRI	Strength recovery index
SG	Strength gain
SL	Strength loss
SF	Silica fume
SFS	Steel furnace slag
SCM	Supplementary cementitious materials
SEM	Scanning electron microscope
TOC	Total organic carbon
TGA	Thermogravimetric analysis
UCS	Unconfined compressive strength
UPV	Ultrasonic pulse velocity
w/b	Water-to-binder ratio
XRD	X-ray diffraction

TABLE OF CONTENT

LIST OF FIGURES

LIST OF TABLES

Chapter 1. Introduction

It is unanimously reported that the demand for portland cement (PC) and concrete, which are critical as the most-used construction materials in the world, has been significantly increasing due to global urbanization [1]. In 2021, around 92 million metric tons of portland cement were produced in the U.S., and a total of 4.4 billion tons were manufactured worldwide [2]. Cement production has a significant environmental cost, since it consumes natural resources and requires a significant amount of energy for calcination, heating, grinding, and transportation. Roughly one ton of carbon dioxide (CO_2) is emitted to the atmosphere for the generation of one ton of portland cement, accounting for an estimated 5 % to 8 % of the global CO_2 production [3–9]. While there was a yearly increase of around 1.5% in the direct CO_2 intensity of cement production from 2015 to 2021, urgent annual declines of 3% until 2030 are necessary to be in line with the Net Zero Emissions by 2050 Scenario [10]. As academia, industry, and governments are giving significant attention to the production of long-life carbon-reduced and carbon-neutral concrete [5,11–14], there is a strong emphasis on the use of recycled aggregates, supplementary cementitious materials (SCMs), and carbon capture technologies to offset the CO_2 footprint of cement clinker and concrete production in general. These approaches are believed to have the potential to solve the environmental issues of the production of concrete and cementitious materials and thus attaining sustainable development in this industry [15]. However, there are problems and knowledge gaps that researchers are facing and need to be dealt with for a comprehensive understanding and application of these essential materials.

1.1 Research objectives

To address some of the sustainability questions concerning the cement and concrete industries, the **objectives** of this dissertation are to (1) determine the physicochemical interactions between treated end-of-life tire (ELT) rubber aggregates and different infrastructure materials (*i.e.*, cement matrix, stabilized soil matrix, and asphalt concrete matrix); (2) study the hydration kinetics of alternative cementitious materials; and (3) establish a new test method to measure CO_2 uptake in construction materials. These objectives are expected to fill the knowledge gap in carbon neutral construction materials research, including increasing the use of low-carbon aggregates (*e.g.*, waste aggregates, recycled aggregates) and alternative cementitious binders, as well as developing new test methods that can support measuring the effectiveness of these reduced carbon cementitious materials. The objectives will be met by specifically achieving the following **research aims**:

1. *Establishing novel infrastructure applications for treated ELT rubber.* One of the challenges with ELT rubber is zinc leachability, since zinc is a heavy metal and is detrimental to aquatic and plant life. The hypothesis driving this research is that the zinc leachability can be reduced through a pretreatment and that any remaining leachable zinc can be captured through the engineering of infrastructure materials, including stabilized soils, cement-based materials, and asphalt concrete.
2. *Deriving hydration mechanisms in clay soils stabilized by steel industry by-products.* The hypothesis in this study is that the available free lime in steel furnace slag can be used to stabilize clay soils. While previous studies have shown that steel slag will stabilize clay soils,

the evidence is not clear if the stabilization mechanism is chemical and/or mechanical. In this study, isothermal calorimetry (IC) is applied to quantify the heat of hydration of the mixture to assess the chemical aspects of the stabilization.

3. *Innovating a new test method to quantify the amount of CO_2 that can be captured by concrete and other industrial materials.* The hypothesis in this study is that the determination of CO_2 content mineralized in cement-based and other industrial materials can be accurately assessed through a Digestion-Titration Method (DTM). The DTM test offers a lower experimental cost, easier access, and less interference from other phases than the current approach using thermogravimetric analysis (TGA).

The **intellectual merit** of this dissertation is that it offers novel advancements towards infrastructure applications with lower environmental impact, including considerations of heavy metal leachates and CO_2. In summary, this dissertation provides the following contributions to intellectual merit: (1) immobilizing zinc leachate from treated ELT rubber in stabilized soils, cement-based materials, and asphalt concrete; (2) applying IC for the first time in the literature to understand hydration kinetics during clay stabilization; and (3) establishing a new test method for quantifying mineralized CO_2 in cement-based and other industrial materials.

Sustainability is a general theme throughout this dissertation, with specific **broader impacts**: (1) immobilizing any zinc leached from treated ELT rubber, since zinc poses a threat to plant and animal life; (2) reducing the carbon footprint of infrastructure materials through the use of waste materials (*i.e.*, ELT rubber, steel furnace slag); and (3) establishing a standardizable test method for quantifying CO_2 mineralization, which would allow for direct comparison of proposed new technologies in carbon mineralization in concrete.

1.2 Research tasks

This dissertation is comprised of three specific research aims, which is comprised of five main tasks that correspond to six manuscripts to meet the three aims:

1) Task 1 (Aim 1) proposes an approach to stabilize soft clayey soils using ELT rubber while simultaneously immobilizing any leached zinc from the rubber particles. In addition to the engineering properties, the stabilized soil is expected to absorb the zinc and other heavy metals leached from the ELT rubber through the cation exchange capacity (CEC) of the clay. This task will consider untreated ELT rubber and ELT rubber that has undergone a hydrometallurgical process to remove the zinc.
2) Task 2 (Aim 1) focuses on utilizing ELT rubber before and after the zinc extraction process to partially replace fine aggregate (up to 30 % of volume) in a cement mortar. Engineering properties were investigated for the rubberized mortars. The effects of ELT rubber on the hydration process of the rubberized mortars were studied. In addition, the leachability of zinc and carbon content in ELT rubber when being used in the rubberized mortar were investigated. Finally, the effects of using silica fume in recovering the loss in engineering property performance and zinc and organic carbon leaching in the rubberized mortar were examined.

3) Task 3 (Aim 1) is to understand the effects of untreated and treated ELT rubber (a 20 % replacement of sand volume) on rubberized asphalt concrete's engineering properties and behavior. Environmentally, this task examines the leaching potential of zinc and TOC from the ELT rubber-modified asphalt concrete and how this potential varies under different surrounding weather conditions such as pH, acid rain, saline environment, and exposure time.
4) Task 4 (Aim 2) explores the heat of hydration of clayey soils stabilized by steel furnace slag (SFS) and assess the extent of chemical reactions. This task provides a deeper understanding of the possible mechanical and/or chemical contributions of SFS to the improvement of stabilized soil's engineering properties. More widely, it provides comprehensive heat of hydration curves and characteristics of stabilized soil with typical binders such as cement and lime.
5) Task 5 (Aim 3) adopts a new DTM test setup as well as provide detailed guidelines and calculations for determining the mineralized CO_2 content in cementitious materials. This task proves the benefit of the DTM model over the TGA method which requires specialized equipment that is not readily accessible to all testing laboratories.

1.3 Dissertation organization

The dissertation consists of six manuscripts within eight chapters that cover all of the above-mentioned tasks. The arrangement of the dissertation is as follows:

- **Chapter 1: *Introduction*.** This chapter generally discusses the knowledge gaps and problems in cement-based construction materials and provide general background knowledge employed in this dissertation. This also entails the problem statement, objectives, and the organization of the dissertation.
- **Chapter 2: *A comprehensive review on treatment methods for end-of-life tire rubber used for rubberized cementitious materials*.** This chapter is part of Task 1, and it presents a comprehensive literature review on how ELT rubber has been physically and/or chemically treated to improve the properties of rubberized cementitious composites. Specifically, this work: (i) summarizes various treatment methods that have been employed to treat the ELT rubber surface before use in rubberized cementitious materials; (ii) presents the hypothesized mechanism(s) behind each treatment method as well as the changes in the ELT rubber's microstructure (if applicable); and (iii) provides discussions and comparisons between the developed pretreatment methods for ELT rubber. As a result, the most effective methods are identified, which can serve as guidelines in the future for other researchers. This paper was published in *Construction and Building Materials*.
- **Chapter 3*: Mitigating zinc leachate from end-of-life tire rubber in stabilized clayey soils.*** This chapter covers Task 1 to investigate the engineering properties and microstructure of ELT rubber-stabilized clay. The clay is not only chemically stabilized with PC as a traditional method but is also mechanically stabilized with ELT rubber (up to 50 % of clay volume). In addition, environmental tests (*i.e.*, pore solution extraction, leaching test) are carried out for the rubberized stabilized soil to verify the hypothesis that clay can absorb the zinc and other heavy metals leached from the ELT rubber through the CEC of the clay component.

- **Chapter 4:** ***Mitigating zinc leachate from end-of-life tire rubber in rubberized mortar***. This chapter covers Task 2 to investigate ELT rubber before and after the zinc extraction process to partially replace fine aggregate (up to 30 % of volume) in a cement mortar and to study the effect of the ELT rubber on engineering properties and microstructure. Simultaneously, isothermal calorimetry is also employed to examine the effects of ELT rubber on the hydration process of the rubberized mortars. In addition, the pore solution and leaching solutions were collected at different curing ages and then analyzed for elemental and total organic carbon contents, primarily to quantify the leachability of zinc. Silica fume is ultimately used to partially replace cement as an effort to possibly recover the loss in engineering property performance and reduce the leachable zinc and organic carbon content.
- **Chapter 5:** ***Effects of end-of-life tire rubber on engineering properties and environmental impacts of rubberized asphalt concrete.*** This chapter covers Task 3 to investigate the effect of treated and untreated ELT rubber on the properties of asphalt concrete and to quantify the immobilization of zinc and TOC. ELT rubber before and after the zinc-recovery process were used to partially replace 20 % sand by volume in asphalt concrete through the dry process. Indirect tensile test-cracking tolerance, asphalt pavement analyzer rutting test, and dynamic modulus test were conducted for the investigations of the engineering properties of rubberized asphalt concrete (RAC). Environmental tests were conducted to examine the leaching potential of zinc and TOC from the RAC and how this potential varies under different simulated weather conditions (*i.e.*, acid rain, deicing solution, deicing solution at pH of 4.0).
- **Chapter 6:** ***Heat of hydration in clays stabilized by a high-alumina steel furnace slag***. As planned in Task 4, this study mainly utilizes IC to quantify hydration kinetics in stabilized soil using SFS. This chapter aims to explore the heat of hydration of SFS-stabilized clayey soils and confirm that chemical reactions are occurring. This chapter provides a deeper understanding of the possible mechanical and/or chemical contributions of SFS to the improvement of stabilized soil's engineering properties. More widely, it provides comprehensive heat of hydration curves and characteristics of stabilized soil with typical binders such as cement, lime, and SCMs. The research for this manuscript was published in *Cleaner Materials*.
- **Chapter 7:** ***Measuring mineralized carbon in cementitious materials by an acid digestion-titration method***. This work follows Task 5 to optimize the DTM test setup and to provide detailed guidelines and calculations for determining the carbonate content in cementitious materials. The acid digestion data were validated against TGA data, thereby producing a robust dataset to compare test methods. This chapter proves the benefit of the DTM method over the TGA method, which requires specialized equipment that is not readily accessible to all testing laboratories.
- **Chapter 8:** ***Conclusions and recommendations.*** The purpose of this chapter is to provide a summary of the six manuscripts included in this dissertation, along with recommendations for future research and practical implications of the findings.

References

[1] International Energy Agency, Cement Sustainability Initiative, Technology Roadmap: Low-Carbon Transition in the Cement Industry, World Business Council for Sustainable Development, 2018.

[2] A.K. Hatfield, Cement, in: Miner. Commod. Summ., USGS, Reston, 2022.

[3] C. Meyer, The greening of the concrete industry, Cem. Concr. Compos. 31 (2009) 601–605. https://doi.org/10.1016/j.cemconcomp.2008.12.010.

[4] R.M. Andrew, Global CO2 emissions from cement production, Earth Syst. Sci. Data. 10 (2018) 195–217. https://doi.org/10.5194/essd-10-195-2018.

[5] M. Schneider, The cement industry on the way to a low-carbon future, Cem. Concr. Res. 124 (2019) 105792. https://doi.org/10.1016/j.cemconres.2019.105792.

[6] S.A. Miller, A. Horvath, P.J.M. Monteiro, Readily implementable techniques can cut annual CO2 emissions from the production of concrete by over 20%, Environ. Res. Lett. 11 (2016) 074029. https://doi.org/10.1088/1748-9326/11/7/074029.

[7] D.N. Huntzinger, T.D. Eatmon, A life-cycle assessment of Portland cement manufacturing: Comparing the traditional process with alternative technologies, J. Clean. Prod. 17 (2009) 668–675. https://doi.org/10.1016/j.jclepro.2008.04.007.

[8] J.S. Damtoft, J. Lukasik, D. Herfort, D. Sorrentino, E.M. Gartner, Sustainable development and climate change initiatives, Cem. Concr. Res. 38 (2008) 115–127. https://doi.org/10.1016/j.cemconres.2007.09.008.

[9] Y. sang Kim, T.Q. Tran, G. o. Kang, T.M. Do, Stabilization of a residual granitic soil using various new green binders, Constr. Build. Mater. 223 (2019) 724–735. https://doi.org/10.1016/j.conbuildmat.2019.07.019.

[10] D. Hodgson, P. Hugues, International Energy Agency (IEA), 2022. https://www.iea.org/reports/cement.

[11] Global Cement and Concrete Association, Concrete Future: The GCCA 2050 Cement and Concrete Industry Roadmap for Net Zero Concrete, Global Cement and Concrete Association, London, 2021.

[12] UN Environment, K.L. Scrivener, V.M. John, E.M. Gartner, Eco-efficient cements: Potential economically viable solutions for a low-CO2 cement-based materials industry, Cem. Concr. Res. 114 (2018) 2–26. https://doi.org/10.1016/j.cemconres.2018.03.015.

[13] Portland Cement Association, Roadmap to Carbon Neutrality, Portland Cement Association, Skokie, 2021.

[14] D.H. Vo, N.D. Do, Y. Mamuye, M.C. Liao, C.L. Hwang, Q.T. Tran, Engineering properties and durability of concrete samples designed by densified mixture design algorithm (DMDA) method incorporating steel reducing slag aggregate, Constr. Build. Mater. 354 (2022) 129180. https://doi.org/10.1016/j.conbuildmat.2022.129180.

[15] GCCA, Concrete Future - The GCCA 2050 Cement and Concrete Industry Roadmap for Net Zero Concrete, Glob. Cem. Concr. Assoc. (2021) 1–48. https://gccassociation.org/concretefuture/wp-content/uploads/2021/10/GCCA-Concrete-Future-Roadmap.pdf.

Chapter 2. A comprehensive review on treatment methods for end-of-life tire rubber used for rubberized cementitious materials[1]

The contributions of the authors to this manuscript are described as follows:

Thien Q. Tran: Conceptualization; Data curation; Formal analysis; Investigation; Methodology; Visualization; Writing - original draft; Writing - review and editing.

Note: Thien Q. Tran was in the main charge of all above-mentioned contribution categories under the supervision of Dr. Alexander S. Brand.

Blessen Skariah Thomas: Methodology; Writing - review and editing.

Wencai Zhang: Funding acquisition; Supervision; Writing - review and editing.

Bin Ji: Writing - review and editing.

Shiyu Li: Writing - review and editing.

Alexander S. Brand: Conceptualization; Funding acquisition; Methodology; Project administration; Supervision; Writing - review and editing.

[1] **Thien Q. Tran**, Blessen Skariah Thomas, Wencai Zhang, Bin Ji, Shiyu Li, and Alexander S. Brand. "A Comprehensive Review on Treatment Methods for End-of-Life Tire Rubber Used for Rubberized Cementitious Materials". *Construction and Building Materials*, 359, 2022. https://doi.org/10.1016/j.conbuildmat.2022.129365

A comprehensive review on treatment methods for end-of-life tire rubber used for rubberized cementitious materials

Thien Q. Tran[1], Blessen Skariah Thomas[2], Wencai Zhang[3], Bin Ji[3], Shiyu Li[3], Alexander S. Brand[1,4*]

[1]The Charles Edward Via, Jr. Department of Civil and Environmental Engineering, Virginia Polytechnic Institute and State University, Blacksburg, Virginia, USA, 24060
[2]Department of Civil Engineering, National Institute of Technology Calicut, Kerala 673601, India
[3]Department of Mining and Minerals Engineering, Virginia Polytechnic Institute and State University, Blacksburg, Virginia, USA, 24060
[4]Department of Materials Science and Engineering, Virginia Polytechnic Institute and State University, Blacksburg, Virginia, USA, 24060
*Corresponding Author: asbrand@vt.edu

2.1 Abstract

The use of end-of-life tire (ELT) rubber in rubberized cementitious materials (RCM) as a partial alternative aggregate has attracted the attention from researchers and industries in the recent decades. While the ELT rubber can be advantageous, such as by increasing fracture toughness, ductility, permeability, and thermal insulation of the concrete, it can negatively impact the other engineering properties, such as elastic modulus, mechanical strength, stiffness, and shrinkage. This reduction in performance may be attributed to the poor interfacial contact and bonding between the rubber particles and cement paste. This manuscript presents a comprehensive literature review on how ELT rubber has been physically and/or chemically treated to improve the properties of the rubberized cementitious composite. Specifically, this work (i) summarizes various treatment methods that have been employed to treat the ELT rubber surface before use in RCM; (ii) presents the hypothesized mechanism(s) behind each treatment method as well as the changes in the ELT rubber's microstructure (if applicable); and (iii) provides discussions and comparisons between the developed pretreatment methods for ELT rubber. Two metrics – strength recovery index (SRI) and strength gain (SG) – are introduced to assist with comparisons. Also, recommendations are provided to assess the most effective pretreatment methods for ELT rubber in RCM in terms of engineering properties.

Keywords: End-of-life tires (ELT), rubberized cementitious materials (RCM), strength recovery index (SRI), strength gain (SG).

2.2 Introduction

In recent decades, waste recycling has received significant attention to improve living conditions, water, air, and ecosystem qualities as well as saving limited resources [1,2]. Recycling is one method to constrain the negative impact as the globe could suffer from the disordered generation of waste as well as the shortage of raw materials [3–5].

End-of-life tires (ELT) present a significant waste issue in many countries in the world. Worldwide, an estimated 3 billion tires are produced annually [6]. According to the U.S. Tire Manufacturers Association, in 2019 approximately 300 million ELTs were produced in the U.S. and an estimated unused stockpile of 56 million tires was reported [7]. The U.S. utilized 76% of available scrap tires, and the three largest usages were tire-derived fuel (37%), ground rubber (24%), and landfilling (15%) [7]. Meanwhile, in China, which has been one of the top producers of ELTs since 2008, there were 232 million cars driving in the country with 14.6 million tons of ELTs discarded in 2018 [8]. This amount of discarded ELTs is around 3.24, 2.81, and 12.17 times larger than that of ELTs generated in the European Union (4.5 million tons), United States (5.2 million tons), and Japan (1.2 million tons), respectively [8]. China has accumulated more than 300 million ELTs, and this number has been increasing by more than 13 million every year [9].

2.2.1 Environmental effects and uses

Tire rubber is a complex combination of various polymers (*e.g.*, polybutadiene, polyisoprene, styrene-butadiene), carbon black, with small amounts of extender oil, zinc oxide, stearic acid, and other compounds [6]. Rubber-based tires are flammable materials, so stockpiling of ELTs can be considered unsafe and a fire hazard [10]. In addition, stockpiled ELTs can expose risks of water, soil, and air pollution [11,12].

One use option for ELT is heat recovery through combustion. The combustion of ELTs at high temperatures emits hazardous gases such as polyaromatic hydrocarbons, sulfur dioxide (SO_2), carbon monoxide (CO), hydrogen chloride (HCl), and nitrogen dioxide (NO_2), all of which are known to negatively affect health and air quality [13,14]. Hence, dealing with ELTs disposal is increasingly becoming significant health, environmental, and aesthetic issue in many countries these days.

Ground and crumb rubber are other options for ELT usage. Depending on the size distribution and particle size, ground and crumb ELT rubber can be used in portland cement concrete [15–18], asphalt concrete [15,19], tire-derived fuels [20], soil modification [21,22], feedstocks for carbon black production [23,24], carbon dioxide absorbants [25], *etc*.

ASTM D6270 [26,27] classifies scrap ELTs into various types based on particle size: (i) rough shredded ELT has a size ranging from 50 mm × 50 mm × 50 mm to 762 mm × 50 mm × 100 mm; (ii) tire-derived aggregate (TDA) ranges in size from 12 mm to 305 mm; (iii) ELT shreds range in size from 50 mm to 305 mm; (iv) ELT chips range from 12 mm to 50 mm; (v) granulated ELT particles range from 0.425 mm to 12 mm; (vi) ground ELT particles are smaller than granulated ELT; and (vii) powdered ELT consists of particles smaller than 0.425 mm but larger than 0.075 mm. There is also a terminology named “crumb rubber” (CR) which has particles in a range of 0.6 mm to 4.75 mm [28]. These categories are presented in Table 2- 1. The summary of the basic information of research studying in RCM is shown in Table 2- 2.

Table 2- 1. Categories of ELT rubber.

Categories	Minimum size (mm)	Maximum size (mm)
Rough shred (RS)	50 × 50 × 50	762 × 50 × 100
Tire derived aggregate (TDA)	12	305
Tire shreds (TS)	50	305
Tire chips (TC)	12	50
Granulated rubber (GRR)	0.425	12
Ground rubber (GR)	0.425	<2
Powdered rubber (PR)	N/A	<0.425

2.2.2 Applications of ELT in concrete

While many other industrial wastes and by-products (*e.g.*, coal ashes, iron and steel slags, agricultural ashes, recycled concrete, *etc*.) have been effectively recycled or reused in civil engineering applications [29–38], rubber waste is reused in this field at only 5 % of its available amount [39] due to some limitations, such as low elastic modulus, reduced compressive strength and poor adhesion [18,40]. Regardless, when ELTs are used to partially to fully replace coarse and/or fine aggregate in concrete mixtures, the rubberized concrete, or rubberized cementitious material (RCM), can remarkably improve mechanical engineering properties such as tenacity, ductility, toughness, and impact resistance as well as electrical, sound, and thermal insulation abilities [41]. In addition, the durability of rubberized concrete, such as freeze-thaw resistance, acid resistance, and chloride permeability resistance, is also improved [18]. These enhanced properties suggest that rubberized concrete can be a good candidate for noise-isolated structures, non-bearing concrete walls, thermal insulation walls or floors in buildings, jersey barriers, railway track beds, pavement, earthquake-resistant structures, high impact-resistant rubberized concrete beams, expansion joints, building facades, and rubberized concrete-filled steel tubes [15,18,41–72]. The low density of rubberized concrete makes it viable to serve as lightweight concrete [73,74]. These positive properties can be motivations for developing sustainable rubberized concrete to achieve greater environmental and economic benefits.

Apart from the many benefits of ELT-used concrete as mentioned above, several barriers have prevented rubberized concrete due to the significant reduction of the mixture strength. The rubber-cement chemical bond, the physical interfacial bond, and porosity are considered to be key factors that strongly affect the engineering properties of RCM. It is well-known that the interfacial transition zone (ITZ) is a porous area surrounding aggregates [75], often referred to as the "weak link" that limits the concrete's strength. When the ELT rubber is added into concrete, there is a lack of bonding between cement matrix and ELT particles at ITZ [71]. In addition, calcium hydroxide (CH) and ettringite gradually decrease in the ITZ with an enhancement in the amount of rubber [71]. Hence, concrete with ELT yields a weaker ITZ, which significantly reduces the strength when compared with the virgin aggregate concrete [71,76,77].

2.2.3 Dosage

A list of studies using ELT for RCM is presented in Table 2- 2. The information of the particle size, treatment methods, quantity of rubber, and tests performed in each study has been demonstrated. ELT partially to fully replaces coarse and/or fine aggregate in the rubberized concrete mixtures. When designing a concrete mixture, it should be noted that the specific gravity of recycled ELT rubber is less than half of the natural aggregates. Hence, in these studies, the added amount of recycled ELTs ranges from 5 % to 100 % of fine and/or coarse aggregate by volume. However, the amount of added recycled ELT should be constrained between the required physical engineering properties and the feasibility of using the rubberized concrete. Particularly, in terms of durability, Kardos and Durham [28] identified the optimum economic replacement of rubber aggregate as 10%. Guo *et al*. [78] noted that the replacement with 25 % of recycled ELT can satisfy the strength requirements for rigid pavement. Meanwhile, Kardos and Durham [28] suggested that a 30 % replacement of fine aggregate (around 5.5 % of total volume) with recycled ELT is acceptable to produce suitable workability and mechanical properties for concrete used in pavement. Liu *et al*. [79] suggested that the recycled ELT content can be at most 20 % of fine aggregate, in case of airport pavement. In general, Issa and Salem [80] recommended that the recycled ELT should not be over 20 % of the total aggregate volume.

In general, Table 2- 2 indicates that ELT rubber replacing aggregate may result in significant reductions in the mechanical properties of RCM, such as modulus and strength. Conversely, increasing the ELT rubber content appears to improve the ductility, toughness, workability, water absorption, thermal insulation, chloride ion permeability, electrical resistivity, conductivity, permeability, energy absorption capacity, impact resistance, and freeze-thaw resistance.

2.2.4 Motivation

Many studies have proved that the key factors that impact the workability, mechanical properties, and durability of rubberized concrete can be attributed to the: (i) rubber content (*i.e.*, volume or weight percentage of aggregate replacement); (ii) morphology of the rubber particles as well as natural aggregates in the rubberized concrete mixture; (iii) admixtures (*e.g.*, supplementary cementitious materials); (iv) mixture design and water-to-cement ratio; and (v) treatment methods (*e.g.*, water washing, NaOH washing, silane coupling agent, chemical treatments) and surface modifications (*e.g.*, coatings) to the rubber particles. This literature review will particularly focus on the treatment methods and surface modifications that are widely applied to improve the feasibility of the use of rubberized concrete. While a number of review articles have already focused on the use of ELT rubber in cementitious applications (*e.g.*, [15–18,41,71,81–84]), there is a lack of a systematic summary and catalog of the currently-used treatment methods for ELT rubber in terms of treatment procedures, treatment mechanisms, and treatment efficiencies. The main purpose of this study is (i) to summarize the mechanism of various recycled ELT rubber pretreatment methods in the literature and their effects on micro- and macrostructure of ELT rubber particles as well as the whole RCM structure and (ii) to provide more comprehensive comparisons between the effectiveness of pretreatment methods for ELT rubber. As a result, the most effective methods will be identified, which can serve as guidelines in the future for other researchers.

Table 2- 2. Summary of the basic information of research studying in RCM.

Study/ Source	ELT type	Treatment method	Dosage (%)	Engineering Properties											
				A	B	C	D	E	F	G	H	I	J	K	L	M
[28]	CR	N/A	FA/10-50 %	X	X	X	X					√		√		√
[42]	25.4 × 25.4 × 5 mm	Saturated NaOH	CA/15%	X	X		X		O							
[43]	#40 mesh	H_2SO_4; HNO_3; $H_2SO4 + HNO_3$;	Total volume/12.2-12.5%		X											
[47]	4.12 mm	Silica fume (SF)	FA/0-50%		X											
[72]	500 µm	NaOH	Total mass/10%	O	X	√										
[78]	FA size	NaOH and SCA	FA/15-50 %		X								√			
[80]	Crushed sand size	N/A	FA/15-100%		X								√			
[85]	0.29-0.59 mm	NaOH; SCA	FA/5-10%		X											
[86]	0-4 mm	N/A	FA/ 0-40%	X			X	X								
[87]	2-6 mm	N/A	FA, CA, FA and CA/5-15%		X		X	X								
[88]	1.18 mm	NaOH	FA/0-18%		X											
[89]	Fractions 2/4 and 4/6	N/A	FA/5-20%		X											
[90]	0.6 mm	N/A	FA/0-5.5 %		X	X										
[91]	4-10 mm	N/A	Gravel/0-25%		X	X										
[92]	2.5-25 mm	N/A	CA/25-100%	X	X	X										
[93]	2-4 mm	Emulsion; ethoxyline resin; synthetic resin; amino-acrylate; chloroprene adhesive; unsaturated resins	FA/5-20 %	X	X		X									
[94]	0.4-0.9 mm	Slag	FA/5-20%	X	X		X									
[95]	2.6 mm	N/A	CA/25-100%	X	X			X								
[96]	10-12 mm (Phase 1)	N/A	Total/5-15% (phase 1)		X	X			√							

Study/ Source	ELT type	Treatment method	Dosage (%)	Engineering Properties											
				A	B	C	D	E	F	G	H	I	J	K	L	M
	10/12 and 16/20 mm (phase 2)		Limestone gravel/10-30% (phase 2)													
[97]	PR Chipped powder: 20 mm	SF	FA/0-40 % CA/2.5 % chipped rubber with 5-20 % PR	X	X	X	X			√	√	√				
[98]	1.18 and 2.36 mm	NaOH; NaOH and SF	FA/20 %		X		X		√							
[99]	TC and CR	N/A	Total aggregate volume/ 10-20 %		X		X							√		
[100]	GR	N/A	FA/10-30 %	X	X	X	X		X							
[101]	0.85 mm	N/A	FA/10-50 %	X	X		X								√	
[102]	GR	N/A	FA/5-20 %	X	X		X								√	
[103]	2 mm	N/A	FA/10- 40 %		X	X	X								√	
[104]	2-6 mm	NaOH; cement paste pre-coating	FA/12.8 %*		X											
[105]	420-840 µm	Ultraviolet (UV) radiation	FA/15%			X										
[106]	0.85 & 2.8 mm	Gamma radiation	FA/30 %	X	X	X	X									
[107]	#40, #30 mesh, 1-5 mm	Heating	FA/40%		X		X									
[108]	0.425-4.75 mm	Cement & silane pre-coating	FA/30 %	X	X		X									
[109]	< 0.6 mm	SCA and CSBR latex	FA/5-30 %		X	X						√				
[110]	0.6-2.5 mm	$Ca(OH)_2$; NaOH; CH_3COOH; H_2SO_4	FA/10%		X	X										
[111]	2-2.36 mm	H_2SO_4; CH_3COOH	FA/30%	X	X											
[112]	300-600 µm	Partial oxidation	FA/6 %*		X	X	X									
[113]	#30-50 mesh	WOSC treating	FA/3, 6 %*		X	X	X									
[114]	#8, 15, 20, 40, & 60 mesh	$MgSO_4$; $CaCl_2$; $Al_2(SO_4)_3$; CCl_4; CS_2; glycerol; acetone soaking	FA/15%		X											
[115]	< 2.3 mm	$CaCO_3$ pre-coating; $CaCO_3$ pre-coating and SF	FA/5-15%		X	X				√						

Study/ Source	ELT type	Treatment method	Dosage (%)	Engineering Properties											
				A	B	C	D	E	F	G	H	I	J	K	L	M
[116]	Sand size	Water soaking	FA/30%		X											
[117]	PR	NaOH and $KMnO_4$ and $NaHSO_3$	Total mass/ 26%		X										√	
[118]	Fine/coarse rubber	Water washing	FA/40%		X											

Note: A: modulus of elasticity; B: compressive strength; C: flexural strength; D: split tensile strength; E: ductility/toughness; F: workability; G: water absorption; H: thermal insulation; I: chloride ion permeability; J: electrical resistivity/conductivity; K: permeability; L: energy absorption capacity/impact resistance; M: freeze–thaw durability; FA and CA denote fine aggregate and coarse aggregate, respectively; X. √, and O denote negative, positive, and insignificant effects of ELT rubber on RCM ; Number with "*" is rubber content in mass unit.

2.3 ELT rubber treatments

A wide variety of ELT rubber treatment methods have been studied for the potential use in RCM. This review paper has categorized and grouped those methods into two main approaches: physical treatments and chemical treatments. Each treatment method uses a different mechanism to treat the ELT rubber and thus has different efficiency on strength recoverability of RCM.

2.3.1 Physical treatments

The physical treatment methods including water treatment, radiation treatment, and heat treatment are explained below.

2.3.1.1 Water treatments

One of the simple and economical methods to pretreat ELT rubber is the water washing method [104,119]. The removal of these impurities is believed to improve the contact between the washed ELT particles and cement paste, resulting in strength recovery for the ELT rubberized concrete**.** This method uses pressurized water to wash the ELT rubber to remove dust and fine rubber particles. The particles are washed for ~5 minutes or until there is little to no dust in the wash water. The washed ELT rubber is filtered and air-dried before mixing in concrete. A similar method called "water soaking-A" proposes to soak the ELT rubber in tap water for 24 hours before being subjected to the washing process. A similar method, termed "water soaking-O," follows the "water soaking-A" except that the ELT rubber is dried at 100 ℃ for 6 hours for faster drying. A study by Najim and Hall [104] found that washing the ELT rubber particles using water prior to mixing could increase the UCS by up to more than 15 %. After the dust and fine particles have been removed, less water in the mixture is absorbed, so the workability of concrete is maintained.

2.3.1.2 Radiation treatments

Radiation treatment includes the treatment with ultraviolet rays, gamma radiation, plasma and microwave treatment.

2.3.1.2.1 Ultraviolet (UV) radiation treatment

Ultraviolet (UV) radiation is known to modify the polymer molecular and/or chemical structure [120]. Due to its high energy, UV radiation has the ability to break the chemical bonds of ELT rubber and generate polar species and unpaired bonds on the ELT rubber particles, which is known to cross-link polymer chains, therefore increasing stiffness of the rubber [121,122]. Ossola and Wojcik [105] effectively applied this technique to modify the ELT rubber used for RCM. The ELT rubber was exposed to UV at ~253 nm for 60 hours and then quickly subjected to mixing within 10 minutes after the UV exposure to avoid any potential temporal impacts. The study found that pretreatment for ELT rubber using UV radiation could effectively reduce the severity of strength loss in flexural strength with only a 6 % reduction when compared to the conventional concrete without added ELT rubber. This improvement was believed to be mainly attributable to the bonding between the rubber and cement matrix.

2.3.1.2.2 Gamma radiation treatment

Similar to UV radiation, gamma radiation can promote the generation of reactive intermediates that can result in free radicals and eventually in hydrogen abstraction, disproportion, arrangement,

and possible new bonds formation in the rubber structure [123,124]. Hence, the ELT particles are believed to be significantly harder and have less cracks on its surfaces; on the other words, the technique is believed to generate a composite material with stiffer particles, which could be able to improve the resistance of RCM. A study by Herrera-Sosa *et al*. [106,125] used 250 kGy gamma rays at 4 kGy/h to modify the physicochemical properties of the ELT rubber at two different sizes (0.85 mm and 2.8 mm) for use in RCM. The research found that some of the observed irradiated ELT rubberized concrete had better compressive strength, splitting tensile strength, and modulus of elasticity when compared to these of non-irradiated ELT rubberized concrete. A later study by the same research group [125] found that the higher energy used for the irradiation process (200 kGy *vs.* 300 kGy) was able to improve the strength. In addition to irradiation doses, the gamma radiation treatment method was found better for larger particles (0.85 mm *vs.* 2.80 mm). For the smaller particle size of ELT rubber (0.85 mm), the treatment method worked most effectively at 30 % of ELT rubber replacement. Conversely, for a larger particle size (2.80 mm), it worked most effectively at 10 % of ELT rubber replacement. In this study, there was no exception reported along with the positive strength improvement as found in their previous study.

2.3.1.2.3 Plasma treatment

Plasmas are also known to chemically modify polymer surfaces and affect bonding [126,127]. Treatment by low-temperature plasma (LTP) has been used, and it has been found to not generate any changes in the bulk properties of the treated materials [128–130]. The LTP treatment introduces chemical functional groups as a function of the process gas as well as the material's chemical composition. An LTP treatment usually requires energy less than 20 eV to break chemical bonds of polymers and then recombine them to create expected functional groups or reactive species [128].

To improve the mechanical properties of a rubberized oil-well cement, Cheng *et al*. [128] treated 0.089 mm ELT rubber by using LTP with oxygen and then subjected to an ethanol LTP polymerization process (LTP-PP) to improve the adhesion of the ELT rubber when blended into the cement matrix. This study generated an oxygen plasma in a chamber at 10 Pa. The treatment involved powers ranging from 60 W to 120 W for 1 min, 2.5 min, and 5 min. Following the plasma treatment, ethanol was vaporized into the chamber. The power for this process was set at 100 W for 20 min, 40 min, and 60 min. The LTP-PP process is presented in Figure 2- 1. The study found that the contact angle of ELT rubber particles can be significantly reduced from 122^{o} to 33^{o} using just LTP. The treatment duration of 2.5 min was found to be much more effective than 1 min but not significantly less effective than the duration of 5 min while the treatment power below 100 W was found to be effective. After being subjected to the ethanol LTP-PP treatment, the contact angle of the ELT rubber was further reduced to 11^{o} after 1 hour of the treatment process. The results suggested that the optimal treatment conditions were LTP at 100 W and 2.5 min coupled with LTP-PP at 100W and 60 min. Indeed, this treatment method for ELT rubber could recover 76.4 % of strength loss in the case of the original mixture with 5 % of rubber. Impressively, tensile strength and flexural strength of the RCM using treated ELT rubber were even improved by 11 % and 9.6 %, respectively, when compared to those of the reference mixture without ELT rubber.

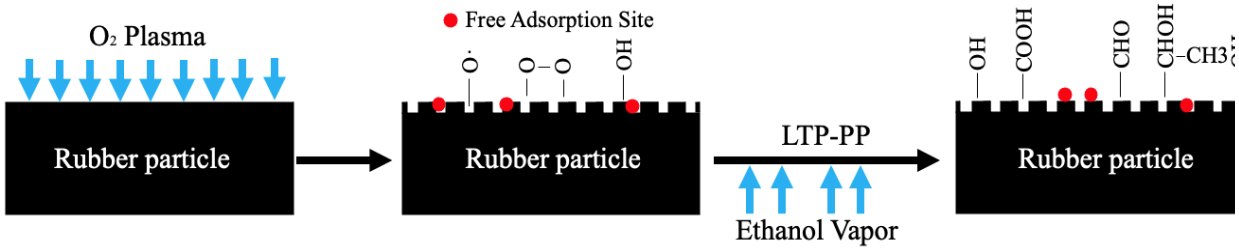

Figure 2- 1. Flowchart of LTP-PP (replicated based on Cheng et al. [128]).

2.3.1.2.4 Microwave treatment

It is worth noting that the treatment for ELT rubber using the microwave is also an effective method. The microwave treatment has the ability to break the crosslinked C-S and S-S bonds of the molecules in rubber. The efficiency of this method depends on the carbon content of ELT rubber, its chemical composition, magneton power, and exposure time [131–138]. However, while microwave treatment methods have been used for ELT rubber in asphalt concrete [136,138,139], to the best of knowledge, the literature on microwave-treated ELT rubber in RCM is not available in any database. Similarly, the microwave treatment coupled with bio-modification or treatment method using cooking oil are also the ones which have been applied only for asphalt, further studies about these methods for RCM are recommended to be discovered.

2.3.1.3 Heat treatment

A recent study by Abd-Elaal *et al*. [107] suggested a thermal treatment method for modifying the ELT rubber particles before mixing. The hypothesis of this method depicts that the relatively high temperature would induce the variation in stiffness of the ELT rubber particle as well as its surface topology. For the treatment procedure, ELT rubber of various sizes (#30 mesh, #40 mesh, 1 mm to 3 mm, and 2 mm to 5 mm) was treated in a 200 ℃ furnace for 1 h to 2 h. The changes in surface morphology were studied by SEM (Figure 2- 2). Impurities on the ELT rubber surface (Figure 2- 2a,b) are believed to consist of cord, steel, fibers, and rubber fines and are argued to negatively impact the bonding between the ELT rubber particles and cement paste. These impurities appear to be removed after thermal treatment (Figure 2- 2 c,d,e). The removal of these impurities could effectively contribute to the interlocking ability between the ELT particles and cement paste, resulting in strength recovery for the ELT rubberized concrete (up to 92.7 % of original compressive strength value in case of using 10 % of rubber).

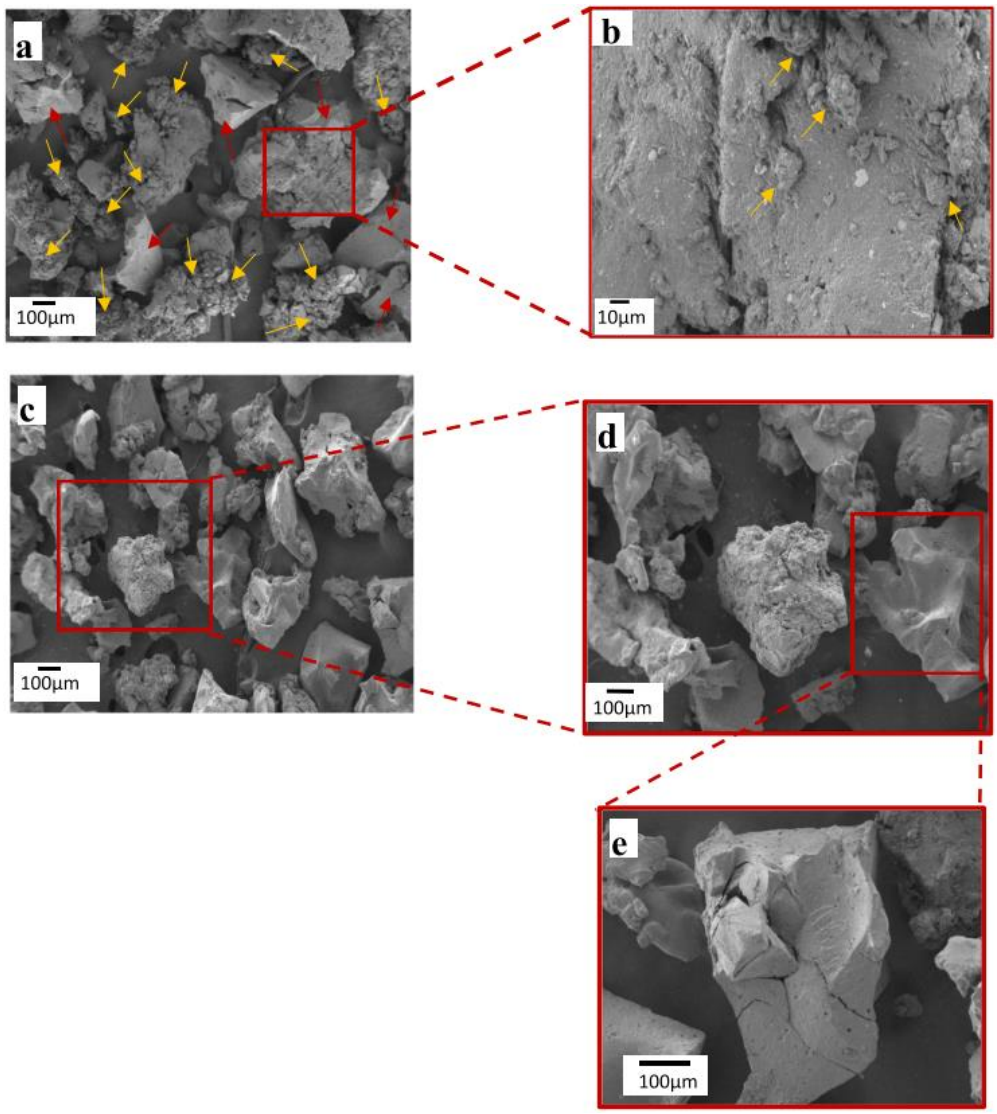

Figure 2- 2. SEM analyses of a and b) untreated and c, d, and e) thermally treated ELT rubber particles [107]. (This figure is reproduced with permission from Elsevier and Copyright Clearance Center).

2.3.2 Chemical treatments

The chemical treatments include coating, silane treatment, use of alkaline and acidic solutions, partial oxidation, and treatments with organic sulphur compounds.

2.3.2.1 Coating treatments

The treatment methods including coating ELT rubber with cement paste and mortar were performed by Najim and Hall [104]. For the cement paste pre-coating, the ELT rubber was immersed in a w/c=1.0 cement paste and then left to air-cure at ambient laboratory conditions for 28 days. For the mortar pre-coating method, a similar method was applied, except that the cement-coated ELT rubber was mixed with fine aggregate (1 mm to 2 mm) prior to curing. It was believed that the coating would create a “hard shell” around the ELT rubber particles by the hydration

products, making it harder and bringing about better bonding between the ELT rubber particles and the cementitious matrix of RCM. The results showed that the two pre-coating methods could effectively recover the strength loss when adding ELT rubber into the conventional concrete. The mortar-coated ELT rubber was found to be more effective than the cement-coated ELT rubber, as the tensile and compressive strengths increased by 19 % and 37 %, respectively, when compared to the uncoated ELT rubber mixture. Also, a significant enhancement in energy absorption, ductility, vibration damping, and dynamic response was found for the mortar-coated ELT rubber concrete. Meanwhile, another investigation [140] identified an increment in strength up to 30% for the cement paste-coated ELT rubber when compared to the untreated ELT rubber. The enhancement in mechanical properties of these coated ELT rubber mixtures could be due to an improvement in interfacial bonding between the cementitious matrix and the coated particle.

With a similar pre-coating concept, Obinna [115] proposed a method that used 3 μm limestone powder (LP) to pre-coat the ELT rubber. The amount of LP and water were 15 % and 5.25 %, respectively (by ELT rubber mass). The coated ELT rubber was air-dried for 24 hours, and then stored for one month before its use in RCM. However, the study found that the LP pre-coated ELT rubber did not significantly improve the compressive strength. Particularly, this treatment method could recover 42 %, 20 %, and 15 % of the strength loss with the LP pre-coated ELT rubber doses of 5 %, 10 %, and 15 %, respectively. To compensate for the marginal strength recovery, the study included a 10 % replacement of cement by silica fume into the RCM. It was believed that this method can enhance the ELT rubber-cement paste interface, and also reduce the porosity of RCM. Indeed, the addition of silica fume could recover around 133 %, 85 %, and 32 % of strength loss of RCM with 5 %, 10 %, and 15 % of LP pre-coated ELT rubber used, respectively.

2.3.2.2 Silane coupling agent used treatments

This involves the combination of a silane coupling agent with cement paste, and carboxylated styrene-butadiene rubber (CSBR) latex.

2.3.2.2.1 Silane coupling agent (SCA) and cement paste coating

A two-stage treatment method using an SCA and cement paste has been proposed by Huang and colleagues [108,141]. Silane is a bifunctional chemical that can act to couple the organic materials (*i.e.*, ELT rubber) to the inorganic materials (*e.g.*, cement paste or aggregate) [142]. The working mechanism of the SCA is presented in Figure 2- 3. An SCA contains a reactive vinyl or epoxy group (X) and methoxy groups (OR). The methoxy groups become hydroxyl groups (OH) due to hydrolysis in the ethanol-water mixture. The hydroxyl groups will be physically bonded by hydrogen bonds or chemically bonded by dehydration condensation to inorganic materials (*e.g.*, cement paste). These strong chemical bonds generated by SCA can be broken with the application of additional energy, resulting in improved RCM engineering properties. In this two-stage mixing process, SCA is first mixed with the ELT rubber particles followed by mixing with a cementitious binder. The role of the second-stage treatment is to generate a ‘‘hard shell’’ around the ELT rubber particles by the hydration of cement coating as well as to enhance the compatibility in the modulus

[141], as presented in Figure 2- 4. Using this approach, the researchers observed a 75% recovery of compressive strength at 15% replacement, and 44% recovery with 30% replacement [108].

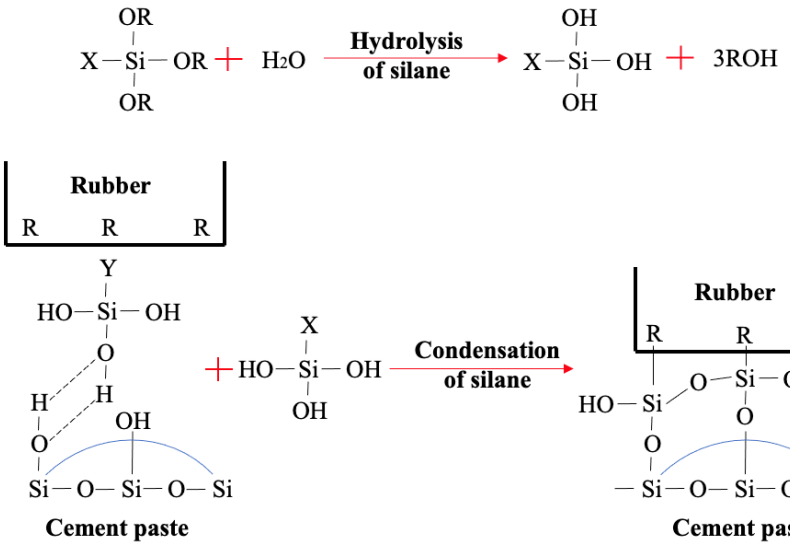

Figure 2- 3. The chemical working mechanism of SCA in an RCM (replicated based on Huang et al. [141]).

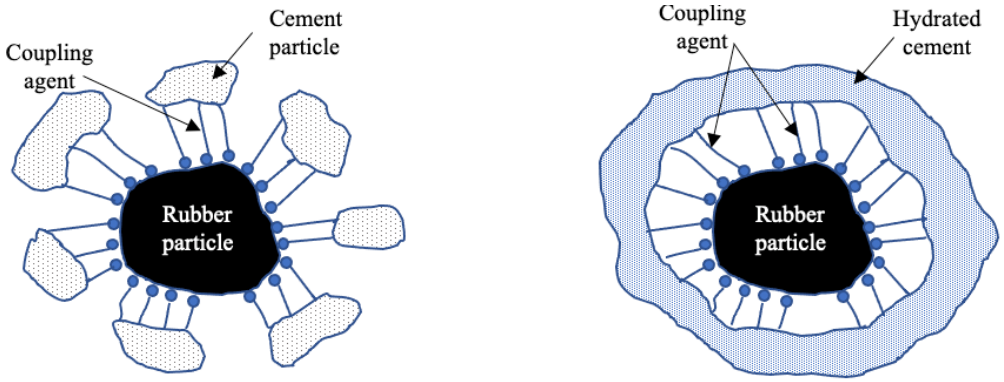

a) Before hydration b) After hydration

Figure 2- 4. Illustration of the SCA action in an RCM (replicated based on Huang et al. [108]).

2.3.2.2.2 Silane coupling agent and carboxylated styrene-butadiene rubber (CSBR) latex

An investigation by Li *et al.* [109] introduced carboxyl and hydroxyl groups using silane and a CSBR latex to treat the ELT rubber, in order to enhance the chemical bonding between the ELT rubber particles and the cementitious matrix. CSBR latex has a strong adhesion capacity [143] and compatibility with both ELT rubber and cementitious materials, which is believed to chemically link the ELT rubber with the cementitious matrix. In addition, CSBR latex can possibly form three-dimensional polymer films in the hardened cementitious materials to seal the voids as well as bridge the matrix's cracks, improving ductile behavior, tensile strength, impact resistance as well

as durability. Indeed, Figure 2- 5 appears to support the effectiveness of the CSBR through a crack arresting mechanism.

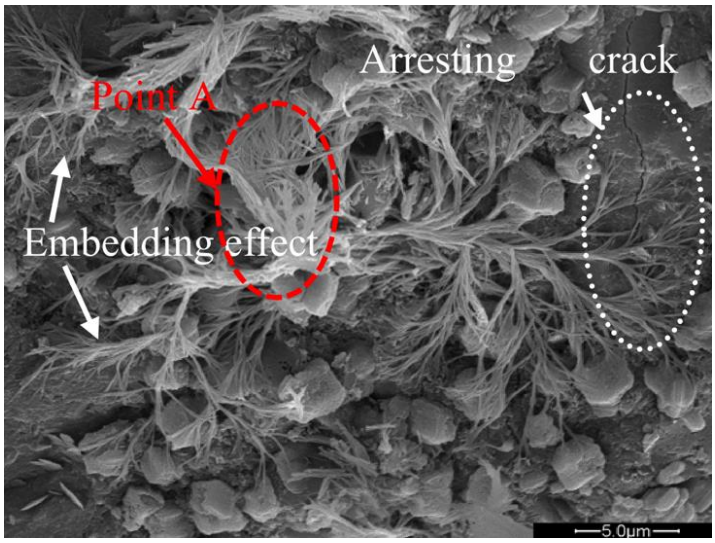

Figure 2- 5. SEM image of a SCA-CSBR-treated RCM showing an apparent crack arrestation [109] (This figure is reproduced with permission from Elsevier and Copyright Clearance Center).

The proposed working mechanism of the SCA-CSBR RCM is postulated as three main stages shown in Figure 2- 6 [109]. Stage I is what exactly happens when SCA is introduced into the ELT rubber as above-mentioned by Huang *et al*. [141] and shown in Figure 2- 3. In Stage II, when the silane-coated rubber interacts with CSBR latex, the carboxyl groups in CSBR latex react with the hydroxyl groups on the ELT rubber particles' surface to generate the chemical bonding at the ELT rubber-CSBR interface. In Stage III, when the SCA-CSBR treated ELT rubber is used in RCM, chemical bonding between the rubber and hydrated cement paste may also be formed. Particularly, as shown in Figure 2- 6, the Ca-OH groups, which are abundant in cement hydration products (*e.g.*, calcium silicate hydrate, calcium sulfoaluminate hydrates, and calcium hydroxide), might react with the COOH groups in the SCA-CSBR treated ELT rubber to create Ca-OO-C bonds. Furthermore, Si-O-Ca bonds can be produced by the reaction between Ca-OH groups in cement hydration products and Si-OH groups in SCA. In addition, the hydrogen bonds between the OH groups in cement hydration products and those in SCA might be formed during the ELT rubber surface treatment, resulting in the enhancement of interface properties. In addition, the van der Waals force may increase as a result of the chemical reactions during the treatment process.

Ultimately, this treatment method was found to increase the compressive and flexural strengths by around 4 % and 13 %, respectively, when compared to the conventional concrete without ELT rubber [109]. Furthermore, the chloride penetration resistance was also increased by 35 % compared to that of conventional concrete [109].

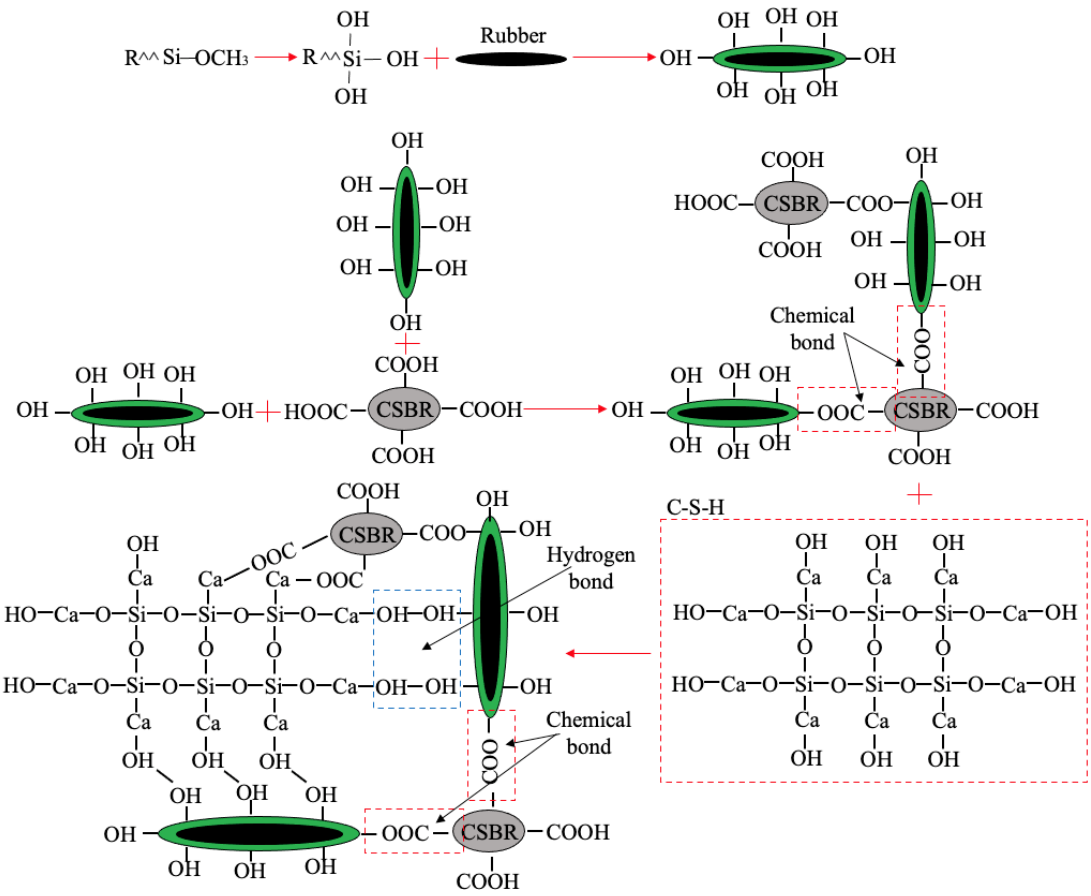

Figure 2- 6. Possible interactions between ELT rubber and C-S-H gel (replicated based on Li et al. [109]).

2.3.2.3 Treatments with alkaline solution

Treating ELT rubber using alkaline solutions, such as sodium hydroxide (NaOH) and calcium hydroxide [$Ca(OH)_2$], has proven to be an effective method to recover the strength loss when using ELT rubber in RCM. Cis-polyisoprene is present in natural rubber, and the carboxyl group in its structure can react with alkaline compounds [78], as shown in Figure 2- 7 for reaction with Na^+. This structure may be able to provide a weak basic condition close to the ELT rubber particles-cement paste interface during the cement hydration and thereby improve bonding.

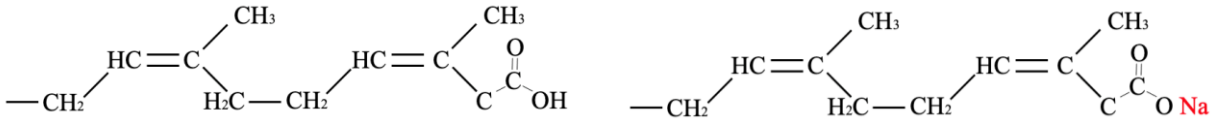

Figure 2- 7. a) The structure of cis-polyisoprene with the carboxylic acid group and b) reaction of the structure in an NaOH solution (replicated based on Guo et al. [78]).

Guo *et al*. [78] stated that treating ELT rubber with NaOH can increase surface hydrophilicity and result in a thinner water film surrounding the ELT rubber surface. As a result, the porosity of the

ITZ could be reduced for better bonding between the ELT rubber particles and cement matrix. Meanwhile, Segre *et al*. [144] believed that zinc stearate, an additive added into tires during their manufacturing, causes poor adhesion due to its diffusion to the ELT rubber's surface. The hypothesized purpose of this method is that NaOH treatment would remove the zinc stearate from the ELT rubber surface, change its surface chemistry, and improve the surface homogeneity. Ultimately, data from multiple studies suggest that NaOH treatment results in better adhesion between the ELT rubber and the hydrated cement matrix [72,105,145].

The general procedure for treating ELT rubber with NaOH involves soaking with or without stirring followed by rinsing and drying. The literature presents different recommendations for NaOH concentration and treatment duration, such as 10 % NaOH treated for 30 min [119], 40 min [78], or 120 min [146] or 1 % NaOH treated for 24 h [145]. Similar procedures are proposed for $Ca(OH)_2$ treatment [110].

Along with NaOH treatment, several studies subjected the NaOH-treated ELT rubber to a second treatment. Feng *et al*. [145] coated dried NaOH-treated ELT rubber with an SCA to facilitate coupling between the ELT rubber and the hydrated cement and found that the SCA could help improve the compressive strength of the RCM by around 3 % compared to that of the cases with ELT rubber treated by NaOH only. Meanwhile, Pelisser *et al*. [147] washed the ELT rubber with 1M NaOH and then added 15 % silica fume to the NaOH-treated ELT rubber for a surface coating modification; the addition of 15 % silica fume was found to result in a compressive strength of 50 MPa, which was equivalent to the reference concrete without silica fume. It appears that the silica fume coating for ELT rubber does not work effectively, and it only contributes to the strength gain of the cementitious mixture by the pozzolanic reaction. Xi *et al.* [47] demonstrated this by comparing the strength improvement of an RCM mixture prepared by (1) coating ELT rubber with 8 % silica fume with a small amount of water for a minute before other components were introduced into the mixture and (2) conventional mixing procedure. The authors found that there were very little to no significant effects when using silica fume to pretreat ELT rubber before its use in RCM.

2.3.2.4 Treatment with acidic solutions

An acidic solution treatment of the ELT rubber has been demonstrated to modify the surface energy of the rubber [110]. Various acidic solutions including hydrochloric acid (HCl) [111], hydrogen peroxide (H_2O_2) [119], nitric acid (HNO_3) [43], sulfuric acid (H_2SO_4) [43,110,119], acetic acid (CH_3COOH) [114], a series of potassium permanganate ($KMnO_4$) oxidation and sodium bisulfite ($NaHSO_3$) sulfonation [117] at different strengths have been explored in the literature. Similar to the process for alkaline solution treatments, ELT rubber are soaked in acidic solution with or without stirring followed by rinsing and drying before mixing into concrete.

Muñoz-Sánchez *et al*. [110] reported that 48 % H_2SO_4 and 48 % CH_3COOH solution could effectively treat the ELT rubber and help recover around 43 % and 13 % of strength loss, respectively, when compared to the RCM using untreated ELT rubber. Abdulla and Ahmed [111] found that HCl treatment for the ELT rubber does not have a remarkable improvement in the RCM,

and there was even a negative impact on the strength of RCM when using 35 % HCl solution. It was reasoned that the strong HCl acid not only dissolved the dirt, oils, and impurities on the ELT rubber particles but also probably dissolved the ELT rubber particles' corners and reduced irregularities that could serve as mechanical interlocking sites. However, Abdulla and Ahmed [111] also found that 5 % H_2SO_4, 35 % H_2SO_4, and 5 % CH_3COOH solutions could effectively treat the ELT rubber and help recover around 36 %, 52 %, and 400 % of strength loss, respectively, when compared to the RCM using untreated ELT rubber. Youssf *et al.* [119] found that H_2O_2 treatment for the ELT rubber does not have any considerable improvement in the RCM while Leung and Grasley [43] had the same conclusion as Abdulla and Ahmed for treatment method using HNO_3.

Apart from the above-mentioned acid treatment methods for ELT rubber, He *et al.* [117] proposed a different method that uses different chemicals at different steps of the treatment process. Particularly, ELT rubber was initially soaked in a 5 % NaOH solution for 1 day before rinsing with water. After that, the ELT rubber was subjected to a 5 % $KMNO_4$ solution while its pH value was adjusted to around 2 to 3 using H_2SO_4. The mixture was heated at 60 ℃ with stirring for 2 hours to facilitate oxidation reactions. After the 2-hour oxidation process, ELT rubber was rinsed with water and then added to saturated $NaHSO_3$ at 60 ℃ for 30 min to 60 min for the sulphonation reactions. The authors found that the adhesion strength of cement paste and the ELT rubber increased by 5 %, 18 %, and 41 % after the ELT rubber surface treatment using NaOH, oxidation, and sulphonation treatments, respectively. As a result, the compressive strength of the RCM using 4 % modified ELT rubber by concrete mass (around 30 ~ 40 % of fine aggregate volume) increased by 49 % compared to that of the untreated ELT rubber. Meanwhile, a study by Youssf *et al.* [119] skipped the NaOH treatment step and directly went to treatment by 5 % $KMNO_4$ oxidation and 5 % $NaHSO_4$ (instead of $NaHSO_3$) sulphonation processes to treat the ELT rubber. The authors found that this treatment process was not effective and even had a negative impact on the RCM's strength improvement. Particularly, with the case of using 20 % ELT rubber by sand volume, there was around a 3 % reduction of strength compared to the original case using untreated ELT rubber.

2.3.2.5 Partial oxidation treatment

A partial oxidation reaction to modify the surface properties of the ELT rubber particles has been employed by Chou *et al.* [112]. This method was believed to generate hydrophilic functional groups, such as S=O and S–O, on the surfaces of ELT rubber. Chou *et al.* argued that these functional groups can improve bonding with hydrated cement, resulting in an increase of mechanical properties of RCM. In this treatment method, air and nitrogen with an oxygen-to-nitrogen ratio of 0.04 are passed through a reactor for 30 min. After 30 min, the gas flow was stopped and the temperature in the reactor is increased up to the designed value (*e.g.*, 150 ℃, 200 ℃, and 250 ℃). The RCM with the ELT rubber treated at 250 ℃ gave a significant enhancement in compressive strength compared with the RCM with untreated ELT rubber. The mortar with treated ELT rubber even achieved a greater compressive strength than the control mortar. Particularly, the authors found that the heating treatment at 250 ℃ could effectively treat the ELT

rubber to totally recover the strength loss along with increasing the compressive strength of RCM by 18 %, when compared to the reference mixture without ELT rubber.

2.3.2.6 Treatment with waste organic sulfur compounds (WOSC)

Chou *et al*. [113] resued WOSC from a petroleum refining plant to improve the hydrophilicity of the ELT rubber particles' surface and to enhance the intermolecular interaction between the ELT rubber and C-S-H to improve the ultimate strength of RCM. The results showed that the ELT rubber particles adsorbed WOSC onto its surface. Since the WOSC is amphiphilic, the WOSC-treated ELT rubber would be more hydrophilic. In addition, the advancing and receding contact angles of the ELT rubber particles changed from 103^{o} to 100^{o} and 59^{o} to 31^{o}, respectively, which indicates an increase in the hydrophilicity. However, these differences might also be due to the changes in surface roughness of the ELT rubber particles after being treated. The intermolecular interaction between untreated and treated ELT rubbers was also studied by atomic force microscopy (AFM), which demonstrated that the intermolecular force between the ELT rubber and C-S-H doubled from 25 nN for the untreated ELT rubber to 55 nN for the WOSC-treated ELT rubber. In the case of using 3 wt.% of ELT rubber, the WOSC treatment method could recover around 38 %, 60 %, and 54 % of compressive, flexural, and tensile strengths of the RCM, respectively. With 6 wt.% of ELT rubber used, these values were around 28 %, 51 %, and 33 %, respectively.

2.3.2.7 Other treatments

Tian *et al*. [114] proposed the use of inorganic metal salt solutions to modify ELT rubber particles. The ELT rubber was soaked in a 10 % $MgSO_4$, 10 % $CaCl_2$, and 10 % $Al_2(SO_4)_3$ solutions for 24 h. After that, ELT rubber was dried and sealed before use. As the ELT rubber was dried, the salt was believed to precipitate on the particle surface and serve as a bonding site. In case of mixtures using 15 % treated ELT rubber by volume of fine aggregate, the result showed that the 10 % $CaCl_2$ solution treatment worked the best among the three with around 37 % recovery of the compressive strength produced, followed by $MgSO_4$ and $Al_2(SO_4)_3$ solution treatments with recoveries of 17 % and 14 %, respectively. Youssf *et al.* [119] also found similar output for $CaCl_2$ solution treatment at 20 % treated ELT rubber used in RCM.

Meanwhile, treatments with organic solutions, such as acetone $(CH_3)_2CO$), glycerol ($C_3H_8O_3$), carbon disulfide (CS_2), and carbon tetrachloride (CCl_4), have also been proposed to improve the ELT rubber surface [114]. The procedure for this treatment method is to soak the ELT rubber in the solution, but the dose was defined based on rubber particle size (specific surface area). The results show that this method could not provide any strength recovery, but had negative effects on the RCM. Particularly, acetone, glycerol, carbon disulfide, and carbon tetrachloride solution treatments caused 13 %, 9 %, 3 %, and 2 % reduction of original compressive strength value in the case of using untreated rubber, respectively. The above-discussed treatment methods for ELT rubber used in RCM are summarized in Table 2- 3 below.

Table 2- 3. Summary of typical treatment methods for ELT rubber used in RCM.

Treatment methods		References
Physical treatments	Water treatments (*i.e.*, water soaking-A, water soaking-O)	[104,119]
	Radiation treatments (*i.e*, Ultraviolet (UV) radiation, gamma radiation, plasma treatment, microwave treatment)	[106,120,125,128,136,138,139]
	Heat treatment	[107]
Chemical treatment	Coating Treatments (*i.e.*, Silane coupling agent (SCA) and cement paste coating, silane coupling agent and carboxylated styrene-butadiene rubber (CSBR) latex)	[104,109]
	Treatments with alkaline solution (*i.e.*, NaOH, $Ca(OH)_2$)	[78]
	Treatment with acidic solutions (*i.e.*, HCl, H_2O_2, HNO_3, H_2SO_4, CH_3COOH, a series of $KMnO_4$ oxidation and $NaHSO_3$ sulfonation)	[43,110,111,114,117,119]
	Partial oxidation treatment	[112]
	Treatment with waste organic sulfur compounds (WOSC)	[113]
Other treatments	Inorganic metal salt solutions (*i.e.*, 10 % $MgSO_4$, 10 % $CaCl_2$, and 10 % $Al_2(SO_4)_3$)	[114,119]
	Organic solutions, such as acetone $(CH_3)_2CO$), glycerol ($C_3H_8O_3$), carbon disulfide (CS_2), and carbon tetrachloride (CCl_4)	[114]

2.3 Discussions and recommendations

The mechanical properties of RCM strongly depend on various factors, such as the amount of aggregate replaced, treatment method, size and size distribution of the ELT rubber particles, mix proportioning, *etc*. Therefore, there is a wide range of recommendations from the literature. For example, Youssf *et al*. [119] identified that the NaOH treatment of the ELT rubber particles produced the best results. However, research by Najim and Hall [104] and Tian *et al*. [114] did not support this finding. Conversely, Abdulla and Ahmed [111] found that certain acidic solution treatments were effective, although Muñoz-Sánchez *et al*. [110], Tian *et al*. [114], and Leung and Grasley [43] reported that acidic solutions did not effectively enhance RCM's mechanical properties. Indeed, it is arguable to definitively conclude which treatment method(s) for the ELT rubber used in RCM can result in the best improvement to combat strength loss. Furthermore, there are very few studies that discussed this matter in-depth with clear approaches and satisfying conclusions. Therefore, this study proposes a comparison metric, termed the strength recovery index (SRI), to quantiatively compare treatment methods. The SRI presents how effective a treatment method can recover the strength loss of RCM relative to control materials. Strength loss is the difference in the 28-day compressive strength between conventional concrete without ELT rubber and RCM with as-received ELT rubber [107]. The SRI is defined as Eq. (1):

$$SRI = \frac{S_T - S_{UT}}{S_C - S_{UT}}, \qquad (1)$$

where S_{UT}, S_T, and S_C are the strengths of RCM with untreated rubber, RCM with treated rubber, and conventional concrete, respectively. Using the SRI, an easier comparison can be performed for the various treatment methods, as shown in Table 2- 4. There are six common ELT rubber dosage ranges in RCM (5 %, 10 %, 15 %, 20 %, 30 %, and 40 %), which are labeled as I to VI in

Table 2- 4. The effectiveness of each treatment method is categorized into five different levels: SRI greater than 0.75 (excellent) is colored in dark green, between 0.50 to 0.75 (very good) is colored in light green, between 0.25 to 0.50 (acceptable) is colored in orange, under 0.25 (ineffective) is colored in yellow, and under 0 (negative) is colored in red. In Table 2- 4, SRIs are arranged in descending order from highest to lowest value for each group.

The strength gain (SG) value is also provided for further evaluations when a treatment method can both totally recover the strength loss and increase the ultimate strength compared to that of conventional concrete. The SG is defined as Eq. (2):

$$SG\ (\%) = \frac{S_T - S_C}{S_C} \times 100, \qquad (2)$$

where S_T and S_C are the strengths of RCM with treated rubber and conventional concrete, respectively.

In this study, it is worth noting that the authors considered and recommend the pretreatment methods as "effective" if they can yield an SRI above 0.5 (very good recoverability) for Groups I, II, and III, and an SRI over 0.25 (acceptable recoverability) for Groups IV, V, and VI.

For Group I (ELT rubber content around 5 %), the data show that pretreatment of the ELT rubber by "SCA and CSBR latex" and "$CaCO_3$ pre-coating and 10 % SF" can give significant recoveries in compressive strength with SRI equal to 5 and 1.3, respectively. These treatment methods can provide a perfect recovery in strength loss and even improve the RCM's strength up to 3.8 % (SCA and CSBR latex method) and 5 % ($CaCO_3$ pre-coating and 10 % SF method), respectively. Meanwhile, pretreatment with LTP and LTP-PP, $CaCO_3$, or WOSC can yield a strength recovery of 76 %, 42 %, and 38 %, respectively. In general, because of the small replacement of ELT rubber, there is a relatively small strength loss that can be effectively recovered by most of the current treatment methods.

For Group II (ELT rubber content around 10 %), the data demonstrate that the "SCA and CSBR latex" treatment method is effective and can recover 100 % strength loss of the RCM. Additional high SRI treatment options include "NaOH washing and 15 % SF", "Heating (1 h)", and "$CaCO_3$ pre-coating and 10 % SF", which have SRI values of 0.93, 0.93, and 0.85, respectively. "NaOH (30 min)" and "$Ca(OH)_2$ (30 min)" are categorized as "very good" treatment methods since they yielded SRI values of 0.65 and 0.58, respectively. The treatment by gamma irradiation brings about inconsistent results since the SRI varies from –1.5 to 2.1 even the mixture proportion is the same between the two studies; therefore the gamma radiation treatment method is not recommended to treat the ELT rubber in this doge range. Further studies should be carried out to confirm the effectiveness of this treatment method.

For Group III (ELT rubber content around 15 %), "Partial oxidation at 250 ℃ (1 hour)" treatment method works as an excellent method with an SRI of 1.35 and it can increase the RCM's strength by 18 %. Additional treatments that produced high SRI values include "Cement and silane pre-

coating", "Ultraviolet (UV) radiation", and "SCA and CSBR latex", which yielded SRI values of 0.75, 0.71, and 0.69, respectively.

For Group IV (ELT rubber content around 20 %), no treatment method was able to completely recover the RCM's strength loss. Only the "Heating (1 h)", "SCA and CSBR latex", and "NaOH (0.5 h)" treatment methods were able to recover more than 50 % of the strength loss. In addition, the treatment by gamma irradiation could provide "acceptable" improvement for the RCM using ELT rubber mesh #7 while it only brought about negative effect to little improvement for the RCM using ELT rubber mesh #20.

For Group V (ELT rubber content around 30 %), no treatment method was able to completely recover the RCM's strength loss. Only the "Mortar pre-coating" and "35 % H_2SO_4 (24 h)" treatment methods were able to recover more than 50 % of the strength loss. Interestingly, the "Gamma radiation" treatment method still maintained "acceptable" performance in strength recovery despite the fact that it was ineffective for a mix with 10 % ELT rubber. Using only NaOH solution to treat the ELT rubber does not appear to be as effective at this ELT dosage, although it was effective at lower ELT dosages. For example, soaking ELT rubber in NaOH solution for 20 min to 60 min can provide very little or even a negative SRI value.

For Group VI (ELT rubber content around 40 %), "Heating (1 h)" and "5 % NaOH (24 h) and 5 % $KMnO_4$ (2 h) and saturated $NaHSO_3$ (1 h)" treatment methods can provide SRI values at "acceptable" recoverability with SRI values of 0.47 and 0.45, respectively. Due to a lack of data in the literature at this high dosage rate, there are fewer options when treating the ELT rubber for RCM.

In a summary, treatment methods appear to be the most effective in mixes with lower (*i.e.*, ≤ 20 %) ELT rubber contents. For Groups I, II, and III, the best pretreatment methods are possibly "SCA and CSBR latex", "$CaCO_3$ pre-coating and 10 % SF", "NaOH washing and 15 % SF", "Heating (1 h)", and "Partial oxidation at 250 °C (1 h)", which have the "excellent recoverability" in RCM's strength loss. Treatment options with "very good recoverability" include "NaOH (30 min)" and "$Ca(OH)_2$ (30 min)". However, it is worth noting that the methods using NaOH appear to have significant variability in the literature.

For Groups IV, V, and VI, "Heating (1 h)", "SCA and CSBR latex", "NaOH (0.5 h)", "Mortar pre-coating", and "35 % H_2SO_4 (24 h)" are recommended to use as they have "very good recoverability" of strength loss in RCM. Treatment options with "acceptable recoverability" include "Gamma radiation", "NaOH (24 h)", "Water soaking (24 h)", "Cement and silane pre-coating", "5 % CH_3COOH (24 h)", "5 % H_2SO_4 (24 h)", "SCA and CSBR latex", and "5 % NaOH (24 h) and 5 % $KMnO_4$ (2 h) and saturated $NaHSO_3$ (1 h)".

For a consolidation of the data, Figure 2- 8 was established based on data from Table 2- 4 to graphically summarize and compare the effectiveness of the outstanding treatment methods at different volume of ELT rubber used in RCM.

In order to have a better understanding of the influence of the "mother concrete" strength on the strength change of the RCM when adding treated ELT rubber, Table 2- 5 was derived based on Table 2- 4. In Table 2- 5, for all groups, the data were arranged and shown from RCM with the highest strength to the lowest strength. The original cementitious materials with strength above 40 MPa were considered as high strength, while the rest were considered as normal strength. The strength loss (SL) of RCMs using untreated and treated ELT rubber is reported from each study. Firstly, the data show that adding ELT rubber decreases the strength of the cementitious material, and the significance of SL generally seems to depend on the original material's strength. Particularly, for high strength cementitious materials, SL is usually smaller than that of normal strength cementitious materials when adding the same amount of ELT rubber. On the other words, the higher the strength the original cementitious material, the lesser the SL is reported when adding ELT rubber. Even with some scatter, this trend is quite clear for the Groups I, II, and III (*i.e.*, ELT rubber content no more than 15 %). When the ELT rubber content is ≥20 %, SL becomes similar regardless of the original strength of cementitious material or type of "mother concrete." More interestingly, when the treatment methods are introduced for ELT rubber, the strength loss of RCM is significantly affected by the type of treatment methods instead of the original strength. For example, for Group III, the "partial oxidation at 250 ℃ (1 hour)" treatment methods could recover all strength loss of the normal strength concrete (34.8 MPa) using treated ELT rubber, while "water soaking-A" could not help the high strength concrete (53.3 MPa) recover any strength loss. This does not follow the tendency mentioned earlier for untreated ELT rubber. This indicates that the selection of treatment methods for ELT rubber plays an essential role in the improvement of RCM's engineering properties further than the original strength of the cementitious material. For Group VI (*i.e.*, ELT rubber content around 40 %), there is too little data available in the literature to draw a reasonable conclusion.

While there are a number of studies on using ELT rubber in RCM, relatively few studies discuss the impact of particle size. The particle size of ELT rubber is one of the main factors which has an effect on the ultimate strength of RCM [47,106,107,125]. However, after being treated, the effect on engineering properties might remain relatively unchanged or may vary; there appears to be a dependence on the treatment method. Herrera-Sosa *et al*. [106,125] found that, at the same replacement percentage of ELT rubber in RCM, the compressive strength of RCMs with small particles is generally lower than the strength with large particles. In their study, the treatment gamma radiation method did not change the main effect of ELT particle size in the RCM, but it did effectively improve the compressive strength when using 30 % of 0.85 mm ELT rubber or 10 % of 2.8 mm ELT rubber. It seems that this treatment method can work effectively at the high replacement percentage of 0.85 mm ELT rubber or low replacement percentage of 2.8 mm ELT rubber. Meanwhile, Abd-Elaal *et al*. [107] found a similar tendency to Herrera-Sosa *et al*. [106,125] for compressive strength of RCM when using untreated ELT rubber at different sizes. However, after being thermally treated, the study reported that the larger size of the treated ELT rubber particle (from mesh #40 to 5 mm) used, the less effective this treatment method could provide. These limited data indicate that the relationship between the particle size of ELT rubber

and a treatment method selected is unpredictable, depending on both ELT rubber size and the type of treatment method applied. Futher study is needed to evaluate this interaction.

Table 2- 4. Comparison of the effectiveness of various ELT rubber pre-treatment methods.

Dose range/ Group	Pre-treatment method	Rubber content (Volume of fine aggregate, %)	Compressive strength				
			S_C (MPa)	S_{UT} (MPa)	S_T (MPa)	Strength Recovery Index (SRI)	Strength Gain (SG) (%)
I	SCA and CSBR latex [109]	5	52.5	52.0	54.5	5.0	3.8
I	$CaCO_3$ pre-coating and 10 % SF [115]	5	40.0	34.0	42.0	1.33	5.0
I	LTP (2.5 min) and LTP-PP (60 min) at 100 W [128]	5	37.3	30.3	35.7	0.76	
I	$CaCO_3$ pre-coating [115]	5	40.0	34.0	36.5	0.42	
I	WOSC treating [113]	3*	31.8	26.8	28.7	0.38	
II	Gamma radiation (mesh #7) [125]	10	24.5	21.0	28.5	2.14	16.3
II	SCA and CSBR latex [109]	10	52.5	48.5	52.5	1.00	
II	NaOH washing and 15 % SF [147]	10	46.0	17.0	44.0	0.93	
II	Heating (1 h) [107]	10	50.9	40.0	50.1	0.93	
II	$CaCO_3$ pre-coating and 10 % SF [115]	10	40.0	30.0	38.5	0.85	
II	NaOH (30 min) [110]	10	39.0	23.5	33.5	0.65	
II	$Ca(OH)_2$ (30 min) [110]	10	39.0	23.5	32.5	0.58	
II	48 % H_2SO_4 (5 min) [110]	10	39.0	23.5	30.2	0.43	
II	$CaCO_3$ pre-coating [115]	10	40.0	30.0	32.0	0.20	
II	Gamma radiation (mesh #20) [125]	10	24.5	15.0	16.5	0.16	
II	CH_3COOH [110]	10	39.0	23.5	25.5	0.13	
II	Gamma radiation (mesh #20) [106]	10	24.1	16.1	15.9	-0.03	
II	SF pre-treating (1 min) [47]	10	4.7	3.6	3.4	-0.18	
II	Gamma radiation (mesh #7) [106]	10	24.1	21.5	17.5	-1.54	
III	Partial oxidation at 250 °C (1 hour) [112]	6*	34.8	16.3	41.2	1.35	18.4
III	Cement and silane pre-coating [108]	15	37.0	25.2	34.0	0.75	
III	Ultraviolet (UV) radiation [105]	15	NA (6.33)	NA (4.98)	NA (5.94)	0.71	
III	SCA and CSBR latex [109]	15	52.5	44.5	50.0	0.69	
III	10 % $CaCl_2$ soaking (24 h) [114]	15	51.3	37.1	42.3	0.37	

Dose range/ Group	Pre-treatment method	Rubber content (Volume of fine aggregate, %)	Compressive strength				
			S_C (MPa)	S_{UT} (MPa)	S_T (MPa)	Strength Recovery Index (SRI)	Strength Gain (SG) (%)
III	$CaCO_3$ pre-coating and 10 % SF [115]	15	40.0	25.3	30.0	0.32	
III	WOSC treating [113]	6*	31.8	18.7	22.4	0.28	
III	10 % $MgSO_4$ soaking (24 h) [114]	15	51.3	37.1	39.5	0.17	
III	Water wash [119]	15	53.3	38.5	40.8	0.16	
III	$CaCO_3$ pre-coating [115]	15	40.0	25.3	27.5	0.15	
III	10 % $Al_2(SO_4)_3$ soaking (24 h) [114]	15	51.3	37.1	39.1	0.14	
III	1 M H_2SO_4 (10 min) [43]	12.2	72.9	17.6	21.6	0.07	
III	3 M HNO3 (30 min) [43]	12.2	72.9	17.6	16.6	-0.02	
III	1.5 M H_2SO_4 + 0.5 M HNO_3 (10 min) [43]	12.2	72.9	17.6	161	-0.03	
III	Carbon tetrachloride (CCl_4) (24 h) [114]	15	51.3	37.1	36.3	-0.06	
III	Carbon disulfide (CS_2) (24 h) [114]	15	51.3	37.1	35.9	-0.08	
III	Water soaking-A [119]	15	53.3	38.5	37.1	-0.09	
III	Water soaking-O [119]	15	53.3	38.5	35.7	-0.19	
III	Glycerol ($C_3H_8O_3$) (24 h) [114]	15	51.3	37.1	33.7	-0.24	
III	Acetone $(CH_3)_2CO$) (24 h) [114]	15	51.3	37.1	32.4	-0.33	
IV	Heating (1 h) [107]	20	50.9	30.5	42.8	0.60	
IV	SCA and CSBR latex [109]	20	52.5	40.5	47.5	0.58	
IV	NaOH (30 min) [148]	20	53.5	41.6	48.1	0.55	
IV	Gamma radiation (mesh #7) [125]	20	24.5	13.0	17.5	0.39	
IV	NaOH (30 min) [98]	20	53.5	35.9	42.1	0.35	
IV	Gamma radiation (mesh #7) [106]	20	24.1	12.9	16.1	0.29	
IV	NaOH (24 h) [149]	20	55.6	27.0	35.0	0.28	
IV	Water soaking (24 h) [116]	20	55.6	27.0	34.9	0.28	
IV	Water soaking (24 h) [150]	20	35.4	21.5	24.6	0.22	
IV	NaOH (1 h) [98]	20	53.5	35.9	38.6	0.15	
IV	Gamma radiation (mesh #20) [125]	20	24.5	12.5	14.0	0.13	

Dose range/ Group	Pre-treatment method	Rubber content (Volume of fine aggregate, %)	Compressive strength				
			S_C (MPa)	S_{UT} (MPa)	S_T (MPa)	Strength Recovery Index (SRI)	Strength Gain (SG) (%)
IV	10 % $CaCl_2$ soaking (24 h) [119]	20	41.5	27.3	29.1	0.13	
IV	NaOH (2 h) [98]	20	53.5	35.9	37.2	0.07	
IV	NaOH (30 min) and 15 % SF [98]	20	53.5	35.9	36.8	0.05	
IV	10 % H_2O_2 (30 min) [119]	20	41.5	27.3	27.5	0.014	
IV	5 % $KMnO_4$ (2 h) and 5 % $NaHSO_4$ (1 h) [119]	20	41.5	27.3	26.5	-0.056	
IV	Gamma radiation (mesh #20) [106]	20	24.1	16.1	15.9	-0.22	
V	Mortar pre-coating [104]	12.8*	54.0	32.0	45.0	0.59	
V	35% H_2SO_4 (24 h) [111]	30	36.5	16.0	26.7	0.52	
V	Cement and silane pre-coating [108]	30	37.0	22.5	28.9	0.44	
V	5 % CH_3COOH (24 h) [111]	30	36.5	16.0	24.3	0.40	
V	Gamma radiation (mesh #20) [125]	30	24.5	5.5	12.5	0.37	
V	5 % H_2SO_4 (24 h) [111]	30	36.5	16.0	23.3	0.36	
V	SCA and CSBR latex [109]	30	52.5	30.5	38.0	0.34	
V	Gamma radiation [111]	30	24.1	11.3	14.8	0.27	
V	Gamma radiation (mesh #7) [106]	30	24.1	11.5	14.8	0.26	
V	Cement paste pre-coating [104]	12.8*	54.0	32.0	37.0	0.23	
V	Gamma radiation (mesh #7) [125]	30	24.5	13.0	15.5	0.22	
V	NaOH (24 h) [149]	30	63.0	27.4	31.4	0.11	
V	Gamma radiation (mesh #20) [106]	30	24.1	5.0	7.0	0.10	
V	Water soaking (24 h) [116]	30	63.0	27.4	30.9	0.10	
V	SF pre-treating (1 min) [47]	30	4.7	1.7	1.9	0.07	
V	NaOH (20 min) [104]	12.8*	54.0	32.0	33.0	0.05	
V	Saturated NaOH (30 min) [42]	10*	39.08	22.33	23.23	0.05	
V	NaOH (40 min) [104]	12.8*	54.0	32.0	32.0	0.00	
V	NaOH (60 min) [104]	12.8*	54.0	32.0	30.5	-0.07	
V	Saturated NaOH (20 min) [72]	10*	43.1	29.4	28.1	-0.09	

Dose range/ Group	Pre-treatment method	Rubber content (Volume of fine aggregate, %)	Compressive strength				
			S_C (MPa)	S_{UT} (MPa)	S_T (MPa)	Strength Recovery Index (SRI)	Strength Gain (SG) (%)
VI	Heating (1 h) [107]	40	50.9	13.7	31.3	0.47	
VI	5 % NaOH (24 h) and $KMnO_4$ (2 h) and saturated $NaHSO_3$ (1 h) [117]	4*	49.2	23.6	35.1	0.45	
VI	Water washing [118]	40	46.8	22.4	26.2	0.16	

Note: Number with "*" is rubber content in mass unit. Green, light green, yellow, orange, and red denote excellent, very good, acceptable, ineffective, and negative strength recoverability, respectively.

Table 2- 5. Strength loss (SL) of normal and high strength RCM with different treatment methods for ELT rubber.

Dose range/ Group	Pre-treatment method	Rubber content (Volume of fine aggregate, %)	Compressive strength				
			S_C (MPa)	S_{UT} (MPa)	S_T (MPa)	S_{UT} Loss (%)	S_T Loss (%)
I	SCA and CSBR latex [109]	5	52.5	52.0	54.5	0.95	-4
I	$CaCO_3$ pre-coating and 10 % SF [115]	5	40.0	34.0	42.0	15.0	-5
I	$CaCO_3$ pre-coating [115]	5	40.0	34.0	36.5	15.0	8.75
I	LTP (2.5 min) and LTP-PP (60 min) at 100 W [128]	5	37.3	30.3	35.7	18.7	4.2
I	WOSC treating [113]	3*	31.8	26.8	28.7	15.7	9.74
II	SCA and CSBR latex [109]	10	52.5	48.5	52.5	7.62	0
II	Heating (1 h) [107]	10	50.9	40.0	50.1	21.41	1.57
II	NaOH washing and 15 % SF [147]	10	46.0	17.0	44.0	63.05	4.35
II	$CaCO_3$ pre-coating and 10 % SF [115]	10	40.0	30.0	38.5	25.0	3.75
II	$CaCO_3$ pre-coating [115]	10	40.0	30.0	32.0	25.0	20.0
II	NaOH (30 min) [110]	10	39.0	23.5	33.5	39.74	14.10
II	$Ca(OH)_2$ (30 min) [110]	10	39.0	23.5	32.5	39.74	16.66
II	48 % H_2SO_4 (5 min) [110]	10	39.0	23.5	30.2	39.74	22.56
II	CH_3COOH [110]	10	39.0	23.5	25.5	39.74	34.61
II	Gamma radiation (mesh #7) [125]	10	24.5	21.0	28.5	14.28	-16.32
II	Gamma radiation (mesh #20) [125]	10	24.5	15.0	16.5	38.77	32.65

Dose range/ Group	Pre-treatment method	Rubber content (Volume of fine aggregate, %)	Compressive strength				
			S_C (MPa)	S_{UT} (MPa)	S_T (MPa)	S_{UT} Loss (%)	S_T Loss (%)
II	Gamma radiation (mesh #7) [106]	10	24.1	21.5	17.5	10.78	27.38
II	Gamma radiation (mesh #20) [106]	10	24.1	16.1	15.9	33.19	34.02
II	SF pre-treating (1 min) [47]	10	4.7	3.6	3.4	23.50	27.65
III	1 M H_2SO_4 (10 min) [43]	12.2	72.9	17.6	21.6	75.85	70.04
III	3 M HNO3 (30 min) [43]	12.2	72.9	17.6	16.6	75.85	77.22
III	1.5 M H_2SO_4 + 0.5 M HNO_3 (10 min) [43]	12.2	72.9	17.6	16.1	75.85	77.91
III	Water wash [119]	15	53.3	38.5	40.8	27.77	23.4
III	Water soaking-A [119]	15	53.3	38.5	37.1	27.76	30.04
III	Water soaking-O [119]	15	53.3	38.5	35.7	27.76	33.02
III	SCA and CSBR latex [109]	15	52.5	44.5	50.0	15.24	4.76
III	10 % $CaCl_2$ soaking (24 h) [114]	15	51.3	37.1	42.3	27.68	17.54
III	10 % $MgSO_4$ soaking (24 h) [114]	15	51.3	37.1	39.5	27.68	23.0
III	10 % $Al_2(SO_4)_3$ soaking (24 h) [114]	15	51.3	37.1	39.1	27.68	23.78
III	Carbon tetrachloride (CCl_4) (24 h) [114]	15	51.3	37.1	36.3	27.68	29.24
III	Carbon disulfide (CS_2) (24 h) [114]	15	51.3	37.1	35.9	27.68	30.0
III	Glycerol ($C_3H_8O_3$) (24 h) [114]	15	51.3	37.1	33.7	27.68	34.31
III	Acetone $(CH_3)_2CO$) (24 h) [114]	15	51.3	37.1	32.4	27.68	36.84
III	$CaCO_3$ pre-coating and 10 % SF [115]	15	40.0	25.3	30.0	36.75	25.0
III	$CaCO_3$ pre-coating [115]	15	40.0	25.3	27.5	36.75	48.40
III	Cement and silane pre-coating [108]	15	37.0	25.2	34.0	31.89	8.11
III	Partial oxidation at 250 ℃ (1 hour) [112]	6*	34.8	16.3	41.2	53.16	-18.40
III	WOSC treating [113]	6*	31.8	18.7	22.4	41.19	29.55
IV	NaOH (24 h) [149]	20	55.6	27.0	35.0	51.43	37.05
IV	Water soaking (24 h) [116]	20	55.6	27.0	34.9	51.43	37.23
IV	NaOH (30 min) [148]	20	53.5	41.6	48.1	22.24	10.09
IV	NaOH (2 h) [98]	20	53.5	35.9	37.2	32.89	30.57

Dose range/ Group	Pre-treatment method	Rubber content (Volume of fine aggregate, %)	Compressive strength				
			S_C (MPa)	S_{UT} (MPa)	S_T (MPa)	S_{UT} Loss (%)	S_T Loss (%)
IV	NaOH (30 min) and 15 % SF [98]	20	53.5	35.9	36.8	32.89	31.21
IV	NaOH (1 h) [98]	20	53.5	35.9	38.6	32.89	27.85
IV	NaOH (30 min) [98]	20	53.5	35.9	42.1	32.64	21.01
IV	SCA and CSBR latex [109]	20	52.5	40.5	47.5	22.85	9.52
IV	Heating (1 h) [107]	20	50.9	30.5	42.8	40.01	15.91
IV	10 % $CaCl_2$ soaking (24 h) [119]	20	41.5	27.3	29.1	34.22	29.88
IV	10 % H_2O_2 (30 min) [119]	20	41.5	27.3	27.5	34.22	33.73
IV	5 % $KMnO_4$ (2 h) and 5 % $NaHSO_4$ (1 h) [119]	20	41.5	27.3	26.5	34.22	36.14
IV	Water soaking (24 h) [150]	20	35.4	21.5	24.6	39.26	30.51
IV	Gamma radiation (mesh #7) [125]	20	24.5	13.0	17.5	46.93	28.57
IV	Gamma radiation (mesh #20) [125]	20	24.5	12.5	14.0	48.98	42.85
IV	Gamma radiation (mesh #7) [106]	20	24.1	12.9	16.1	46.47	33.19
IV	Gamma radiation (mesh #20) [106]	20	24.1	16.1	15.9	33.20	34.02
V	NaOH (24 h) [149]	30	63.0	27.4	31.4	56.51	50.16
V	Water soaking (24 h) [116]	30	63.0	27.4	30.9	56.51	50.95
V	Mortar pre-coating [104]	12.8*	54.0	32.0	45.0	40.74	16.66
V	NaOH (20 min) [104]	12.8*	54.0	32.0	33.0	40.74	38.89
V	NaOH (40 min) [104]	12.8*	54.0	32.0	32.0	40.74	40.74
V	NaOH (60 min) [104]	12.8*	54.0	32.0	30.5	40.74	43.51
V	Cement paste pre-coating [104]	12.8*	54.0	32.0	37.0	40.74	31.48
V	SCA and CSBR latex [109]	30	52.5	30.5	38.0	41.9	27.62
V	Saturated NaOH (20 min) [72]	10*	43.1	29.4	28.1	31.78	34.8
V	Saturated NaOH (30 min) [42]	10*	39.08	22.33	23.23	42.86	40.3
V	Cement and silane pre-coating [108]	30	37.0	22.5	28.9	39.19	21.89
V	35% H_2SO_4 (24 h) [111]	30	36.5	16.0	26.7	56.16	26.84
V	5 % CH_3COOH (24 h) [111]	30	36.5	16.0	24.3	56.16	33.42

Dose range/ Group	Pre-treatment method	Rubber content (Volume of fine aggregate, %)	Compressive strength				
			S_C (MPa)	S_{UT} (MPa)	S_T (MPa)	S_{UT} Loss (%)	S_T Loss (%)
V	Gamma radiation (mesh #7) [125]	30	24.5	13.0	15.5	46.94	36.73
V	Gamma radiation (mesh #20) [125]	30	24.5	5.5	12.5	77.55	48.98
V	Gamma radiation [106]	30	24.1	11.3	14.8	53.11	38.59
V	Gamma radiation (mesh #7) [106]	30	24.1	11.5	14.8	52.28	38.59
V	Gamma radiation (mesh #20) [106]	30	24.1	5.0	7.0	79.25	70.95
V	SF pre-treating (1 min) [47]	30	4.7	1.7	1.9	63.83	59.57
VI	Heating (1 h) [107]	40	50.9	13.7	31.3	73.08	38.51
VI	5 % NaOH (24 h) and $KMnO_4$ (2 h) and saturated $NaHSO_3$ (1 h) [117]	4*	49.2	23.6	35.1	52.03	28.65
VI	Water washing [118]	40	46.8	22.4	26.2	52.13	44.02

Note: Number with "*" is rubber content in mass unit.

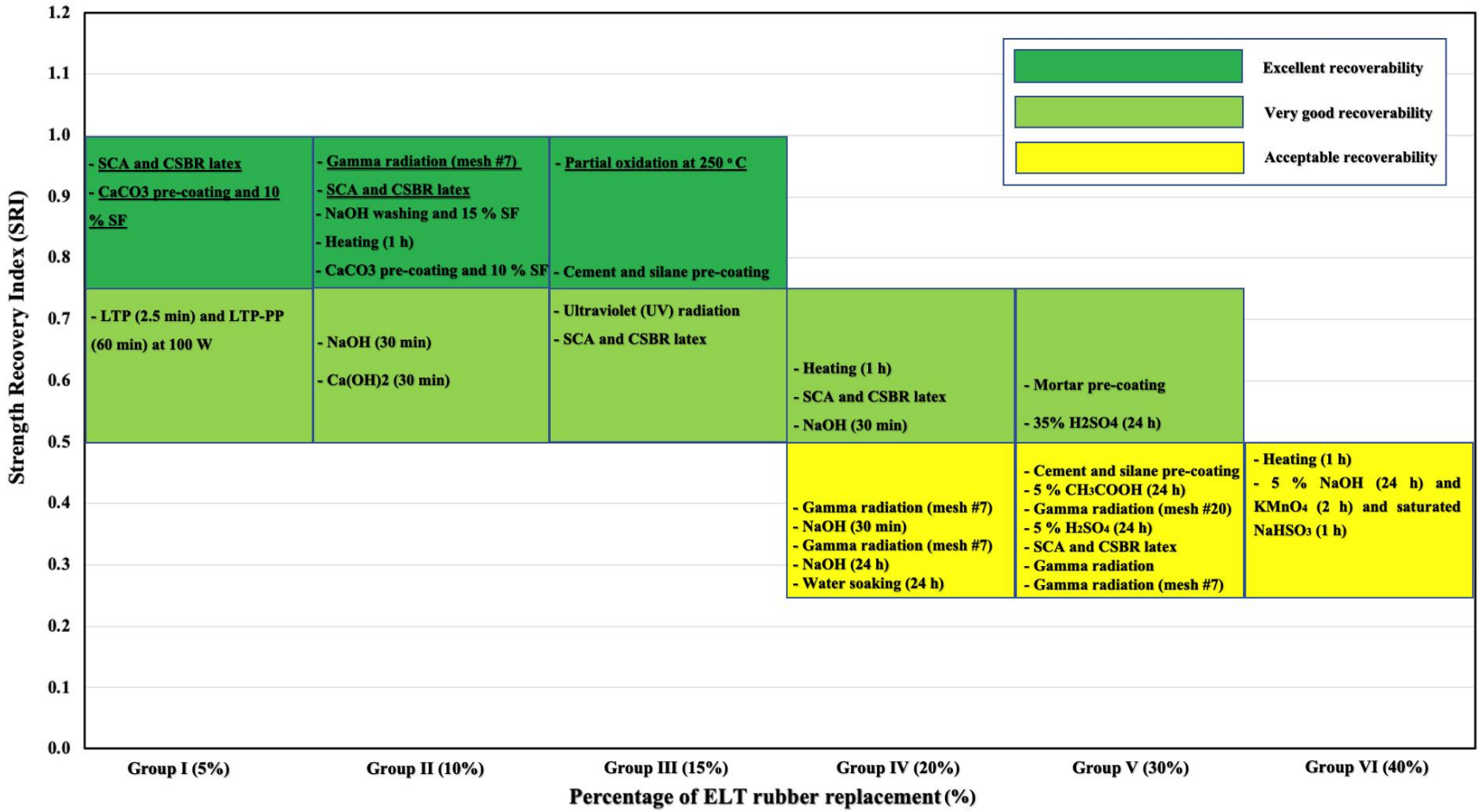

Figure 2- 8. Effectiveness of various ELT rubber pre-treatment methods.The underlined methods are the ones which have SRI > 1 and SG > 0.

2.4 Conclusions

This study summarizes the various treatment methods for end-of-life tire (ELT) rubber in order to recover the reduced strength and also to improve the strength of rubberized cementitious materials (RCM). A comparison of various pretreatment methods for ELT rubber was summarized based on the calculation of a strength recovery index. The main findings of this study are:

1. The strength of RCM tends to decrease with an increase in the ELT rubber content. Some of the treatment methods for ELT rubber can result in a full recovery of strength. The treatment methods such as NaOH and gamma radiation, appear to have conflicting results in the literature. In general, chemical treatments appear to have a greater benefit than physical treatments.
2. The strength recovery index (SRI) and strength gain (SG) can be used as effective metrics to evaluate the efficiency of a treatment method for ELT rubber used in RCM. Based on the calculated SRI, the most effective treatment methods include "SCA and CSBR latex", "$CaCO_3$ pre-coating and 10 % SF", "NaOH washing and 15 % SF", "Heating (1 h)", and "Partial oxidation at 250 ℃ (1 hour)".
3. The significance of strength loss (SL) generally seems to depend on the original material's strength. For high strength cementitious materials, SL is usually smaller than that of normal strength cementitious materials when adding the same amount of ELT rubber when the ELT rubber content no more than 15 %. When the ELT rubber content is ≥20 %, the SL becomes similar regardless of the original strength of cementitious material or type of "mother concrete". More interestingly, when the treatment methods are introduced for ELT rubber, the SL of RCM is significantly affected by the type of treatment methods instead of the original strength.
4. Among the multiple treatment methods, only a few appear to work effectively with proven results. Further studies should focus on these treatments, considering the basic properties of the ELT rubber such as particle size, density, chemical composition, and material sources.

Acknowledgement

This study is the work of research project SUST-2021-D14-4, which was supported by the Center for Tire Research (CenTiRe).

References

[1] X. Bai, T. McPhearson, H. Cleugh, H. Nagendra, X. Tong, T. Zhu, Y.-G. Zhu, Linking urbanization and the environment: Conceptual and empirical advances, Annu. Rev. Environ. Resour. 42 (2017) 215–240. doi:10.1146/annurev-environ-102016-061128.

[2] S.H.A. Koop, C.J. van Leeuwen, The challenges of water, waste and climate change in cities, Environ. Dev. Sustain. 19 (2017) 385–418. doi:10.1007/s10668-016-9760-4.

[3] S. Lehmann, Optimizing urban material flows and waste streams in urban development through principles of zero waste and sustainable consumption, Sustainability. 3 (2011) 155–183. doi:10.3390/su3010155.

[4] F. Grosse, Is recycling "part of the solution"? The role of recycling in an expanding society and a world of finite resources, Sapiens. 3 (2010).

[5] F. Di Maio, P.C. Rem, A robust indicator for promoting circular economy through recycling, J. Environ. Prot. (Irvine,. Calif). 6 (2015). doi:10.4236/jep.2015.610096.

[6] B. Rodgers, Tire Engineering, CRC Press, Boca Raton, 2021. doi:10.1201/9781003022961.

[7] U.S. Tire Manufacturers Association, 2019 U.S. Scrap Tire Management Summary, Washington D.C., 2020.

[8] B. Chen, D. Zheng, R. Xu, S. Leng, L. Han, Q. Zhang, N. Liu, C. Dai, B. Wu, G. Yu, J. Cheng, Disposal methods for used passenger car tires: One of the fastest growing solid wastes in China, Green Energy Environ. (2021). doi:10.1016/j.gee.2021.02.003.

[9] E. Scott, China moves on waste tyres, Tyre Rubber Recycl. (2019). https://www.tyreandrubberrecycling.com/china-moves-on-waste-tyres/.

[10] S.L. Poole Jr., Scrap and Shredded Tire Fires, Report USFA-TR-093, FEMA, Washington D.C., 1998.

[11] M. Gualtieri, M. Andrioletti, C. Vismara, M. Milani, M. Camantini, Toxicity of tire debris leachates, Environ. Int. 31 (2005) 723–730. doi:10.1016/j.envint.2005.02.001.

[12] C. Halsband, L. Sørensen, A.M. Booth, D. Herzke, Car tire crumb rubber: Does leaching produce a toxic chemical cocktail in coastal marine systems?, Front. Environ. Sci. 8 (2020) 125. doi:10.3389/fenvs.2020.00125.

[13] J. Downard, A. Singh, R. Bullard, T. Jayarathne, C.M. Rathnayake, D.L. Simmons, B.R. Wels, S.N. Spak, T. Peters, D. Beardsley, C.O. Stanier, E.A. Stone, Uncontrolled combustion of shredded tires in a landfill – Part 1: Characterization of gaseous and particulate emissions, Atmos. Environ. 104 (2015) 195–204. doi:10.1016/j.atmosenv.2014.12.059.

[14] I. Glushankova, A. Ketov, M. Krasnovskikh, L. Rudakova, I. Vaisman, End of life tires as a possible source of toxic substances emission in the process of combustion, Resources. 8 (2019) 119. doi:10.3390/resources8020113.

[15] X. Shu, B. Huang, Recycling of waste tire rubber in asphalt and portland cement concrete: An overview, Constr. Build. Mater. 67 (2014) 217–224. doi:10.1016/j.conbuildmat.2013.11.027.
[16] B.S. Thomas, R.C. Gupta, A comprehensive review on the applications of waste tire rubber in cement concrete, Renew. Sustain. Energy Rev. 54 (2016) 1323–1333. doi:10.1016/j.rser.2015.10.092.
[17] R. Roychand, R.J. Gravina, Y. Zhuge, X. Ma, O. Youssf, J.E. Mills, A comprehensive review on the mechanical properties of waste tire rubber concrete, Constr. Build. Mater. 237 (2020) 117651. doi:10.1016/j.conbuildmat.2019.117651.
[18] P. Kara De Maeijer, B. Craeye, J. Blom, L. Bervoets, Crumb rubber in concrete—The barriers for application in the construction industry, Infrastructures. 6 (2021) 1–20. doi:10.3390/infrastructures6080116.
[19] L.G. Picado-Santos, S.D. Capitão, J.M.C. Neves, Crumb rubber asphalt mixtures: A literature review, Constr. Build. Mater. 247 (2020) 118577. doi:10.1016/j.conbuildmat.2020.118577.
[20] R. Gonçalves dos Santos, C. Lucas Rocha, F. Lopes Souza Felipe, F. Tonon Cezario, P.J. Correia, S. Rezaei-Gomari, Tire waste management: An overview from chemical compounding to the pyrolysis-derived fuels, J. Mater. Cycles Waste Manag. 22 (2020) 628–241. doi:10.1007/s10163-020-00986-8.
[21] B.R. Madhusudhan, A. Boominathan, S. Banerjee, Factors affecting strength and stiffness of dry sand-rubber tire shred mixtures, Geotech. Geol. Eng. 37 (2019) 2763–2780. doi:10.1007/s10706-018-00792-y.
[22] J.S. Yadav, S.K. Tiwari, The impact of end-of-life tires on the mechanical properties of fine-grained soil: A Review, Environ. Dev. Sustain. 21 (2019) 485–568. doi:10.1007/s10668-017-0054-2.
[23] S.M.R. Costa, D. Fowler, G.A. Carreira, I. Portugal, C.M. Silva, Production and upgrading of recovered carbon black from the pyrolysis of end-of-life tires, Materials. 15 (2022) 2030. doi:10.3390/ma15062030.
[24] A.D. La Rosa, E. Pergolizzi, D. Maragna, G. Recca, G. Cicala, Reuse of carbon black from end-of-life tires in new pneumatic formulations and life-cycle assessment of the thermolysis process, J. Elastomers Plast. 51 (2019) 740–754. doi:10.1177/0095244318819242.
[25] K. Panploo, B. Chalermsinsuwan, S. Poompradub, Natural rubber latex foam with particulate fillers for carbon dioxide adsorption and regeneration, RSC Adv. 9 (2019) 28916–28923. doi:10.1039/c9ra06000f.
[26] D 6270 – 98 (Reapproved 2004), Standard Practice for Use of Scrap Tires in Civil Engineering Applications, Annu. B. ASTM Stand. (2004).
[27] C.D. Conditions, O. Matter, O.O. Soils, S. Soils, ASTM D6270 − 20: Standard Practice for Use of Scrap Tires in Civil Engineering Applications, (2011) 1–22. doi:10.1520/D6270-20.2.

[28] A.J. Kardos, S.A. Durham, Strength, durability, and environmental properties of concrete utilizing recycled tire particles for pavement applications, Constr. Build. Mater. 98 (2015) 832–845. doi:10.1016/j.conbuildmat.2015.08.065.
[29] T.Q. Tran, Y. Kim, G. Kang, B.H. Dinh, T.M. Do, Feasibility of reusing marine dredged clay stabilized by a combination of by-products in coastal road construction, Transp. Res. Rec. (2019) 036119811986819. doi:10.1177/0361198119868196.
[30] G. Kang, Y. Kim, T.Q. Tran, N.A. Dan, Strength Monitoring of Dredged Marine Clay Stabilized with Basic Oxygen Furnace Steel Slag Using Non-Destructive Method, 29th Int. Ocean Polar Eng. Conf. (2019) ISOPE-I-19-476.
[31] T.M. Do, Y. Kim, T.Q. Tran, N. Vu, Effect of Lime on Engineering Properties of CLSM Made with Fly Ash-Red Mud-Lime-Gypsum Binder, in: Korean Society of Civil Engineers Conferences, Busan, 2017: pp. 31–32.
[32] T.M. Do, Y.-S. Kim, G.-O. Kang, M.Q. Dang, T.Q. Tran, Thermal conductivity of controlled low strength material (CLSM) made entirely from by-products, 2018. doi:10.4028/www.scientific.net/KEM.773.244.
[33] Y. Kim, T.Q. Tran, G. Kang, T.M. Do, Stabilization of a residual granitic soil using various new green binders, Constr. Build. Mater. 223 (2019) 724–735. doi:10.1016/j.conbuildmat.2019.07.019.
[34] T.T. Le, S.S. Park, J.C. Lee, D.E. Lee, Strength characteristics of spent coffee grounds and oyster shells cemented with GGBS-based alkaline-activated materials, Constr. Build. Mater. 267 (2021) 120986. doi:10.1016/j.conbuildmat.2020.120986.
[35] A.S. Brand, P. Singhvi, E.O. Fanijo, E. Tutumluer, Stabilization of a clayey soil with ladle metallurgy furnace slag fines, Materials. 13 (2020) 1–19. doi:10.3390/MA13194251.
[36] T.Q. Tran, A. Behravan, A.S. Brand, Heat of hydration in clays stabilized by a high-alumina steel furnace slag, Clean. Mater. 5 (2022) 100105. doi:10.1016/j.clema.2022.100105.
[37] Saloni, Parveen, T.M. Pham, Y.Y. Lim, S.S. Pradhan, Jatin, J. Kumar, Performance of rice husk Ash-Based sustainable geopolymer concrete with Ultra-Fine slag and Corn cob ash, Constr. Build. Mater. 279 (2021) 122526. doi:10.1016/j.conbuildmat.2021.122526.
[38] Saloni, Parveen, T.M. Pham, Enhanced properties of high-silica rice husk ash-based geopolymer paste by incorporating basalt fibers, Constr. Build. Mater. 245 (2020) 118422. doi:10.1016/j.conbuildmat.2020.118422.
[39] U.S. Tire Manufacturers Association, 2019 U.S. Scrap Tire Market Summary, Washington D.C., 2020.
[40] A. Alsaif, S.A. Bernal, M. Guadagnini, K. Pilakoutas, Freeze-thaw resistance of steel fibre reinforced rubberised concrete, Constr. Build. Mater. 195 (2019) 450–458. doi:10.1016/j.conbuildmat.2018.11.103.
[41] L. Lavagna, R. Nisticò, M. Sarasso, M. Pavese, An analytical mini-review on the compression strength of rubberized concrete as a function of the amount of recycled tires crumb rubber, Materials. 13 (2020) 1234. doi:10.3390/ma13051234.

[42] G. Li, M.A. Stubblefield, G. Garrick, J. Eggers, C. Abadie, B. Huang, Development of waste tire modified concrete, Cem. Concr. Res. 34 (2004) 2283–2289. doi:10.1016/j.cemconres.2004.04.013.
[43] C.K. Leung, Z.C. Grasley, Effect of micrometric and nanometric viscoelastic inclusions on mechanical damping behavior of cementitious composites, Constr. Build. Mater. 35 (2012) 444–451. doi:10.1016/j.conbuildmat.2012.04.021.
[44] C.K. Lu, C.H. Lee, I.F. Wang, Improving properties of rubberized mortar with polyacrylamide, Appl. Mech. Mater. 528 (2014) 77–82. doi:10.4028/www.scientific.net/AMM.528.77.
[45] N. Segre, P.J.M. Monteiro, G. Sposito, Surface characterization of recycled tire rubber to be used in cement paste matrix, J. Colloid Interface Sci. 248 (2002) 521–523. doi:10.1006/jcis.2002.8217.
[46] Z. Chen, L. Li, Z. Xiong, Investigation on the interfacial behaviour between the rubber-cement matrix of the rubberized concrete, J. Clean. Prod. 209 (2019) 1354–1364. doi:10.1016/j.jclepro.2018.10.305.
[47] Y. Xi, Y. Li, High Toughness Rubber-Modified Concrete (RMC), 2003.
[48] R. Roychand, R.J. Gravina, Y. Zhuge, X. Ma, J.E. Mills, O. Youssf, Practical rubber pre-treatment approch for concrete use—an experimental study, J. Compos. Sci. 5 (2021) 1–17. doi:10.3390/jcs5060143.
[49] B.S. Thomas, R.C. Gupta, V. John Panicker, Experimental and modelling studies on high strength concrete containing waste tire rubber, Sustain. Cities Soc. 19 (2015) 68–73. doi:10.1016/j.scs.2015.07.013.
[50] B.S. Thomas, S. Kumar, P. Mehra, R.C. Gupta, M. Joseph, L.J. Csetenyi, Abrasion resistance of sustainable green concrete containing waste tire rubber particles, Constr. Build. Mater. 124 (2016) 906–909. doi:10.1016/j.conbuildmat.2016.07.110.
[51] B.S. Thomas, R.C. Gupta, Long term behaviour of cement concrete containing discarded tire rubber, J. Clean. Prod. 102 (2015) 78–87. doi:10.1016/j.jclepro.2015.04.072.
[52] B.S. Thomas, R.C. Gupta, P. Mehra, S. Kumar, Performance of high strength rubberized concrete in aggressive environment, Constr. Build. Mater. 83 (2015) 320–326. doi:10.1016/j.conbuildmat.2015.03.012.
[53] B.S. Thomas, R. Chandra Gupta, Properties of high strength concrete containing scrap tire rubber, J. Clean. Prod. 113 (2016) 86–92. doi:10.1016/j.jclepro.2015.11.019.
[54] B.S. Thomas, R.C. Gupta, V.J. Panicker, Recycling of waste tire rubber as aggregate in concrete: Durability-related performance, J. Clean. Prod. 112 (2016) 504–513. doi:10.1016/j.jclepro.2015.08.046.
[55] B.S. Thomas, R.C. Gupta, P. Kalla, L. Cseteneyi, Strength, abrasion and permeation characteristics of cement concrete containing discarded rubber fine aggregates, Constr. Build. Mater. 59 (2014) 204–212. doi:10.1016/j.conbuildmat.2014.01.074.

[56] N.P. Pham, A. Toumi, A. Turatsinze, Evaluating damage of rubberized cement-based composites under aggressive environments, Constr. Build. Mater. 217 (2019) 234–241. doi:10.1016/j.conbuildmat.2019.05.066.

[57] N.P. Pham, A. Toumi, A. Turatsinze, Effect of an enhanced rubber-cement matrix interface on freeze-thaw resistance of the cement-based composite, Constr. Build. Mater. 207 (2019) 528–534. doi:10.1016/j.conbuildmat.2019.02.147.

[58] N.P. Pham, A. Toumi, A. Turatsinze, Rubber aggregate-cement matrix bond enhancement: Microstructural analysis, effect on transfer properties and on mechanical behaviours of the composite, Cem. Concr. Compos. 94 (2018) 1–12. doi:10.1016/j.cemconcomp.2018.08.005.

[59] T.M. Pham, J. Liu, P. Tran, V.L. Pang, F. Shi, W. Chen, H. Hao, T.M. Tran, Dynamic compressive properties of lightweight rubberized geopolymer concrete, Constr. Build. Mater. 265 (2020) 120753. doi:10.1016/j.conbuildmat.2020.120753.

[60] T.M. Pham, N. Renaud, V.L. Pang, F. Shi, H. Hao, W. Chen, Effect of rubber aggregate size on static and dynamic compressive properties of rubberized concrete, Struct. Concr. 23 (2022) 2510–2522. doi:10.1002/suco.202100281.

[61] T.M. Pham, W. Chen, A.M. Khan, H. Hao, M. Elchalakani, T.M. Tran, Dynamic compressive properties of lightweight rubberized concrete, Constr. Build. Mater. 238 (2020) 117705. doi:10.1016/j.conbuildmat.2019.117705.

[62] M.C. Bignozzi, F. Sandrolini, Tyre rubber waste recycling in self-compacting concrete, Cem. Concr. Res. 36 (2006) 735–739. doi:10.1016/j.cemconres.2005.12.011.

[63] T.M. Pham, W. Chen, M. Elchalakani, A. Karrech, H. Hao, Experimental investigation on lightweight rubberized concrete beams strengthened with BFRP sheets subjected to impact loads, Eng. Struct. 205 (2020) 110095. doi:10.1016/j.engstruct.2019.110095.

[64] T.M. Pham, M. Elchalakani, H. Hao, J. Lai, S. Ameduri, T.M. Tran, Durability characteristics of lightweight rubberized concrete, Constr. Build. Mater. 224 (2019) 584–599. doi:10.1016/j.conbuildmat.2019.07.048.

[65] T.M. Pham, X. Zhang, M. Elchalakani, A. Karrech, H. Hao, A. Ryan, Dynamic response of rubberized concrete columns with and without FRP confinement subjected to lateral impact, Constr. Build. Mater. 186 (2018) 207–218. doi:10.1016/j.conbuildmat.2018.07.146.

[66] T.M. Pham, J. Kingston, G. Strickland, W. Chen, H. Hao, Effect of crumb rubber on mechanical properties of multi-phase syntactic foams, Polym. Test. 66 (2018) 1–12. doi:10.1016/j.polymertesting.2017.12.033.

[67] E. Ganjian, M. Khorami, A.A. Maghsoudi, Scrap-tyre-rubber replacement for aggregate and filler in concrete, Constr. Build. Mater. 23 (2009) 1828–1836. doi:10.1016/j.conbuildmat.2008.09.020.

[68] M. Fakhri, F. Saberik, The effect of waste rubber particles and silica fume on the mechanical properties of Roller Compacted Concrete Pavement, J. Clean. Prod. 129 (2016) 521–530. doi:10.1016/j.jclepro.2016.04.017.

[69] J. Xue, M. Shinozuka, Rubberized concrete: A green structural material with enhanced energy-dissipation capability, Constr. Build. Mater. 42 (2013) 196–204. doi:10.1016/j.conbuildmat.2013.01.005.
[70] M. Valente, A. Sibai, Rubber/crete: Mechanical properties of scrap to reuse tire-derived rubber in concrete; A review, J. Appl. Biomater. Funct. Mater. 17 (2019) 228080001983548. doi:10.1177/2280800019835486.
[71] J. Xu, Z. Yao, G. Yang, Q. Han, Research on crumb rubber concrete: From a multi-scale review, Constr. Build. Mater. 232 (2020) 117282. doi:10.1016/j.conbuildmat.2019.117282.
[72] N. Segre, I. Joekes, Use of tire rubber particles as addition to cement paste, Cem. Concr. Res. 30 (2000) 1421–1425. doi:10.1016/S0008-8846(00)00373-2.
[73] P. Pongsopha, P. Sukontasukkul, H. Zhang, S. Limkatanyu, Thermal and acoustic properties of sustainable structural lightweight aggregate rubberized concrete, Results Eng. 13 (2022) 100333. doi:10.1016/j.rineng.2022.100333.
[74] J.O. Akinyele, R.W. Salim, W.K. Kupolati, Production of lightweight concrete from waste tire rubber crumb, Eng. Struct. Technol. 8 (2016) 108–116. doi:10.3846/2029882X.2016.1209727.
[75] K.L. Scrivener, A.K. Crumbie, P. Laugesen, The interfacial transition zone (ITZ) between cement paste and aggregate in concrete, Interface Sci. 12 (2004) 411–421. doi:10.1023/B:INTS.0000042339.92990.4c.
[76] J. Wang, Z. Guo, Q. Yuan, P. Zhang, H. Fang, Effects of ages on the ITZ microstructure of crumb rubber concrete, Constr. Build. Mater. 254 (2020) 119329. doi:10.1016/j.conbuildmat.2020.119329.
[77] A.-T. Akono, J. Chen, S. Kaewunruen, Friction and fracture characteristics of engineered crumb-rubber concrete at microscopic lengthscale, Constr. Build. Mater. 175 (2018) 735–745. doi:10.1016/j.conbuildmat.2018.04.141.
[78] S. Guo, Q. Dai, R. Si, X. Sun, C. Lu, Evaluation of properties and performance of rubber-modified concrete for recycling of waste scrap tire, J. Clean. Prod. 148 (2017) 681–689. doi:10.1016/j.jclepro.2017.02.046.
[79] F. Liu, L.Y. Meng, G.F. Ning, L.J. Li, Fatigue performance of rubber-modified recycled aggregate concrete (RRAC) for pavement, Constr. Build. Mater. 95 (2015) 207–217. doi:10.1016/j.conbuildmat.2015.07.042.
[80] C.A. Issa, G. Salem, Utilization of recycled crumb rubber as fine aggregates in concrete mix design, Constr. Build. Mater. 42 (2013) 48–52. doi:10.1016/j.conbuildmat.2012.12.054.
[81] R.A. Assaggaf, M.R. Ali, S.U. Al-Dulaijan, M. Maslehuddin, Properties of concrete with untreated and treated crumb rubber – A review, J. Mater. Res. Technol. 11 (2021) 1753–1798. doi:10.1016/j.jmrt.2021.02.019.
[82] M. Valente, A. Sibai, Rubber/crete: Mechanical properties of scrap to reuse tire-derived rubber in concrete; A review, J. Appl. Biomater. Funct. Mater. 17 (2019). doi:10.1177/2280800019835486.

[83] A. Adesina, O.D. Atoyebi, Effect of crumb rubber aggregate on the performance of cementitious composites: A review, IOP Conf. Ser. Earth Environ. Sci. 445 (2020) 012032. doi:10.1088/1755-1315/445/1/012032.
[84] M.A. Musarat, W.S. Alaloul, S. Ayub, M.B.A. Rabbani, W. Farooq, M. Altaf, Chemical and physical behavior of rubberized concrete: A review, in: 2021 Int. Conf. Decis. Aid Sci. Appl., IEEE, 2021: pp. 441–445. doi:10.1109/DASA53625.2021.9682385.
[85] C. Albano, N. Camacho, J. Reyes, J.L. Feliu, M. Hernández, Influence of scrap rubber addition to Portland I concrete composites: Destructive and non-destructive testing, Compos. Struct. 71 (2005) 439–446. doi:10.1016/j.compstruct.2005.09.037.
[86] A.C. Ho, A. Turatsinze, R. Hameed, D.C. Vu, Effects of rubber aggregates from grinded used tyres on the concrete resistance to cracking, J. Clean. Prod. 23 (2012) 209–215. doi:10.1016/j.jclepro.2011.09.016.
[87] K.B. Najim, M.R. Hall, Mechanical and dynamic properties of self-compacting crumb rubber modified concrete, Constr. Build. Mater. 27 (2012) 521–530. doi:10.1016/j.conbuildmat.2011.07.013.
[88] A. Gholampour, T. Ozbakkaloglu, R. Hassanli, Behavior of rubberized concrete under active confinement, Constr. Build. Mater. 138 (2017) 372–382. doi:10.1016/j.conbuildmat.2017.01.105.
[89] G. Girskas, D. Nagrockienė, Crushed rubber waste impact of concrete basic properties, Constr. Build. Mater. 140 (2017) 36–42. doi:10.1016/j.conbuildmat.2017.02.107.
[90] K. Bisht, P. V. Ramana, Evaluation of mechanical and durability properties of crumb rubber concrete, Constr. Build. Mater. 155 (2017) 811–817. doi:10.1016/j.conbuildmat.2017.08.131.
[91] A. Turatsinze, M. Garros, On the modulus of elasticity and strain capacity of Self-Compacting Concrete incorporating rubber aggregates, Resour. Conserv. Recycl. 52 (2008) 1209–1215. doi:10.1016/j.resconrec.2008.06.012.
[92] C. Bing, L. Ning, Experimental Research on Properties of Fresh and Hardened Rubberized Concrete, J. Mater. Civ. Eng. 26 (2014) 04014040. doi:10.1061/(asce)mt.1943-5533.0000923.
[93] H. Liu, X. Wang, Y. Jiao, T. Sha, Experimental investigation of the mechanical and durability properties of crumb rubber concrete, Materials. 9 (2016) 1–12. doi:10.3390/ma9030172.
[94] E. Ozbay, M. Lachemi, U.K. Sevim, Compressive strength, abrasion resistance and energy absorption capacity of rubberized concretes with and without slag, Mater. Struct. Constr. 44 (2011) 1297–1307. doi:10.1617/s11527-010-9701-x.
[95] L. Zheng, X.S. Huo, Y. Yuan, Strength, Modulus of Elasticity, and Brittleness Index of Rubberized Concrete, J. Mater. Civ. Eng. 20 (2008) 692–699. doi:10.1061/(asce)0899-1561(2008)20:11(692).

[96] Z. Boudaoud, M. Beddar, Effects of Recycled Tires Rubber Aggregates on the Characteristics of Cement Concrete, Open J. Civ. Eng. 02 (2012) 193–197. doi:10.4236/ojce.2012.24025.
[97] G.N. Kumar, V. Sandeep, Ch. Sudharani, Using Tyres Wastes As Aggregates in Concrete To Form Rubcrete – Mix for Engineering Applications, Int. J. Res. Eng. Technol. 03 (2014) 500–509. doi:10.15623/ijret.2014.0311086.
[98] O. Youssf, J.E. Mills, R. Hassanli, Assessment of the mechanical performance of crumb rubber concrete, Constr. Build. Mater. 125 (2016) 175–183. doi:10.1016/j.conbuildmat.2016.08.040.
[99] M. Gesoğlu, E. Güneyisi, G. Khoshnaw, S. Ipek, Investigating properties of pervious concretes containing waste tire rubbers, Constr. Build. Mater. 63 (2014) 206–213. doi:10.1016/j.conbuildmat.2014.04.046.
[100] B.S. Mohammed, N.J. Azmi, Strength reduction factors for structural rubbercrete, Front. Struct. Civ. Eng. 8 (2014) 270–281. doi:10.1007/s11709-014-0265-7.
[101] W. Feng, F. Liu, F. Yang, L. Li, L. Jing, Experimental study on dynamic split tensile properties of rubber concrete, Constr. Build. Mater. 165 (2018) 675–687. doi:10.1016/j.conbuildmat.2018.01.073.
[102] N.N. Gerges, C.A. Issa, S.A. Fawaz, Rubber concrete: Mechanical and dynamical properties, Case Stud. Constr. Mater. 9 (2018). doi:10.1016/j.cscm.2018.e00184.
[103] E. Khalil, M. Abd-Elmohsen, A.M. Anwar, Impact Resistance of Rubberized Self-Compacting Concrete, Water Sci. 29 (2015) 45–53. doi:10.1016/j.wsj.2014.12.002.
[104] K.B. Najim, M.R. Hall, Crumb rubber aggregate coatings/pre-treatments and their effects on interfacial bonding, air entrapment and fracture toughness in self-compacting rubberised concrete (SCRC), Mater. Struct. Constr. 46 (2013) 2029–2043. doi:10.1617/s11527-013-0034-4.
[105] G. Ossola, A. Wojcik, UV modification of tire rubber for use in cementitious composites, Cem. Concr. Compos. 52 (2014) 34–41. doi:10.1016/j.cemconcomp.2014.04.004.
[106] E.S. Herrera-Sosa, G. Martínez-Barrera, C. Barrera-Díaz, E. Cruz-Zaragoza, Waste tire particles and gamma radiation as modifiers of the mechanical properties of concrete, Adv. Mater. Sci. Eng. 2014 (2014). doi:10.1155/2014/327856.
[107] E.S. Abd-Elaal, S. Araby, J.E. Mills, O. Youssf, R. Roychand, X. Ma, Y. Zhuge, R.J. Gravina, Novel approach to improve crumb rubber concrete strength using thermal treatment, Constr. Build. Mater. 229 (2019) 116901. doi:10.1016/j.conbuildmat.2019.116901.
[108] Q. Dong, B. Huang, X. Shu, Rubber modified concrete improved by chemically active coating and silane coupling agent, Constr. Build. Mater. 48 (2013) 116–123. doi:10.1016/j.conbuildmat.2013.06.072.
[109] G. Li, Z. Wang, C.K.Y. Leung, S. Tang, J. Pan, W. Huang, E. Chen, Properties of rubberized concrete modified by using silane coupling agent and carboxylated SBR, J. Clean. Prod. 112 (2016) 797–807. doi:10.1016/j.jclepro.2015.06.099.

[110] B. Muñoz-Sánchez, M.J. Arévalo-Caballero, M.C. Pacheco-Menor, Influence of acetic acid and calcium hydroxide treatments of rubber waste on the properties of rubberized mortars, Mater. Struct. Constr. 50 (2017). doi:10.1617/s11527-016-0912-7.
[111] A.I. Abdulla, S.H. Ahmed, Effect of rubber treated by acidic solution on some mechanical properties of rubberize cement mortar, Eng. Technol. J. 29 (2011) 2793–2806.
[112] L.H. Chou, C.K. Yang, M.T. Lee, C.C. Shu, Effects of partial oxidation of crumb rubber on properties of rubberized mortar, Compos. Part B Eng. 41 (2010) 613–616. doi:10.1016/j.compositesb.2010.09.009.
[113] L.H. Chou, C.N. Lin, C.K. Lu, C.H. Lee, M.T. Lee, Improving rubber concrete by waste organic sulfur compounds, Waste Manag. Res. 28 (2010) 29–35. doi:10.1177/0734242X09103843.
[114] S. Tian, T. Zhang, Y. Li, Research on modifier and modified process for rubber-particle used in rubberized concrete for road, Adv. Mater. Res. 243–249 (2011) 4125–4130. doi:10.4028/www.scientific.net/AMR.243-249.4125.
[115] O. Onuaguluchi, Effects of surface pre-coating and silica fume on crumb rubber-cement matrix interface and cement mortar properties, J. Clean. Prod. 104 (2015) 339–345. doi:10.1016/j.jclepro.2015.04.116.
[116] I. Mohammadi, H. Khabbaz, K. Vessalas, In-depth assessment of Crumb Rubber Concrete (CRC) prepared by water-soaking treatment method for rigid pavements, Constr. Build. Mater. 71 (2014) 456–471. doi:10.1016/j.conbuildmat.2014.08.085.
[117] L. He, Y. Ma, Q. Liu, Y. Mu, Surface modification of crumb rubber and its influence on the mechanical properties of rubber-cement concrete, Constr. Build. Mater. 120 (2016) 403–407. doi:10.1016/j.conbuildmat.2016.05.025.
[118] S. Raffoul, R. Garcia, K. Pilakoutas, M. Guadagnini, N.F. Medina, Optimisation of rubberised concrete with high rubber content: An experimental investigation, Constr. Build. Mater. 124 (2016) 391–404. doi:10.1016/j.conbuildmat.2016.07.054.
[119] O. Youssf, R. Hassanli, J.E. Mills, W. Skinner, X. Ma, Y. Zhuge, R. Roychand, R. Gravina, Influence of mixing procedures, rubber treatment, and fibre additives on rubcrete performance, J. Compos. Sci. 3 (2019). doi:10.3390/jcs3020041.
[120] J.F. Rabek, Photodegradation of Polymers: Physical Characteristics and Applications, Springer, Berlin, 1996. doi:10.1007/978-3-642-80090-0.
[121] M.G. Aboelkheir, J.G. Lima Junior, R.D. Toledo Filho, F.G. Souza Junior, C.Y. dos Santos Siqueira, Thermo-oxidative degradation of vulcanized SBR: A comparison between ultraviolet (UV) and microwave as recovery techniques, J. Polym. Res. 28 (2021) 141. doi:10.1007/s10965-021-02497-y.
[122] R. Celestino, M.G. Aboelkheir, Recovery of tire rubber waste after UV treatment as a recycled aggregate in cementitious composites, Mater. Today Proc. (2022). doi:https://doi.org/10.1016/j.matpr.2022.02.552.

[123] S.R. Scagliusi, E.L.C. Cardoso, A.B. Lugao, Effect of gamma radiation on chlorobutyl rubber vulcanized by three different crosslinking systems, Radiat. Phys. Chem. 81 (2012) 1370–1373. doi:10.1016/j.radphyschem.2012.01.037.

[124] M.M. Phiri, M.J. Phiri, K. Formela, S.P. Hlangothi, Chemical surface etching methods for ground tire rubber as sustainable approach for environmentally-friendly composites development– a review, Compos. Part B Eng. 204 (2021) 108429. doi:10.1016/j.compositesb.2020.108429.

[125] E.S. Herrera-Sosa, G. Martínez-Barrera, C. Barrera-Díaz, E. Cruz-Zaragoza, F. Ureña-Núñez, Recovery and Modification of Waste Tire Particles and Their Use as Reinforcements of Concrete, Int. J. Polym. Sci. 2015 (2015). doi:10.1155/2015/234690.

[126] E.M. Liston, Plasma treatment for improved bonding: A review, J. Adhes. 30 (1989) 199–218. doi:10.1080/00218468908048206.

[127] D. Hegemann, H. Brunner, C. Oehr, Plasma treatment of polymers for surface and adhesion improvement, Nucl. Instruments Methods Phys. Res. Sect. B Beam Interact. with Mater. Atoms. 208 (2003) 281–286. doi:10.1016/S0168-583X(03)00644-X.

[128] C. Xiaowei, H. Sheng, G. Xiaoyang, D. Wenhui, Crumb waste tire rubber surface modification by plasma polymerization of ethanol and its application on oil-well cement, Appl. Surf. Sci. 409 (2017) 325–342. doi:10.1016/j.apsusc.2017.03.072.

[129] X. Cheng, D. Long, S. Huang, Z. Li, X. Guo, Time effectiveness of the low-temperature plasma surface modification of ground tire rubber powder, J. Adhes. Sci. Technol. 29 (2015) 1330–1340. doi:10.1080/01694243.2015.1026958.

[130] X.G. Xiaowei Cheng, Haitao Chen, Sheng Huang, Zaoyan Li, Improvement of the Properties of Plasma-Modified Ground Tire Rubber-Filled Cement Paste Xiaowei, J. Appl. Polym. Sci. 116 (2010) 2658–2667. doi:10.1002/app.

[131] X. Colom, A. Faliq, K. Formela, J. Cañavate, FTIR spectroscopic and thermogravimetric characterization of ground tyre rubber devulcanized by microwave treatment, Polym. Test. 52 (2016) 200–208. doi:10.1016/j.polymertesting.2016.04.020.

[132] J. Yin, S. Wang, F. Lv, Improving the short-term aging resistance of asphalt by addition of crumb rubber radiated by microwave and impregnated in epoxidized soybean oil, Constr. Build. Mater. 49 (2013) 712–719. doi:10.1016/j.conbuildmat.2013.08.067.

[133] G.X. Yu, Z.M. Li, X.L. Zhou, C.L. Li, Crumb rubber-modified asphalt: Microwave treatment effects, Pet. Sci. Technol. 29 (2011) 411–417. doi:10.1080/10916460903394102.

[134] F.D.B. de Sousa, C.H. Scuracchio, G.H. Hu, S. Hoppe, Devulcanization of waste tire rubber by microwaves, Polym. Degrad. Stab. 138 (2017) 169–181. doi:10.1016/j.polymdegradstab.2017.03.008.

[135] O. Xu, L. Cong, F. Xiao, S.N. Amirkhanian, Rheology investigation of combined binders from various polymers with GTR under a short term aging process, Constr. Build. Mater. 93 (2015) 1012–1021. doi:10.1016/j.conbuildmat.2015.05.051.

[136] M. Liang, S. Ren, W. Fan, H. Wang, W. Cui, P. Zhao, Characterization of fume composition and rheological properties of asphalt with crumb rubber activated by microwave and TOR, Constr. Build. Mater. 154 (2017) 310–322. doi:10.1016/j.conbuildmat.2017.07.199.
[137] C. H. Scuracchio, D. A. Waki, M. L. C. P. da Silva, Thermal analysis of ground tire rubber devulcanized by microwaves, J. Therm. Anal. Calorim. 87 (2007) 893–897.
[138] X. Yang, A. Shen, B. Li, H. Wu, Z. Lyu, H. Wang, Z. Lyu, Effect of microwave-activated crumb rubber on reaction mechanism, rheological properties, thermal stability, and released volatiles of asphalt binder, J. Clean. Prod. 248 (2020). doi:10.1016/j.jclepro.2019.119230.
[139] M. Ateeq, A. Al-Shamma'a, Experimental study on the microwave processing of waste tyre rubber aggregates to enhance their surface properties for their use in rubberized bituminous mixtures, Microw. Opt. Technol. Lett. 59 (2017) 2951–2960. doi:10.1002/mop.30868.
[140] Z. Li, F. Li, J.S.L. Li, Properties of concrete incorporating rubber tyre particles, Mag. Concr. Res. 50 (1998) 297–304. doi:10.1680/macr.1998.50.4.297.
[141] B. Huang, X. Shu, J. Cao, A two-staged surface treatment to improve properties of rubber modified cement composites, Constr. Build. Mater. 40 (2013) 270–274. doi:10.1016/j.conbuildmat.2012.11.014.
[142] S. Ebnesajjad, Adhesion promoters, in: Surf. Treat. Mater. Adhes. Bond., 2nd ed., William Andrew, Oxford, 2014: pp. 301–329. doi:10.1016/C2013-0-12914-5.
[143] P. Piltonen, P. Karinkanta, J. Niinimäki, The effect of styrene–butadiene latex carboxylation on adhesion, Int. J. Adhes. Adhes. 54 (2014) 82–85. doi:10.1016/j.ijadhadh.2014.05.007.
[144] N. Segre, C. Ostertag, P.J.M. Monteiro, Effect of tire rubber particles on crack propagation in cement paste, Mater. Res. 9 (2006) 311–320. doi:10.1590/S1516-14392006000300011.
[145] L.Y. Feng, A.J. Chen, H.D. Liu, Effect of Waste Tire Rubber Particles on Concrete Abrasion Resistance Under High-Speed Water Flow, Int. J. Concr. Struct. Mater. 15 (2021). doi:10.1186/s40069-021-00475-8.
[146] A. Kashani, T.D. Ngo, P. Hemachandra, A. Hajimohammadi, Effects of surface treatments of recycled tyre crumb on cement-rubber bonding in concrete composite foam, Constr. Build. Mater. 171 (2018) 467–473. doi:10.1016/j.conbuildmat.2018.03.163.
[147] F. Pelisser, N. Zavarise, T.A. Longo, A.M. Bernardin, Concrete made with recycled tire rubber: Effect of alkaline activation and silica fume addition, J. Clean. Prod. 19 (2011) 757–763. doi:10.1016/j.jclepro.2010.11.014.
[148] O. Youssf, M.A. Elgawady, J.E. Mills, X. Ma, An experimental investigation of crumb rubber concrete confined by fibre reinforced polymer tubes, Constr. Build. Mater. 53 (2014) 522–532. doi:10.1016/j.conbuildmat.2013.12.007.
[149] I. Mohammadi, H. Khabbaz, K. Vessalas, Enhancing mechanical performance of rubberised concrete pavements with sodium hydroxide treatment, Mater. Struct. Constr. 49 (2016) 813–827. doi:10.1617/s11527-015-0540-7.
[150] O. Youssf, R. Hassanli, J.E. Mills, M. Abd Elrahman, An experimental investigation of the mechanical performance and structural application of LECA-Rubcrete, Constr. Build. Mater. 175 (2018) 239–253. doi:10.1016/j.conbuildmat.2018.04.184.

Chapter 3. Mitigating zinc leachate from end-of-life tire rubber in stabilized clayey soils[2]

The contributions of the authors to this manuscript are described as follows:

Thien Q. Tran: Conceptualization; Data curation; Formal analysis; Investigation; Methodology; Visualization; Writing - original draft; Writing - review and editing.

Note: Thien Q. Tran was in the main charge of all above-mentioned contribution categories under the supervision of Dr. Alexander S. Brand.

Shiyu Li: Investigation; Writing - review and editing.

Bin Ji: Investigation; Writing - review and editing.

Xiang Zhao: Investigation.

Wencai Zhang: Funding acquisition; Supervision; Writing - review and editing.

Alexander S. Brand: Conceptualization; Funding acquisition; Methodology; Project administration; Supervision; Writing - original draft; Writing - review and editing.

[2] **Thien Q. Tran,** Shiyu Li, Bin Ji, Xiang Zhao, Wencai Zhang, Alexander S. Brand. " Mitigating zinc leachate from end-of-life tire rubber in stabilized clayey soils" (Under review)

Mitigating zinc leachate from end-of-life tire rubber in stabilized clayey soils

Thien Q. Tran[1], Shiyu Li[2], Bin Ji[2], Xiang Zhao[1], Wencai Zhang[2], Alexander S. Brand[1,3*]

[1]The Charles Edward Via, Jr. Department of Civil and Environmental Engineering, Virginia Polytechnic Institute and State University, Blacksburg, Virginia, USA, 24061
[2]Department of Mining and Minerals Engineering, Virginia Polytechnic Institute and State University, Blacksburg, Virginia, USA, 24061
[3]Department of Materials Science and Engineering, Virginia Polytechnic Institute and State University, Blacksburg, Virginia, USA, 24061
*Corresponding Author: asbrand@vt.edu

3.1 Abstract

This study proposes the use of rubberized stabilized soil (RSS) in which clayey soils (*e.g.*, kaolin and bentonite) were stabilized by portland cement (PC) and end-of-life tire (ELT) rubber particles. The authors previously developed a methodology to extract zinc from the ELT rubber, so this study explores the potential for RSS to immobilize the leachate from the ELT rubber before and after this treatment. Three main topics are addressed in this study: 1) the capability of clay to capture leached zinc under ambient and alkaline aqueous conditions; 2) engineering properties of RSS with 0 %, 10 %, 30 %, and 50 % ELT rubber added by clay volume; and 3) pore solution and leachability tests of RSS. The results showed that the clayey soils and ELT rubber are synergistic in terms of engineering properties and the capturability of zinc and total organic carbon (TOC). While the ELT rubber and PC strengthen the clay structure, the clay absorbs leached zinc and TOC from the ELT rubber particles. Adding untreated ELT rubber into PC-stabilized clays significantly increased the RSS strength, but this improvement was less significant for the treated ELT rubber. Ultimately, the results proved that the environmental and mechanical performance of RSS makes it a viable construction material.

Keywords: end-of-life tire (ELT) rubber; rubberized stabilized soil (RSS); total organic carbon (TOC); zinc leachate; clay stabilization.

3.2 Introduction

Waste recycling, particularly in urban areas, is of critical concern to ensure quality of life, maintain or improve the ecosystem, and preserve natural resources (Bai *et al*., 2017; Koop and van Leeuwen, 2017). End-of-life tire (ELT) is one waste issue that presents numerous challenges to recycle (Abbas-Abadi *et al*., 2022). An estimated 3 billion ELTs are discarded worldwide every year (Rodgers, 2021). In the U.S., 4.46 million tons of ELT were generated in 2019, the majority of which was used as fuel, recycled into ground rubber, and other uses, but an estimated 14.3% was land disposed such as in landfills (U.S. Tire Manufacturers Association, 2020). The U.S. has an estimated stockpile of 56 million ELTs (U.S. Tire Manufacturers Association, 2020). Meanwhile, China generates the most ELTs, including 14.6 million tons of ELT in 2018 (B. Chen

et al., 2021). Therefore, sustainable practices and management of ELTs are of concern (Araujo-Morera *et al.*, 2021).

Tire rubber is a complex formulation of various polymers (*e.g.*, polyisoprene, polybutadiene, styrene-butadiene) and carbon black with small amounts of zinc oxide, extender oil, stearic acid, and others (Rodgers, 2021). Storage of ELTs can pose a fire hazard (Poole Jr., 1998), since these materials are flammable, and can pose a risk to soil, groundwater, and air pollution (Gualtieri *et al.*, 2005; Halsband *et al*., 2020). Of particular concern is zinc, which is added as a vulcanizing agent and comprises 1 % to 2 % of the tire rubber by mass (Rodgers, 2021), since it can be leached into the living environment during landfilling (Buck *et al.*, 2021; Councell *et al.*, 2004; Liu *et al.*, 2018; Rhodes *et al.*, 2012; Smolders and Degryse, 2002). A study by Smolders and Degryse (Smolders and Degryse, 2002) found that, during a one-year weathering period, 10 % to 40 % of the zinc in 100 μm ELT particles was leached. If the average amount of zinc in tire rubber is 1.5 % *wt.*, then an estimated 286 thousand tons of zinc can be potentially leached into the environment based on the current yearly production of ELTs in the U.S. and China alone. Zinc not only causes damage to the stomach lining in living organisms but also exhibits toxicity towards a wide range of organisms including plants, invertebrates, and fish (Li *et al*., 2023; Tran *et al.*, 2022b). This can result in severe harm to ecosystems and have long-lasting effects on the environment (Liu *et al.*, 2018).

Ground ELT rubber has found usage in civil engineering applications, including portland cement concrete (Kara De Maeijer *et al.*, 2021; Lavagna *et al*., 2020; Shu and Huang, 2014; Tran *et al.*, 2022b), asphalt concrete (Ma *et al.*, 2022; Picado-Santos *et al.*, 2020; Shu and Huang, 2014; Song *et al.*, 2018; Wang *et al.*, 2018), cement-stabilized base materials (Liu *et al.*, 2023), and soil stabilization (Al-Bared *et al.*, 2018). However, the potential for zinc to be leached from the ELT rubber in these applications has seen little research. Some researchers have found higher concentrations of zinc are leached from rubber-modified asphalt concrete (Sampson *et al.*, 2014; Vashisth *et al.*, 1998), although using ELT rubber in asphalt concrete reduces the rate of zinc leached (Liu *et al.*, 2018). Zinc has been found to leach into soil that is stabilized by ground ELT rubber (Smolders and Degryse, 2002), although some researchers have proposed this methodology to improve soil quality in zinc-deficient soils (Taheri *et al.*, 2011). Cement hydration appears to immobilize any zinc remaining after using tire-derived fuel in a cement kiln during the clinkering process (Trezza and Scian, 2009).

When considering the fate of zinc leached from ELT rubber, no studies have evaluated the ability of a clayey soil to capture the leached zinc in a rubberized stabilized soil (RSS). A few studies have shown that ELT rubber can be used to engineer soil properties (Al-Bared *et al.*, 2018; Yoon *et al.*, 2006) and that portland cement (PC) stabilization can be further used to modify the soil properties (Saberian and Rahgozar, 2016; Yadav and Tiwari, 2017). Clay soils are of particular interest in this capacity, given that certain clays can capture heavy metals through cation exchange (Ahmed *et al.*, 2021; Esmaeili *et al.*, 2019; Farrah *et al.*, 1980; Lothenbach *et al.*, 1998). Heavy metal cations, such as Zn^{2+}, are captured by negatively charged clay in the soil via electrostatic

forces in which negative soil particles attract the positive cations (Matthews, 2014). This cation exchange capacity (CEC) strongly depends on clay content, particle size and type of clay in the soil, organic matter content, and soil pH (Bellir *et al*., 2013; Kennedy, 1965; Vangronsveld *et al*., 1995; Zhang *et al*., 2011).

This study proposes an approach to stabilize soft clayey soil using ELT rubber and PC that also acts to immobilize any leached zinc. Specifically, ELT rubber before and after treatment will be compared. The treatment follows a hydrometallurgical process to pre-leach the zinc from the rubber to recover it as zinc oxide for other industries (Li *et al*., 2023). This treatment process was developed in an effort to control the environmental impact of leached zinc from ELT rubber. The main purposes of this study are to evaluate if clays can immobilize: 1) zinc leached from untreated ELT rubber and 2) any remaining leachable zinc from the treated ELT rubber. Furthermore, PC will be used to chemically stabilize the soil in addition to the ELT rubber. Specifically, along with chemical reactions between the PC and clay, the addition of ELT rubber is believed to mechanically change the stabilized soil structure, resulting in a significant improvement in strength. Beyond the engineering properties, the stabilized soil is expected to absorb the zinc leached from the ELT rubber through the CEC of the clay. The study is novel because it considers the fate of the zinc in conjunction with engineering properties of RSS, which has not been considered previously in the literature.

3.3 Experimental program

3.3.1 Materials

In this study, two typical clays were used, kaolin and bentonite, with specific gravities of 2.63 and 2.62, respectively. The kaolin and bentonite have liquid limit (LL) values of 57 % and 513 %, respectively. The CEC was determined following ASTM C837 (Kennedy, 1965), which was 15.75 meq/100g and 71.75 meq/100g, respectively, for kaolin and bentonite. The median particle size (D_{50}) for kaolin, bentonite, and Type I/II PC was 3.8 μm, 1.4 μm, and 6.7 μm, respectively, and the particle size distribution is shown in Figure 3- 1.

The ELT rubber was received from the manufacturer as a reduced particle size and was reported to consist of natural rubber, butadiene rubber, and styrene-butadiene rubber. In this study, the ELT rubber particles were used in the "as-received" form, herewith referred to as untreated ELT rubber, and in the processed form where the zinc was extracted, herewith referred to as treated ELT rubber. The hydrometallurgical treatment process was based on a previous methodology (Li *et al*., 2023) where 2.0 M HNO_3 was used to leach and subsequently recover the zinc from the ELT rubber. The treatment batch had a solid concentration of 200 g L^{-1}. The treatment process was carried out at a leaching temperature of 90 ℃ and was agitated for 5 h using a PTFE-coated magnetic stirrer at 600 rpm, resulting in a leaching recovery of zinc of around 95 %. The specific gravity of untreated and treated ELT rubber was 1.20 and 1.18, respectively. The particle size distribution of the ELT rubber is shown in in Figure 3- 1; the D_{50} for untreated and treated ELT rubber was 0.34 mm and 0.45 mm, respectively. The ELT rubber particles expanded slightly after treatment.

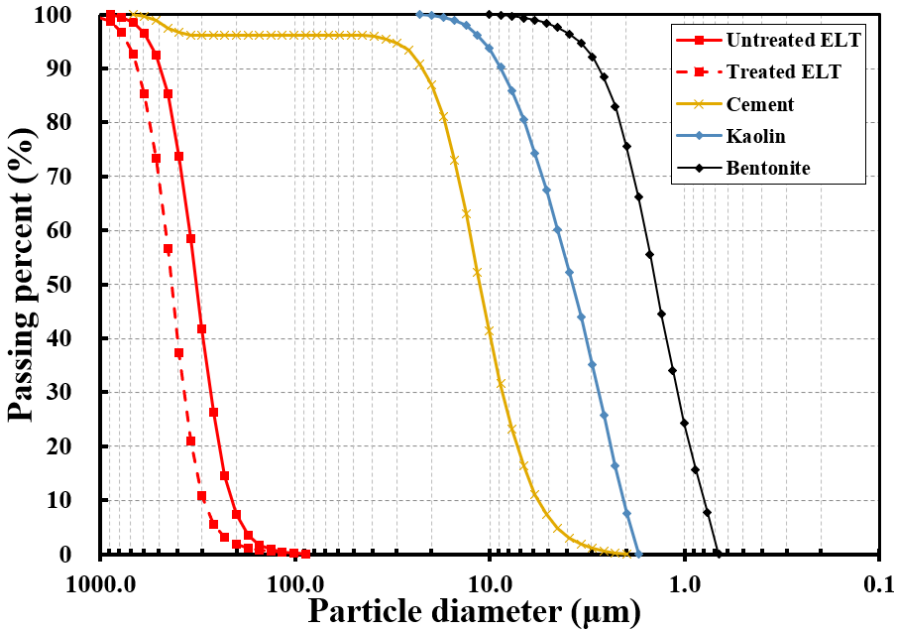

Figure 3- 1. Particle size distribution curves of PC, kaolin, bentonite, and ELT rubber particles.

A Bruker D8 X-ray diffractometer with Cu Kα radiation was employed for mineralogical analysis of the clays. The kaolin clay was found to consist of only kaolinite, while the bentonite clay was composed of montmorillonite and quartz (Tran *et al*., 2022a).

The major metals in the untreated ELT rubber were Mg, Al, Ca, Fe, and Zn, as determined after digestion of the rubber in strong acid, at concentrations of 567 mg kg^{-1}, 219 mg kg^{-1}, 627 mg kg^{-1}, 131 mg kg^{-1}, and 10,389 mg kg^{-1}, respectively (Li *et al*., 2023). The chemical composition of the kaolin, bentonite, and PC was determined by X-ray fluorescence analysis and presented in Table 3- 1.

Table 3- 1. Chemical composition of kaolin, bentonite, and PC.

Chemical composition (%)	Kaolin	Bentonite	PC
CaO	0.3	1.1	56.7
SiO_2	43.0	50.2	30.1
Al_2O_3	20.3	12.9	8.4
MgO	0.6	1.6	2.1
Fe_2O_3	1.3	3.8	2.9
TiO_2	1.3	0.1	0.2
K_2O	0.3	0.3	0.5
Na_2O	-	1.3	-
P_2O_5	-	0.1	-
Loss of ignition (LOI)	33.0	28.4	0.0

3.3.2 Experimental methodology

3.3.2.1 Zinc capture test

To test the hypothesis that clay can absorb leached zinc, a soaking test was employed in this study. The test was performed by soaking clay and ELT rubber with a liquid-to-ELT solid ratio of 40 (L/S = 40) at 23 °C. Different aqueous solutions, including deionized water, 0.05 M NaOH, 0.18 M $Ca(OH)_2$, and 0.45 M $Ca(OH)_2$, were employed for this test to simulate different conditions of leaching when the clay mixture is interacting with hydrating PC or exposed to different environmental conditions. After 1 day, 7 days, and 28 days of soaking, the pH and zinc concentration of the leaching solution were determined using a pH meter and inductively coupled plasma mass spectrometry (ICP-MS), respectively. The soaking proportion of clay-rubber mixtures with different chemical solutions is presented in Table 3- 2.

Table 3- 2. Soaking proportion of clay-rubber mixtures.

Mix code	Solid (g)			Liquid/chemical solution			Measured pH		
	Kaolin (g)	Bentonite (g)	Untreated ELT rubber (g)	Water (g)	0.18 M or 0.45 M $Ca(OH)_2$ (mL)	0.05 M NaOH (mL)	1 d	7 d	28 d
1R_40W			5.0	200			9.4	7.2	7.2
1K_40W	5.0			200			8.9	8.2	8.0
1B_40W		5.0		200			10.2	9.9	9.9
1K_1R_40W	5.0		5.0	200			8.6	8.0	8.0
1K_1R_40W_0.2CaO	5.0		5.0		200		13.0	12.6	12.4
1K_1R_40W_0.5CaO	5.0		5.0		200		13.0	12.6	12.6
1K_1R_40W_NaOH	5.0		5.0			200	13.0	12.5	12.5
1B_1R_40W		5.0	5.0	200			10.2	9.6	9.3
1B_1R_40W_0.2CaO		5.0	5.0		200		13.0	12.6	12.3
1B_1R_40W_0.5CaO		5.0	5.0		200		13.0	12.6	12.5
1B_1R_40W_NaOH		5.0	5.0			200	12.9	12.4	12.2

Note: K: kaolin; B: bentonite; CaO: lime; W: water; NaOH: sodium hydroxide

3.3.2.2 Engineering property tests

Untreated and treated ELT rubber was mixed with clay and PC. For the kaolin clay experiments, the ELT rubber content was 0 %, 10 %, 30 %, and 50 % by clay volume. For the bentonite clay experiments, the ELT rubber content was 0 % and 50 % by clay volume. RSS with kaolin used a water content of 2.0 LL of kaolin while RSS with bentonite used a water content of 0.5 LL of bentonite. PC was added at 20 % by solid mass. After mixing, the flowability of each fresh RSS mixture was immediately determined according to ASTM D6103 (D 6103 – 04, 2017). Cylindrical specimens with lengths of 100 mm and diameters of 50 mm were prepared *via* the dynamic compaction method (Kitazume *et al.*, 2015) and cured in a curing chamber conditioned at 23 °C ± 2 °C and 95 % ± 2 % of relative humidity until the testing time. The unconfined compressive strength (UCS) after 3 days, 7 days, and 28 days were determined in accordance with ASTM

D2166 (ASTM C2166, 2000). The mixture proportions and performed experiments for different mixtures are presented in Table 3- 3.

Table 3- 3. Proportion of RSS and performed experiments.

Note	Mix code	ELT rubber content (% clay volume)	C/S ratio	Clay (kg/m^3)	Cement (PC) (kg/m^3)	ELT Rubber (kg/m^3)	Water (kg/m^3)	Performed experiments					
								UCS	Flow	IC	SEM	PSE	Leaching test
Stabilized kaolin	Ref-K	0	0.2	627.4	147.9	0	715.23	√	√	√	√	√	√
Stabilized kaolin with untreated ELT rubber	URK-10	10	0.2	610.0	158.2	27.78	695.42	√	√	√			
	URK-30	30	0.2	578.0	177.1	78.95	658.9	√	√	√			
	URK-50	50	0.2	549.2	194.2	125.0	626.1	√	√	√	√	√	√
Stabilized kaolin with treated ELT rubber	TRK-10	10	0.2	610.0	158.0	27.36	695.5	√	√	√			
	TRK-30	30	0.2	578.1	176.55	77.8	659.1	√	√	√			
	TRK-50	50	0.2	549.4	193.3	123.2	626.3	√	√	√	√	√	√
Stabilized bentonite	Ref-B	0	0.2	331.1	78.34	0	849.2	√	√		√		√
Stabilized bentonite with untreated/treated ELT rubber	URB-50	50	0.2	307.8	109.3	70.4	789.6	√	√		√		√
	TRB-50	50	0.2	307.9	108.7	69.29	789.75	√	√		√		√
Untreated and treated ELT rubber-cement mixture without clay	(U)ELT-C	50	-	-	194.2	125.0	626.1						√
	(T)ELT-C	50	-	-	193.3	123.2	626.3						√

Note: K: kaolin; B: bentonite; C/S: cement-to-solid ratio in volume; PC: cement UCS: unconfined compressive strength; IC: isothermal calorimetry; PSE: pore solution extraction; SEM: scanning electron microscopy.

3.3.2.3 Isothermal calorimetry

Isothermal calorimetry (IC) was conducted using a Calmetrix I-Cal Flex to observe the thermal power (W/g cement) and total heat (J/g cement) of various RSS mixtures. While IC is commonly used to understand cement hydration kinetics (Wadsö *et al.*, 2016), it has recently been applied to study reactions in stabilized soils (Tran *et al.*, 2022a). After the RSS mixtures were thoroughly mixed in 15 mL plastic vials, the vials were transferred to the isothermal chamber which was set to 23 ^{o}C. The heat of hydration was quantified for up to 3 days of curing time. To investigate the heat development in the RSS matrix and how it was different from the one without ELT rubber added, mixtures coded Control-K, URK-10, URK-30, URK-50, TRK-10, TRK-30, and TRK-50 were subjected to the IC test.

3.3.2.4 Microstructure study

Scanning electron microscopy (SEM) was employed to study the microstructure of the ELT rubber particles. A JEOL IT-500HR SEM with a Schottky field emission electron source was used. Samples were sputter-coated with a ~12 nm thick platinum/palladium layer. For these analyses, samples were vacuum-dried to remove moisture prior to the tests following the method in a study by Kim *et al.* (Kim *et al.*, 2019).

3.3.2.5 Pore solution extraction (PSE) and environmental tests

PSE was used to understand the chemical composition in the pore solution of mixture Ref-K, URK-50, and TRK-50. The PSE device in this study was based on the Barneyback and Diamond system (Barneyback Jr. and Diamond, 1981). The applied pressure to extract the pore solution at curing ages of 7 days and 28 days from the cylindrical samples (50 mm in diameter and 100 mm in length) was increased from 0 MPa to 22.5 MPa until 5 mL to 10 mL of pore fluid was collected. The collected pore solution was then filtered and immediately acidified with 12.1 M HCl at 2 % by volume of solution to prevent precipitation. Finally, the extracted solution was analyzed using a Thermo Electron iCAP-RQ ICP-MS and a Shimadzu TOC-VCSN to quantify the zinc and TOC concentrations, respectively, during the hydration process of the RSS. These two analyses were also employed for the leachate of the crushed UCS samples soaked in deionized water at L/S ratio of 8 to check whether the proposed material satisfies the environmental requirements. Along with the three above-mentioned mixture, two more mixtures were prepared by eliminating the clay content in mixtures URK-50 and TRK-50 for the leaching test to investigate the effects of clay in zinc and TOC immobilization in the leachate.

3.4 Results and discussion

3.4.1 Zinc capture test

Figure 3- 2 depicts the zinc concentration of various leachates at different soaking times. As shown, the leachates of mixtures of kaolin with water (1K_40) and bentonite with water (1K_40) did not expose any significant concentration of zinc after 28 days of the soaking process. Meanwhile, the zinc leached out from the ELT rubber into the distilled water (mixture 1R_40W) was dramatically high since its concentration increased more than 270 times from 27.1 ppb (1 day) to 7387 ppb (28 days). This clearly indicates that ELT rubber possesses a potential for zinc to leach

into the surrounding environment. When kaolin or bentonite was introduced to the mixtures, the 28-day zinc concentration of all the leachates significantly decreased by 95 % (*i.e.*, from 7387 ppb to less than 300 ppb). Increasing the pH with 0.18 M $Ca(OH)_2$, 0.45 M $Ca(OH)_2$, and 1 M NaOH accelerated the zinc leaching rate at the early soaking times (1 day) relative to water. The increased pH appeared to be effective with bentonite to increase its cation absorbability, hence, it could absorb more free zinc from leachate (*i.e.*, zinc concentration decreased from 7387 ppb to around 30 ppb). Meanwhile, the increased pH did not have a remarkable effect on the zinc absorbability of kaolin as it could not absorb more free zinc from leachate compared to the mixture soaked in distilled water (1K_1R_40W). This might be explained that because the CEC of kaolin is much smaller (around 5 times) than that of bentonite, it might reach its maximum capacity to absorb more ions.

Another explanation for the reduction in zinc concentration in Figure 3- 2 is that it precipitated out of solution. Above pH ~10, Zn^{2+} can precipitate out of solution as ZnO and/or $Zn(OH)_2$ (Aimable *et al.*, 2010; Sinha *et al.*, 2016). Similarly, Lothenbach *et al.* (Lothenbach *et al.*, 1998) found that zinc concentration in a clay-free system dropped dramatically when pH was greater than 9. However, no white precipitates were observed in these solutions, which would have been indicative of ZnO and/or $Zn(OH)_2$. It is possible that part of Zn^{2+} could be converted into hydroxides in alkaline conditions and precipitate on the surface of the clay (Zhang *et al.*, 2011). In addition, clay has multiple micropores so that zinc might diffuse and be captured into the pore spaces of the clay structure. All three of these hypotheses can occur simultaneously during this experiment. Since all clay-rubber mixtures significantly reduced the zinc concentration, the immobilization of zinc is most likely attributed to the CEC of clays.

In addition to zinc, the only other heavy metal identified in the ELT rubber in appreciable quantity was iron, as presented in Section 3.3.1. Therefore, it is worth noting that the clay was also able to immobilize any leached iron, as shown in Figure 3- 3, and that the pH modification significantly enhanced the iron immobilization. Other heavy metals, including lead, chromium, cobalt, cadmium, and arsenic, were detected in extremely low (*e.g.*, less than 30 ppb) to zero concentrations in the leachates detected by ICP-MS.

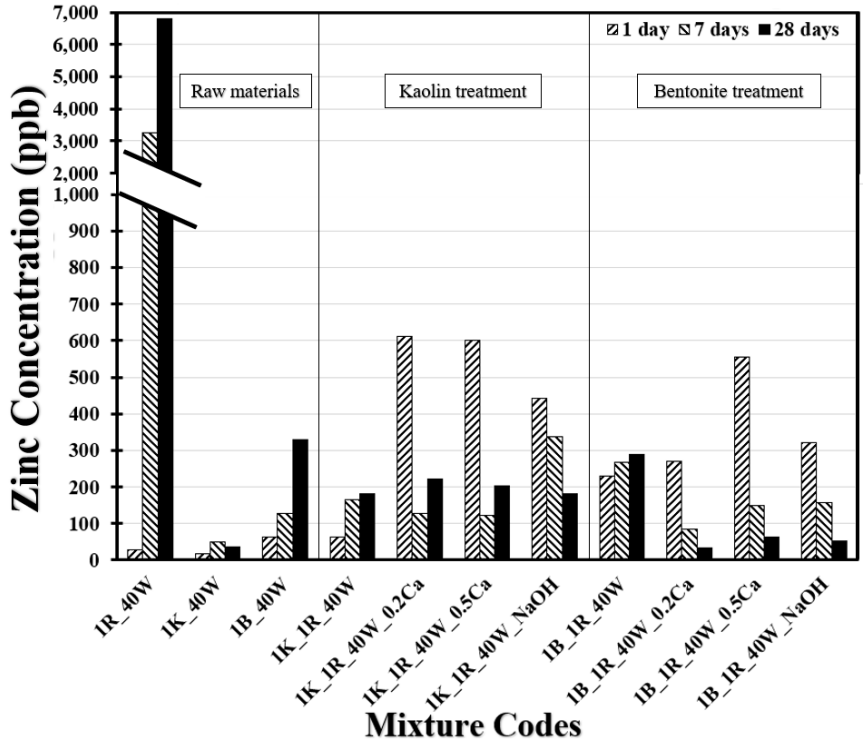

Figure 3- 2. Zinc concentration of various leachates at different soaking times.

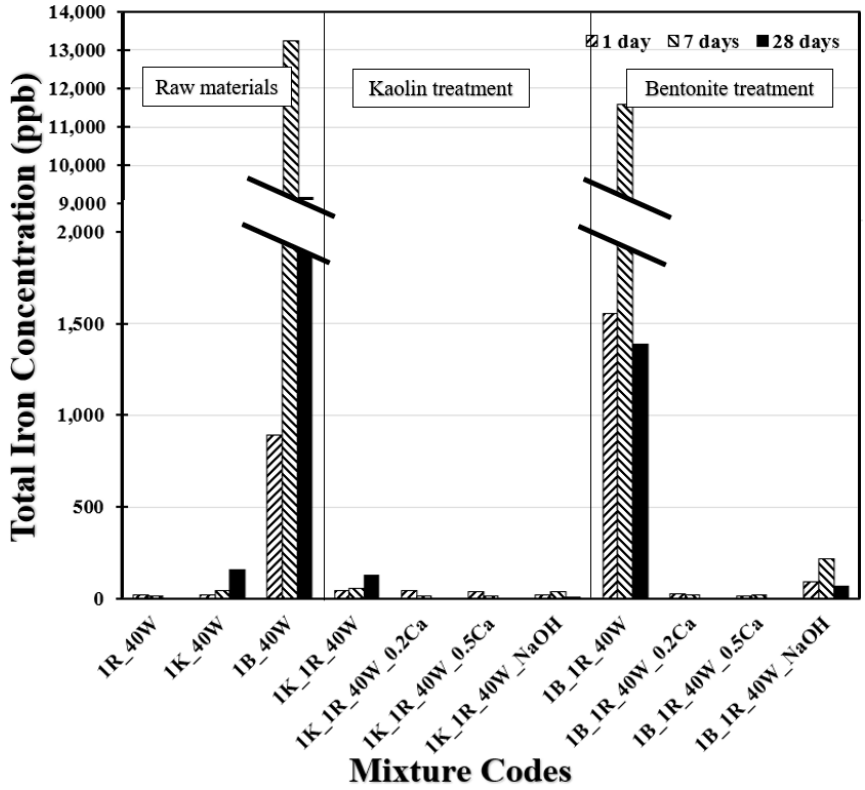

Figure 3- 3. Total iron concentration of various leachates at different soaking times.

3.4.2 Unconfined compressive strength (UCS)

Figure 3- 4 shows the UCS of conventional cement-stabilized soil (*i.e.*, Ref-K and Ref-B), RSS with untreated ELT rubber (*i.e.*, URK-10, URK-13, and URK-50), and RSS with treated ELT rubber (*i.e.*, TRK-10, TRK-13, and TRK-50). The conventional mixtures exhibited low UCS values as well as slow strength development during the curing time. However, when different amounts of untreated ELT rubber were introduced, the strength of stabilized clays remarkably improved. In general, a higher replacement percentage of treated ELT rubber yielded a greater strength. The 28-day strength of rubberized stabilized kaolin with 50 % of untreated ELT rubber (URK-50) was 1019 kPa, which roughly doubled the conventional stabilized kaolin without any rubber added (523 kPa). This improvement was nearly three times in the case of rubberized stabilized bentonite (558 kPa compared to 179 kPa). However, the treated ELT rubber was not as effective as the untreated ELT rubber. The 28-day strength of RSS with 50 % of treated ELT rubber (TRK-50) was decreased by 65 % (from 1019 kPa to 654 kPa) compared to the untreated ELT rubber used case, which was just 25 % higher than that of conventional stabilized kaolin. This happened similarly in the case of rubberized stabilized bentonite (388 kPa *vs.* 558 kPa).

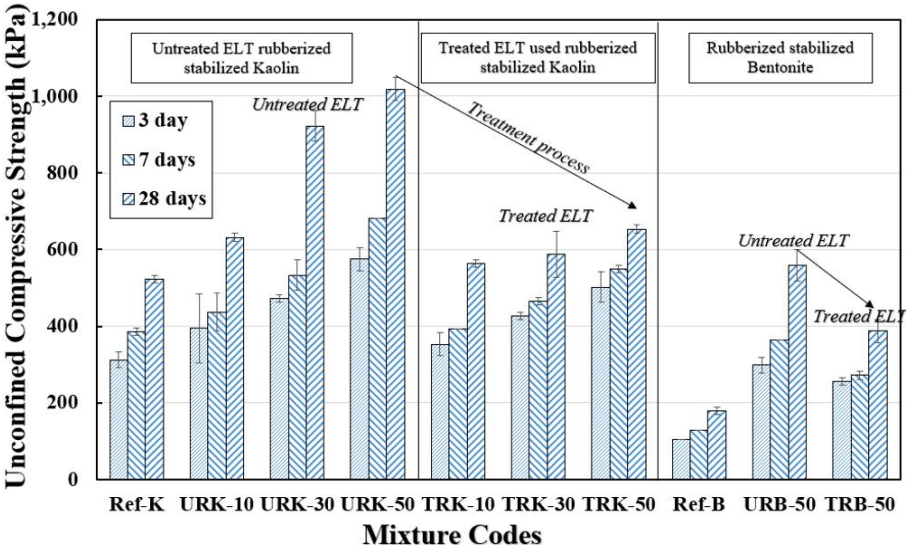

Figure 3- 4. Unconfined compressive strength of rubberized stabilized clays.

3.4.3 Flowability

The flowability of different RSS mixtures is presented in Figure 3- 5. Generally, untreated and treated ELT rubber enhanced the flowability of rubberized stabilized kaolin up to 35 %, increasing from around 8 cm (Ref-K) to 11 cm (mixtures URK-10 and TRK 30). The hydrophobic nature of the ELT rubber (*e.g.*, (C. Y. Chen *et al.*, 2021; Di Mundo *et al.*, 2018)) could be one reason for the increased flowability, as the rubber particles act to repel water. In addition, since the cohesion of clay is high, the clay particles tend to agglomerate in the presence of water. The ELT rubber particles disrupt that cohesion and act to disperse the clay particles. Meanwhile, the ELT rubber only slightly improved the flowability of the stabilized bentonite; this is understandable since the selected water content of the rubberized stabilized bentonite mixture was only 50 % of its liquid

limit value. The improvement of the flowability of RSS when ELT rubber is added can be helpful in the application of controlled low-strength materials.

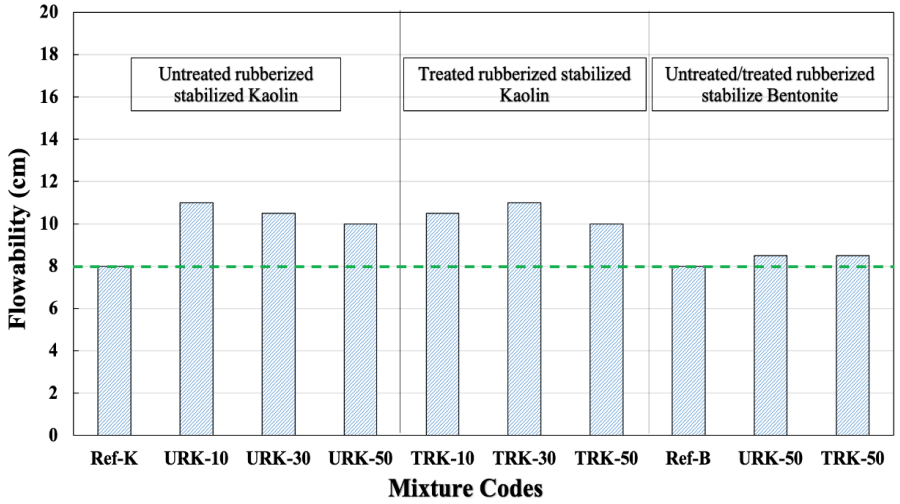

Figure 3- 5. Flowability of different RSS.

3.4.4 Isothermal calorimetry (IC)

The thermal power generated from different RSS mixtures is graphically presented in Figure 3- 6. It can be seen that, during the hydration process, RSS mixtures generally generated much higher thermal power (from 1.2 to 1.35 times) than that of the reference mixture (around 0.011 W/g_{cement}). This could be explained that, due to the hydrophobicity of the used ELT rubber, there is more "free" water available in RSS skeleton, which provides more sufficient water for the mineral diffusion for the hydration process of the mixtures. Second, the leached zinc in the RSS matrix probably could homogeneously incorporate into the C–S–H to increase the growth rate of C–S–H and give higher peak of hydration. This observation is in good agreement with a previous study by Bazzoni *et al.* (Bazzoni *et al.*, 2014). In addition, the mechanical and physical engineering properties of ELT rubber are believed to be more efficient than clay in helping improve the mixtures' strength development.

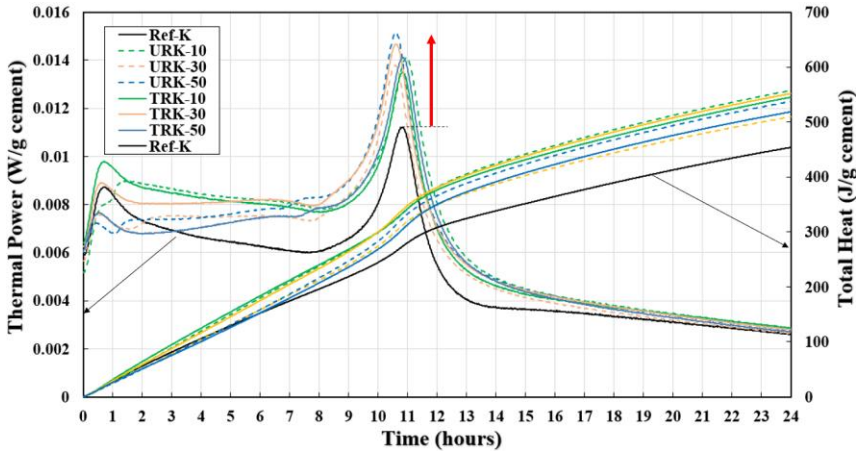

Figure 3- 6. The thermal power generated from different RSS.

Secondly, the data show that the peak of thermal power curves of the rubberized stabilized kaolin was mostly maintained with just a few minute shifts. In addition, possible retardations in the hydration due to the contamination of the hydration media in the mixture's matrix *via* zinc, reported in some previous studies by Garg and White (Garg and White, 2017) and Ataie *et al* (Ataie *et al*., 2015), were not found yet in this case. The peak differences (hour) and peak value (W/g_{cement}) of various RSS are shown in Table 3- 4.

Table 3- 4. Hydration thermal power of different RSSs.

Mix code	Peak (h)	Peak delay (h)	Peak (W/g_{cement})	Peak value difference (%)
Ref-K	10.8	N/A	$1.12x10^{-2}$	N/A
URK-10	10.9	0.1	$1.41x10^{-2}$	25.9
URK-30	10.7	-0.1	$1.38x10^{-2}$	23.2
URK-50	10.7	-0.1	$1.51x10^{-2}$	34.8
TRK-10	10.8	0.0	$1.35x10^{-2}$	20.5
TRK-30	10.7	-0.1	$1.47x10^{-2}$	31.3
TRK-50	10.8	0.0	$1.41x10^{-2}$	25.9

Table 3- 5. Hydration total heat generated from different RSSs

Mix code	Total heat (J/g_{cement}) (percent difference between modified mixtures and PC)			
	12 h	24 h	48 h	72 h
Ref-K	$3.09x10^2$	$4.54x10^2$	$5.87x10^2$	$6.13x10^2$
URK-10	$3.81x10^2$ (23.3)	$5.58x10^2$ (22.9)	$7.03x10^2$ (19.8)	$7.38x10^2$ (20.4)
URK-30	$3.50x10^2$ (13.3)	$5.09x10^2$ (12.1)	$6.46x10^2$ (10.1)	$6.83x10^2$ (11.4)
URK-50	$3.65x10^2$ (18.1)	$5.37x10^2$ (18.3)	$6.81x10^2$ (16.0)	$7.25x10^2$ (18.3)
TRK-10	$3.76x10^2$ (21.7)	$5.45x10^2$ (20.0)	$6.92x10^2$ (17.9)	$7.30x10^2$ (19.1)
TRK-30	$3.82x10^2$ (23.6)	$5.52x10^2$ (21.6)	$6.93x10^2$ (17.9)	$7.30x10^2$ (19.1)
TRK-50	$3.50x10^2$ (13.3)	$5.18x10^2$ (14.1)	$6.59x10^2$ (12.3)	$7.01x10^2$ (14.4)

Along with thermal power, Figure 3- 6 simultaneously reports the total heat recorded from mixing to 24 h, and the detailed total heat of each mixture over time up to 72 h of curing is shown in Table 3- 5. The data reveal that using ELT rubber in stabilized kaolin mixtures remarkably increased the total hydration heat. After 72 h, the increases were up to 20 % for 10 % of untreated ELT rubber used and up to 19 % for both 10 % and 30 % of treated ELT rubber used. Interestingly, the increases were less significant when using more ELT rubber (up to 50 %) in the mixtures. This tendency is not totally in agreement with the UCS development shown in Figure 3- 4. While other studies have demonstrated that IC data can directly relate to strength development in cementitious composites (e.g., (Tanesi and Ardani, 2013)), this study does appear to demonstrate similar trends for RSS. However, the data indicate that the change of thermal power peak and total heat during the hydration can be possibly used to predict the strength changing tendency of the stabilized soil mixtures, but it cannot completely reflect the strength development behavior of the mixtures.

3.4.5 Microstructure

Secondary electron imaging with SEM was performed on the ELT rubber particles. Figure 3- 7 a and Figure 3- 7 c show that the untreated ELT rubber particles possessed irregular and angular shapes with no visible microcracks. In contrast, there were significant cracks observed on the treated ELT rubber surface as a result of the treatment process, as shown in Figure 3- 7 b and Figure 3- 7 d. This change to the particle morphology after treatment was reported previously and is the reason for the increased specific surface area of the ELT rubber (Li *et al*., 2023). In addition, the treated ELT rubber particle appeared to have many small scales on its surface due to the formed cracks which are close to the particle edges, as can be seen in Figure 7d. These cracks and scales weaken the ELT rubber particle and are likely the reason for the reduced mechanical performance of the treated ELT rubber compared to the untreated ELT rubber in Figure 3- 4.

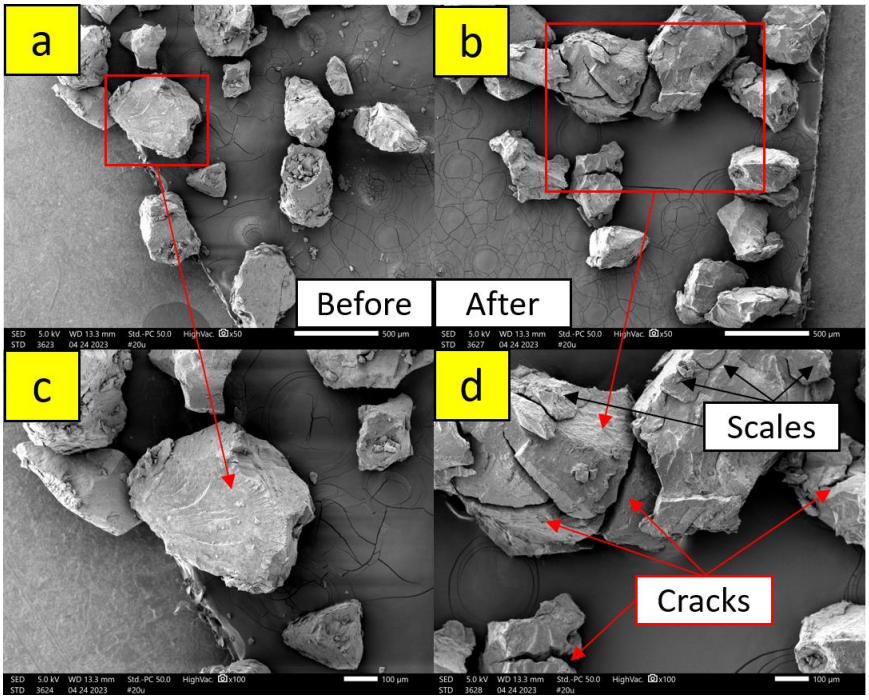

Figure 3- 7. SEM images of the (a, c) untreated ELT rubber particles and (b, d) treated ELT rubber particles.

3.4.6 Environmental tests

Figure 3- 8 presents zinc concentration in the extracted pore solution of RSS mixtures Ref-K, URK-50, and TRK-50. At early curing times (7 days), the zinc concentration in the pore solution of all mixtures was relatively high. However, there is an apparent immobilization of the zinc at 28 days relative to 7 days, which is attributed to the CEC of the clay in the RSS matrix. The result is in good agreement with the findings from the zinc capture test in Figure 3- 2. In addition, the results show that the zinc-recovery treatment could not completely remove all zinc in the ELT rubber particle, which agrees with the previous study (Li *et al*., 2023).

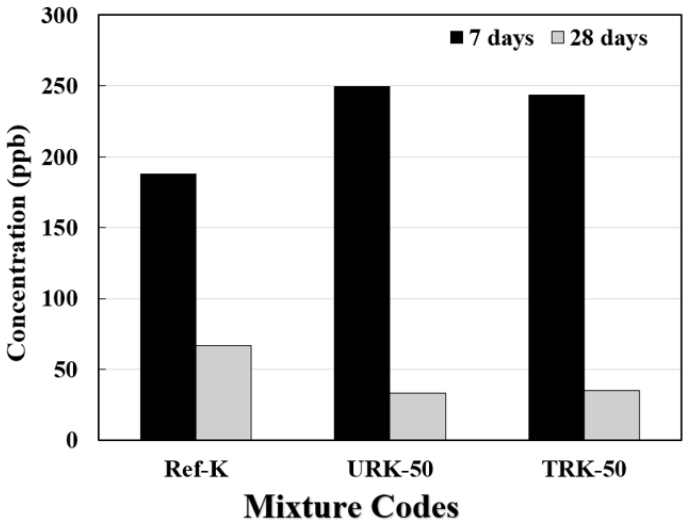

Figure 3- 8. Zinc concentration in the extracted pore solution of kaolin with ELT rubber.

Figure 3- 9 compares the zinc concentration in the leachate of RSS mixtures and the ELT rubber-cement mixtures without kaolin ((U)ELT-C and (T)ELT-C). At 7 days of soaking, the mixtures (U)ELT-C and (T)ELT-C exposed around 25 ppb to 40 ppb of zinc in the leachate, which were generally much higher than the RSS mixtures (*i.e.*, URK-50, TRK-50, URB-50, and TRB-50) that yielded negligible zinc concentrations. After 150 days, all leached zinc was evidently immobilized by clay in RSS mixtures while there were still small amounts of zinc still left in the leachate of the ELT rubber-cement mixtures without clays. The CEC of hydration products from cementitious materials, such as C–S–H, has been reported to possess the ability to capture heavy metals (Bernard *et al*., 2021), which is also observed in this study through the zinc concentration reduction in the leachate of rubber-cement mixtures, (U)ELT-C and (T)ELT-C, between 7 days and 28 days. Even though the zinc concentration recorded in the leachate of all mixtures satisfied the requirement for zinc content in drinking water (< 5 ppm) (Agency for Toxic Substances and Disease Registry (ATSDR), 2005), it is worth noting that the zinc immobilization of the RSS was enhanced more effectively due to the presence of clay.

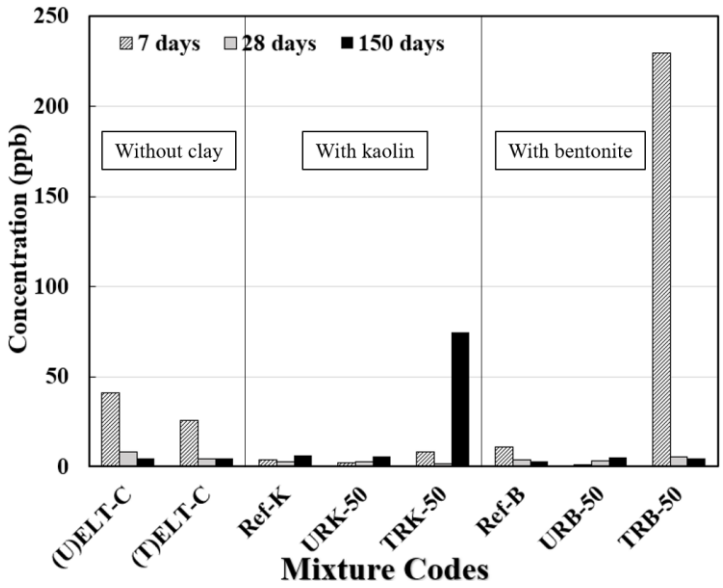

Figure 3- 9. Zinc concentration in the leachate of RSS mixtures.

Figure 3- 10 illustrates the TOC content in the extracted pore solution of RSS mixtures including Ref-K, URK-50, and TRK-50. It can be noted that the amount of leached TOC in the pore solution was relatively high after 7 days of curing time and was significantly reduced after 28 days (*i.e.*, decreased to the level yielded by the reference mixture).

Figure 3- 11 shows the TOC content in the leachate of the RSS mixtures, including Ref-K, URK-50, TRK-50, URB-50, and TRB-50. The TOC content in the leachate of the RSS mixtures increased over time. After 150 days of soaking, mixtures with kaolin could immobilize around 50 % of the leached TOC when compared to the amount leached TOC from rubber-cement mixtures, keeping the TOC concentration in the leachate of rubberized stabilized kaolin marginally under the zinc threshold for drinking water (25 mg/L) (Standard Methods for the Examination of Water and Wastewater, 2018). More noticeably, around 75 % of leached TOC was immobilized for mixture RSS mixtures with bentonite. These findings indicate that clays not only can absorb zinc, but they can also immobilize the TOC leached from ELT rubber particles.

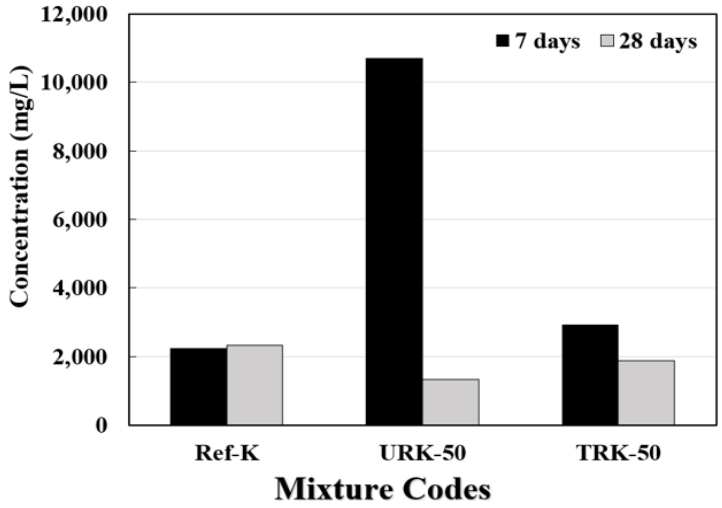

Figure 3- 10. TOC in the pore solution of rubberized stabilized kaolin.

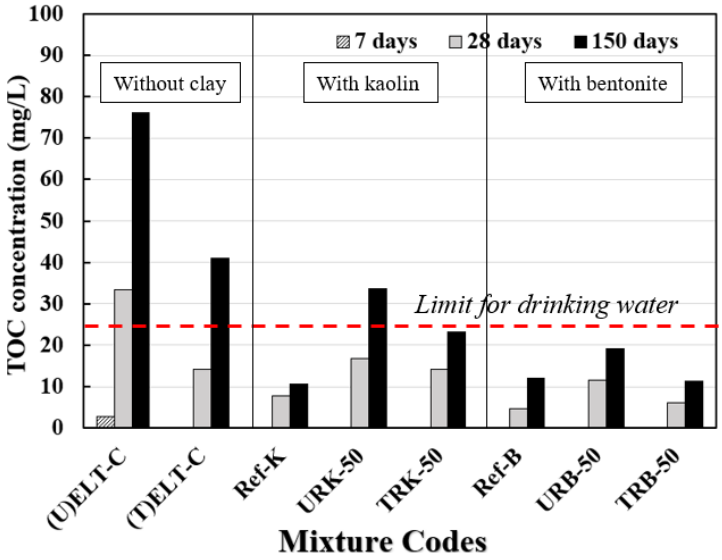

Figure 3- 11. TOC in the leachate of RSS mixtures.

3.5 Conclusions

In this study, the feasibility of using ELT rubber for soil stabilization was investigated in terms of engineering and environmental aspects. The effects of zinc-recovered treatment on ELT rubber were also discussed. The main conclusions taken from this study are:

1. The results successfully proved the hypothesis that clays possess a strong ability for zinc immobilization.
2. While the treatment process for zinc recovery from ELT rubber could provide a more environmentally conscious material, it adversely affected the engineering properties of the RSS.
3. ELT rubber enhanced the flowability of stabilized clay mixtures, possibly due to its hydrophobicity.

4. While adding untreated ELT rubber into stabilized clay could significantly enhance the strength of the mixture by up to roughly 95 % (for kaolin mixture) and 300 % (for bentonite mixture), the zinc-recovery treatment process on ELT rubber negatively affected the significance of strength improvement in the RSS mixtures.
5. The peak heat of hydration was exaggerated up to 1.35 times due to the addition of ELT rubber in the stabilized clay mixture. The change of thermal power peak and total heat during the hydration can possibly be used to predict the strength changing tendency of the stabilized soil mixtures, but it cannot completely reflect the strength development behavior of the mixtures.
6. Kaolin and bentonite could effectively immobilize leached zinc and TOC contents in the RSS.

Acknowledgement

This study was supported by the Center for Tire Research (CenTiRe), Project SUST-2021-D14-4. The authors acknowledge Lehigh Technologies for providing the waste tire rubber and Short Mountain Silica company for providing the kaolin and bentonite for this work. The authors thank Jeffrey Parks, Jody Smiley, Madeline E. Schreiber, and Aaron J. Prussin II, for their assistance with ICP-MS and TOC analyses.

References

Abbas-Abadi, M.S., Kusenberg, M., Shirazi, H.M., Goshayeshi, B., Van Geem, K.M., 2022. Towards full recyclability of end-of-life tires: Challenges and opportunities. J. Clean. Prod. 374, 134036. https://doi.org/https://doi.org/10.1016/j.jclepro.2022.134036

Agency for Toxic Substances and Disease Registry (ATSDR), 2005. Toxicological Profile for Zinc, Public Health Statement.

Ahmed, A.M., Ayad, M.I., Eledkawy, M.A., Darweesh, M.A., Elmelegy, E.M., 2021. Removal of iron, zinc, and nickel-ions using nano bentonite and its applications on power station wastewater. Heliyon 7, e06315. https://doi.org/10.1016/j.heliyon.2021.e06315

Aimable, A., Buscaglia, M.T., Buscaglia, V., Bowen, P., 2010. Polymer-assisted precipitation of ZnO nanoparticles with narrow particle size distribution. J. Eur. Ceram. Soc. 30, 591–598. https://doi.org/10.1016/j.jeurceramsoc.2009.06.010

Al-Bared, M.A.M., Marto, A., Latifi, N., 2018. Utilization of Recycled Tiles and Tyres in Stabilization of Soils and Production of Construction Materials – A State-of-the-Art Review. KSCE J. Civ. Eng. 22, 3860–3874. https://doi.org/10.1007/s12205-018-1532-2

Araujo-Morera, J., Verdejo, R., López-Manchado, M.A., Hernández Santana, M., 2021. Sustainable mobility: The route of tires through the circular economy model. Waste Manag. 126, 309–322. https://doi.org/https://doi.org/10.1016/j.wasman.2021.03.025

ASTM C2166, 2000. Standard Test Method for Unconfined Compressive Strength of Cohesive Soil 1. Current 04.

Ataie, F.F., Juenger, M.C.G., Taylor-Lange, S.C., Riding, K.A., 2015. Comparison of the retarding mechanisms of zinc oxide and sucrose on cement hydration and interactions with supplementary cementitious materials. Cem. Concr. Res. 72, 128–136. https://doi.org/10.1016/j.cemconres.2015.02.023

Bai, X., McPhearson, T., Cleugh, H., Nagendra, H., Tong, X., Zhu, T., Zhu, Y.-G., 2017. Linking urbanization and the environment: Conceptual and empirical advances. Annu. Rev. Environ. Resour. 42, 215–240. https://doi.org/10.1146/annurev-environ-102016-061128

Barneyback Jr., R.S., Diamond, S., 1981. Expression and analysis of pore fluids from hardened cement pastes and mortars. Cem. Concr. Res. 11, 279–285. https://doi.org/10.1016/0008-8846(81)90069-7

Bazzoni, A., Suhua, M., Wang, Q., Shen, X., Cantoni, M., Scrivener, K.L., 2014. The effect of magnesium and zinc ions on the hydration kinetics of C3S. J. Am. Ceram. Soc. 97, 3684–3693. https://doi.org/10.1111/jace.13156

Bellir, K., Lehocine, M.B., Meniai, A.H., 2013. Zinc removal from aqueous solutions by adsorption onto bentonite. Desalin. Water Treat. 51, 5035–5048. https://doi.org/10.1080/19443994.2013.808786

Bernard, E., Yan, Y., Lothenbach, B., 2021. Effective cation exchange capacity of calcium silicate hydrates (C-S-H). Cem. Concr. Res. 143, 106393. https://doi.org/10.1016/j.cemconres.2021.106393

Buck, T., Cooper Doherty, A., Ernst, M., Garland, M., Goings, M., 2021. Rationale Document for Motor Vehicle Tires Containing Zinc.

Chen, B., Zheng, D., Xu, R., Leng, S., Han, L., Zhang, Q., Liu, N., Dai, C., Wu, B., Yu, G., Cheng, J., 2021. Disposal methods for used passenger car tires: One of the fastest growing solid wastes in China. Green Energy Environ. https://doi.org/10.1016/j.gee.2021.02.003

Chen, C.Y., Shen, Z.Y., Lee, M.T., 2021. On developing a hydrophobic rubberized cement paste. Materials (Basel). 14. https://doi.org/10.3390/ma14133687

Councell, T.B., Duckenfield, K.U., Landa, E.R., Callender, E., 2004. Tire-wear particles as a source of zinc to the environment. Environ. Sci. Technol. 38, 4206–4214. https://doi.org/10.1021/es034631f

D 6103 – 04, 2017. Standard Test Method for Flow Consistency of Controlled Low Strength Material (CLSM). ASTM Stand. 3–5.

Di Mundo, R., Petrella, A., Notarnicola, M., 2018. Surface and bulk hydrophobic cement composites by tyre rubber addition. Constr. Build. Mater. 172, 176–184. https://doi.org/10.1016/j.conbuildmat.2018.03.233

Esmaeili, A., Mobini, M., Eslami, H., 2019. Removal of heavy metals from acid mine drainage by native natural clay minerals, batch and continuous studies. Appl. Water Sci. 9, 1–6. https://doi.org/10.1007/s13201-019-0977-x

Farrah, H., Hatton, D., Pickering, W.F., 1980. The affinity of metal ions for clay surfaces. Chem. Geol. 28, 55–68. https://doi.org/10.1016/0009-2541(80)90035-2

Garg, N., White, C.E., 2017. Mechanism of zinc oxide retardation in alkali-activated materials: An: in situ X-ray pair distribution function investigation. J. Mater. Chem. A 5, 11794–11804. https://doi.org/10.1039/c7ta00412e

Gualtieri, M., Andrioletti, M., Vismara, C., Milani, M., Camantini, M., 2005. Toxicity of tire debris leachates. Environ. Int. 31, 723–730. https://doi.org/10.1016/j.envint.2005.02.001

Halsband, C., Sørensen, L., Booth, A.M., Herzke, D., 2020. Car tire crumb rubber: Does leaching produce a toxic chemical cocktail in coastal marine systems? Front. Environ. Sci. 8, 125. https://doi.org/10.3389/fenvs.2020.00125

Kara De Maeijer, P., Craeye, B., Blom, J., Bervoets, L., 2021. Crumb rubber in concrete—the barriers for application in the construction industry. Infrastructures 6, 1–20. https://doi.org/10.3390/infrastructures6080116

Kennedy, B.V.C., 1965. Mineralogy and Cation-Exchange Capacity of Sediments from Selected Streams. Geol. Surv. Prof. Pap. 433-D 28.

Kim, Y. sang, Tran, T.Q., Kang, G. o., Do, T.M., 2019. Stabilization of a residual granitic soil using various new green binders. Constr. Build. Mater. 223, 724–735. https://doi.org/10.1016/j.conbuildmat.2019.07.019

Kitazume, M., Grisolia, M., Leder, E., Marzano, I.P., Correia, A.A.S., Oliveira, P.J.V., Åhnberg, H., Andersson, M., 2015. Applicability of molding procedures in laboratory mix tests for quality control and assurance of the deep mixing method. Soils Found. 55, 761–777. https://doi.org/10.1016/j.sandf.2015.06.009

Koop, S.H.A., van Leeuwen, C.J., 2017. The challenges of water, waste and climate change in cities. Environ. Dev. Sustain. 19, 385–418. https://doi.org/10.1007/s10668-016-9760-4

Lavagna, L., Nisticò, R., Sarasso, M., Pavese, M., 2020. An analytical mini-review on the compression strength of rubberized concrete as a function of the amount of recycled tires crumb rubber. Materials (Basel). 13. https://doi.org/10.3390/ma13051234

Li, S., Tran, T.Q., Li, Q., Ji, B., Brand, A.S., Zhang, W., 2023. Resources , Conservation & Recycling Zn leaching recovery and mechanisms from end-of-life tire rubber 194. https://doi.org/10.1016/j.resconrec.2023.107004

Liu, L., Wang, C., Liang, Q., Chen, F., Zhou, X., 2023. A state-of-the-art review of rubber modified cement-based materials: Cement stabilized base. J. Clean. Prod. 392, 136270. https://doi.org/https://doi.org/10.1016/j.jclepro.2023.136270

Liu, X., Wang, J., Gheni, A., ElGawady, M.A., 2018. Reduced zinc leaching from scrap tire during pavement applications. Waste Manag. 81, 53–60. https://doi.org/https://doi.org/10.1016/j.wasman.2018.09.045

Lothenbach, B., Krebs, R., Furrer, G., Gupta, S.K., Schulin, R., 1998. Immobilization of cadmium and zinc in soil by Al-montmorillonite and gravel sludge. Eur. J. Soil Sci. 49, 141–148. https://doi.org/10.1046/j.1365-2389.1998.00140.x

Ma, Y., Wang, S., Zhou, H., Hu, W., Polaczyk, P., Huang, B., 2022. Recycled polyethylene and crumb rubber composites modified asphalt with improved aging resistance and thermal stability. J. Clean. Prod. 334, 130102. https://doi.org/10.1016/j.jclepro.2021.130102

Matthews, J.A., 2014. Cation Exchange Capacity (Cec). Encycl. Environ. Chang. https://doi.org/10.4135/9781446247501.n583

Picado-Santos, L.G., Capitão, S.D., Neves, J.M.C., 2020. Crumb rubber asphalt mixtures: A literature review. Constr. Build. Mater. 247, 118577. https://doi.org/10.1016/j.conbuildmat.2020.118577

Poole Jr., S.L., 1998. Scrap and Shredded Tire Fires, Report USFA-TR-093. FEMA, Washington D.C.

Rhodes, E.P., Ren, Z., Mays, D.C., 2012. Zinc leaching from tire crumb rubber. Environ. Sci. Technol. 46, 12856–12863. https://doi.org/10.1021/es3024379

Rodgers, B., 2021. Tire Engineering. CRC Press, Boca Raton. https://doi.org/10.1201/9781003022961

Saberian, M., Rahgozar, M.A., 2016. Geotechnical properties of peat soil stabilised with shredded waste tyre chips in combination with gypsum, lime or cement. Mires Peat 18, 1–16. https://doi.org/10.19189/MaP.2015.OMB.211

Sampson, L.C., Houston, A. V, Randall, J., Barrett, M.E., Street, G., 2014. Technical Report: Water Quality and Hydraulic Performance of Permeable Friction Course on Curbed Sections of Highways.

Shu, X., Huang, B., 2014. Recycling of waste tire rubber in asphalt and portland cement concrete: An overview. Constr. Build. Mater. 67, 217–224. https://doi.org/10.1016/j.conbuildmat.2013.11.027

Sinha, M.K., Sahu, S.K., Pramanik, S., Prasad, L.B., Pandey, B.D., 2016. Recovery of high value copper and zinc oxide powder from waste brass pickle liquor by solvent extraction. Hydrometallurgy 165, 182–190. https://doi.org/10.1016/j.hydromet.2015.09.012

Smolders, E., Degryse, F., 2002. Fate and effect of zinc from tire debris in soil. Environ. Sci. Technol. 36, 3706–3710. https://doi.org/10.1021/es025567p

Song, W., Huang, B., Shu, X., 2018. Influence of warm-mix asphalt technology and rejuvenator on performance of asphalt mixtures containing 50% reclaimed asphalt pavement. J. Clean. Prod. 192, 191–198. https://doi.org/10.1016/j.jclepro.2018.04.269

Standard Methods for the Examination of Water and Wastewater, 2018. , Standard Methods for the Examination of Water and Wastewater. American Public Health Association. https://doi.org/doi:10.2105/SMWW.2882.104

Taheri, S., Khoshgoftarmanesh, A.H., Shariatmadari, H., Chaney, R.L., 2011. Kinetics of zinc release from ground tire rubber and rubber ash in a calcareous soil as alternatives to Zn fertilizers. Plant Soil 341, 89–97. https://doi.org/10.1007/s11104-010-0624-7

Tanesi, J., Ardani, A., 2013. Isothermal calorimetry as a tool to evaluate early-age performance of fly ash mixtures. Transp. Res. Rec. 42–53. https://doi.org/10.3141/2342-06

Tran, T.Q., Behravan, A., Brand, A.S., 2022a. Heat of hydration in clays stabilized by a high-alumina steel furnace slag. Clean. Mater. 5, 100105. https://doi.org/10.1016/j.clema.2022.100105

Tran, T.Q., Skariah Thomas, B., Zhang, W., Ji, B., Li, S., Brand, A.S., 2022b. A comprehensive review on treatment methods for end-of-life tire rubber used for rubberized cementitious materials. Constr. Build. Mater. 359, 129365. https://doi.org/10.1016/j.conbuildmat.2022.129365

Trezza, A.., Scian, N.., 2009. Scrap Tire Ashes in Portland Cement Production 12, 489–494. https://doi.org/10.1590/S1516-14392009000400019

U.S. Tire Manufacturers Association, 2020. 2019 U.S. Scrap Tire Management Summary. Washington D.C.

Vangronsveld, J., Van Assche, F., Clijsters, H., 1995. Reclamation of a Bare Industrial Area Contaminated by Non-ferrous Metals : In-situ Metal Immobilization and Revegetation. Environ. Pollut. 87, 51–59.

Vashisth, P., Lee, K.W., Wright, R.M., 1998. Assessment of water pollutants from asphalt pavement containing recycled rubber in Rhode Island. Transp. Res. Rec. 1626, 95–104. https://doi.org/10.3141/1626-12

Wadsö, L., Winnefeld, F., Riding, K., Sandberg, P., 2016. Calorimetry, in: Scrivener, K., Snellings, R., Lothenbach, B. (Eds.), A Practical Guide to Microstructural Analysis of Cementitious Materials. CRC Press, Boca Raton, pp. 37–74.

Wang, T., Xiao, F., Zhu, X., Huang, B., Wang, J., Amirkhanian, S., 2018. Energy consumption and environmental impact of rubberized asphalt pavement. J. Clean. Prod. 180, 139–158. https://doi.org/10.1016/j.jclepro.2018.01.086

Yadav, J.S., Tiwari, S.K., 2017. A study on the potential utilization of crumb rubber in cement treated soft clay. J. Build. Eng. 9, 177–191. https://doi.org/https://doi.org/10.1016/j.jobe.2017.01.001

Yoon, S., Prezzi, M., Siddiki, N.Z., Kim, B., 2006. Construction of a test embankment using a sand-tire shred mixture as fill material. Waste Manag. 26, 1033–1044. https://doi.org/10.1016/j.wasman.2005.10.009

Zhang, H., Tong, Z., Wei, T., Tang, Y., 2011. Removal characteristics of Zn(II) from aqueous solution by alkaline Ca-bentonite. Desalination 276, 103–108. https://doi.org/10.1016/j.desal.2011.03.026

Chapter 4. Mitigation of zinc and organic carbon leached from end-of-life tire rubber in cementitious composites[3]

The contributions of the authors to this manuscript are described as follows:

Thien Q. Tran: Conceptualization; Data curation; Formal analysis; Investigation; Methodology; Visualization; Writing - original draft; Writing - review and editing.

Note: Thien Q. Tran was in the main charge of all above-mentioned contribution categories under the supervision of Dr. Alexander S. Brand.

Shiyu Li: Investigation; Writing - review and editing.

Bin Ji: Investigation; Writing - review and editing.

Xiang Zhao: Investigation.

Md Hasibul Hasan Rahat: Investigation.

Tu-Nam Nguyen: Investigation.

Bao-Chau Le: Investigation.

Wencai Zhang: Funding acquisition; Supervision; Writing - review and editing.

Alexander S. Brand: Conceptualization; Funding acquisition; Methodology; Project administration; Supervision; Writing - original draft; Writing - review and editing.

[3] **Thien Q. Tran,** Shiyu Li, Bin Ji, Xiang Zhao, Md Hasibul Hasan Rahat, Tu-Nam Nguyen, Bao-Chau Le, Wencai Zhang, Alexander S. Brand. Mitigation of zinc and organic carbon leached from end-of-life tire rubber in cementitious composites" (Under review)

Mitigation of zinc and organic carbon leached from end-of-life tire rubber in cementitious composites

Thien Q. Tran[1], Shiyu Li[2], Bin Ji[2], Xiang Zhao[1], Md Hasibul Hasan Rahat[1], Tu-Nam Nguyen[1], Bao-Chau Le[1], Wencai Zhang[2], and Alexander S. Brand[1,3*]

[1]The Charles Edward Via, Jr. Department of Civil and Environmental Engineering, Virginia Polytechnic Institute and State University, Blacksburg, Virginia, USA, 24061
[2]Department of Mining and Minerals Engineering, Virginia Polytechnic Institute and State University, Blacksburg, Virginia, USA, 24061
[3]Department of Materials Science and Engineering, Virginia Polytechnic Institute and State University, Blacksburg, Virginia, USA, 24061
*Corresponding Author: asbrand@vt.edu

4.1 Abstract

End-of-life tire (ELT) rubber has been widely researched to replace fine or coarse aggregates in cementitious composites. While most studies paid attention to its effect on the engineering properties, very few considered chemical reactions with pore solution and the potential for environmental leachate. Recently the authors developed a methodology to remove zinc from the ELT rubber, since zinc can be toxic if it is leached into the environment. In this study, the authors utilized ELT rubber before and after the zinc extraction process to partially replace fine aggregate in a mortar. Flowability, compressive strength, flexural strength, and ultrasonic pulse velocity were measured for the engineering properties of rubberized mortars. Simultaneously, isothermal calorimetry was also employed to investigate the effects of ELT rubber on the hydration process of the rubberized mortars. In addition, the pore solution and leaching solutions were taken at different curing ages and then analyzed for elemental and total organic carbon (TOC) contents. The results showed a remarkable loss in engineering properties of rubberized mortar when ELT rubber was utilized, and the decrease in performance was more pronounced in the samples with zinc-extracted ELT rubber. The pore solution was found to contain significant quantities of zinc and TOC. However, the authors also found that using silica fume to partially replace cement could effectively recover the loss in strength and could reduce the leachability of zinc and TOC.

Keywords: Rubberized mortar; unconfined compressive strength; isothermal calorimetry; end-of-life tires; zinc leachate.

4.2 Introduction

To ensure the quality of life, particularly in urban areas, to protect and improve the ecosystem, and to preserve natural resources, waste recycling emerges as a critical concern [1–4]. End-of-life tires (ELT) are one of the wastes that has received significant attention (*e.g.*, [5–8]). Three billion ELTs are estimated to be generated yearly around the world [9]. China, the largest ELT producer, discarded around 14.6 million tons of ELTs in 2018 [10]; only 39 % was recovered and the fate of the remaining ELTs was unspecified [11]. Meanwhile, the U.S. discarded 4.46 million tons of

ELTs in 2019, the majority which was recycled, but around 14.3% was landfilled [12], and the U.S. has stockpiled around 56 million ELTs [12]. Some countries generate fewer ELTs but have poorer recycling strategies; for instance, Nigeria and Russia generated 113 thousand tons and 800 thousand tons of ELTs in 2017 and only recycled 5 % and 20 %, respectively [11]. Among the amount of ELT recycled reported by World Business Council for Sustainable Development, there is a relatively small proportion of ELT rubber in civil engineering applications; in particular, this number was only 8.8 % in the U.S., 3 % in Europe, 0.1 % in Japan, and zero in many different countries with large populations including China, India, Indonesia, Brazil, and Nigeria [11].

Tire rubber contains various polymers, such as polybutadiene, polyisoprene, and styrene-butadiene, and carbon black with small amounts of extender oil, stearic acid, zinc oxide, and others [9]. In addition, this material can be detrimental to soil, groundwater, and the atmosphere [13,14]. Particularly, one of the potential polluting agents in ELTs is zinc, which is introduced with 1 % to 2 % of the tire rubber by mass during the vulcanizing process of tire manufacture [9]. According to the findings by Smolders and Degryse [15], up to 40 % of zinc can be leached out from ELT particles (< 100 μm) into the environment after a one-year weathering period during landfilling. Based solely on the current yearly production of ELTs in China and the U.S., there is an estimation of 286 thousand tons of zinc that can be potentially released into the environment if all zinc in the ELT rubber is leached. Zinc exhibits toxicity not only towards a diverse array of organisms, including plants, invertebrates, and fish but also induces damage to the stomach lining in living organisms [16]. The unexpected leaching of zinc from ELTs can lead to adverse harm to ecosystems and cause enduring impacts on the environment [16].

While many traditional industrial wastes and by-products (*e.g.*, recycled concrete aggregates, iron and steel slags, coal ashes, agricultural ashes, *etc*.) are very familiar in cement-based civil engineering applications, ELT rubber has received less attention [17–26]. This is due to some performance limitations, such as low elastic modulus and poor adhesion [25,27]. Meanwhile, although ELT rubber can improve many mechanical engineering properties and durability of portland cement concrete, such as impact resistance, acid resistance, freeze–thaw resistance, and chloride permeability resistance, ELT rubber adversely causes significant reductions in strength [26,28,29]. This is considered the main challenge preventing industries and practitioners from reusing ELT rubber in cement-based materials.

In addition, the zinc leaching potential when using ELT rubber in portland cement concrete has received no attention to the best of the authors' knowledge, and there are no explicit conclusions about this yet. When discussing the fate of zinc leached from ELT rubber, higher zinc concentrations leached from rubber-modified asphalt concrete were reported by some previous studies [30,31], although asphalt concrete reduces the rate of zinc leached from ELT rubber [16]. Zinc has also been reported to leach into soil that is modified by ground ELT rubber [15,32]. Therefore, the zinc leachability of ELT rubber is also considered an environmental issue when using this material in cementitious materials.

In this study, the authors utilized ELT rubber before and after a zinc extraction process to partially replace fine aggregate in a mortar. The treatment process was employed in an attempt to mitigate the environmental effects of leachable zinc from ELT rubber and to collect the zinc in the form of zinc oxide for other markets. First, the effects of "as-received" ELT rubber and treated, zinc-extracted ELT rubber on different engineering properties of the rubberized mortar will be investigated. Also, the zinc leaching potential from these rubberized mortar mixtures will be observed *via* their pore solution and leachate. Second, the work examines whether the presence of silica fume can recover the engineering property loss as well as immobilize the leached zinc from untreated ELT rubber and the remaining leachable zinc from the ELT rubber after the treatment process. The hypothesis behind the silica fume treatment is that it produces additional calcium silicate hydrate (C–S–H) and accordingly increases the cation exchange capacity of the rubberized mixture, thereby immobilizing any zinc and TOC leached from the ELT rubber. While the use of ELT rubber in cementitious composites is not a new topic, the work in this study is novel because it takes into account the fate of the zinc in ELT rubber in conjunction with the engineering properties of rubberized mortar. More significantly, this study takes advantage of silica fume to not only recover the strength loss of rubberized mortar but also immobilize the leached zinc and TOC from the used ELT rubber, which has not been considered previously in the literature.

4.3 Experimental program

4.3.1 Materials

In this study, the ELT rubber was used in the form of powder. Along with an "as-received" form, named "untreated ELT rubber," the rubberized mortars also used the ELT rubber that went through a process where the zinc was extracted, named "treated ELT rubber." The hydrometallurgical treatment process was based on the authors' previously developed methodology [33], where 2.0 M HNO_3 was used to leach the zinc from the ELT rubber and then recover it as ZnO. A solid concentration of 200 g L^{-1} was used for the treatment batch. The treatment process was conducted in a leaching environment of 90 ℃ with agitation at 600 rpm for 5 h, which was able to leach 95 % of the total zinc in the ELT rubber. The specific gravity of untreated and treated ELT rubber was 1.17 and 1.15, respectively. The particle size distribution of the untreated ELT rubber, treated ELT rubber, sand, silica fume, and cement is shown in Figure 4- 1; the median particle size (D_{50}) for each of these materials respectively was 0.375 mm, 0.423 mm, 55.9 µm, 19.7 µm, and 11.2 µm. The ELT rubber particles expanded slightly after treatment, which is evident by the gradation in Figure 4- 1.

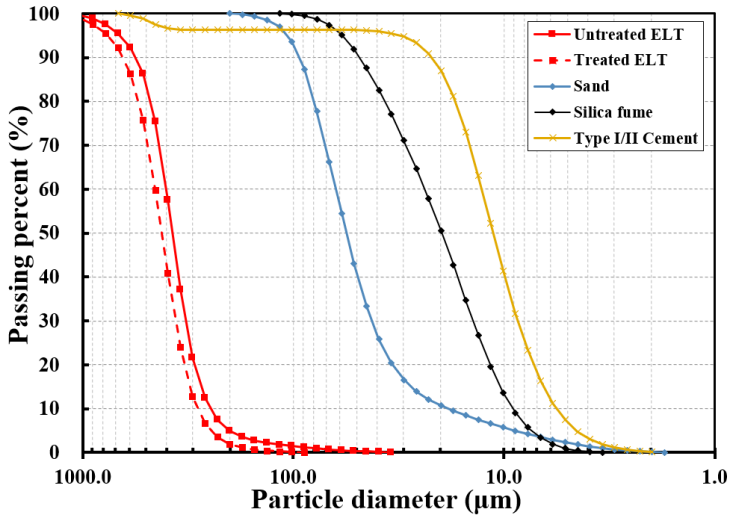

Figure 4- 1. Particle size distribution curves of untreated ELT rubber, treated ELT rubber, sand, silica fume, and cement.

The major metals in the untreated ELT rubber were Mg, Al, Ca, Fe, and Zn, as determined after digestion of the rubber in strong acid, at concentrations of 322 mg kg^{-1}, 505 mg kg^{-1}, 1195 mg kg^{-1}, 503 mg kg^{-1}, and 20,509 mg kg^{-1}, respectively. The chemical composition of cement was determined by X-ray fluorescence analysis and is shown in Table 4- 1.

Table 4- 1. Chemical composition of PC.

Chemical composition (%)	CaO	SiO_2	Al_2O_3	MgO	Fe_2O_3	TiO_2	K_2O
Cement	56.7	30.1	8.4	2.1	2.9	0.2	0.5

4.3.2 Experimental methodology

4.3.2.1 Experimental program and engineering property tests

In this study, a set of experiments was performed to determine the mechanical properties, chemical composition of the pore solution, heat of hydration, and zinc and TOC leaching potential. Untreated and treated ELT rubber were used to replace sand in mortars at 0 % (mixture coded Ref-M), 10 % (mixtures coded URM-10% and TRM-10%), 20 % (mixtures coded URM-20% and TRM-20%), and 30 % (mixtures coded URM-30% and TRM-30%) by sand volume. Cement was used at a dosage of 450 kg/m^3, and the water-to-cement ratio was 0.65. Component materials were mixed following ASTM C305 [34]. After mixing, flowability was immediately measured following ASTM C1437 [35]. For each mix, nine 50-mm cubes and nine 2.5 cm by 2.5 cm by 30 cm beams were cast and tested according to ASTM C109 [36] for the compressive strength and ASTM C78 [37] for the flexural strength, respectively. The samples were stored in a curing room at 23 °C ± 2 °C and 95 % ± 2 % of relative humidity until testing at curing ages of 3 days, 7 days, and 28 days with three replicates. Before each compressive strength test, the ultrasonic pulse velocity (UPV) was measured for each sample according to ASTM C597 [38]. In order to ascertain if the strength loss from ELT rubber could be mitigated, 7.5 % of silica fume was used to replace

cement by its mass in mixtures URM-30% (with 30 % untreated ELT rubber) and TRM-30% (with 30 % treated ELT rubber) to produce two mixtures coded URM-30-SF7.5% and TRM-30-SF7.5%. These two mixtures were also subjected to all of the tests mentioned earlier.

In terms of durability, the rapid chloride penetrability test (RCPT) was performed for all investigated mixtures following ASTM 1202 [39]. The RCPT value can be one of the key factors indicative of the diffusivity of concrete, which is closely related to the initiation of concrete deterioration [40]. Multiple 100 mm diameter by 200 mm high cylindrical specimens were prepared and cured for 28 days for each mixture. The mixture proportions and performed experiments for different rubberized mortar mixtures are presented in Table 4- 2.

Isothermal calorimetry (IC) was performed using a Calmetrix I-Cal Flex to quantify the thermal power (W/g_{cement}) along with the total heat (J/g_{cement}) of various rubberized mortar mixtures during the hydration process. After the rubberized mortar mixtures were well mixed in 15-mL plastic vials, the vials were then immediately transferred to the 23 ℃ isothermal chamber. The heat of hydration was observed for up to a curing time of 60 hours. Data were collected after 30 minutes of adding the vial to the chamber to allow for thermal equilibrium. To examine the hydration heat evolution in the rubberized mortar mixtures and how it differs from the reference mixture without ELT rubber added, mixtures labeled Ref-M, URM-10%, URM-20%, URM-30%, TRM-10%, TRM-20%, and TRM-30%, were subjected to the IC experiments.

Scanning electron microscopy (SEM) was used to study the changes in the microstructure of the ELT rubber particles before and after the zinc-recovery treatment process. For these analyses, samples were vacuum-dried to remove moisture prior to the tests. A JEOL IT-500HR SEM with a source of Schottky field emission electron was employed for this work. A ~12 nm thick platinum/palladium layer was used to coat the samples before the investigation.

For the pore solution extraction (PSE), cylindrical specimens with diameters of 50 mm and lengths of 100 mm were prepared. The PSE device used in this investigation was configured following the Barneyback and Diamond system [41]. PSE was performed after 3 days, 7 days, and 14 days of curing for mixtures URM-30% and TRM-30% (without silica fume added) versus URM-30-SF7.5% and TRM-30-SF7.5% (with silica fume added). The applied pressure for extracting the solution from pores was increased from 0 MPa to 450 MPa until 5 mL to 10 mL of solution was obtained. The obtained pore solution was then filtered (if needed) and instantly acidified by 2 % of 12.1 N HCl by the solution volume to prevent precipitation. Ultimately, the extracted pore solution at a certain curing time was analyzed for zinc concentration using a Thermo Electron iCAP-RQ inductively coupled plasma mass spectrometer (ICP-MS) and for TOC concentration using a Shimadzu TOC-VCSN.

The leaching test was performed by soaking the crushed compressive strength samples of the four above-mentioned mixtures in deionized water at a liquid-to-solid (L/S) ratio equal to 8. After 3 days, 7 days, and 28 days of soaking, 20 mL of the leachate of each mixture was taken, acidified with the same procedure described earlier, and subjected to ICP-MS and TOC analyses for zinc and TOC concentration measurements, respectively.

Table 4- 2. Proportion of mixtures and performed experiments.

Note	Codes	w/b ratio	Mortar proportion (kg/m^3)					Performed experiments							
			Cement	Silica Fume	Sand	Rubber	Water	UCS	FS	RCPT	UPV	IC	SEM	PSE	Leaching test
Untreated ELT rubber	-	-	-	-	-	-	-	-	-	-	-	-	√	-	-
Treated ELT rubber	-	-	-	-	-	-	-	-	-	-	-	-	√	-	-
Control mixture	Ref-M	0.65	450	-	1350	0.00	292.5	√	√	√	√	√	-	-	-
RM-10 (10% rubber)	URM-10%	0.65	450	-	1214	59.63	292.5	√	√	√	√	√	-	-	-
	TRM-10%	0.65	450	-	1214	58.70	292.5	√	√	√	√	√	-	-	-
RM-20 (20% rubber)	URM-20%	0.65	450	-	1079	119.26	292.5	√	√	√	√	√	-	-	-
	TRM-20%	0.65	450	-	1079	117.41	292.5	√	√	√	√	√	-	-	-
RM-30 (30% rubber)	URM-30%	0.65	450	-	944	178.89	292.5	√	√	√	√	√	-	√	√
	TRM-30%	0.65	450	-	944	176.11	292.5	√	√	√	√	√	-	√	√
RM-30-7.5 % -(30 % rubber + 7.5% Silica)	URM-30-SF7.5%	0.65	416.25	33.75	944	161.00	270.5625	√	√	√	√		-	√	√
	TRM-30-SF7.5%	0.65	416.25	33.75	944	158.50	270.5625	√	√	√	√		-	√	√

Note: UCS: unconfined compressive strength; FS: flexural strength; RCPT: rapid chloride penetration test; IC: isothermal calorimetry; SEM: scanning electron microscopy; SPE: pore solution extraction.

4.4 Results and discussion

4.4.1 Flowability

Figure 4- 2 compares the flowability of the reference mortar versus different rubberized mortar mixtures. The data suggest that untreated ELT rubber enhanced the flowability of rubberized mortar from 6 % (*i.e.*, mixtures URM-10% and URM-30%) to 12 % (*i.e.*, mixture URM-20%). Meanwhile, only 10 % of treated ELT rubber added (*i.e.*, mixtures TRM-10%) increased the mixture's flowability by around 5 %, and the addition of 20 % and 30 % (*i.e.*, mixtures TRM-20% and TRM-30%) reduced the flow by up to 6 %. When silica fume was added, the flowability of mixtures URM-30% and TRM-30% remarkably reduced by 6 % and 13 %, respectively; this reduction in flowability is attributed to the higher water demand of silica fume compared to cement.

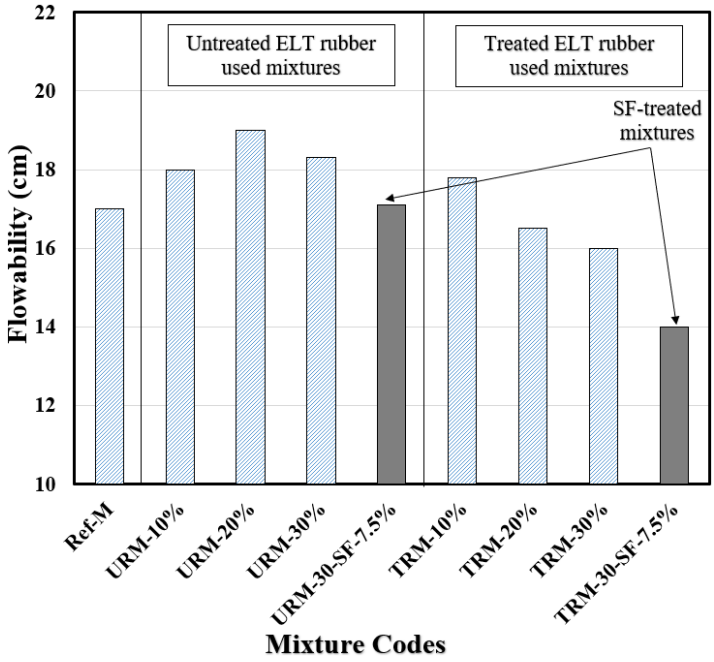

Figure 4- 2. Flowability of different rubberized mortars.

4.4.2 Unconfined compressive strength (UCS)

Figure 4- 3 illustrates the UCS of the reference mortar relative to the different rubberized mortar mixtures. The compressive strength of the reference mixture reached 18.3 MPa after 28 days of curing. The strength of the mortar dropped significantly with the introduction of ELT rubber. Specifically, 36 %, 55 %, and 64 % of strength was lost with the addition of 10 %, 20 %, and 30 % of untreated ELT rubber, respectively. These losses increased to be 40 %, 62 %, and 72 %, respectively, when treated ELT rubber was used.

The effect of the zinc-recovery treatment process on the UCS of rubberized cementitious mixtures was not recognizable at 10 % of ELT rubber replacement since the means of UCS values of mixtures URM-10% and TRM-10% were found not to be different by a one-tailed paired t-test with a confidence of 95 %. It became clearer when the replacement percentage increased (*i.e.*, 20

% and 30 %) that treated ELT rubber reduced the UCS more than the untreated ELT rubber; the means of UCS of mixtures URM-20% and TRM-20% and URM-30% and TRM-30% were found to be different by a one-tailed paired t-test with confidences of 95 % and 94 %, respectively.

However, with the addition of SF, the strength of rubberized mortars using 30 % of untreated ELT rubber and 30 % of treated ELT rubber was enhanced by 48 % and 37 %, respectively, relative to the mixtures without SF; these means were confirmed to be different by one-tailed t-test with a confidence of 95 %. It is well-known that SF undergoes a pozzolanic reaction with the calcium hydroxide produced during cement hydration to yield C–S–H [42,43], so it is likely that this is the primary reason for the increased UCS.

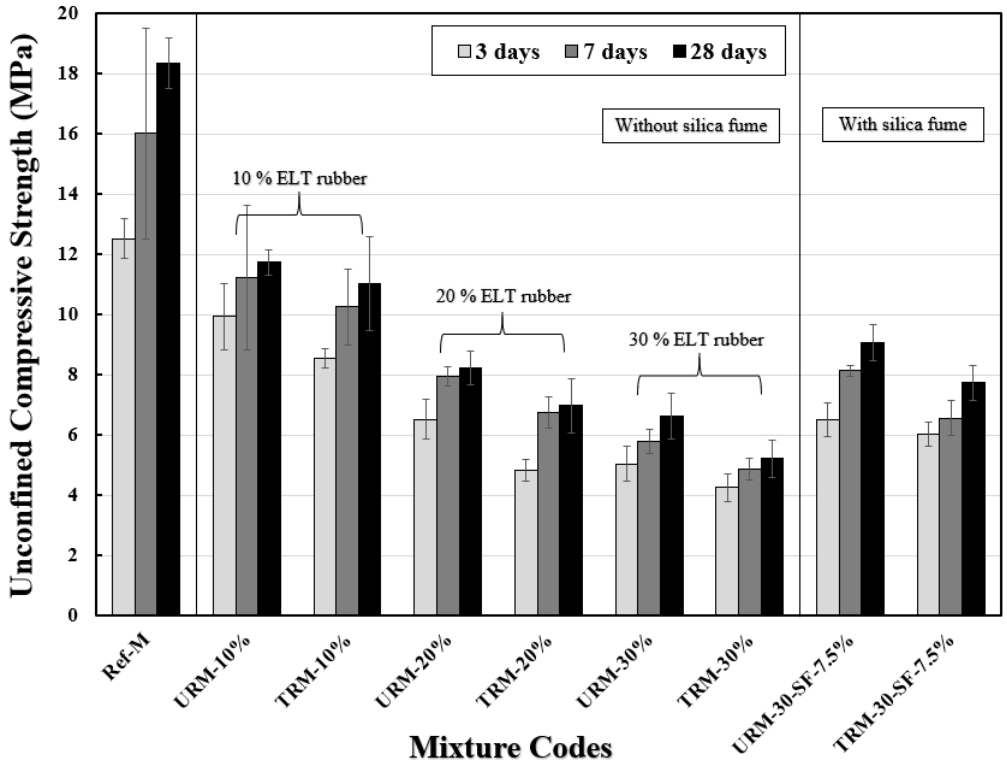

Figure 4- 3. Unconfined compressive strength of different rubberized mortars.

4.4.3 Flexural strength

The flexural strength of reference mortar relative to the different rubberized mortars is presented in Figure 4- 4. The flexural strength of the reference mortar reached 6.2 MPa at 28 days of curing time. In general, the introduction of ELT rubber dramatically reduced the flexural strength of the mortar. Specifically, 22 %, 42 %, and 50 % of the mortar flexural strength was lost with the addition of 10 %, 20 %, and 30 % of untreated ELT rubber, respectively. These losses were 29 %, 45 %, and 64 %, respectively, when treated ELT rubber was used. In line with what was observed from the UCS results, the ELT rubber treatment process seemed to result in worse flexural strength performance. However, the effect of the zinc-recovery treatment process on the flexural strength of rubberized cementitious mixtures was not clear at 10 % and 20 % of ELT rubber replacement since the means of flexural strength of mixtures URM-10% and TRM-10% and URM-20% and

TRM-20% were not found to be different by a one-tailed paired t-test with a confidence of 95 %. The reduction was more recognizable when the replacement percentage was 30 %; the means of flexural strength values of mixtures URM-30% and TRM-30% were found to be different by one-tailed paired t-test with a confidence of 95 %.

In addition, while SF could effectively improve the UCS strength of the rubberized mortar, it was slightly detrimental to the flexural strength. In particular, the flexural strength of rubberized mortars using 30 % of untreated ELT rubber and 30 % of treated ELT rubber respectively dropped by 10 % and 18 % when SF was used relative to the mixtures without SF; even though these means were confirmed to be similar by one-tailed paired t-test with a confidence of 95 %. However, Figure 4- 4 visibly shows that the SF had negative to no effects on the flexural strength improvement. It is known that the addition of SF can embrittle cementitious materials [44], so this is postulated as the likely cause of the reduced performance.

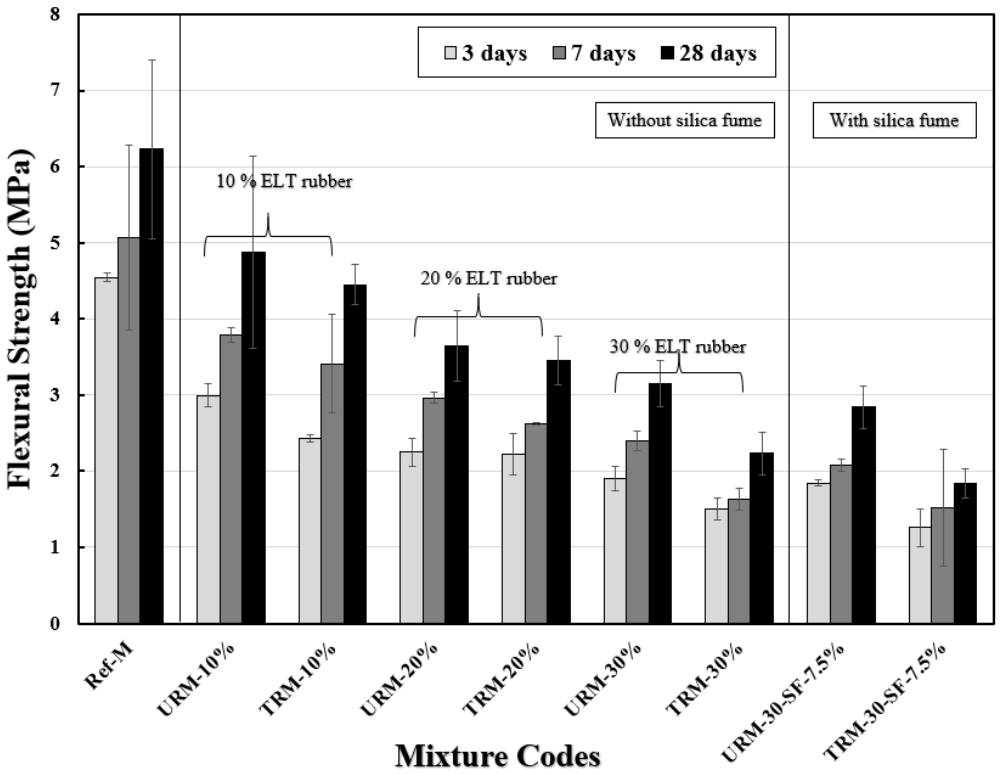

Figure 4- 4. Flexural strength of different rubberized mortars.

4.4.4 Ultrasonic pulse velocity (UPV)

Figure 4- 5 shows the UPV of the reference mortar relative to the different rubberized mortars. The reference mortar had a UPV value of 4026 m/s after 28 days of curing. Similarly, the use of ELT rubber reduced the UPV of the mortar by 8 %, 19 %, and 27 % with the addition of 10 %, 20 %, and 30 % of untreated ELT rubber, respectively. These losses were increased to 10 %, 24 %, and 30 %, respectively, when treated ELT rubber was used. The effect of the zinc-recovery treatment process on the UPV of rubberized cementitious mixtures was not recognizable at 10 % of ELT rubber replacement since the means of UPV of mixtures URM-10% and TRM-10% were

not found to be different by a one-tailed paired t-test with a confidence of 95 %. It became clearer when the replacement percentage increased (*i.e.*, 20 % and 30 %) that treated ELT rubber reduced the UPV more than the untreated ELT rubber; the means of UPV values of mixtures URM-20% and TRM-20% and URM-30% and TRM-30% were found to be different by one-tailed paired t-test with a confidence of 95 %. The addition of SF was ineffective, since the UPV kept mostly unchanged with insignificant standard deviation when SF was used for the mixtures with 30 % ELT rubber; the means were not different by a one-tailed paired t-test with a confidence of 95 %.

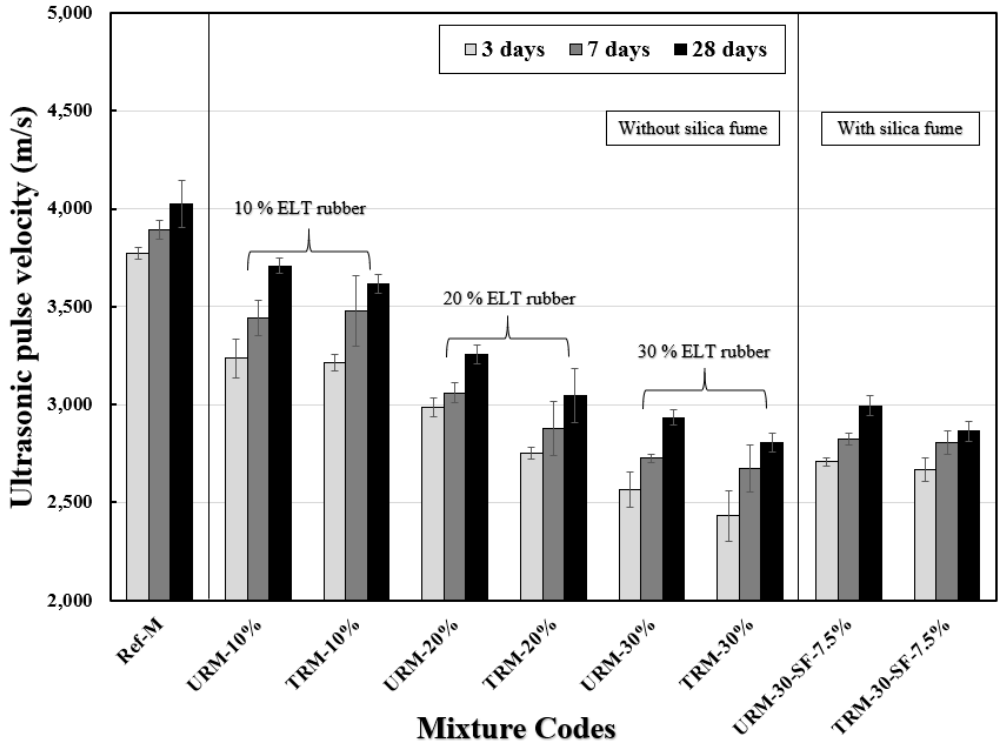

Figure 4- 5. UPV of different rubberized mortars.

4.4.5 Rapid chloride penetrability test (RCPT)

Figure 4- 6 shows the RCPT results of the reference mortar relative to the different rubberized mortars. The use of untreated ELT rubber could effectively reduce the RCPT value by up to 7 % (with 30 % ELT rubber added) relative to the reference mixture; these means were confirmed to be different by one-tailed paired t-test with a confidence of 95 %. Meanwhile, the treated ELT rubber insignificantly increased the RCPT value by up to 3 % (with 30 % ELT rubber added), which is negligible since the means were not different by a one-tailed paired t-test with a confidence of 95 %. For the untreated ELT rubber, the RCPT value, in general, decreased with increasing ELT rubber content, which agrees with Oikonomou and Mavridou [45], although the treated ELT rubber did not appear to follow the same trend.

With the addition of SF, the RCPT value decreased by up to 84 % for both mixtures with 30 % of ELT rubber. This indicates that the SF is very beneficial in chloride migration resistance of the conventional mortar since its RCPT value decreased from the range of 8000 to 9000 Coulombs

(classified as a material with high chloride ion penetrability) to the range of 1484 to 1599 Coulombs (low chloride ion penetrability). These findings are in very good agreement with Bentz's commentary [40] that the C–S–H resulting from the pozzolanic reaction of SF possess a diffusivity that is 25 times less than that of regular C–S–H produced by cement hydration.

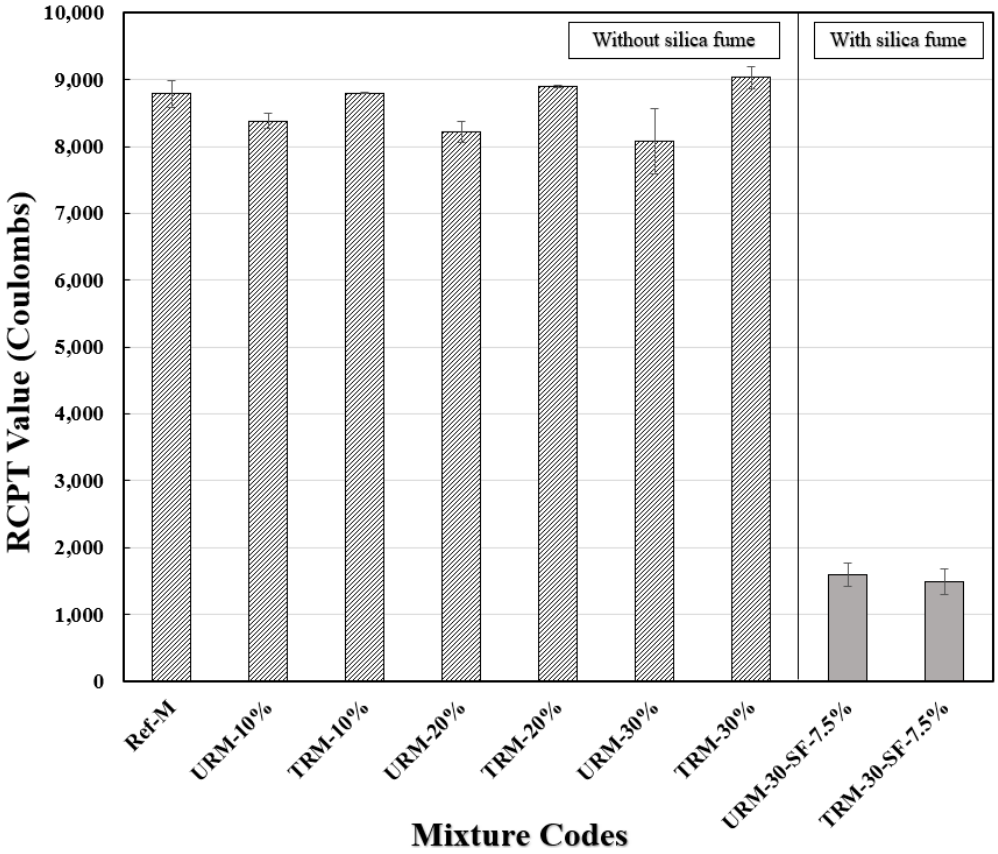

Figure 4- 6. RCPT results of different rubberized mortars.

4.4.6 Isothermal calorimetry (IC)

The thermal power generated from reference mortar and different rubberized mortar mixtures is graphically shown in Figure 4- 7. The data reveal that, during the hydration process, most rubberized mortar mixtures (up to 20 % of ELT replacement) generally generated similar peak thermal power compared to that of the reference mixture with a variation of around 4 %. However, rubberized mortars using 30 % of untreated ELT rubber (URM-30%) and 30 % of treated ELT rubber (TRM-30%) resulted in peak thermal power that were 8 % and 12 % higher than the reference mixture. A study by Bazzoni *et al*. [46] found that zinc could homogeneously incorporate into the C–S–H, increasing the C–S–H nucleation and growth, thereby inducing a higher thermal power peak as a result. These findings are in line with what the authors observed in this study.

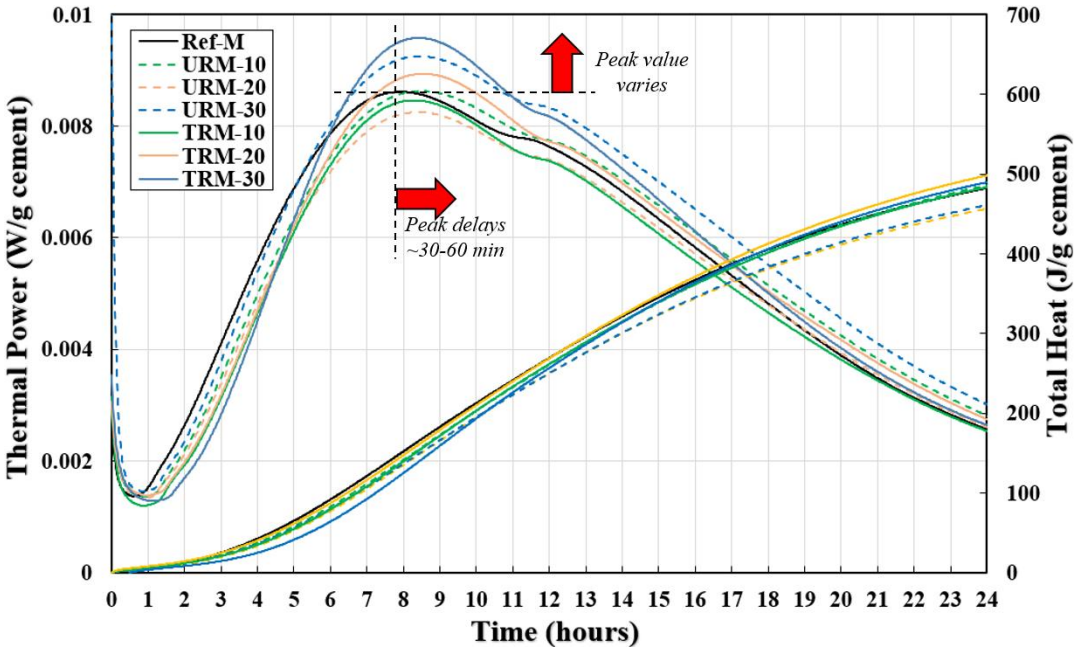

Figure 4- 7. The thermal power generated from different rubberized mortars.

Secondly, it can be seen that the peak of thermal power curves of all rubberized mortars was delayed by around one hour compared to the peak of the reference case, which indicates that the presence of ELT rubber slightly delays the hydration process of the mortar. The retardations might be attributed to the contamination of the hydration media *via* zinc leached from the ELT rubber to the mortar mixture's pore solution. These findings are in good agreement with some previous studies by Ataie *et al.* [47] and Garg and White [48]. It is also possible that organic compounds leached from the ELT rubber could detrimentally affect hydration [49]. The peak differences (hour) and peak value (W/g_{cement}) of various rubberized mortars are presented in Table 4- 3.

Table 4- 3. Hydration thermal power of different rubberized mortars.

Mix code	1st Peak (h)	1st Peak delay (h)	1st Peak (W/g_{cement})	Peak value difference (%)	2nd Peak (h)	2nd Peak delay (h)
Ref-M	7.5	N/A	$0.86x10^{-2}$	N/A	10.8	N/A
URM-10%	8.5	1.0	$0.86x10^{-2}$	0.0	12.0	1.2
TRM-10%	8.5	1.0	$0.85x10^{-2}$	-1.2	11.8	1.0
URM-20%	8.5	1.0	$0.83x10^{-2}$	-3.5	11.8	1.0
TRM-20%	8.7	1.2	$0.89x10^{-2}$	3.5	12.3	1.5
URM-30%	8.5	1.0	$0.93x10^{-2}$	8.1	11.5	0.7
TRM-30%	8.5	1.0	$0.96x10^{-2}$	11.6	12.0	1.2

Table 4- 4. Hydration total heat generated from different rubberized mortars.

Mix code	Total heat (J/g_{cement}) (percent difference between modified mixtures and PC)			
	12 h	24 h	48 h	60 h
Ref-M	269	483	595	626
URM-10%	261 (-2.9)	486 (0.6)	606 (1.8)	638 (1.9)
TRM-10%	250 (-7.1)	484 (0.2)	565 (-5.0)	595 (-5.0)
URM-20%	250 (-7.1)	461 (-4.5)	570 (-4.2)	599 (-4.3)
TRM-20%	262 (-2.6)	484 (0.2)	599 (0.67)	630 (0.6)
URM-30%	268 (-0.4)	497 (2.9)	620 (4.2)	652 (4.2)
TRM-30%	257 (-4.5)	490 (1.4)	610 (2.52)	643 (2.7)

In addition to the thermal power, Figure 4- 7 simultaneously presents the total heat measured from mixing to 24 hours. Due to the retardation in hydration induced by the ELT rubber, rubberized mortars generated less heat (up to 7 % less) than the reference mixture in the first 12 h. This difference was only around 5 % after 24 h and up to 60 h of hydration. The detailed total heat of each mortar mixture over time up to 60 h of curing can be seen in Table 4- 4.

4.4.7 Microstructure study

Secondary electron imaging with SEM was conducted on the untreated (Figure 4- 8a) and treated (Figure 4- 8b) ELT rubber particles. As can be seen in Figure 4- 8a, the untreated ELT rubber particle appeared with a rough surface and angular and irregular shapes with no visible microcracks. In contrast, Figure 4- 8b reveals that the treated ELT rubber developed appreciable cracks on its surface as a result of the zinc-recovery treatment process. This phenomenon observed after the zinc-recovery treatment was previously reported and is believed to increase the ELT rubber's specific surface area [33]. These cracks would suggest that the treated ELT rubber particles would fracture more easily under load, thereby reducing the mechanical performance of the mortar, as was observed in the compressive and flexural strength tests.

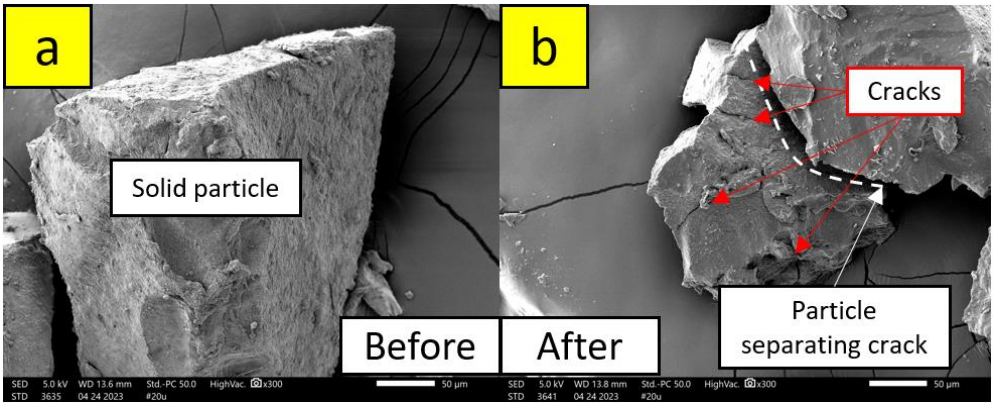

Figure 4- 8. SEM images of the (a) untreated ELT rubber particles and (b) treated ELT rubber particles.

4.4.8 Environmental tests

Figure 4- 9 compares the zinc concentration in the extracted pore solution of rubberized mortar mixtures with SF (URM-30% and URM-30%) and without SF (URM-30-SF7.5% and TRM-30-SF7.5%). First, it can be recognized that the rubberized mortar using 30 % treated ELT rubber leached more zinc than the one using 30 % untreated ELT rubber after 14 days of curing, which indicates that the zinc-recovery treatment could not remove all zinc in the ELT rubber particle completely. This agrees with the previous study by Li *et al.* [33]. The remaining zinc in the ELT rubber particles seems to be more leachable than the one in the untreated particles due to the higher specific surface and more porous character with cracks in the treated particles, as was seen in Figure 4- 9. Second, it can be seen that there was not much difference between the zinc concentration recorded in the extracted pore solution of rubberized mortars with and without SF added.

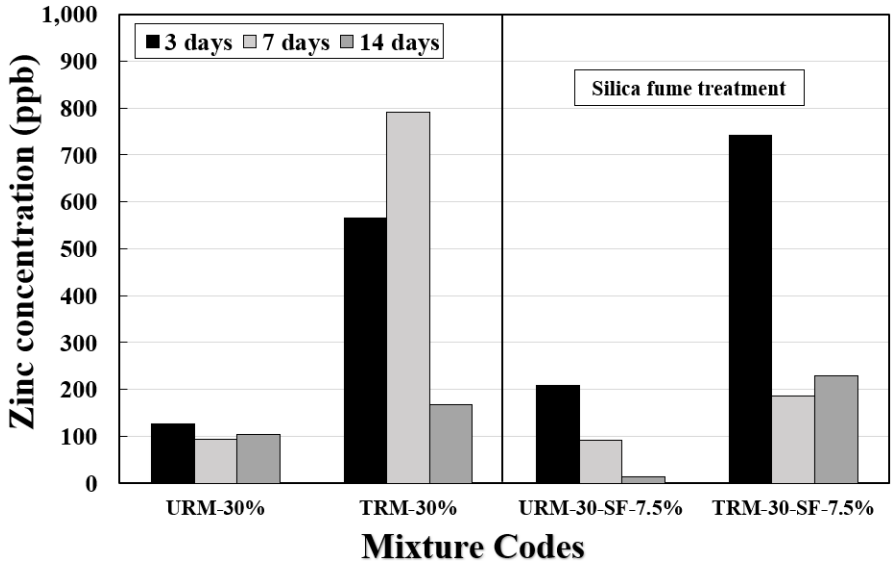

Figure 4- 9. Zinc concentration in the extracted pore solution of rubberized mortar mixtures.

Figure 4- 10 compares the zinc concentration in the leachate of rubberized mortar mixtures with SF (URM-30% and URM-30%) and without SF (URM-30-SF7.5% and TRM-30-SF7.5%). After 28 days of soaking, the mixtures URM-30% and URM-30% respectively yielded 57 ppb to 65 ppb of zinc in the leachate. This amount was reduced by 74 % and 57 %, respectively, after the addition of SF. Since the rubberized mortars with SF yielded negligible zinc concentrations in their leachate, this indicates that the SF addition was very effective in zinc immobilization for rubberized mortar. The mechanism of zinc captureability of SF can be explained by the cation exchange capacity (CEC) of the main hydration product, C–S–H, which has been shown to have the ability to capture heavy metals [50]. As mentioned earlier, the addition of SF promotes the formation C–S–H through the pozzolanic reaction, hence increasing the total CEC of the rubberized mortar. The additional C–S–H produced by the presence of SF should densify the rubberized cementitious matrix, which would help to restrain the leached zinc from releasing into solution. Eventually, more zinc was immobilized compared to the mixtures without SF used.

Although the zinc concentration monitored in all mixtures' leachates satisfied the zinc content requirement for drinking water (< 5 ppm) [51], it deserves to note that the zinc immobilization of the rubberized mortar mixtures was improved more effectively due to the existence of SF in the mixtures.

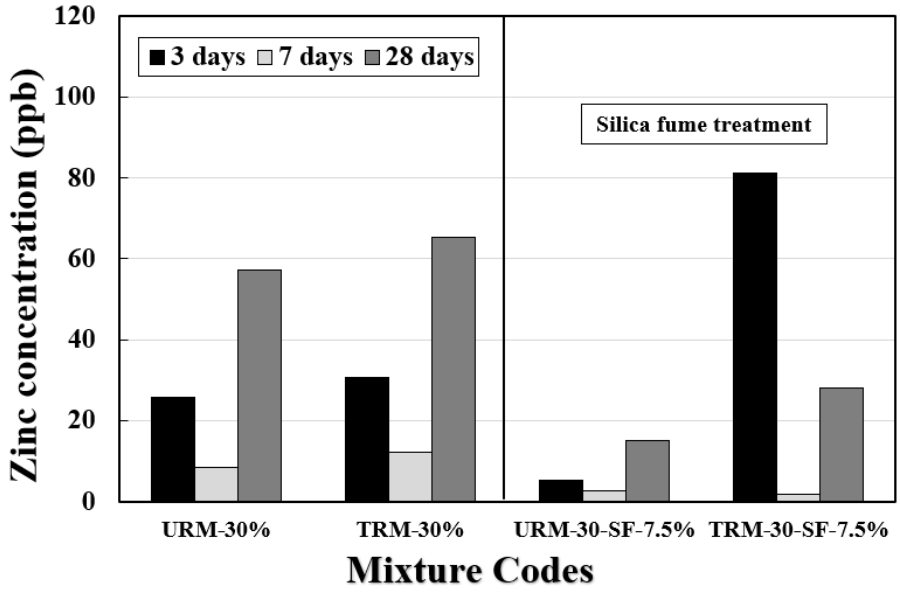

Figure 4- 10. Zinc concentration in the leachate of rubberized mortar mixtures.

Figure 4- 11 compares the TOC concentration in the extracted pore solution of rubberized mortar mixtures without SF (URM-30% and URM-30%) and with SF (URM-30-SF7.5% and TRM-30-SF7.5%). Similar to the zinc concentration observed earlier, TOC concentration in the pore solution of the rubberized mortar using 30 % treated ELT (11.8 g/L) more than doubled that of the one using 30 % untreated ELT rubber (0.5 g/L). This is attributed to the higher specific surface and more porous character with cracks of the treated ELT particles (Figure 4- 8), which could allow carbon content to leach out more easily.

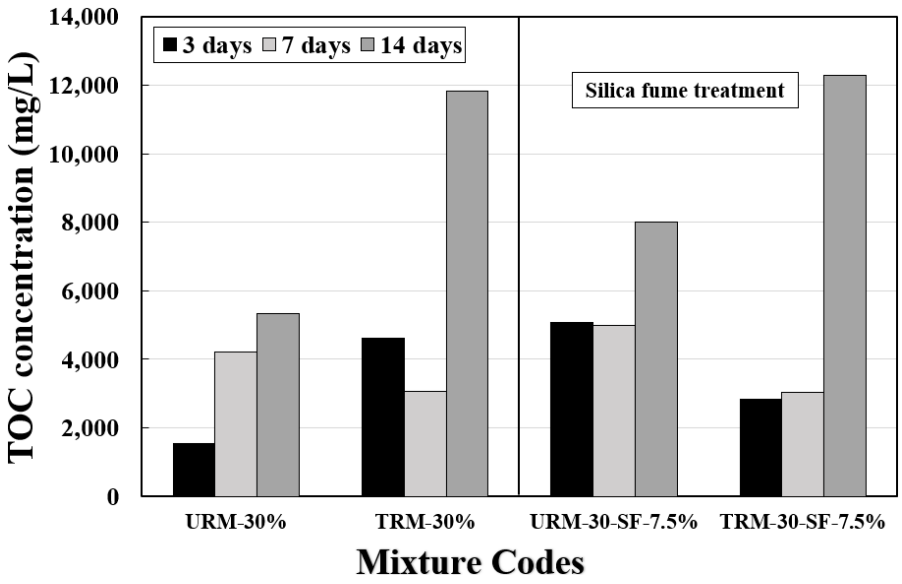

Figure 4- 11. TOC in the pore solution of rubberized mortar mixtures.

Figure 4- 12 compares the TOC concentration in the leachate of rubberized mortar mixtures without SF (URM-30% and URM-30%) and with SF (URM-30-SF7.5% and TRM-30-SF7.5%). Generally, the TOC content in the leachate of all rubberized mortar mixtures increased over time. At 28 days of soaking, the mixtures URM-30% and URM-30% respectively released 841 mg/L to 360 mg/L of TOC concentration in the leachate, which were much higher than the TOC threshold for drinking water (25 mg/L) [52]. However, the addition of SF could reduce the TOC is the leachate by more than 80 %. This significant reduction can be explained by densification of the microstructure when SF is used [53], which can be expected to decrease the transport properties of the mortar. These findings indicate that silica fume not only can immobilize zinc but can also capture the TOC leached from ELT rubber particles.

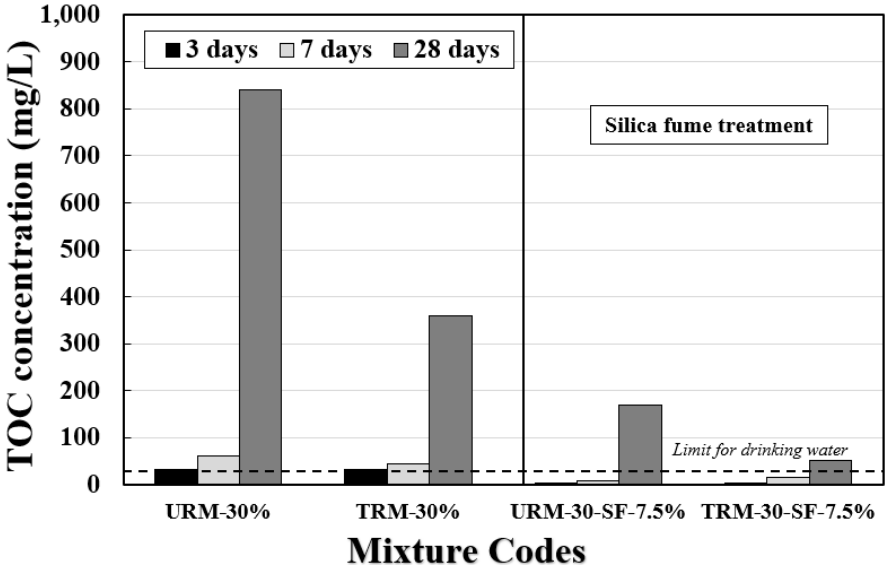

Figure 4- 12. TOC in the leachate of rubberized mortar mixtures.

4.5 Conclusions

In this study, the effects of untreated ELT rubber and the zinc-recovered treated ELT rubber on rubberized mortar mixtures were investigated in terms of engineering and environmental aspects. The effects of silica fume were also explored. The main conclusions drawn from this research are:

1. Untreated ELT rubber enhanced the flowability of the rubberized mortars. Meanwhile, a high percentage of treated ELT rubber addition (*i.e.*, 20 % and 30 %) and the presence of silica fume decreased the flowability of the rubberized mortars.
2. The engineering properties of mortars (*i.e.*, UCS, flexural strength, and UPV) dropped significantly as higher amounts of ELT rubber were used. The treatment process for zinc recovery from ELT rubber further reduced these properties.
3. The results successfully proved that silica fume could effectively recover the lost strength and significantly mitigate the RCPT value of rubberized mortar.
4. The utilization of ELT rubber generally delayed the hydration peak of the mortar for roughly one hour. The existence of ELT rubber at a high percent (30%) slightly increased the hydration peak value and accumulated hydration heat.
5. The zinc-recovery treatment process seemed to allow the remaining zinc to leach out from the treated ELT rubber more easily than the untreated one.
6. Silica fume proved to be very efficient in zinc and TOC immobilization since it could capture up to 74 % of leachable zinc and 86 % of TOC contents in the leachate of rubberized mortars after 28 days of soaking.

Acknowledgement

This study was supported by the Center for Tire Research (CenTiRe), Project SUST-2021-D14-4. The authors acknowledge Lehigh Technologies for providing the waste tire rubber and Short Mountain Silica for providing sand for this work. The authors thank Jeffrey Parks, Jody Smiley, Madeline E. Schreiber, and Aaron J. Prussin II, for their assistance with ICP-MS and TOC analyses.

References

[1] X. Bai, T. McPhearson, H. Cleugh, H. Nagendra, X. Tong, T. Zhu, Y.-G. Zhu, Linking urbanization and the environment: Conceptual and empirical advances, Annu. Rev. Environ. Resour. 42 (2017) 215–240. https://doi.org/10.1146/annurev-environ-102016-061128.

[2] S.H.A. Koop, C.J. van Leeuwen, The challenges of water, waste and climate change in cities, Environ. Dev. Sustain. 19 (2017) 385–418. https://doi.org/10.1007/s10668-016-9760-4.

[3] S. Khan, R. Anjum, S.T. Raza, N.A. Bazai, M. Ihtisham, Technologies for municipal solid waste management: Current status, challenges, and future perspectives, Chemosphere. 288 (2022) 132403. https://doi.org/10.1016/j.chemosphere.2021.132403.

[4] B. Esmaeilian, B. Wang, K. Lewis, F. Duarte, C. Ratti, S. Behdad, The future of waste management in smart and sustainable cities: A review and concept paper, Waste Manag. 81 (2018) 177–195. https://doi.org/10.1016/j.wasman.2018.09.047.

[5] J. Araujo-Morera, R. Verdejo, M.A. López-Manchado, M. Hernández Santana, Sustainable mobility: The route of tires through the circular economy model, Waste Manag. 126 (2021) 309–322. https://doi.org/https://doi.org/10.1016/j.wasman.2021.03.025.

[6] M.S. Abbas-Abadi, M. Kusenberg, H.M. Shirazi, B. Goshayeshi, K.M. Van Geem, Towards full recyclability of end-of-life tires: Challenges and opportunities, J. Clean. Prod. 374 (2022) 134036. https://doi.org/https://doi.org/10.1016/j.jclepro.2022.134036.

[7] S. Dabic-Miletic, V. Simic, S. Karagoz, End-of-life tire management: A critical review, Environ. Sci. Pollut. Res. 28 (2021) 68053–68070. https://doi.org/10.1007/s11356-021-16263-6.

[8] J. Thomas, R. Patil, The road to sustainable tire materials: Current state-of-the-art and future perspectives, Environ. Sci. Technol. 57 (2023) 2209–2216. https://doi.org/10.1021/acs.est.2c07642.

[9] B. Rodgers, Tire Engineering, CRC Press, Boca Raton, 2021. https://doi.org/10.1201/9781003022961.

[10] B. Chen, D. Zheng, R. Xu, S. Leng, L. Han, Q. Zhang, N. Liu, C. Dai, B. Wu, G. Yu, J. Cheng, Disposal methods for used passenger car tires: One of the fastest growing solid wastes in China, Green Energy Environ. (2021). https://doi.org/10.1016/j.gee.2021.02.003.

[11] WBCSD, Global ELT Management-A global state of knowledge on regulation, management systems, impacts of recovery and technologies, World Bus. Counc. Sustain. Dev. (2019) 57. https://docs.wbcsd.org/2019/12/Global_ELT_Management - A global state of knowledge on regulation management systems impacts of recovery and technologies.

[12] U.S. Tire Manufacturers Association, 2019 U.S. Scrap Tire Management Summary, Washington D.C., 2020.
[13] M. Gualtieri, M. Andrioletti, C. Vismara, M. Milani, M. Camantini, Toxicity of tire debris leachates, Environ. Int. 31 (2005) 723–730. https://doi.org/10.1016/j.envint.2005.02.001.
[14] C. Halsband, L. Sørensen, A.M. Booth, D. Herzke, Car tire crumb rubber: Does leaching produce a toxic chemical cocktail in coastal marine systems?, Front. Environ. Sci. 8 (2020) 125. https://doi.org/10.3389/fenvs.2020.00125.
[15] E. Smolders, F. Degryse, Fate and effect of zinc from tire debris in soil, Environ. Sci. Technol. 36 (2002) 3706–3710. https://doi.org/10.1021/es025567p.
[16] X. Liu, J. Wang, A. Gheni, M.A. ElGawady, Reduced zinc leaching from scrap tire during pavement applications, Waste Manag. 81 (2018) 53–60. https://doi.org/10.1016/j.wasman.2018.09.045.
[17] R.A. Assaggaf, M.R. Ali, S.U. Al-Dulaijan, M. Maslehuddin, Properties of concrete with untreated and treated crumb rubber – A review, J. Mater. Res. Technol. 11 (2021) 1753–1798. https://doi.org/10.1016/j.jmrt.2021.02.019.
[18] M. Valente, A. Sibai, Rubber/crete: Mechanical properties of scrap to reuse tire-derived rubber in concrete; A review, J. Appl. Biomater. Funct. Mater. 17 (2019). https://doi.org/10.1177/2280800019835486.
[19] A. Adesina, O.D. Atoyebi, Effect of crumb rubber aggregate on the performance of cementitious composites: A review, IOP Conf. Ser. Earth Environ. Sci. 445 (2020) 012032. https://doi.org/10.1088/1755-1315/445/1/012032.
[20] R. Roychand, R.J. Gravina, Y. Zhuge, X. Ma, O. Youssf, J.E. Mills, A comprehensive review on the mechanical properties of waste tire rubber concrete, Constr. Build. Mater. 237 (2020) 117651. https://doi.org/10.1016/j.conbuildmat.2019.117651.
[21] X. Shu, B. Huang, Recycling of waste tire rubber in asphalt and portland cement concrete: An overview, Constr. Build. Mater. 67 (2014) 217–224. https://doi.org/https://doi.org/10.1016/j.conbuildmat.2013.11.027.
[22] B.S. Thomas, R.C. Gupta, A comprehensive review on the applications of waste tire rubber in cement concrete, Renew. Sustain. Energy Rev. 54 (2016) 1323–1333. https://doi.org/10.1016/j.rser.2015.10.092.
[23] J. XU, Z. Yao, G. Yang, Q. Han, Research on crumb rubber concrete: From a multi-scale review, Constr. Build. Mater. 232 (2020) 117282. https://doi.org/10.1016/j.conbuildmat.2019.117282.
[24] L. Lavagna, R. Nisticò, M. Sarasso, M. Pavese, An analytical mini-review on the compression strength of rubberized concrete as a function of the amount of recycled tires crumb rubber, Materials (Basel). 13 (2020). https://doi.org/10.3390/ma13051234.
[25] P. Kara De Maeijer, B. Craeye, J. Blom, L. Bervoets, Crumb Rubber in Concrete—The Barriers for Application in the Construction Industry, Infrastructures. 6 (2021). https://doi.org/10.3390/infrastructures6080116.

[26] T.Q. Tran, B. Skariah Thomas, W. Zhang, B. Ji, S. Li, A.S. Brand, A comprehensive review on treatment methods for end-of-life tire rubber used for rubberized cementitious materials, Constr. Build. Mater. 359 (2022) 129365. https://doi.org/10.1016/j.conbuildmat.2022.129365.
[27] A. Alsaif, S.A. Bernal, M. Guadagnini, K. Pilakoutas, Freeze-thaw resistance of steel fibre reinforced rubberised concrete, Constr. Build. Mater. 195 (2019) 450–458. https://doi.org/10.1016/j.conbuildmat.2018.11.103.
[28] N.P. Pham, A. Toumi, A. Turatsinze, Rubber aggregate-cement matrix bond enhancement: Microstructural analysis, effect on transfer properties and on mechanical behaviours of the composite, Cem. Concr. Compos. 94 (2018) 1–12. https://doi.org/10.1016/j.cemconcomp.2018.08.005.
[29] G. Ossola, A. Wojcik, UV modification of tire rubber for use in cementitious composites, Cem. Concr. Compos. 52 (2014) 34–41. https://doi.org/10.1016/j.cemconcomp.2014.04.004.
[30] P. Vashisth, K.W. Lee, R.M. Wright, Assessment of water pollutants from asphalt pavement containing recycled rubber in Rhode Island, Transp. Res. Rec. 1626 (1998) 95–104. https://doi.org/10.3141/1626-12.
[31] L.C. Sampson, A. V Houston, J. Randall, M.E. Barrett, G. Street, Technical Report: Water Quality and Hydraulic Performance of Permeable Friction Course on Curbed Sections of Highways, 2014.
[32] S. Taheri, A.H. Khoshgoftarmanesh, H. Shariatmadari, R.L. Chaney, Kinetics of zinc release from ground tire rubber and rubber ash in a calcareous soil as alternatives to Zn fertilizers, Plant Soil. 341 (2011) 89–97. https://doi.org/10.1007/s11104-010-0624-7.
[33] S. Li, T.Q. Tran, Q. Li, B. Ji, A.S. Brand, W. Zhang, Resources , Conservation & Recycling Zn leaching recovery and mechanisms from end-of-life tire rubber, 194 (2023). https://doi.org/10.1016/j.resconrec.2023.107004.
[34] ASTM C305, Standard Practice for Mechanical Mixing of Hydraulic Cement Pastes and Mortars of Plastic Consistency, ASTM Int. (2020).
[35] ASTM C1437, Standard Test Method for Flow of Hydraulic Cement Mortar, ASTM Int. (2015).
[36] ASTM C109, Standard test method for compressive strength of hydraulic cement mortars, Annu. B. ASTM Stand. (2021).
[37] ASTM C78, Standard Test Method for Flexural Strength of Concrete (Using Simple Beam with Third-Point Loading), ASTM Int. (2022).
[38] ASTM C597, Ultrasonic Pulse Velocity Through Concrete, ASTM Int. (2022).
[39] ASTM C1202, Standard Test Method for Electrical Indication of Concrete's Ability to Resist Chloride Ion Penetration, Am. Soc. Test. Mater. (2012).
[40] D.P. Bentz, Influence of silica fume on diffusivity in cement-based materials. II. Multi-scale modeling of concrete diffusivity, Cem. Concr. Res. 30 (2000) 1121–1129. https://doi.org/10.1016/S0008-8846(00)00263-5.

[41] R.S. Barneyback Jr., S. Diamond, Expression and analysis of pore fluids from hardened cement pastes and mortars, Cem. Concr. Res. 11 (1981) 279–285. https://doi.org/10.1016/0008-8846(81)90069-7.
[42] P.K. Mehta, P.J.M. Monteiro, Concrete: Microstructure, Properties, and Materials, 4th ed., McGraw-Hill, 2016.
[43] H.F.W. Taylor, Cement Chemistry, 2nd ed., Thomas Telford, London, 1997.
[44] S. Mindess, L. Qu, M.G. Alexander, The influence of silica fume on the fracture properties of paste and microconcrete, Adv. Cem. Res. 6 (1994) 103–107. https://doi.org/10.1680/adcr.1994.6.23.103.
[45] N. Oikonomou, S. Mavridou, Improvement of chloride ion penetration resistance in cement mortars modified with rubber from worn automobile tires, Cem. Concr. Compos. 31 (2009) 403–407. https://doi.org/10.1016/j.cemconcomp.2009.04.004.
[46] A. Bazzoni, M. Suhua, Q. Wang, X. Shen, M. Cantoni, K.L. Scrivener, The effect of magnesium and zinc ions on the hydration kinetics of C3S, J. Am. Ceram. Soc. 97 (2014) 3684–3693. https://doi.org/10.1111/jace.13156.
[47] F.F. Ataie, M.C.G. Juenger, S.C. Taylor-Lange, K.A. Riding, Comparison of the retarding mechanisms of zinc oxide and sucrose on cement hydration and interactions with supplementary cementitious materials, Cem. Concr. Res. 72 (2015) 128–136. https://doi.org/10.1016/j.cemconres.2015.02.023.
[48] N. Garg, C.E. White, Mechanism of zinc oxide retardation in alkali-activated materials: An: in situ X-ray pair distribution function investigation, J. Mater. Chem. A. 5 (2017) 11794–11804. https://doi.org/10.1039/c7ta00412e.
[49] A.S. Brand, J.R. Roesler, Bonding in cementitious materials with asphalt-coated particles: Part I – The interfacial transition zone, Constr. Build. Mater. 130 (2017) 171–181. https://doi.org/10.1016/j.conbuildmat.2016.10.019.
[50] E. Bernard, Y. Yan, B. Lothenbach, Effective cation exchange capacity of calcium silicate hydrates (C-S-H), Cem. Concr. Res. 143 (2021) 106393. https://doi.org/10.1016/j.cemconres.2021.106393.
[51] Agency for Toxic Substances and Disease Registry (ATSDR), Toxicological Profile for Zinc, 2005.
[52] Standard Methods For the Examination of Water and Wastewater, American Public Health Association, 2018. https://doi.org/doi:10.2105/SMWW.2882.104.
[53] ACI Committee 234, Guide for the Use of Silica Fume in Concrete, Report ACI 234R-06, American Concrete Institute, Farmington Hills, 2006.

Chapter 5. Zinc and total organic carbon leachability from end-of-life tire rubber in rubberized asphalt concrete[4]

The contributions of the authors to this manuscript are described as follows:

Thien Q. Tran: Conceptualization; Data curation; Formal analysis; Investigation; Methodology; Visualization; Writing - original draft; Writing - review and editing.

Note: Thien Q. Tran was in the main charge of all above-mentioned contribution categories under the supervision of Dr. Alexander S. Brand.

Bilin Tong: Investigation; Methodology; Writing - review and editing.

Shiyu Li: Investigation; Writing - review and editing.

Bin Ji: Investigation; Writing - review and editing.

Md Hasibul Hasan Rahat: Investigation.

Wencai Zhang: Funding acquisition; Supervision; Writing - review and editing.

Gerardo W. Flintsch: Conceptualization; Methodology; Supervision; Writing - review and editing.

Alexander S. Brand: Conceptualization; Funding acquisition; Methodology; Project administration; Supervision; /Writing - original draft; Writing - review and editing.

[4] **Thien Q. Tran,** Bilin Tong, Shiyu Li, Bin Ji, Md Hasibul Hasan Rahat, Wencai Zhang, Gerardo W. Flintsch, Alexander S. Brand. "Zinc and total organic carbon leachability from end-of-life tire rubber in rubberized asphalt concrete" (Under review)

Zinc and total organic carbon leachability from end-of-life tire rubber in rubberized asphalt concrete

Thien Q. Tran[1], Bilin Tong[1,2], Shiyu Li[3], Bin Ji[3], Md Hasibul Hasan Rahat[1], Wencai Zhang[3], Gerardo W. Flintsch[1,2], Alexander S. Brand[1,4*]

[1]The Charles E. Via, Jr. Department of Civil and Environmental Engineering, Virginia Polytechnic Institute and State University, Blacksburg, Virginia, USA, 24061
[2]Center for Sustainable and Resilient Infrastructure, Virginia Tech Transportation Institute, Blacksburg, VA, USA, 24061
[3]Department of Mining and Minerals Engineering, Virginia Polytechnic Institute and State University, Blacksburg, Virginia, USA, 24061
[4]Department of Materials Science and Engineering, Virginia Polytechnic Institute and State University, Blacksburg, Virginia, USA, 24061
*Corresponding Author: asbrand@vt.edu

5.1 Abstract

End-of-life tire (ELT) rubber has been widely studied and utilized as a binder additive or aggregate in asphalt concrete. While most research focused on the effects on the engineering properties of rubberized asphalt concrete (RAC), very few considered the leaching potential of heavy metals or organic carbon content from ELT rubber, which can be detrimental to the living environment. The authors recently developed a metallurgical treatment process to remove and recover zinc from the ELT rubber for environmental and recycling purposes. In this study, the hypothesis to be tested is that the asphalt binder will serve to immobilize any remaining leachable zinc and total organic carbon (TOC) content from ELT rubber. The authors used ELT rubber before and after the zinc-recovery process to partially replace 20 % sand by volume in asphalt concrete through the dry process. Indirect tensile test-cracking tolerance, asphalt pavement analyzer rutting test, and dynamic modulus test were conducted for the investigations of the engineering properties of RAC. A total of three mixtures were evaluated: control, 20 % untreated ELT rubber, and 20 % treated ELT rubber. Environmental tests were conducted to examine the leaching potential of zinc and TOC from the RAC and how this potential varies under different conditions. While the presence of ELT rubber caused a negative impact on the tensile strength and cracking tolerance index, it improved the rutting resistance and the dynamic modulus when the materials were subjected to high-temperature conditions. Environmentally, there were still remarkable amounts of zinc leached out from ELT rubber to the environment and the zinc recovery treatment process even induced more zinc leaching. Conversely, the asphalt binder effectively immobilized TOC, since no TOC was detected in the leaching environments.

Keywords: Rubberized asphalt concrete; indirect tensile test-cracking tolerance; asphalt pavement analyzer rutting; stress sweep rutting; dynamic modulus; end-of-life tire rubber; zinc leachate; and total organic carbon content.

5.2 Introduction

End-of-life tire (ELT) rubber is a waste that commands significant attention from many researchers as well as industries recently for recycling and environmental purposes. Around three billion ELTs are discarded yearly worldwide [1]. The largest ELTs producer in the world is China, discarding around 14.6 million tons of ELTs in 2018 [2]. As the second largest, the U.S. discarded 4.46 million tons of ELTs in 2019 [3]. While a portion of this waste has been stockpiled, the others have been reused as tire-derived fuel, ground rubber, landfilling, and civil engineering applications. Various polymers (i.e., polybutadiene, polyisoprene, and styrene-butadiene) and carbon black are the main components of rubber tires. ELTs also contain small amounts of additives such as stearic acid, extender oil, and zinc oxide (ZnO) [1]. Additionally, ELTs can be detrimental to the living environment, including groundwater, soil, and the atmosphere [4,5]. ELTs contain 1 % to 2 % ZnO by mass, which is added for vulcanizing process [1], and Smolders and Degryse [6] reported that powdered ELT particles (< 100 μm) can potentially release up to 40 % of its zinc into the living environment after one year exposed to weathering conditions. According to the current ELT generation in China and the U.S., it is estimated that around 286 thousand tons of zinc can be potentially leached out into the environment if all zinc within the ELT rubber is leachable. Zinc harms the organisms, including invertebrates, fish, and plants [7]. Meanwhile, the organic carbon released from ELT rubber can be problematic to the ecosystem and human health. TOC in water can be broken down by micro-organisms and oxidized which might use up a lot of oxygen in the environment, which threatens the lives of the aquatic animals [8]. Even without oxygen, TOC promote the development of anaerobic bacteria which can generate sulfate salts to damage the living aquatic and human life [9].

ELT rubber has been found use in civil engineering materials such as asphalt concrete [10,11], portland cement concrete [12–14], and soil stabilization [15,16]. The most attention from researchers, professionals, and industries has been paid to rubberized portland cement concrete and RAC. ELT rubber can improve some engineering properties (i.e., resilient modulus, elasticity, fatigue resistance, rutting resistance, permanent deformation resistance) of asphalt concrete [17] while it is reported to decrease tensile strength [18]. The ELT rubber can be added to the asphalt concrete by the dry process or the wet process. In the dry process, ELT rubber is blended into the aggregates prior to the addition of asphalt binder, and the wet process requires ELT rubber to be pre-blended into the asphalt binder [11,19].

The effect of ELT rubber on the engineering properties of asphalt concrete has received more attention than the environmental aspects. There are a few studies investigating the environmental impacts of using ELT rubber in asphalt concrete from different aspects, such as CO_2, N_2, CO, SO_2, NO_x, and CH_4 emissions during its production [20], greenhouse gas emissions [21], and heavy metal leachability [22–24]. The leaching potential of heavy metals such as zinc from the ELT

rubber particles used in RAC has not been adequately researched. In addition, the risk of organic carbon content leaching from ELT rubber in asphalt concrete has not been investigated in the literature.

The main purpose of this study is to test if the asphalt binder can serve to immobilize any leachable zinc and organic content from ELT rubber in RAC. The authors used ELT rubber before and after a zinc extraction process to partially replace 20 % sand by volume in asphalt concrete through the dry process. As mentioned earlier, the engineering property tests were first conducted to investigate the effects of ELT rubber on RAC. A total of three mixtures were evaluated: control, 20 % untreated ELT rubber, and 20 % treated ELT rubber. Environmental tests were conducted to examine the leaching potential of zinc and TOC from the RAC and how this potential varies under different conditions, such as extreme pH, saline, and acidic environments. The novelty of this study is that it furthers the knowledge about the fate of zinc and TOC in ELT rubber-modified asphalt concrete, which has not previously been explored in the literature.

5.3 Experimental program

5.3.1 Materials

The control asphalt concrete mixture (coded C-AC) was a common surface course mix used in the region. The by mass mix proportion included 38 % #8 quartzite, 19 % #10 quartzite, 13 % sand, 30 % reclaimed asphalt pavement (RAP), and 5.8 % asphalt binder. The used binder was PG 64S-22 type with 0.5 wt% of a liquid anti-strip additive. The RAP was found to have 5.25 % residual binder according to AASHTO T 308 [26]. The RAP residual binder content was accounted in the mix by accordingly adjusting the asphalt binder proportioning. The combined gradation of aggregates used in the control mixture is shown in Table 5- 1.

Table 5- 1. Gradation of aggregates for the control asphalt concrete design approved by Virginia department of transportation (VDOT) used in this study.

Sieve size (mm)	Acceptance range (%)		Passing (%)
	Min	Max	Control mix (C-AC)
12.5	99.0	100.0	100.0
9.50	89.2	94.8	92.0
4.75	55.2	60.8	58.0
2.36	38.2	43.8	41.0
0.60	20.9	25.1	23.0
0.075	5.6	7.0	6.3
Asphalt binder	5.59	6.01	5.8

It should be noted that 20 % of sand volume was replaced by two types of ELT rubber, untreated and treated, to produce RAC (i.e., UR-AC and TR-AC, respectively) in this study. The mixing

process complied to the regular asphalt concrete mixing procedure in accordance with AASHTO R 30 [27]. The ELT rubber was added into heated aggregates and pre-mixed for 15 seconds before the asphalt binder was introduced, which allows for softening the ELT rubber powder hence easing its blend and connection with asphalt binder eventually [19]. The ELT rubber was provided by Lehigh Technologies in the form of a powder. In addition to the "as-received" form, referred to as untreated ELT rubber, the RAC incorporated ELT rubber that had undergone a process to extract zinc, known as treated ELT rubber. The method for hydrometallurgical treatment was based on a previously developed procedure by the authors [28], involving the use of 2.0 M HNO_3 to dissolve zinc from the ELT rubber and subsequently recover it. The treatment batch had a solid concentration of 200 g L^{-1}. This treatment was carried out in a leaching environment at 90 ℃, with continuous agitation at 600 rpm for a duration of 5 hours, resulting in 95 % zinc leaching recovery rate. The treated ELT rubber was washed by clean water to bring its pH value back to 7.0, the material was then allowed to dry in a 60 ℃ oven for 24 hours before its use. The main metallic elements found in the untreated ELT rubber by digestion in a strong acid were magnesium with 322 mg kg^{-1}, aluminum with 505 mg kg^{-1}, calcium with 1195 mg kg^{-1}, iron with 503 mg kg^{-1}, and zinc with 20,509 mg kg^{-1} [28].

5.3.2 Experimental methodology

5.3.2.1 Engineering property experiments

In terms of engineering properties, cracking performance assessment and rutting performance assessment were investigated on all proposed asphalt concrete mixtures. While the cracking performance investigation included a basic indirect tensile test cracking tolerance (IDT-CT) test and dynamic modulus test, the rutting performance was evaluated using the asphalt pavement analyzer (APA) rut test.

Five IDT-CT specimens for each mixture with the dimensions of 62 mm in height and 150 mm in diameter were prepared and tested at 25 ℃ complying to ASTM D8225 [29]. For dynamic modulus testing, three samples for each mixture were created with dimensions of 150 mm in height and 100 mm in diameter by coring the gyratory-compacted samples that were originally 180 mm height by 150 mm diameter. The dynamic modulus specimens were uniaxially tested using an Asphalt Mixture Performance Tester machine with a maximum stress level up to 2800 kPa (400 psi). The test was performed at 4.4 ℃, 21.1 ℃, and 37.8 ℃ with six different frequencies ranging from 0.1 Hz to 25 Hz in accordance with AASHTO T 378-17 [30] to determine the dynamic modulus, |E*|.

With same diameter with IDT-CT specimens, four APA rutting test samples for each mixture were made with 75 mm in height. These samples were conditioned at 64 ℃ for 6 hours before testing according to AASHTO T 340 [32] in which each sample was subjected to 8000 cycles of loading by a 45.4 kg (100 lbs) wheel.

All samples were prepared by gyratory compaction method following AASHTO T 312 [33] with a target bulk specific gravity (Gmb) of 7 % ± 0.5 %. The maximum specific gravity (Gmm) of mixtures C-AC, UR-AC, and TR-AC was 2.487, 2.424, and 2.442, respectively.

In order to microstructurally distinguish the morphology of the ELT rubber before and after the zinc recovery treatment process, scanning electron microscopy (SEM) was employed. Samples in powder form were first vacuum-dried prior to being sputter coated by a ~12 nm thick platinum/palladium layer. A JEOL IT-500HR SEM with a Schottky field emission electron gun was used.

5.3.2.2 Environmental experiments

Leaching tests were performed for all mixtures including C-AC, UR-AC, and TR-AC. Broken IDT-CT samples were heated up at 160 ℃ for 2 hours before being dispersed to be used as leaching samples. Around 1.25 kg of dispersed asphalt concrete for each mixture was soaked with different soaking solutions with a liquid-to-solid (L/S) ratio of 8 by volume. Four types of soaking solutions were prepared, including: 1) deionized water, 2) pH 4.0 solution to simulate the leaching condition induced by acid rain, 3) 0.1 M NaCl solution to simulate the leaching condition induced by deicing chemicals, and 4) pH 4.0 and 0.1 M NaCl solution to serve as a combination of the earlier extreme leaching conditions. 20 mL of the leachate for each mixture at different leaching conditions were periodically collected at 3 days, 7 days, and 28 days. The obtained leachates were then filtered and immediately acidified by 2 % of 12.1 N HCl by sample volume to prevent precipitation. The leachate samples were analyzed for zinc concentration and TOC concentration using a Thermo Electron iCAP-RQ ICP-MS and a Shimadzu TOC-VCSN, respectively.

5.4 Results and discussion

5.4.1 Indirect tensile test - cracking tolerance (IDT-CT)

Figure 5- 1a reports the indirect tensile strength (ITS) and CT index of the three mixes. The ITS of C-AC, UR-AC, and TR-AC were respectively 1.19 MPa, 0.90 MPa, and 1.14 MPa. The ITS of the control mix decreased by 24 % when 20 % of the sand volume of the mixture was replaced by untreated ELT rubber (mixture UR-AC), meanwhile, the same replacement of sand by treated ELT rubber (mixture TR-AC) did not introduce significant reduction in ITS which was only 4 %. By a one-tailed paired t-test, the ITS of C-AC and TR-AC were not significantly different with 95 % confidence.

The CT index of both UR-AC (42.8) and TR-AC mixtures (41.6) was roughly 50 % lower than that of C-AC (81.1). There was no appreciable improvement in CT index when treated ELT rubber was used to replace sand regardless of its previously recorded enhancement in tensile strength. This is understandable since tensile strength of asphalt concretes relies on the cross-sectional area of samples and peak loads alone, while the CT index depends on various factors such as fracture energy (i.e., area of the load versus vertical displacement curve and area of cracking face), slope of the load-displacement curve (modulus parameter), and specimen diameter [34,35]. By a one-tailed paired t-test, the CT index between UR-AC and TR-AC were not significantly different at 95 % confidence, but C-AC was significantly different from UR-AC and TR-AC. This engineering trend has been observed in the literature [36,37].

Figure 5- 1 b shows typical load-displacement curves of C-AC versus the UR-AC and TR-AC. It can be seen that the asphalt concrete using ELT rubber yielded lower ultimate loads as well as 20 % to 30 % lower threshold displacement compared to those of the control.

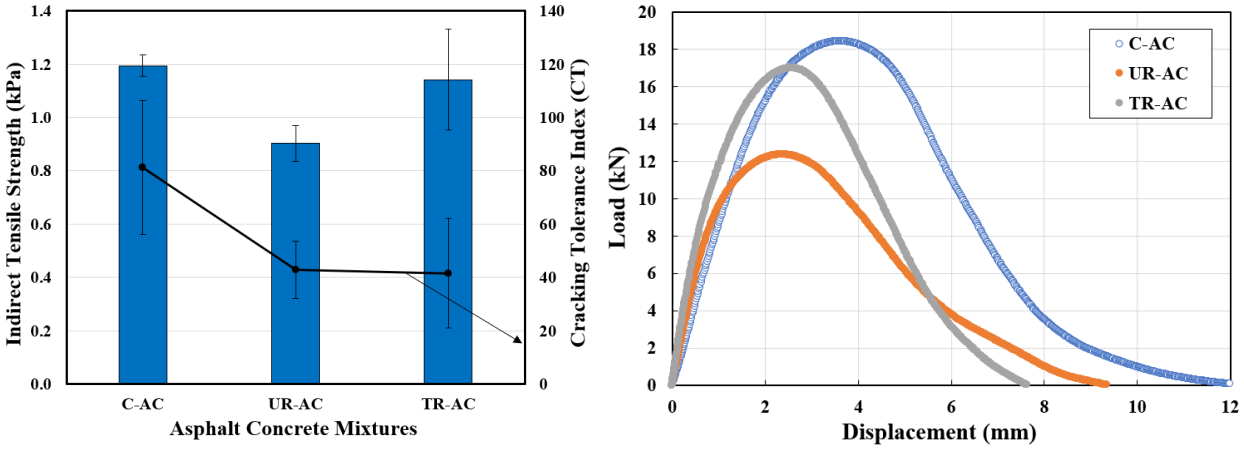

a) b)

Figure 5- 1. a) Indirect tensile strength and b) typical load-displacement curves of conventional asphalt concrete and asphalt concretes using untreated ELT rubber and treated ELT rubber.

5.4.2 Asphalt pavement analyzer (APA) rutting test

Figure 5- 2 shows the time-dependent rutting depth of the three mixes within a loading cycle up to 8000. Apart from the negative effects in cracking resistance of asphalt concrete, it is evident from Figure 5- 2 and Figure 5- 3 that using ELT rubber improved the rutting resistance of the asphalt concrete. After 8000 loading cycles the concrete-AC, UR-AC, and TR-AC mixes resulted in average final rutting depths of 2.62 mm, 1.72 mm, and 1.94 mm, respectively. The final rutting depth decreased by 34 % and 26 % when untreated and treated ELT rubber was used, respectively. This increased rutting resistance behavior has been reported in the literature [19,38–41].

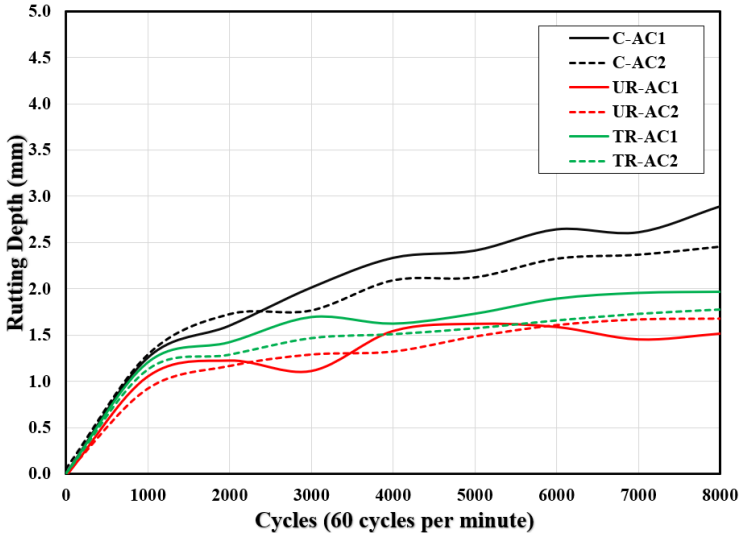

Figure 5- 2. Rutting depth observation of conventional asphalt concrete and asphalt concretes using untreated ELT rubber and treated ELT rubber.

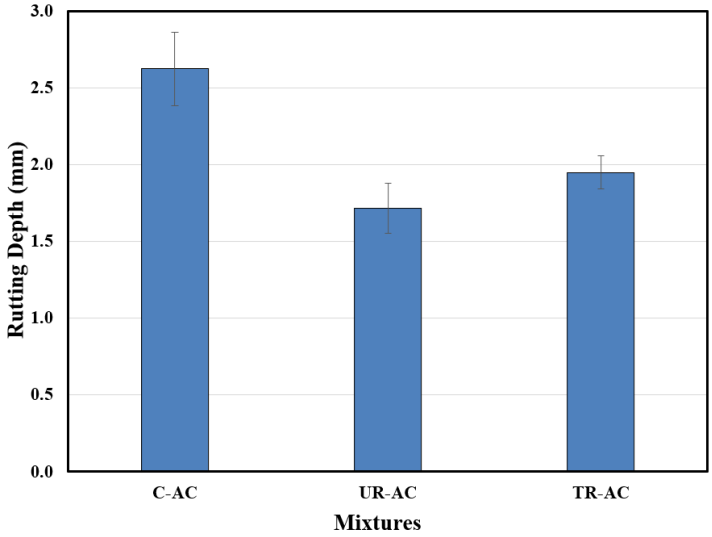

Figure 5- 3. Final rutting depth values after 8000 loading cycles of the three studied asphalt concretes.

5.4.3 Dynamic modulus

The stress-strain relationship under a continuous sinusoidal loading was monitored and the dynamic modulus, |E*|, was determined (Figure 5- 4). Master curves of dynamic modulus were constructed at a reference temperature of 21.1 ℃ by shifting the data at various temperatures until data points merge into a smooth function. The magnitude of |E*| decreased with increasing temperature frequencies for all mixes. At lower frequencies and higher temperatures, the mixes with ELT rubber demonstrated a higher |E*| than the control, while the opposite trend was observed at higher frequencies. An asphalt concrete with higher |E*| at higher temperature often

possesses higher rutting resistance [42], which was observed in the rutting tests. This performance trend agrees with the findings in previous studies [41,43].

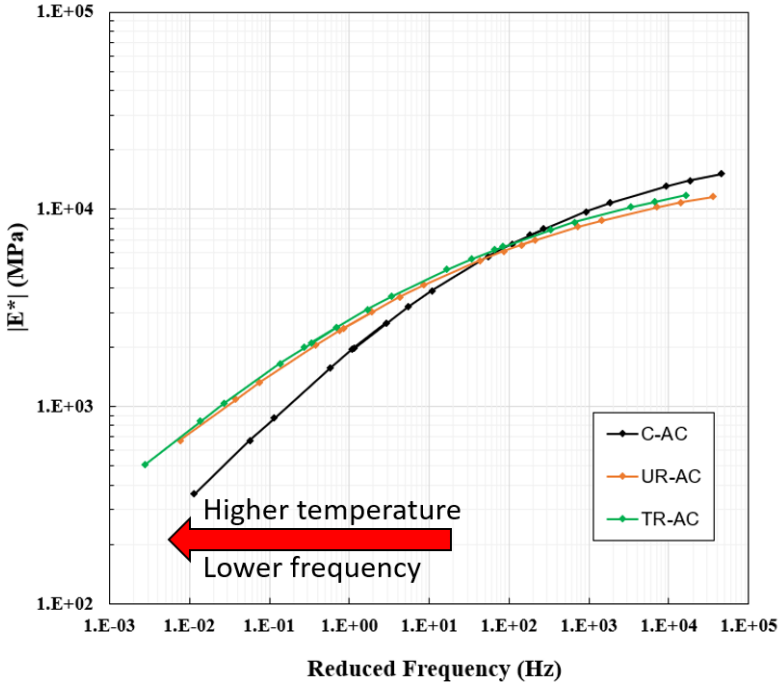

Figure 5- 4. Dynamic modulus |E| in master curves of conventional asphalt concrete, asphalt concrete using untreated ELT rubber, and treated ELT rubber.*

5.4.4 Microstructure study

Untreated (Figure 5- 5a) and treated (Figure 5- 5b) ELT rubber particles were imaged by secondary electron imaging with SEM. As can be noticed in Figure 5a, the as-received ELT rubber particle showed a rough surface and irregular and angular shapes with no appreciable microcracks. Conversely, the treated ELT rubber particles shown in Figure 5b appeared with visible cracks on its surface induced by the zinc-recovery treatment. In addition, the strong oxidation environment during the treatment process made the ELT rubber more porous and caused an increase in its specific surface area, which were previously reported in the authors' previous work [28]. As a result, the ELT rubber may possibly absorb more asphalt binder, leading to a lower asphalt content in the mix, which may make it more susceptible to cracking. Also, the degradation of treated ELT rubber induced by the zinc-recovery treatment process might be the reason why the RAC with treated ELT rubber did not provide improvement in rutting resistance as significant as the RAC using untreated ELT rubber.

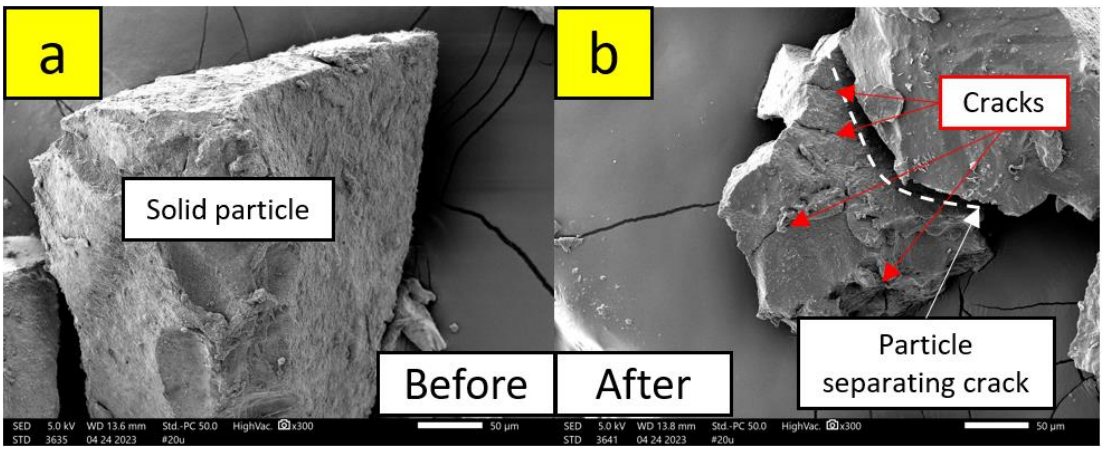

Figure 5- 5. SEM images of the (a) untreated ELT rubber particles and (b) treated ELT rubber particles.

5.4.5 Environmental tests

Figure 5- 6 compares zinc concentration in leachates of conventional asphalt concrete and asphalt concretes using untreated and treated ELT rubbers in differently extreme leaching environments. It is found that asphalt concretes using ELT rubber tend to release much more zinc than conventional asphalt concrete after 7 days of being exposed to normal and extreme environments. In normal leaching condition, mixtures UR-AC and TR-AC respectively released zinc roughly 23 times and 40 times more than mixture C-AC. In the extreme leaching environment, the deicing simulating solution (0.1 M NaCl) did not appear to promote the leachability of zinc. On the other hand, the acidic rain solution (pH 4.0) greatly increased the leaching and increased the measured zinc concentration by 114 % and 32 % in the leachate of mixtures UR-AC and TR-AC when compared to the control, respectively. This phenomenon occurred similarly but less significantly in the combined leaching solution of pH 4.0 and 0.1 M NaCl in which the zinc concentration increase was 53 % and 16 %, respectively. In addition, it is recognized that the RAC with treated ELT rubber released even more zinc to the leaching environments than the one using untreated ELT rubber. As discussed earlier, since the zinc recovery treatment caused more pores, cracks, and higher specific surface area in ELT rubber particles, and some residual zinc left in the particles have larger contact with surrounding environment which might cause the leachability taking place more easily. The zinc concentration kept increasing in the leachate of mixtures UR-AC and TR-AC for 28 days of leaching. While the pH 4.0 solution increased the leachable zinc in mixture TR-AC by 35 %, 0.1 M NaCl solution and 0.1 M NaCl solution (at pH 4.0) nearly doubled the leached zinc of mixture UR-AC. Generally, all of the adverse leaching conditions introduced negative impacts on the zinc immobilization of asphalt concrete. When running the leaching test on the same amount of untreated ELT rubber alone under deionized water, the leachable zinc concentrations after 3 days, 8 days, and 28 days were 555 ppb, 963 ppb, and 1309 ppb, respectively. The results indicate that RAC could reduce the leachable zinc from ELT rubber by around 82 %, 91 %, and 82 %, respectively. However, these positive reductions in leachable zinc

were lessened under extreme leaching conditions. The values for TOC concentration were 4.0 mg/L, 5.8 mg/L, and 5.7 mg/L, respectively.

While still significant amounts of zinc were found in the leaching environments, there was no signal of TOC content after 28 days of soaking. It indicates that RAC could effectively immobilize TOC leaching out from ELT rubber particles. In a comparison, bitumen binder was found to outplay stabilized soil and mortar in terms of TOC immobilization, which were explored in the authors' previous studies (chapters 2 and 3).

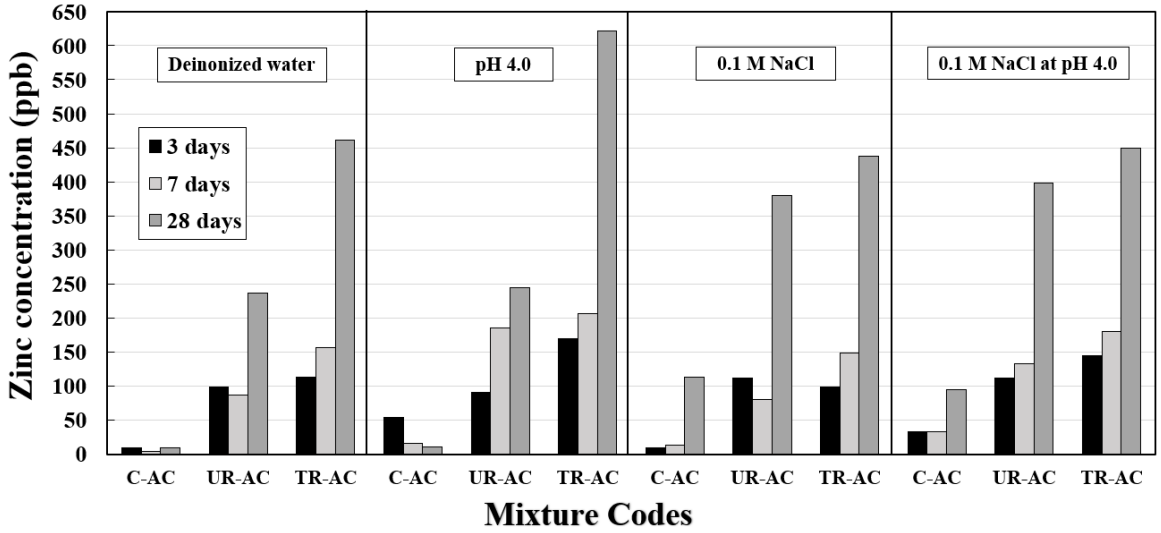

Figure 5- 6. Zinc concentration in leachates of conventional asphalt concrete and asphalt concretes using untreated and treated ELT rubbers in differently leaching environments.

5.5 Results and discussion

In this study, the effects of untreated and the zinc-recovered treated ELT rubbers on the asphalt concrete were examined in engineering and environmental terms. The main conclusions drawn from this work are:

1. Using ELT rubber in asphalt concrete generally reduced ITS value and CT index. This happened for both of rubber types. The treated ELT rubber helped improve ITS of the RAC remarkably, but it did not have significant impact in CT index.
2. ELT rubber effectively improved the rutting resistance of asphalt concrete.
3. ELT rubber improved the dynamic modulus |E*| of asphalt concrete when the material was subjected to higher temperature conditions.
4. Asphalt concretes using ELT rubber tend to release more zinc than conventional asphalt concrete after 28 days of being exposed to normal and extreme environments. The simulated acid rain solution (pH 4.0), simulated deicing solution, and simulated deicing solution at pH of 4.0 greatly exacerbated the leaching of zinc compared to deionized water.
5. RAC with treated ELT rubber released even more zinc to the leaching environments than the one using untreated ELT rubber. The zinc recovery treatment caused more pores, cracks, and higher specific surface area in ELT rubber particles, and some residual zinc left

in the particles have larger contact with surrounding environment, leading to easier leachability.

6. When contrasting with the leached zinc concentration, no signal of TOC content was found in any leaching environments. RAC is believed to effectively immobilize TOC leaching out from ELT rubber particles.

Acknowledgement

This study was supported by the Center for Tire Research (CenTiRe), Project SUST-2021-D14-4. The authors acknowledge Lehigh Technologies for providing the waste tire rubber and Adams Construction Company, Inc. for the aggregates and asphalt binders for this work. The authors also greatly thank Billy Hobbs and all technicians at Virginia Tech Transportation Institute for their assistance with the research, facilities, and equipment.

References

[1] B. Rodgers, Tire Engineering, CRC Press, Boca Raton, 2021. https://doi.org/10.1201/9781003022961.

[2] B. Chen, D. Zheng, R. Xu, S. Leng, L. Han, Q. Zhang, N. Liu, C. Dai, B. Wu, G. Yu, J. Cheng, Disposal methods for used passenger car tires: One of the fastest growing solid wastes in China, Green Energy Environ. (2021). https://doi.org/10.1016/j.gee.2021.02.003.

[3] U.S. Tire Manufacturers Association, 2019 U.S. Scrap Tire Management Summary, Washington D.C., 2020.

[4] M. Gualtieri, M. Andrioletti, C. Vismara, M. Milani, M. Camantini, Toxicity of tire debris leachates, Environ. Int. 31 (2005) 723–730. https://doi.org/10.1016/j.envint.2005.02.001.

[5] C. Halsband, L. Sørensen, A.M. Booth, D. Herzke, Car tire crumb rubber: Does leaching produce a toxic chemical cocktail in coastal marine systems?, Front. Environ. Sci. 8 (2020) 125. https://doi.org/10.3389/fenvs.2020.00125.

[6] E. Smolders, F. Degryse, Fate and effect of zinc from tire debris in soil, Environ. Sci. Technol. 36 (2002) 3706–3710. https://doi.org/10.1021/es025567p.

[7] X. Liu, J. Wang, A. Gheni, M.A. ElGawady, Reduced zinc leaching from scrap tire during pavement applications, Waste Manag. 81 (2018) 53–60. https://doi.org/10.1016/j.wasman.2018.09.045.

[8] E.E. Agency, Total Organic Carbon (TOC), (2023). https://www.eea.europa.eu.

[9] UNICERT, Total Organic Carbon, (2023). https://unicertglobal.com.

[10] L.G. Picado-Santos, S.D. Capitão, J.M.C. Neves, Crumb rubber asphalt mixtures: A literature review, Constr. Build. Mater. 247 (2020) 118577. https://doi.org/10.1016/j.conbuildmat.2020.118577.

[11] X. Shu, B. Huang, Recycling of waste tire rubber in asphalt and portland cement concrete: An overview, Constr. Build. Mater. 67 (2014) 217–224. https://doi.org/https://doi.org/10.1016/j.conbuildmat.2013.11.027.

[12] T.Q. Tran, B. Skariah Thomas, W. Zhang, B. Ji, S. Li, A.S. Brand, A comprehensive review on treatment methods for end-of-life tire rubber used for rubberized cementitious materials, Constr. Build. Mater. 359 (2022) 129365. https://doi.org/10.1016/j.conbuildmat.2022.129365.

[13] B.S. Thomas, R.C. Gupta, A comprehensive review on the applications of waste tire rubber in cement concrete, Renew. Sustain. Energy Rev. 54 (2016) 1323–1333. https://doi.org/10.1016/j.rser.2015.10.092.

[14] R. Roychand, R.J. Gravina, Y. Zhuge, X. Ma, O. Youssf, J.E. Mills, A comprehensive review on the mechanical properties of waste tire rubber concrete, Constr. Build. Mater. 237 (2020) 117651. https://doi.org/10.1016/j.conbuildmat.2019.117651.
[15] M.A.M. Al-Bared, A. Marto, N. Latifi, Utilization of Recycled Tiles and Tyres in Stabilization of Soils and Production of Construction Materials – A State-of-the-Art Review, KSCE J. Civ. Eng. 22 (2018) 3860–3874. https://doi.org/10.1007/s12205-018-1532-2.
[16] L. Liu, C. Wang, Q. Liang, F. Chen, X. Zhou, A state-of-the-art review of rubber modified cement-based materials: Cement stabilized base, J. Clean. Prod. 392 (2023) 136270. https://doi.org/https://doi.org/10.1016/j.jclepro.2023.136270.
[17] N.A. Hassan, G.D. Airey, R.P. Jaya, N. Mashros, M.A. Aziz, A review of crumb rubber modification in dry mixed rubberised asphalt mixtures, J. Teknol. 70 (2014) 127–134. https://doi.org/10.11113/jt.v70.3501.
[18] D. Jin, D. Ge, J. Wang, L. Malburg, Z. You, Reconstruction of Asphalt Pavements with Crumb Rubber Modified Asphalt Mixture in Cold Region: Material Characterization, Construction, and Performance, Materials (Basel). 16 (2023). https://doi.org/10.3390/ma16051874.
[19] L. da Silva, A. Benta, L. Picado-Santos, Asphalt rubber concrete fabricated by the dry process: Laboratory assessment of resistance against reflection cracking, Constr. Build. Mater. 160 (2018) 539–550. https://doi.org/10.1016/j.conbuildmat.2017.11.081.
[20] T. Wang, F. Xiao, X. Zhu, B. Huang, J. Wang, S. Amirkhanian, Energy consumption and environmental impact of rubberized asphalt pavement, J. Clean. Prod. 180 (2018) 139–158. https://doi.org/10.1016/j.jclepro.2018.01.086.
[21] F. Bartolozzi, I., Antunes, I., Rizzi, The environmental impact assessment of asphalt rubber: life cycle assessment, in: 2012.
[22] California Department of Transportation, Water Quality and Toxicity Evaluation of Discharge Generated from Asphalt Pavement Surfacing Materials, (2008). https://doi.org/10.7922/G27W69JM.
[23] P. Vashisth, K.W. Lee, R.M. Wright, Assessment of water pollutants from asphalt pavement containing recycled rubber in Rhode Island, Transp. Res. Rec. 1626 (1998) 95–104. https://doi.org/10.3141/1626-12.
[24] L.C. Sampson, A. V Houston, J. Randall, M.E. Barrett, G. Street, Water Quality and Hydraulic Performance of Permeable Friction Course on Curbed Sections of Highways, 7 (2014).
[25] S.C. department of T. SCDOT, Qualified products list for liquid anti-strip additives for asphalt mixtures, 2018.
[26] AASHTO T 308, Determining the Asphalt Binder Content of Asphalt Mixtures by the Ignition Method, (2018) 1–8.
[27] AASHTO R 30-02, Standard Practice for Mixture Conditioning of Hot Mix Asphalt (HMA), (2015).
[28] S. Li, T.Q. Tran, Q. Li, B. Ji, A.S. Brand, W. Zhang, Resources , Conservation & Recycling Zn leaching recovery and mechanisms from end-of-life tire rubber, 194 (2023). https://doi.org/10.1016/j.resconrec.2023.107004.

[29] ASTM D8225, Standard Test Method for Determination of Cracking Tolerance Index of Asphalt Mixture Using the Indirect Tensile Cracking Test at, Astm, D8825. (2019) 1–6. https://doi.org/10.1520/D8225-19.Copyright.
[30] AASHTO T 378-17, Standard Method of Test for Determining the Dynamic Modulus and Flow Number for Asphalt Mixtures Using the Asphalt Mixture Performance Tester (AMPT), 3 (2018).
[31] C.E. Dougan, J.E. Stephens, J. Mahoney, G. Hansen, Dynamic Modulus Test Protocol - Problems and Solutions, FHWA Rep. (2003).
[32] AASHTO TP 63-03, Standard Method of Test for Determining the Rutting Susceptibility of Asphalt Paving Mixtures Using the Asphalt Pavement Analyzer (APA), Am. Assoc. State Highw. Transp. Off. 10 (2012) 10–12.
[33] AASHTO T312, Standard Method for Preparing and Determining the Density of Hot Mix Asphalt (HMA) Specimens By Means of the SHRP Gyratory Compactor, Am. Assoc. State Highw. Transp. Off. Washingt. DC. (2015) 1–6.
[34] F. Zhou, Development of an IDEAL Cracking Test for Asphalt Mix Design , Quality Control and Quality Assurance Final Report for NCHRP IDEA Project 195 Innovations Deserving Exploratory Analysis (IDEA) Programs Managed by the Transportation Research Board, NCHRP-IDEA Progr. Proj. 195 (2019). IDEAL CT.
[35] F. Pérez-jiménez, R. Botella, K. Moon, M. Marasteanu, M. Fakhri, E.H. Kharrazi, F. Berto, K.E. Haslett, Evaluation of Cracking Indices for Asphalt Mixtures Using SCB Tests at Different Temperatures and Loading Rates, Honor. Theses Capstones. 380 (2018) 1067–1071.
[36] P. Saha Chowdhury, S.L.A. Noojilla, M.A. Reddy, Evaluation of fatigue characteristics of asphalt mixtures using Cracking Tolerance index (CTIndex), Constr. Build. Mater. 342 (2022) 128030. https://doi.org/10.1016/j.conbuildmat.2022.128030.
[37] H. Nair, S. Hossain, Performance of Ground Tire Rubber Modified Asphalt Mixture Overlays Over Jointed Concrete Pavements on US 60 in the Virginia Department o f Transportation ' s Richmond District, Virginia Transp. Res. Counc. (2022).
[38] W. Zhang, J. Tang, Z. Dong, T. Ma, M.A. Akber, X. Huang, J. Zhu, Y. Luan, Performance Characterization of Recycled-Asphalt Pavement with Stabilized Rubber–Modified Asphalt Using Balanced Mix Design Method, J. Mater. Civ. Eng. 32 (2020). https://doi.org/10.1061/(asce)mt.1943-5533.0003486.
[39] Y. Ma, S. Wang, H. Zhou, W. Hu, P. Polaczyk, B. Huang, Potential Alternative to Styrene–Butadiene–Styrene for Asphalt Modification Using Recycled Rubber–Plastic Blends, J. Mater. Civ. Eng. 33 (2021) 1–10. https://doi.org/10.1061/(asce)mt.1943-5533.0003946.
[40] X. Shu, B. Huang, Recycling of waste tire rubber in asphalt and portland cement concrete: An overview, Constr. Build. Mater. 67 (2014) 217–224. https://doi.org/10.1016/j.conbuildmat.2013.11.027.

[41] Y. Ma, S. Wang, H. Zhou, W. Hu, P. Polaczyk, M. Zhang, B. Huang, Compatibility and rheological characterization of asphalt modified with recycled rubber-plastic blends, Constr. Build. Mater. 270 (2021) 121416. https://doi.org/10.1016/j.conbuildmat.2020.121416.
[42] S. Diefenderfer, I. Boz, J. Habbouche, Balanced Mix Design for Surface Asphalt Mixtures : Phase I : Initial Roadmap Development and Specification Verification, (2021) 66.
[43] S. Zhao, B. Huang, X. Shu, X. Jia, M. Woods, Laboratory performance evaluation of warm-mix asphalt containing high percentages of reclaimed asphalt pavement, Transp. Res. Rec. (2012) 98–105. https://doi.org/10.3141/2294-11.

Chapter 6. Heat of hydration in clays stabilized by a high-alumina steel furnace slag[5]

The contributions of the authors to this manuscript are described as follows:

Thien Q. Tran: Conceptualization; Data curation; Formal analysis; Investigation; Methodology; Visualization; Writing - original draft; Writing - review and editing.

Note: Thien Q. Tran was in the main charge of all above-mentioned contribution categories under the supervision of Dr. Alexander S. Brand.

Amir Behravan: Investigation; Writing - review and editing.

Alexander S. Brand: Conceptualization; Methodology; Project administration; Supervision; Writing - original draft; Writing - review and editing.

[5] **Thien Q. Tran,** Alexander S. Brand, Amir Behravan. "Heat of hydration in clays stabilized by a high-alumina steel furnace slag". *Cleaner Materials*, 5, 2022. https://doi.org/10.1016/j.clema.2022.100105

Heat of hydration in clays stabilized by a high-alumina steel furnace slag

Thien Q. Tran,[1] Amir Behravan,[1] and Alexander S. Brand[1,2*]

[1] The Charles Edward Via, Jr. Department of Civil and Environmental Engineering, Virginia Polytechnic Institute and State University, Blacksburg, VA, 24060, USA
[2] Department of Materials Science and Engineering, Virginia Polytechnic Institute and State University, Blacksburg, VA, 24060, USA
*Corresponding Author: asbrand@vt.edu

6.1 Abstract

This investigation utilized isothermal calorimetry (IC) to quantify the heat of hydration of steel furnace slag (SFS)-stabilized clays to assess the chemical aspects of the stabilization. Specifically, kaolin and bentonite clays were each blended with 40% of SFS by mass at water-to-binder ratios ranging from 1.0 to 1.5. The hydration properties of stabilized mixtures using lime (CaO) or portland cement (PC) were also tested for comparison at the same experimental conditions. The obtained thermal power and total heat curves of stabilized mixtures could contribute to confirming that there is a hydration process taking place in clay stabilized by SFS. Relative to lime and PC, the SFS performed similarly in terms of hydration heat behavior. When blended into clays, SFS provided a more significant hydration heat behavior than cement, but that was much milder than lime. X-ray diffraction (XRD) and thermogravimetric analysis (TGA) were also employed to qualitatively analyze the mineralogy of the stabilized mixtures.
Keywords: Steel furnace slag (SFS); kaolin; bentonite; isothermal calorimetry (IC); X-ray diffraction (XRD); thermogravimetric analysis (TGA).

6.2 Introduction

Due to urgent requirements to limit CO_2 emission from portland cement (PC) production as well as preserve depleting natural resources [1], recent research has focused on reducing the carbon footprint of stabilized soils by using recycled, by-product, or marginal materials [2–11]. In particular, supplementary cementitious materials (SCMs), such as fly ash or ground granulated blast furnace slag (GGBFS), have been used as a partial to full replacement of PC in stabilized soils [12–15]. SFS is one alternative material that has not received as much attention as fly ash or GGBFS for soil stabilization, possibly due to the fact that SFS properties can vary widely [16], which may explain the varying effectiveness of SFS as an SCM [17]. SFS is a by-product of steel production [18–20], including basic oxygen furnace (BOF), electric arc furnace (EAF), and ladle furnace (LF) processes. For the application of SFS in construction and building materials, it has been utilized in portland cement concretes and mortars, asphalt concretes, unbound and bound base courses, and soil stabilization as an alkali-activated material or as a cementitious binder [4,5,20–24], although its effects on the composite material are highly variable depending on the chemical and mineral composition, aggregate shape and texture, reactivity, *etc*., of the SFS [16].

While there has been significant research on the stabilization of clays and clayey soils using lime and portland cement, fewer studies have focused on the application of SFS. However, from the studies that have examined SFS-stabilized clay, it is generally unclear if the stabilization effect is mechanical, chemical, or a combination of both. Mechanically, Akinwumi [25] hypothesized that the SFS reduced the optimum water content of stabilized clay, hence condensing the soil matrix to produce lower plasticity, a smaller swelling potential, and, eventually, a higher strength. In addition, the improvement was believed to be due to the increase in shear strength and internal friction of clay particles by adding SFS. Similarly, Brand *et al*. [3] argued that the increased mechanical properties in a clayey soil stabilized by SFS fines were attributed to mechanical rather than a chemical stabilization mechanism. Meanwhile, Poh *et al*. [26] stated that the SFS has cementitious properties, which means that the chemical reactions would occur in the stabilized soil mixture. However, the reactions take place slowly to form binding gels – such as calcium silicate hydrate (C-S-H) and calcium aluminate hydrate (C-A-H) – hence, alkaline activators, such as quick lime, NaOH, Na_2SiO_3-$5H_2O$, *etc*., have been added to accelerate the chemical reactions. Goodarzi *et al*. [27] concluded that there are also pozzolanic reactions under strongly alkaline environments that can generate the linking products in SFS-stabilized clays. In addition, Akinwumi [25] and Montenegro *et al*. [28] believed that the cation exchange capacity (CEC) of clay might play an important role in the stabilized mixture's engineering properties, *i.e.*, SFS will be more effective in clays with higher CEC values. A number of studies have suggested that SFS can chemically stabilize clay soils based on the remarkable improvement in mechanical properties, such as unconfined compressive strength, split tensile strength, California bearing ratio (CBR), swelling potential, *etc*. [25,26,29–31], while a few other studies strengthened this hypothesis by using scanning electron microscopy (SEM) [27,32], energy-dispersive X-ray spectroscopy (EDS) [4], X-ray diffraction (XRD) [28], or thermogravimetric analysis (TGA) [28,33,34].

When considering if SFS would react either pozzolanically or hydraulically, a recent review found that, as an SCM, SFS is generally detrimental to the mechanical properties of the cementitious composites [17]. For instance, while dicalcium silicate, if present, in SFS exists as the β and/or γ-polymorph [19,35], the β-polymorph is found to be relatively nonreactive in SFS [36], even though it is reactive in portland cements [37], and the γ polymorph is not hydraulically active [38]. Regardless, SFS studies have shown that the calcium silicate and calcium aluminate phases can be reactive [39–42]. In addition, SFS will often contain both free CaO and free MgO [18,43], both of which are hydraulic to form $Ca(OH)_2$ and $Mg(OH)_2$ [44], respectively. It is well-established that $Ca(OH)_2$ will chemically stabilize clay soils [45–47], which suggests that, depending on the free CaO content of SFS, there should be at least some chemical reaction. However, certain SFS, such as some EAF sources, may have little to no free CaO [43], which may therefore not have any chemical stabilization effect and instead may offer a mechanical stabilization effect.

For the possible pozzolanic reaction between SFS and clay, this may be considered as a secondary process taking place in soil stabilization, assuming that the cation exchange is the primary reaction. In the high pH environment when $Ca(OH)_2$ is present, the solubility of the alumina and silica from the clay will increase [48]. These dissolved ions will then react with available calcium ions released

from the SFS to possibly form C-(A)-S-H surrounding the clay particle surface as well as condensing the soil matrix, resulting in an improvement in the clay mixture [5]. These pozzolanic reactions tend to occur slowly over years, so the reaction can continue to strengthen the clay matrix, fill the pores, and reduce plasticity over time [49]. However, there are very few studies taking an in-depth look at the possibility of this pozzolanic reaction [4,5,48], and many studies have only confirmed this process by showing SEM [4,5,27,32] or EDS [4] data. However, these data may not be considered to be comprehensive, since it is unclear which products can be attributable to hydraulic *vs*. pozzolanic reactions.

The hydration process in a cementitious material occurs through a number of exothermic chemical reactions [37]. Aside from methods that can typically only be used to study mixes at certain curing times (*e.g.*, SEM, EDS, XRD), calorimetric measurements can provide continuous observation of the thermal changes taking place in hydrating cementitious materials from the start of the hydration process [50]. It is known that the amount and rate of the heat generated from the hydration process are significantly dependent on the physical properties and chemical compositions of the used components (*e.g.*, cement, SCMs, chemical admixtures) [51]. In addition, the mixture proportions and curing conditions also play essential roles in the hydration of the cementitious materials [51]. The heat generated over curing time reflects the increases in hydration product content and can be used to explain various reactions between the used binders, base material, and water. As a result, the proper information from the calorimetric analysis can be used to study setting behavior, workability, strength development, or pore structure development of the cementitious materials [51].

In order to explicitly evaluate the chemical reactivity of an SFS with clay soil, this study utilizes isothermal calorimetry (IC). While IC is commonly used in cement and concrete studies to quantify hydration kinetics [50], it has yet to be applied to soil or clay stabilization studies. Therefore, this study aims to explore the heat of hydration of SFS-stabilized clayey soils and confirm the statement that there are chemical reactions in SFS-stabilized clayey soil by calorimetric analysis along with other microstructural analyses such as XRD and TGA. This study is expected to provide a deeper understanding of the possible mechanical and/or chemical contributions of SFS to the improvement of stabilized soil's engineering properties, and this would be a stepping stone for the upcoming work to thoroughly clarify this topic.

6.3 Experimental program

6.3.1 Materials

In this work, two commercial clays were studied: kaolin and bentonite. Using Cu Kα radiation, XRD analyses of the clays are shown in **Error! Reference source not found.**. The kaolin clay was found to consist of kaolinite, while the bentonite clay was composed of montmorillonite and quartz. The specific gravities of the kaolin and bentonite were 2.63 and 2.62, respectively.

The SFS in this study was reportedly from an EAF source. The SFS specific gravity was 2.89. In order to determine the chemical composition of the SFS by inductively coupled plasma mass spectrometry (ICP-MS), 0.5 g of SFS powder was digested in 50 ml of 6 N HCl. The ICP-MS

results indicated a composition of 49.50 % CaO, 33.23 % Al_2O_3, 7.61 % MgO, 5.53 % FeO, 2.24 % SiO_2, 0.69 % MnO, 0.61 % Na_2O, 0.37 ZnO, 0.19 % BaO, and a trace amount of other elements. These data suggest that this particular SFS has a particularly high alumina content, considering that most EAF slags are reported to have Al_2O_3 contents of 3 % to 10 % [43]. Figure 6- 1 shows the XRD pattern of the SFS, indicating the presence of tricalcium aluminate ($Ca_3Al_2O_6$), mayenite ($Ca_{12}Al_{14}O_{33}$), and periclase (MgO). Typically, the calcium aluminate phases in EAF slags are reported to be mayenite and brownmillerite ($Ca_2(Al, Fe)_2O_5$) [16], although tricalcium aluminate ($Ca_3Al_2O_6$) has been reported in LF slags [41,52–56]. Therefore, while the SFS source was identified as EAF from the supplier, it is likely that this SFS is an LF slag originating from an EAF process.

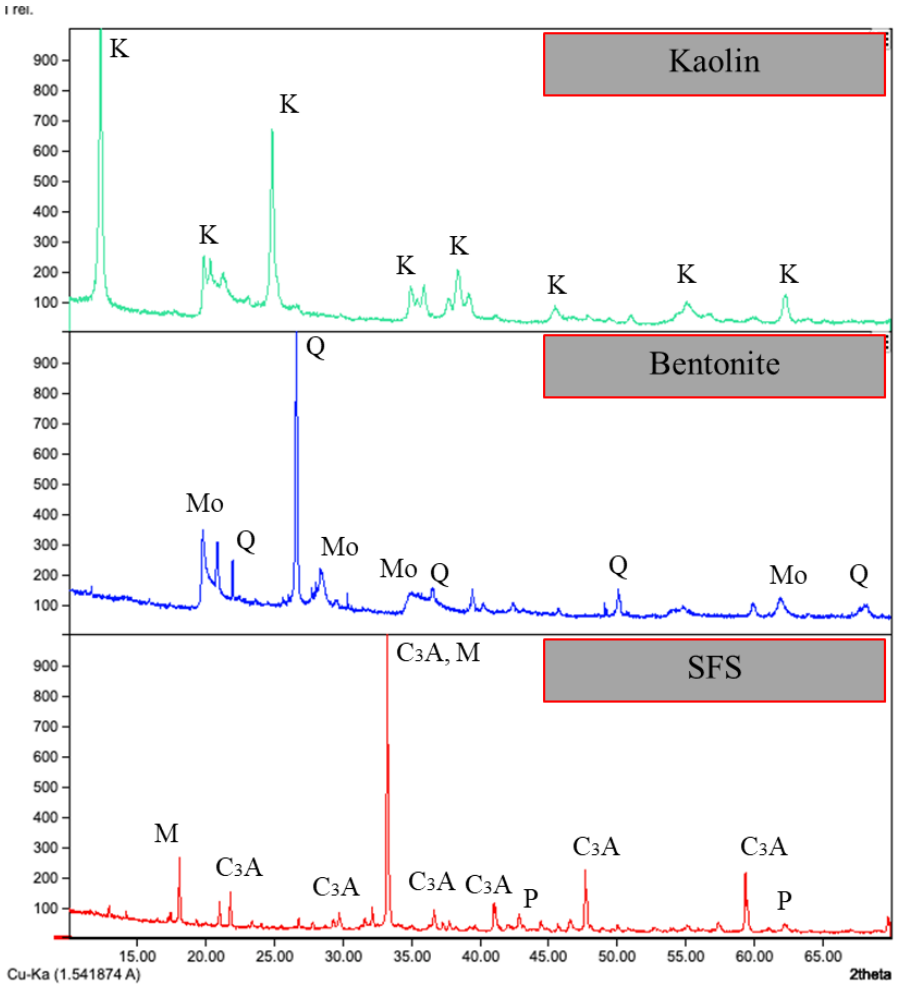

Figure 6- 1. XRF analysis of kaolin and bentonite clays and the SFS. Identified peaks: kaolinite (K), montmorillonite (Mo), quartz (Q), mayenite (M), tricalcium aluminate (C3A), and periclase (P).

Since the SFS particles were too coarse, rolling and ball mills were used to grind the SFS particles to be as fine as conventional PC. Pictures of the SFS before and after grinding are shown in Figure 6- 2. The particle size distributions of ground SFS, kaolin, and bentonite are shown in Figure 6- 3.

After ball milling, Figure 6- 3 shows that the ground SFS had a similar particle size distribution to PC. The median particle size (D_{50}) for ground SFS, PC, kaolin, and bentonite were 4.5 μm, 6.7 μm, 3.8 μm, and 1.4 μm, respectively.

The free CaO and $Ca(OH)_2$ contents of the SFS were found to be 3.0 % and 2.1%, respectively, using the ethylene glycol method [57,58] in combination with TGA. In addition, the TGA-quantified amount of $CaCO_3$ was found to be 2.27 %.

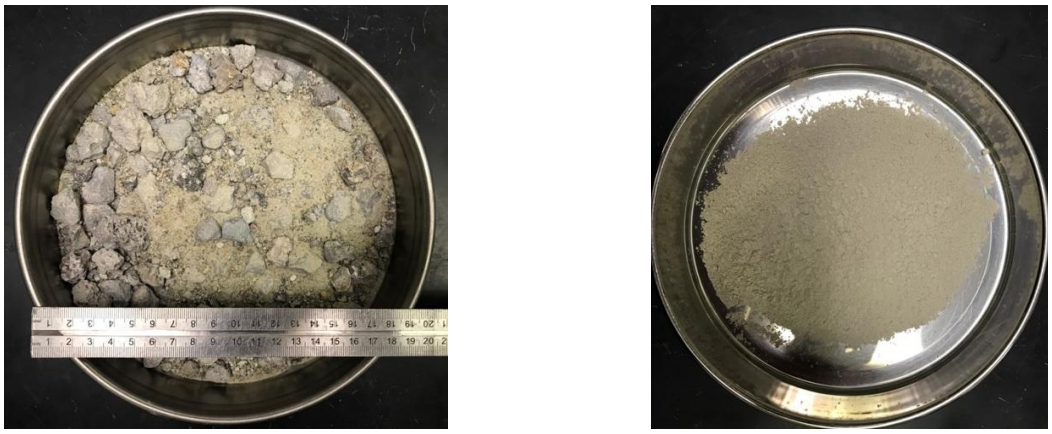

a) b)

Figure 6- 2. SFS before (a) and after (b) processing by roller and ball milling.

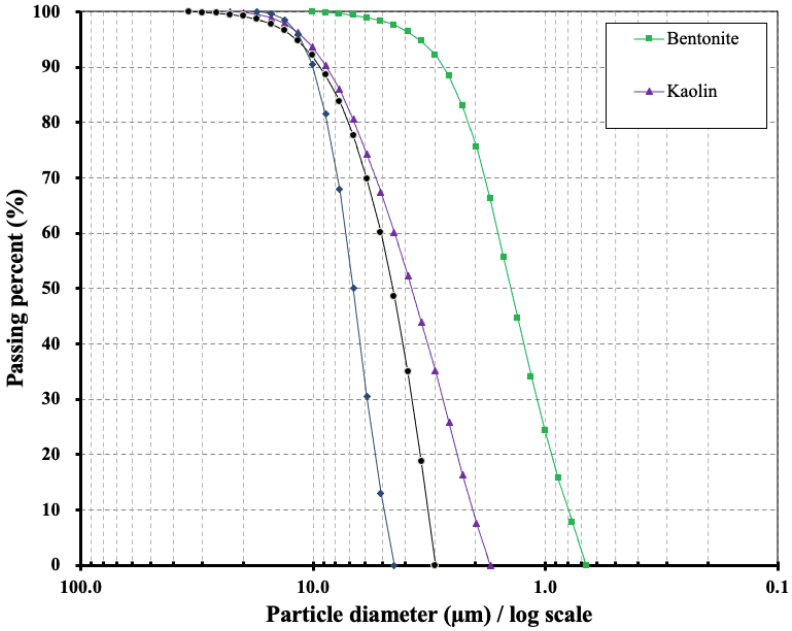

Figure 6- 3. Particle size distribution curves of PC, SFS, kaolin, and bentonite.

6.3.2 Experimental procedures and program

Isothermal calorimetry was performed using a Calmetrix I-Cal Flex to quantify the total heat (J/g binder) and thermal power (W/g binder) of various clay mixtures. Then the mixtures were manually mixed thoroughly in 15 mL plastic vials. The isothermal chamber was set to 23 ˚C. The heat of hydration was observed for up to 90 hours of curing time. In order to investigate the heat development in the stabilized clay matrix, kaolin and bentonite were each mixed with 40% of ground SFS by mass at the water-to-binder (w/b) ratios of 1.0 and 1.5. At the same experimental conditions, the heat evolution of stabilized mixtures with 40% by mass CaO or PC was also evaluated for comparison. The CaO was freshly prepared by calcining $CaCO_3$.

In addition, in order to exaggerate the effects of SFS on clay mixtures, the amount of ground SFS was increased to 100% and 300% by clay mass at w/b = 0.5 for XRD and TGA analysis. The XRD and TGA samples were oven-dried at 60 ˚C for 24 hours to remove moisture and then were then pulverized and sieved through a mesh size of 75-μm before the tests. A total of 14 experimental cases were performed, as detailed in Table 6- 1.

Table 6- 1. Mix design for stabilized clays.

Mix code	*w/b*	Binder (%)	Clay (kg/m^3)	SFS (kg/m^3)	PC (kg/m^3)	CaO (kg/m^3)	Water ($liter/m^3$)
Kao-40%SFS-1.0w/b	1.0	40	1088.6	435.4			435.4
Ben-40%SFS-1.0w/b	1.0	40	1086.9	434.7			434.7
Kao-40%PC-1.0w/b	1.0	40	1102.3		440.9		440.9
Ben-40%PC-1.0w/b	1.0	40	1100.5		440.2		440.2
Kao-40%SFS-1.5w/b	1.5	40	894.0	357.6			536.4
Ben-40%SFS-1.5w/b	1.5	40	892.8	357.1			535.7
Kao-40%PC-1.5w/b	1.5	40	903.2		361.3		541.9
Ben-40%PC-1.5w/b	1.5	40	902.0		360.8		541.2
Kao-2%CaO-30w/b	30	2	1013.7			20.3	608.2
Ben-2%CaO-30w/b	30	2	1012.2			20.2	607.3
Kao-100%SFS-0.5w/b*	0.5	100	815.5	815.5			407.8
Kao-300%SFS-0.5w/b*	0.5	100	814.5	814.5			407.3
Ben-100%SFS-0.5w/b*	0.5	300	342.7	1028.0			514.0
Ben-300%SFS-0.5w/b*	0.5	300	342.5	1027.5			514.7

Note: Kao: kaolin; Ben: bentonite; SFS: steel furnace slag; PC: Portland cement; CaO: lime; w/b: water-to-binder ratio. Mixtures with "*" are considered only for XRD and TGA analysis.

6.4 Results and discussion

6.4.1 Thermal power in calorimetric analysis

The thermal power generated from stabilized mixtures using SFS and PC at 1.0 and 1.5 *w/b* ratios is graphically shown in Figure 6- 4 with a logarithmic time scale. It can be seen that the thermal power curves of stabilized mixtures at a *w/b* ratio of 1.0 (blue curves) generally reach their peaks earlier than those at a *w/b* ratio of 1.5 (red curves) regardless of binder types. This can be explained that, with the same binder amount used and higher water content applied, the ion diffusion process

lasts longer and there are more water-filled spaces that the ions can be released from the binders into it. Hence, the mixtures with *w/b* = 1.5 can produce more heat compared to the other cases. This is confirmed in Fig. 4 since it shows that thermal power values of the stabilized mixtures with *w/b* = 1.5 range from around 0.4 to 0.7 W/g_{binder}, while those of stabilized mixtures with *w/b* = 1.0 can reach only the range of 0.05 to 0.2 W/g_{binder}.

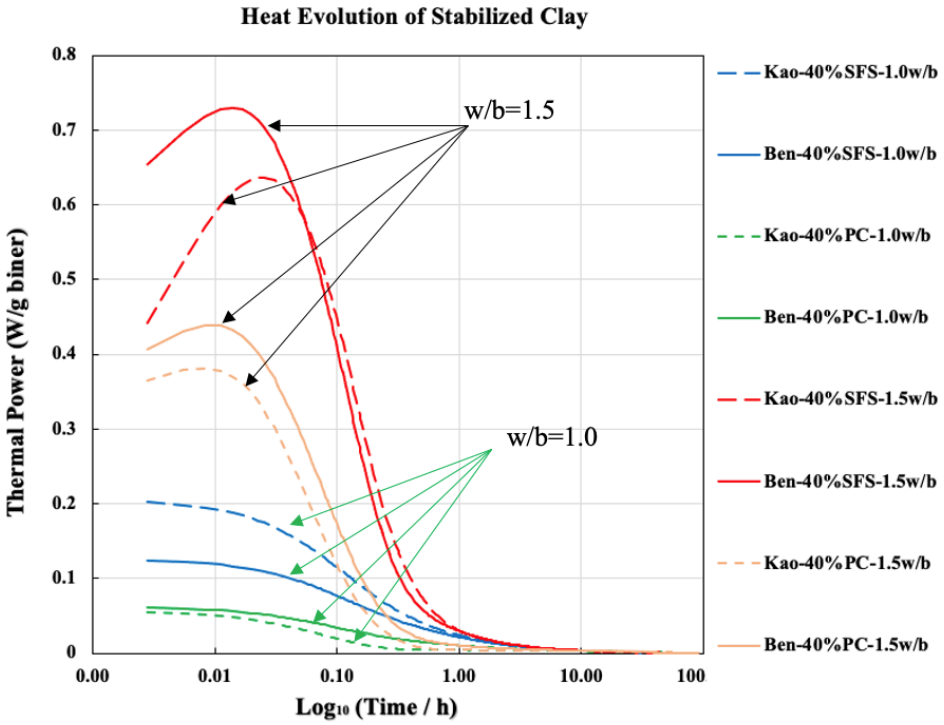

Figure 6- 4. Thermal power of kaolin and bentonite stabilized by SFS or PC at the water-to-binder ratios of 1.0 and 1.5.

In addition, it should be noted that the mixtures stabilized by SFS generated more heat compared to the ones stabilized by PC. This can be explained by the hydraulic reactions occurring in the SFS attributable to the C_3A, mayenite, and free CaO present. In the presence of water, C_3A reacts very rapidly [59] through an exothermic reaction that forms metastable calcium aluminate hydrate phases that eventually convert to the stable phase hydrogarnet [37]. Similarly, the hydration of mayenite is also exothermic in the initial formation of metastable calcium aluminate hydrate phases that convert to hydrogarnet [60,61]. Lastly, the hydration of CaO to form $Ca(OH)_2$ is also exothermic [62]. However, the free CaO in this SFS is only around 3 %, whereas the XRD data (**Error! Reference source not found.**) shows a predominance of C_3A and mayenite. Therefore, it is likely that the hydration of C_3A and/or mayenite were the cause for the high heat of hydration in Figure 6- 4.

It is also worth noting that, in a high pH environment, the cation exchange capacity (CEC) of clay is increased as its interlayers can effectively exchange more ions (*i.e.*, attract more Ca^{2+} ions available on binder particles surface) [25,26,63], resulting in a very fast and high heat generation. In addition to the exothermic reaction of pure CaO to form $Ca(OH)_2$, the increased CEC may also

explain why the lime-stabilized mixtures in Figure 6- 5 resulted in significantly greater thermal power values than the SFS- or PC-stablized mixtures. Meanwhile, a considerable amount of free CaO in SFS was converted into $Ca(OH)_2$ in advance of mixing time as mentioned above; hence, it should be expected that there would not be as significant of an exothermic reaction in the SFS mixes compared to the pure CaO mixes. This is not mention to that the free CaO in SFS is not necessarily all immediately available for reaction, since some of it may be present inside SFS particles. Additionally, the free CaO may not in fact be pure CaO and may have some impurities (*e.g.*, Mg) that may affect its reactivity. The maximum thermal power of mixtures Kao-2%CaO-30w/b and Ben-2%CaO-30w/b reached around 8.3 and 10.4 W/g_{binder}, respectively, all other mixtures were only under 1.0 in W/g_{binder} in general.

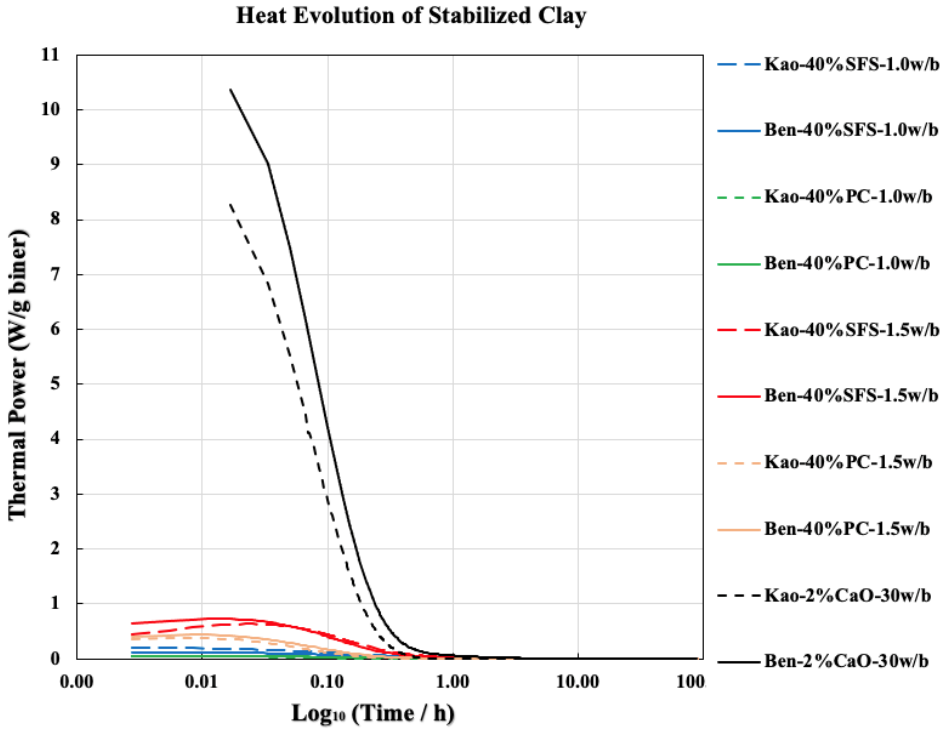

Figure 6- 5. Thermal power of kaolin and bentonite stabilized by lime compared to SFS and PC at the equivalent water-to-binder ratios of 1.5.

From Figure 6- 5, it is worth noting that the external mixing method in sample preparation could not provide the thermal power immediately after mixing, resulting in a lack of data in the very early curing time for the hydration stages I – initial reaction, II – induction period, and III – acceleration (for the case of *w/b* = 1.0). This is in good agreement with a previous finding [64].

6.4.2 Total heat in calorimetric analysis

The thermal power value depicts the real-time heat that a sample generates at a certain moment, while total heat (J/g_{binder}) shows the accumulated heat at a certain moment recorded from the mixing time [50]. Total heat values of various stabilized mixtures in this study are presented in Figure 6- 6.

Figure 6- 6 shows that the total heat values in mixtures Kao-40%SFS-1.5w/b and Ben-40%SFS-1.5w/b reach the highest value of around 1100 and 1200 J/g_{binder} after 90 hours of curing, respectively. These values dropped by from 30% to 40% when cement is used to stabilize the clays instead of using SFS (*i.e.*, Kao-40%PC-1.5w/b and Ben-40%PC-1.5w/b). In general, this trend is applicable for the stabilized mixtures at a *w/b* ratio of 1.0. However, as explained above, the total heat in these cases (*w/b* = 1.0 cases) is smaller due to inadequate water for perfect hydration.

Interestingly, at the same condition, the stabilized kaolin's hydration takes place more significantly (in terms of heat generation) over that of bentonite during the very early curing time while this trend is opposite after that. This can be closely related to the water absorbability as well as the specific surface area of the used clays. With the same water amount used, bentonite tends to retain more water surrounding its particle surface and absorb more water in its structure (interlayers) than kaolin, resulting in a lack of water for ion diffusion at the very early curing time. The absorbed and retained water is then moved out of clay particles gradually to the mixture matrix for an equilibrium status since the water there is consumed to form linking gels. Hence, the chemical reactions in stabilized bentonite seemed to be more steadily significant than kaolin in later ages. Furthermore, it is widely known that bentonite has a very high CEC value that can strongly exchange the needed ions and accelerate the chemical reactions as mentioned above.

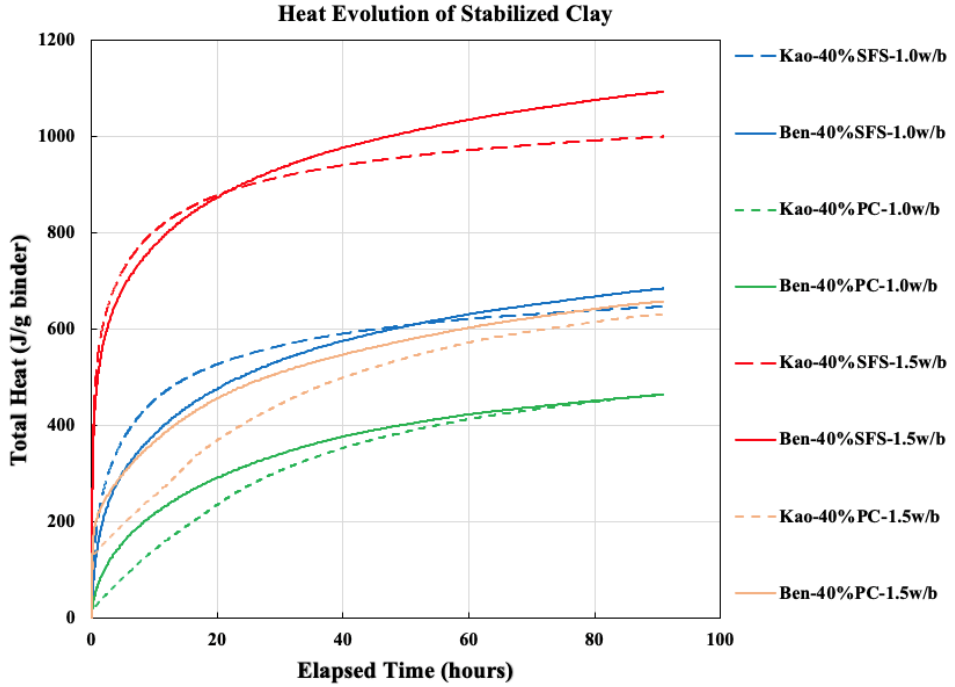

Figure 6- 6. Total heat of kaolin and bentonite stabilized by SFS and PC at the water-to-binder ratios of 1.0 and 1.5.

Figure 6- 7 compares the accumulated total heat of the two CaO-stabilized clays with the SFS- and PC-stabilized mixtures during the hydration process with curing times up to 90 hours. The accumulated total heat of stabilized mixtures using CaO is the largest (around 3000 and 5000

J/g_{binder} for Kao-2%CaO-30w/b and Ben-2%CaO-30w/b mixtures, respectively) among the stabilized ones, followed by cases of using SFS (around 1000 J/g_{binder}) and PC (around 700 J/g_{binder}), respectively.

In terms of stage III of hydration, acceleration, Figure 6- 5 and Figure 6- 7 reveal that, at this stage of the hydration process, all of the SFS stabilized mixtures generally took place significantly in the first five to ten minutes after mixing, which is much faster than that of conventional PC-based materials [65]. This is likely attributable to the very rapid reaction of C_3A, which can form metastable hydrate phases within seconds of reacting with water [59,66]. After this stage, the binder's particles are usually covered by reaction products such as C-S-H and CH while there is less "free" space and water for linking gels to grow significantly [67], resulting in a slow reaction as well as lower thermal power generated in the soil matrix. The total heat of each pair of the stabilized mixtures (*i.e.*, Kao-40%PC-1.5w/b *vs.* Ben-40%PC-1.5w/b, Kao-40%SFS-1.5w/b *vs.* Ben-40%SFS-1.5w/b, or Kao-40%SFS-1.0w/b *vs.* Ben-40%SFS-1.0w/b) keeps gradually increasing and finally reaches similar values in the curing time of 90 hours. Exceptionally, for the cases of clay mixtures stabilized by CaO, there is no increase of heat recorded after this accelerating time. It is believed that the CaO in the mixture was consumed and completely transferred to $Ca(OH)_2$ when the accelerating time is over. After that, the $Ca(OH)_2$ is dissolved in the remaining solution to reach equilibrium and to possibly contribute additional Ca^{2+} to any CEC reactions, which is process that can be exothermic or endothermic [68]. Also, the precipitation of $Ca(OH)_2$ in cementitious systems has been reported to be an endothermic process [69], which could be a contributing cause a slight decrease in total hydration heat.

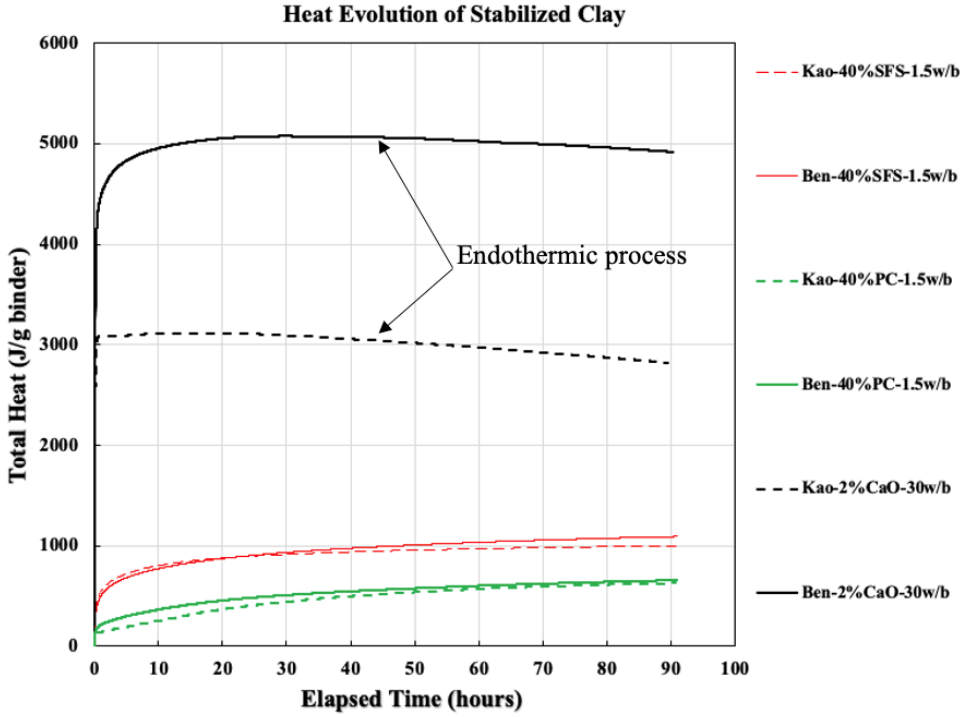

Figure 6- 7. Thermal power of kaolin and bentonite stabilized by lime compared to SFS and PC at the equivalent water-to-binder ratios of 1.5.

6.4.3 XRD analysis

In addition to calorimetric analysis, XRD of various mixtures was also analyzed to possibly explain the hydration heat discussed above. According to Figure 6- 8, bentonite mainly contains quartz (Q) and montmorillonite (M). When it is mixed with SFS, new hydration products are recognized. Particularly, with 40 % of SFS blended, the XRD result shows that there are reaction products from the SFS hydration, including hydrogarnet (H) and hydroxy-AFm phases (Hy). It is known that hydrogarnet is the major component in the alumina-rich systems [70]. Furthermore, both hydrogarnet and hydroxy-AFm phases (*e.g.*, C_4AH_{19}, C_4AH_{13}) will form from the reaction of C_3A and mayenite in the presence of water [37,59,66,71–73].

The hydration products of kaolin mixtures mixed with SFS are similar to those of bentonite, shown in Figure 6- 9. Predominantly, the hydration products included hydrogarnet and hydroxy-AFm.

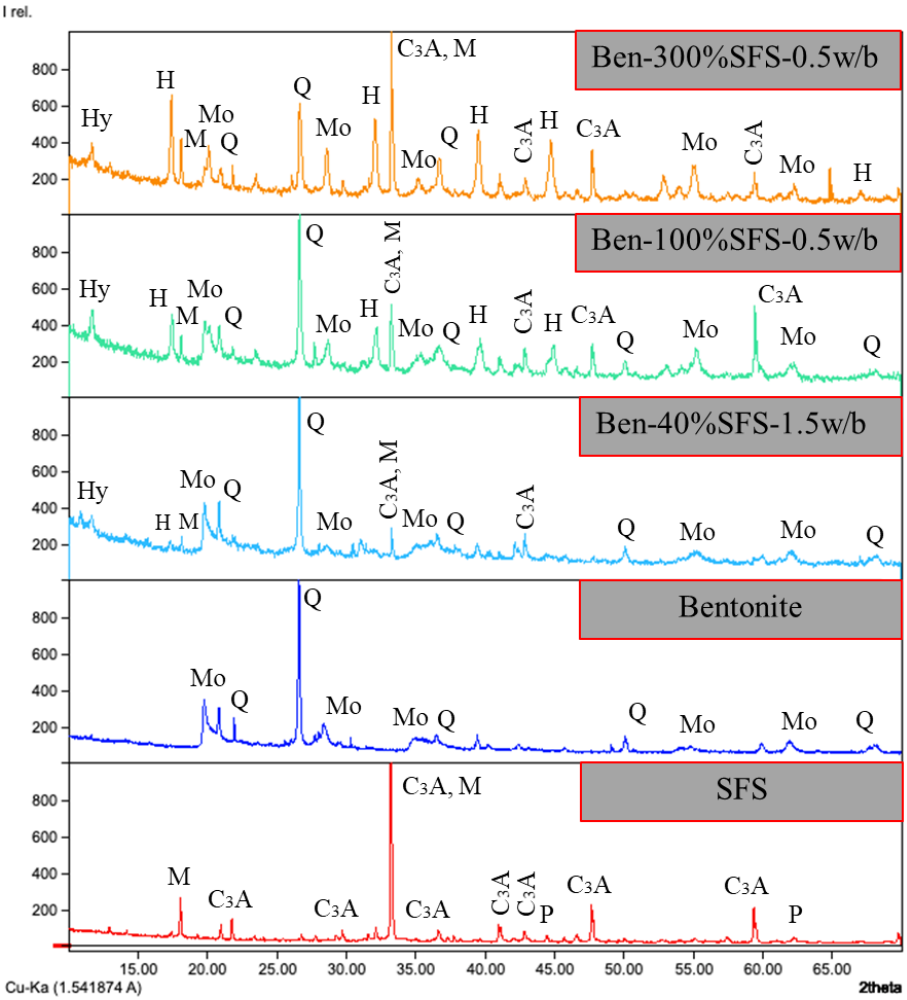

Figure 6- 8. Qualitative XRD analysis of SFS, bentonite, and bentonite mixtures mixed with SFS at different ratios. Identified peaks: montmorillonite (Mo), quartz (Q), mayenite (M), tricalcium aluminate (C_3A), periclase (P), hydrogarnet (H), and hydroxy-AFM (Hy).

For both bentonite and kaolinite mixtures, there is a clear hydration reaction of the SFS owing to the presence of C_3A and mayenite. While there is free CaO and free MgO identified in the SFS that could contribute to clay stabilization, the amount of reaction, if present, is not observable by XRD. Therefore, while these data do indeed indicate that this particular SFS was hydraulic, it is unclear if any reaction with the clay occurred.

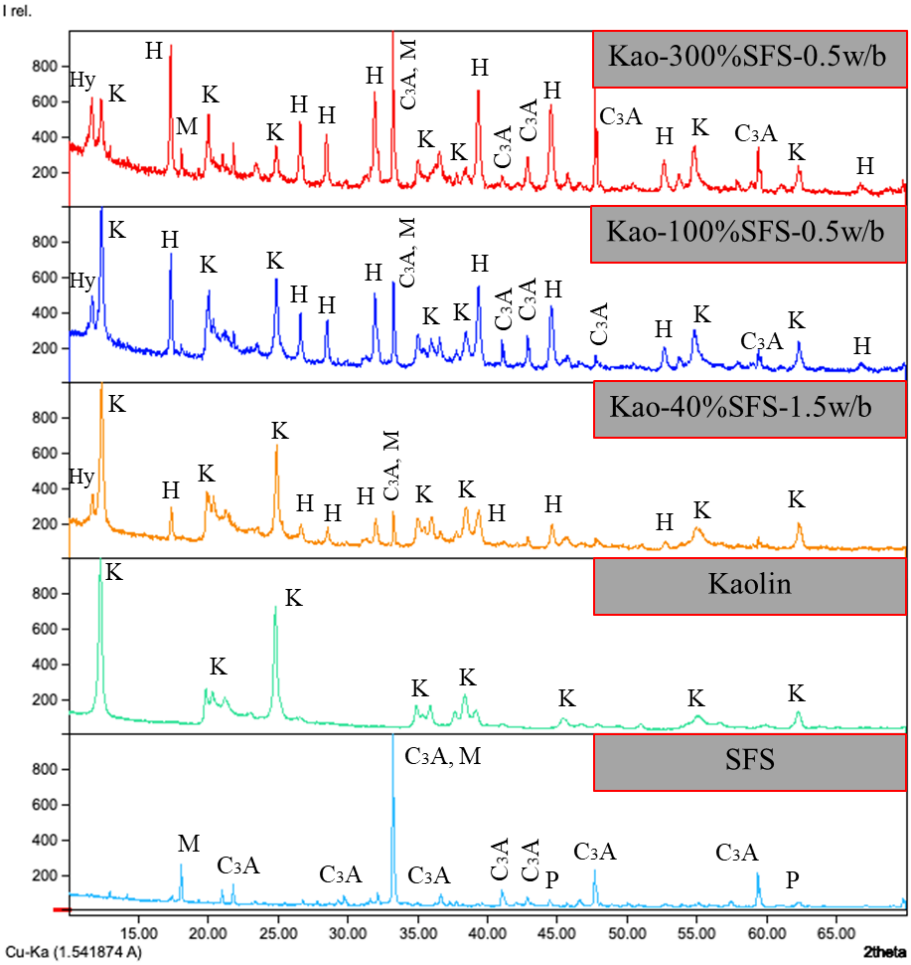

Figure 6- 9. Qualitative XRD analysis of SFS, kaolinite, and kaolinite mixtures mixed with SFS at different ratios. Identified peaks: kaolinite (K), mayenite (M), tricalcium aluminate (C_3A), periclase (P), hydrogarnet (H), and hydroxy-AFM (Hy).

6.4.4 TGA analysis

Figure 6- 10 shows TGA curves of bentonite and stabilized bentonite mixtures mixed with CaO and SFS at different ratios. At around 100 ˚C the TGA plots show weight loss in all bentonite mixtures due to the loss of free water. From 100 ˚C to around 600 ˚C (black rectangle), there are weight losses of 2 % and 4 % in mixes Ben-0.4SFS-1.5wb and Ben-0.02CaO-30wb, respectively, which are larger than that in the unstabilized bentonite. This provides an evidence that there are probably some binding phases formed in the bentonite structure such as portlandite and hydrogarnet. When the temperature exceeds 600 ˚C, there are weight losses (around 3 %) probably due to the loss of structural water [74]. It should be noted that the weight loss after 600 ˚C (green

rectangle) is contributed by the decomposition of calcite ($CaCO_3$). The trend is similar for the case Ben-1.0SFS-0.5wb and Ben-3.0SFS-0.5wb. However, there is significant weight loss recorded (around 6 % and 10 % for mixes Ben-1.0SFS-0.5wb and Ben-3.0SFS-0.5wb, respectively) during the temperature range of 250 – 400 ˚C (red rectangle). This is believed to be caused due to the decomposition of the hydrogarnet phase found in the XRD analysis above [75].

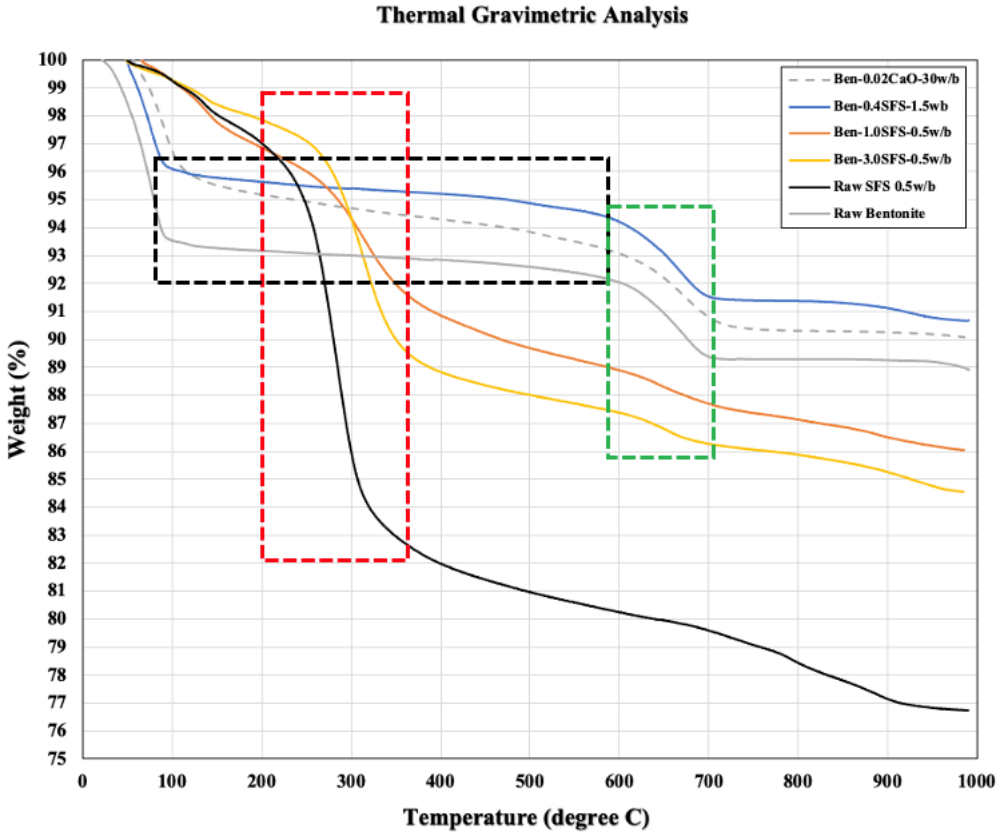

Figure 6- 10. TGA analysis of raw bentonite and bentonite mixtures mixed with SFS at different ratios.

6.5 Conclusion

In this study, isothermal calorimetry was employed to observe the hydration heat evolution of kaolin and bentonite stabilized by SFS compared to conventional portland cement and lime. The use of calorimetric techniques is promising to further assess and understand the stabilization reactions and mechanisms for conventional stabilizing binders as well as industrial by-products. The main conclusions taken from this study can be drawn as below:

1. The hydration process of all SFS stabilized mixtures generally occurred faster than that of portland cement or lime. The SFS in this study had a high calcium aluminate content, which rapidly reacts with water and was likely the main cause for the rapid heat generation.
2. The clay type, particle size, and specific surface area affected the hydration behavior of stabilized clay.

3. The “peak delay” of the thermal power curve strongly depends on the amount of water available in the soil matrix. In addition, at the same condition, the stabilized kaolin’s hydration takes place more significantly over that of bentonite during the very early curing time while this trend is opposite after that.
4. In a clay mixture, the hydration of SFS generates more heat than that of cement, but much less heat than that of CaO.
5. Hydration of SFS and PC keep gradually generating heat as time goes by while it likely generates no heat in the cases of CaO.
6. The external mixing method in sample preparation could not provide the thermal power data immediately after mixing, resulting in a lack of data in the very early curing time. For deeper studies, internal mixing should be employed for dealing with this issue.

Acknowledgement

The authors would like to thank the Short Mountain Silica company for providing the kaolin and bentonite for this work. This research received no external funding. The authors declare no conflict of interest.

References

[1] M. Schneider, The cement industry on the way to a low-carbon future, Cem. Concr. Res. 124 (2019) 105792. https://doi.org/10.1016/j.cemconres.2019.105792.

[2] M.U. Hossain, L. Wang, L. Chen, D.C.W. Tsang, S.T. Ng, C.S. Poon, V. Mechtcherine, Evaluating the environmental impacts of stabilization and solidification technologies for managing hazardous wastes through life cycle assessment: A case study of Hong Kong, Environ. Int. 145 (2020) 106139. https://doi.org/10.1016/j.envint.2020.106139.

[3] A.S. Brand, P. Singhvi, E.O. Fanijo, E. Tutumluer, Stabilization of a clayey soil with ladle metallurgy furnace slag fines, Materials (Basel). 13 (2020) 1–19. https://doi.org/10.3390/MA13194251.

[4] Y. sang Kim, T.Q. Tran, G. o. Kang, T.M. Do, Stabilization of a residual granitic soil using various new green binders, Constr. Build. Mater. 223 (2019) 724–735. https://doi.org/10.1016/j.conbuildmat.2019.07.019.

[5] T.Q. Tran, Y. Kim, G. Kang, B.H. Dinh, T.M. Do, Feasibility of Reusing Marine Dredged Clay Stabilized by a Combination of By-Products in Coastal Road Construction, Transp. Res. Rec. J. Transp. Res. Board. (2019) 036119811986819. https://doi.org/10.1177/0361198119868196.

[6] M. Tavakol, M. Hossain, S.E. Tucker-Kulesza, Subgrade soil stabilization using low-quality recycled concrete aggregate, in: C.L. Meehan, S. Kumar, M.A. Pando, J.T. Coe (Eds.), Geo-Congress 2019, ASCE, Reston, 2019: pp. 235–244. https://doi.org/10.1061/9780784482124.025.

[7] T.M. Do, Y. Kim, T.Q. Tran, N. Vu, Effect of Lime on Engineering Properties of CLSM Made with Fly Ash-Red Mud-Lime-Gypsum Binder, in: Korean Society of Civil Engineers Conferences, Busan, 2017: pp. 31–32.

[8] T.Q. Tran, Y. Kim, G. Kang, J. Kim, T.M. Do, Stabilization of weathered granite soil using new cementless binders, in: Korean Society of Civil Engineers Conferences, Gyeongju, 2018: pp. 176–177.

[9] T.M. Do, Y. Kim, G. Kang, M.Q. Dang, T.Q. Tran, Thermal Conductivity of Controlled Low Strength Material (CLSM) Made Entirely from By-Products, 773 (2018) 244–248. https://doi.org/10.4028/www.scientific.net/KEM.773.244.

[10] H. Tung, A. James, C. Bora, I. Kaoru, C. Sun-Gyu, Sand and Silty-Sand Soil Stabilization Using Bacterial Enzyme Induced Calcite Precipitation (BEICP), Can. Geotech. J. (2018) 1–66.

[11] M.J. Cui, H.J. Lai, T. Hoang, J. Chu, One-phase-low-pH enzyme induced carbonate precipitation (EICP) method for soil improvement, Acta Geotech. 16 (2021) 481–489. https://doi.org/10.1007/s11440-020-01043-2.

[12] T.B. Edil, H.A. Acosta, C.H. Benson, Stabilizing Soft Fine-Grained Soils with Fly Ash, J. Mater. Civ. Eng. 18 (2006) 283–294. https://doi.org/10.1061/(asce)0899-1561(2006)18:2(283).
[13] R.M. Brooks, Soil Stabilization With Flyash and Rice Husk Ash, Int. J. Res. Rev. Appl. Sci. 1 (2009) 2076–734.
[14] A.K. Sharma, P. V. Sivapullaiah, Ground granulated blast furnace slag amended fly ash as an expansive soil stabilizer, Soils Found. 56 (2016) 205–212. https://doi.org/10.1016/j.sandf.2016.02.004.
[15] R. Siddique, Ground Granulated Blast Furnace Slag, Waste Mater. By-Products Concr. (2007) 1–39. https://doi.org/10.1007/978-3-540-74294-4_1.
[16] A.S. Brand, E.O. Fanijo, A review of the influence of steel furnace slag type on the properties of cementitious composites, Appl. Sci. 10 (2020) 8210. https://doi.org/10.3390/app10228210.
[17] A.M. Rashad, A synopsis manual about recycling steel slag as a cementitious material, J. Mater. Res. Technol. 8 (2019) 4940–4955. https://doi.org/10.1016/j.jmrt.2019.06.038.
[18] I.Z. Yildirim, M. Prezzi, Chemical, mineralogical, and morphological properties of steel slag, Adv. Civ. Eng. 2011 (2011). https://doi.org/10.1155/2011/463638.
[19] C. Shi, Steel slag—its production, processing, characteristics, and cementitious properties, J. Mater. Civ. Eng. 16 (2004) 230–236. https://doi.org/10.1061/(ASCE)0899-1561(2004)16:3(230).
[20] G.C. Wang, The Utilization of Slag in Civil Infrastructure Construction, Woodhead Publishing, Cambridge, UK, 2016. https://doi.org/10.1016/C2014-0-03995-0.
[21] T.T. Le, S.S. Park, J.C. Lee, D.E. Lee, Strength characteristics of spent coffee grounds and oyster shells cemented with GGBS-based alkaline-activated materials, Constr. Build. Mater. 267 (2021) 120986. https://doi.org/10.1016/j.conbuildmat.2020.120986.
[22] G. Kang, Y. Kim, T.Q. Tran, N.A. Dan, Strength Monitoring of Dredged Marine Clay Stabilized with Basic Oxygen Furnace Steel Slag Using Non-Destructive Method, 29th Int. Ocean Polar Eng. Conf. (2019) ISOPE-I-19-476.
[23] H. Hoàng, J. Choi, H. Kim, B. Yeon, Mechanical properties and self-healing capacity of eco-friendly ultra-high ductile fiber-reinforced slag-based composites, Compos. Struct. 229 (2019) 111401. https://doi.org/10.1016/j.compstruct.2019.111401.
[24] Y. sang Kim, B.H. Dinh, T.M. Do, G. o. Kang, Development of thermally enhanced controlled low-strength material incorporating different types of steel-making slag for ground-source heat pump system, Renew. Energy. 150 (2020) 116–127. https://doi.org/10.1016/j.renene.2019.12.129.
[25] I. Akinwumi, Soil modification by the application of steel slag, Period. Polytech. Civ. Eng. 58 (2014) 371–377. https://doi.org/10.3311/PPci.7239.
[26] H.Y. Poh, G.S. Ghataora, N. Ghazireh, Soil stabilization using basic oxygen steel slag fines, J. Mater. Civ. Eng. 18 (2006) 229–240. https://doi.org/10.1061/(ASCE)0899-1561(2006)18:2(229).

[27] A.R. Goodarzi, M. Salimi, Stabilization treatment of a dispersive clayey soil using granulated blast furnace slag and basic oxygen furnace slag, Appl. Clay Sci. 108 (2015) 61–69. https://doi.org/10.1016/j.clay.2015.02.024.
[28] J.M. Montenegro, M. Celemín-Matachana, J. Cañizal, J. Setién, Ladle Furnace Slag in the Construction of Embankments: Expansive Behavior, J. Mater. Civ. Eng. 25 (2013) 972–979. https://doi.org/10.1061/(asce)mt.1943-5533.0000642.
[29] D.H. Diniz, J.M.F. de Carvalho, J.C. Mendes, R.A.F. Peixoto, Blast Oxygen Furnace Slag as Chemical Soil Stabilizer for Use in Roads, J. Mater. Civ. Eng. 29 (2017) 04017118. https://doi.org/10.1061/(asce)mt.1943-5533.0001969.
[30] I. Barišić, S. Dimter, T. Rukavina, Strength properties of steel slag stabilized mixes, Compos. Part B Eng. 58 (2014) 386–391. https://doi.org/10.1016/j.compositesb.2013.11.002.
[31] M. Shahbazi, M. Rowshanzamir, S.M. Abtahi, S.M. Hejazi, Optimization of carpet waste fibers and steel slag particles to reinforce expansive soil using response surface methodology, Appl. Clay Sci. 142 (2017) 185–192. https://doi.org/10.1016/j.clay.2016.11.027.
[32] W. Shen, M. Zhou, W. Ma, J. Hu, Z. Cai, Investigation on the application of steel slag-fly ash-phosphogypsum solidified material as road base material, J. Hazard. Mater. 164 (2009) 99–104. https://doi.org/10.1016/j.jhazmat.2008.07.125.
[33] J.M. Manso, V. Ortega-López, J.A. Polanco, J. Setién, The use of ladle furnace slag in soil stabilization, Constr. Build. Mater. 40 (2013) 126–134. https://doi.org/10.1016/j.conbuildmat.2012.09.079.
[34] V. Ortega-López, J.M. Manso, I.I. Cuesta, J.J. González, The long-term accelerated expansion of various ladle-furnace basic slags and their soil-stabilization applications, Constr. Build. Mater. 68 (2014) 455–464. https://doi.org/10.1016/j.conbuildmat.2014.07.023.
[35] J.D. Gupta, W.A. Kneller, R. Tamirisa, E. Skrzypczak-Jankun, Characterization of base and subbase iron and steel slag aggregates causing deposition of calcareous tufa in drains, Transp. Res. Rec. 1434 (1994) 8–16.
[36] J.J. Emery, Slag utilization in pavement construction, in: Extending Aggreg. Resour. (ASTM Spec. Tech. Publ. 774), American Society for Testing and Materials, Philadelphia, 1982.
[37] H.F.W. Taylor, Cement Chemistry, 2nd ed., Thomas Telford, London, 1997.
[38] K.H. Jost, B. Ziemer, Relations between the crystal structures of calcium silicates and their reactivity against water, Cem. Concr. Res. 14 (1984) 177–184. https://doi.org/10.1016/0008-8846(84)90102-9.
[39] P.Y. Mahieux, J.E. Aubert, G. Escadeillas, M. Measson, Quantification of hydraulic phase contained in a basic oxygen furnace slag, J. Mater. Civ. Eng. 26 (2014) 593–598. https://doi.org/10.1061/(ASCE)MT.1943-5533.0000867.
[40] M. Mahoutian, Y. Shao, A. Mucci, B. Fournier, Carbonation and hydration behavior of EAF

and BOF steel slag binders, Mater. Struct. 48 (2015) 3075–3085. https://doi.org/10.1617/s11527-014-0380-x.
[41] E. Adesanya, H. Sreenivasan, A.M. Kantola, V.-V. Telkki, K. Ohenoja, P. Kinnunen, M. Illikainen, Ladle slag cement–Characterization of hydration and conversion, Constr. Build. Mater. 193 (2018) 128–134. https://doi.org/10.1016/j.conbuildmat.2018.10.179.
[42] S. Choi, J.-M. Kim, D. Han, J.-H. Kim, Hydration properties of ladle furnace slag powder rapidly cooled by air, Constr. Build. Mater. 113 (2016) 682–690. https://doi.org/10.1016/j.conbuildmat.2016.03.089.
[43] N. Balcázar, M. Kühn, J.M. Baena, A. Formoso, J. Piret, Summary Report on RTD in Iron and Steel Slags: Development and Perspectives, Proceedings No. EUR 19066 EN, European Commission, Luxembourg, 1999.
[44] B. Erlin, D. Jana, Forces of hydration that can cause havoc in concrete, Concr. Int. 25 (2003) 51–57.
[45] F.G. Bell, Lime stabilization of clay minerals and soils, Eng. Geol. 42 (1996) 223–237. https://doi.org/10.1016/0013-7952(96)00028-2.
[46] S. Diamond, E.B. Kinter, Mechanisms of soil-lime stabilization: An interpretive review, Highw. Res. Rec. 92 (1965) 83–102.
[47] C. Cherian, D.N. Arnepalli, A critical appraisal of the role of clay mineralogy in lime stabilization, Int. J. Geosynth. Gr. Eng. 1 (2015) 8. https://doi.org/10.1007/s40891-015-0009-3.
[48] J.R. Prusinski, S. Bhattacharja, Effectiveness of Portland cement and lime stabilizing clay soils, Transp. Res. Rec. (1999) 215–227. https://doi.org/10.3141/1652-28.
[49] S. Bhattacharja, J.I. Bhatty, H.A. Todres, Stabilization of clay soils by portland cement or lime–a critical review of literature, PCA R&D Ser. (2003) 60.
[50] L. Wadsö, F. Winnefeld, K. Riding, P. Sandberg, Calorimetry, in: K. Scrivener, R. Snellings, B. Lothenbach (Eds.), A Pract. Guid. to Microstruct. Anal. Cem. Mater., CRC Press, Boca Raton, 2016: pp. 37–74.
[51] P. Ii, R. January, Developing a Simple and Rapid Test for Monitoring the Heat Evolution of Concrete Mixtures for Both Laboratory and Field Applications, (2007).
[52] D. Adolfsson, F. Engström, R. Robinson, B. Björkman, Cementitious phases in ladle slag, Steel Res. Int. 82 (2011) 398–403. https://doi.org/10.1002/srin.201000176.
[53] D. Adolfsson, R. Robinson, F. Engström, B. Björkman, Influence of mineralogy on the hydraulic properties of ladle slag, Cem. Concr. Res. 41 (2011) 865–871. https://doi.org/10.1016/j.cemconres.2011.04.003.
[54] J. Setién, D. Hernández, J.J. González, Characterization of ladle furnace basic slag for use as a construction material, Constr. Build. Mater. 23 (2009) 1788–1794. https://doi.org/10.1016/j.conbuildmat.2008.10.003.
[55] V.Z. Serjun, B. Mirtič, A. Mladenovič, Evaluation of ladle slag as a potential material for building and civil engineering, Mater. Tehnol. 47 (2013) 543–550.
[56] J. Vlček, R. Švrčinová, J. Burda, M. Topinková, M. Klárová, H. Ovčačiková, D. Jančar, M.

Velička, Hydraulic properties of ladle slags, Metalurgija. 55 (2016) 399–402.
[57] M.P. Javellana, I. Jawed, Extraction of free lime in portland cement and clinker by ethylene glycol, Cem. Concr. Res. 12 (1982) 399–403. https://doi.org/10.1016/0008-8846(82)90088-6.
[58] H.-S. Lee, H.-S. Lim, M.A. Ismail, Quantitative evaluation of free CaO in electric furnace slag using the ethylene glycol method, Constr. Build. Mater. 131 (2017) 676–681. https://doi.org/10.1016/j.conbuildmat.2016.11.047.
[59] A.C. Jupe, X. Turrillas, P. Barnes, S.L. Colston, C. Hall, D. Häusermann, M. Hanfland, Fast in situ x-ray-diffraction studies of chemical reactions: A synchrotron view of the hydration of tricalcium aluminate, Phys. Rev. B. 53 (1996) R14697–R14700. https://doi.org/10.1103/PhysRevB.53.R14697.
[60] Z. He, Y. Li, The influence of mayenite employed as a functional component on hydration properties of ordinary portland cement, Materials (Basel). 11 (2018) 1958. https://doi.org/10.3390/ma11101958.
[61] R.N. Edmonds, A.J. Majumdar, The hydration of $12CaO.7A_{12}O_3$ at different temperatures, Cem. Concr. Res. 18 (1988) 473–478. https://doi.org/10.1016/0008-8846(88)90082-8.
[62] A. Gupta, P.D. Armatis, P. Sabharwall, B.M. Fronk, V. Utgikar, Thermodynamics of Ca(OH)2/CaO reversible reaction: Refinement of reaction equilibrium and implications for operation of chemical heat pump, Chem. Eng. Sci. 230 (2021) 116227. https://doi.org/10.1016/j.ces.2020.116227.
[63] E. Bernard, Y. Yan, B. Lothenbach, Effective cation exchange capacity of calcium silicate hydrates (C-S-H), Cem. Concr. Res. 143 (2021) 106393. https://doi.org/10.1016/j.cemconres.2021.106393.
[64] O. Linderoth, L. Wadsö, D. Jansen, Long-term cement hydration studies with isothermal calorimetry, Cem. Concr. Res. 141 (2021). https://doi.org/10.1016/j.cemconres.2020.106344.
[65] K. Scrivener, A. Ouzia, P. Juilland, A. Kunhi Mohamed, Advances in understanding cement hydration mechanisms, Cem. Concr. Res. 124 (2019) 105823. https://doi.org/10.1016/j.cemconres.2019.105823.
[66] A.S. Brand, S.B. Feldman, P.E. Stutzman, A.V. Ievlev, M. Lorenz, D.C. Pagan, S. Nair, J.M. Gorham, J.W. Bullard, Dissolution and initial hydration behavior of tricalcium aluminate in low activity sulfate solutions, Cem. Concr. Res. 130 (2020) 105989. https://doi.org/10.1016/j.cemconres.2020.105989.
[67] J.W. Bullard, H.M. Jennings, R.A. Livingston, A. Nonat, G.W. Scherer, J.S. Schweitzer, K.L. Scrivener, J.J. Thomas, Mechanisms of cement hydration, Cem. Concr. Res. 41 (2011) 1208–1223. https://doi.org/10.1016/j.cemconres.2010.09.011.
[68] B. Rotenberg, J.P. Morel, V. Marry, P. Turq, N. Morel-Desrosiers, On the driving force of cation exchange in clays: Insights from combined microcalorimetry experiments and molecular simulation, Geochim. Cosmochim. Acta. 73 (2009) 4034–4044. https://doi.org/10.1016/j.gca.2009.04.012.

[69] D. Damidot, A. Nonat, C3S hydration in diluted and stirred suspensions: (I) study of the two kinetic steps, Adv. Cem. Res. 6 (1994) 27–35. https://doi.org/10.1680/adcr.1994.6.21.27.

[70] K. Kyritsis, N. Meller, C. Hall, Chemistry and morphology of hydrogarnets formed in cement-based CASH hydroceramics cured at 200° to 350°C, J. Am. Ceram. Soc. 92 (2009) 1105–1111. https://doi.org/10.1111/j.1551-2916.2009.02958.x.

[71] L.G. Baquerizo, T. Matschei, K.L. Scrivener, M. Saeidpour, L. Wadsö, Hydration states of AFm cement phases, Cem. Concr. Res. 73 (2015) 143–157. https://doi.org/10.1016/j.cemconres.2015.02.011.

[72] L. Black, C. Breen, J. Yarwood, C.S. Deng, J. Phipps, G. Maitland, Hydration of tricalcium aluminate (C_3A) in the presence and absence of gypsum - Studied by Raman spectroscopy and X-ray diffraction, J. Mater. Chem. 16 (2006) 1263–1272. https://doi.org/10.1039/b509904h.

[73] A.N. Christensen, T.R. Jensen, N.V.Y. Scarlett, I.C. Madsen, J.C. Hanson, Hydrolysis of pure and sodium substituted calcium aluminates and cement clinker components investigated by in situ synchrotron X-ray powder diffraction, J. Am. Ceram. Soc. 87 (2004) 1488–1493. https://doi.org/10.1111/j.1551-2916.2004.01488.x.

[74] M. Sarkar, K. Dana, S. Ghatak, A. Banerjee, Polypropylene-clay composite prepared from Indian bentonite, Bull. Mater. Sci. 31 (2008) 23–28. https://doi.org/10.1007/s12034-008-0005-5.

[75] S. Karen, R. Snellings, B. Lothenbach, A Practical Guide to Microstructural Analysis of Cementitious Materials, 2018. https://doi.org/10.1201/b19074.

Chapter 7. Measuring mineralized carbon in cementitious materials by an acid digestion-titration method[6]

The contributions of the authors to this manuscript are described as follows:

Thien Q. Tran: Data curation; Formal analysis; Investigation; Methodology; Visualization; Writing - original draft; Writing - review and editing.

Note: Thien Q. Tran was in the main charge of the above-mentioned contribution categories under the supervision of Dr. Alexander S. Brand.

Rachel Cook: Data curation; Investigation; Writing - review and editing.

Olajide Ipindoala: Investigation.

Ebenezer O. Fanijo: Methodology.

Aron Newman: Supervision; Writing - review and editing.

Paul E. Stutzman: Conceptualization; Writing - review and editing.

Alexander S. Brand: Conceptualization; Funding acquisition; Methodology; Project administration; Supervision; Writing - original draft; Writing - review and editing.

[6] **Thien Q. Tran,** Rachel Cook, Olajide Ipindoala, Ebenezer O. Fanijo, Aron Newman, Paul E. Stutzman, and Alexander S. Brand. "Measuring mineralized carbon in cementitious materials by an acid digestion-titration method" (Under review)

Measuring mineralized carbon in cementitious materials by an acid digestion-titration method

Thien Q. Tran,[1] Rachel Cook[2], Olajide Ipindoala[3], Ebenezer O. Fanijo[1,4], Aron Newman[2], Paul E. Stutzman[2], and Alexander S. Brand[1,5*]

[1] The Charles E. Via, Jr. Department of Civil and Environmental Engineering, Virginia Polytechnic Institute and State University, Blacksburg, VA 24060, U.S.A.
[2] Infrastructure Materials Group, Materials and Structural Systems Division, Engineering Laboratory, National Institute of Standards and Technology, Gaithersburg, MD 20899, U.S.A.
[3]Department of Civil Engineering, Morgan State University, 1700 East Cold Spring Lane, Baltimore, MD 21251, U.S.A.
[4] School of Building Construction, Georgia Institute of Technology, Atlanta, GA 30332, U.S.A.
[5] Department of Materials Science and Engineering, Virginia Polytechnic Institute and State University, Blacksburg, VA 24060, U.S.A.
*Corresponding Author: asbrand@vt.edu

7.1 Abstract

As carbon dioxide (CO_2) sequestration technology begins to emerge in the construction and building materials sectors, industry stakeholders require quantifiable assurance of emerging carbonated products. This study adapts a Digestion-Titration Method (DTM) for the determination of mineralized CO_2 content in cementitious materials based on tests that were originally developed in the early 1900s. The experimental conditions were optimized with a systematic design of experiments (DOE) approach. The method utilizes hydrochloric acid to digest carbonate minerals (*i.e.*, $CaCO_3$, $MgCO_3$) under vacuum conditions. The liberated CO_2 from acid digestion is captured by a barium hydroxide solution to precipitate barium carbonate. Titration is used to quantify the remaining barium hydroxide, yielding a back-estimation of the total CO_2 content. We performed our study on mixtures of fixed compositions, portland cement, and a carbonated cementitious commercial product. DTM results were compared to thermogravimetric analysis (TGA) of the same samples. The outcomes of this work demonstrate that DTM can provide consistent results to TGA for samples containing a singular carbonate phase and yield more consistent quantification of mineralized CO_2 for samples containing multiple reaction products.

Keywords: Digestion-titration method (DTM); design of experiments (DOE); thermogravimetric analysis (TGA); mineralized carbon

7.2 Introduction

Demand for construction materials — predominately portland cement concrete — has been significantly increasing due to global urbanization [1,2]. Concrete is the most utilized man-made material globally. The production of cement contributes approximately 8 % to 9 % of global anthropogenic carbon dioxide (CO_2) emissions as a consequence [3]. Cement chemists are studying cement-based materials' ability to effectively absorb CO_2 through carbonation of various

cementitious phases such as calcium hydroxide ($Ca(OH)_2$) [4,5] and brucite ($Mg(OH)_2$) [6] to offset those emissions. Research has been ongoing (*e.g.*, [7–10]) with regard to this technology as well as the various cementitious materials (*e.g.*, magnesia-based cements [6], wollastonite-based cements [11,12], slaked lime [13,14]) that accompany it.

Reliable quantitative characterization techniques are needed to accurately report the degree of carbonation in these material mixtures. Commonly utilized characterization techniques for this application include X-ray diffraction (XRD), scanning electron microscopy coupled with energy-dispersive X-ray spectroscopy (SEM-EDS), solid-state nuclear magnetic resonance (NMR) spectroscopy, and thermogravimetric analysis (TGA). Each technique has relative advantages and disadvantages. XRD is a powerful technique that can identify phases present in a prepared powdered sample based on atomic interplanar spacings and quantify crystalline phases [15]. Identification and quantification of amorphous, nanocrystalline, and glassy phases (*e.g.*, calcium silicate hydrate, amorphous $CaCO_3$) can be challenging despite modern refinements of the techniques (*e.g.*, Partial Or No Known Crystal Structures [16,17]). SEM-EDS is a characterization technique that allows for targeted elemental analysis of a sample's surface and mapping elemental concentrations, regardless of crystallinity. The technique measures the X-ray energy and intensity distribution produced by the electron beam interacting with the sample's subsurface (*i.e.*, penetrating the sample ≈ 0.02 μm to 1.0 μm) [18,19]. SEM-EDS has reduced quantitative accuracy for lighter elements, such as carbon and oxygen, and cannot measure hydrogen directly. It is commonly used *via* point analyses as an approximation technique [19]. Solid-state NMR has been gaining acceptance as a characterization technique [20]. For multi-component mixtures like cement-based materials, solid-state NMR provides the ability to detect and isolate phases *via* nuclear spin isotope selection for short and long-range structural ordering in amorphous and crystalline phases. Examples include quantitative NMR (*e.g.*, [21,22]), $\{^1H\}^{29}Si$ cross-polarization magic-angle-spinning (CPMAS) NMR (*e.g.*, [23]), and *in situ* solid-state NMR (*e.g.*, [24]). To the best of the authors knowledge NMR has not been implemented to quantify mineralized CO_2 contents in cementitious materials. TGA operates by measuring the mass of a sample as a function of increasing temperature typically in an inert atmosphere, allowing for the quantification of phase(s) present based on mass loss in specified temperature ranges [25]. TGA is able to identify both crystalline and amorphous phases when used in tandem with other techniques such as XRD. Additionally, once an acceptable method (*e.g.*, ASTM C1872 [26]) is established, TGA will require relatively minimal training in operation. However, for cement-based materials, the determination of CO_2 content from TGA is not necessarily straightforward due to convolution from overlapping thermal phenomena.

Overlapping thermal phenomena complicates identification and quantification by TGA. In the context of this study, thermal decomposition signatures of carbonates can purportedly occur between 105 °C and 1000 °C [27] due to the following factors. The mass lost observed between 550 °C and 830 °C is typically associated with $CaCO_3$ thermal decomposition [27–29] but can also be associated with iron oxidation [25]. Calcite typically decomposes above 600 °C but amorphous $CaCO_3$ partially thermally decomposes between 400 °C and 600 °C [30], crystallizes, and then

decomposes entirely above 600 °C. The polymorphs of calcium carbonate (*i.e.*, calcite, aragonite, and vaterite) can exhibit different thermal phenomena due to bound water contents [31]. For magnesia-based cements, magnesite ($MgCO_3$) decomposition occurs between 550 °C and 650 °C [32]. Thermal decomposition of calcium silicate hydrate occurs over a wide range from 50 °C to 600 °C with an additional dehydroxylation mass loss at 800 °C [27], thus overlapping with the thermal decomposition temperature ranges of $CaCO_3$ and $MgCO_3$. Decomposition range of $CaCO_3$ can vary due to experimental configuration [27] and other factors [33,34], such as vapor pressure, sample mass, and particle size. Discrepancies in decomposition ranges can consequently lead to underestimated reports of $CaCO_3$ content [35]. Thus, it is challenging to utilize TGA as a standalone technique for both phase identification and quantification of a complex cementitious mixture. TGA coupled with mass spectrometry (TGA-MS) analysis of the evolved gas could provide a more accurate measurement of CO_2 content with temperature [36], although TGA-MS instruments are less common. The acid digestion-titration technique (DTM) this publication focuses on provides a cost-effective method to quantify mineralized CO_2, regardless of composition and crystallinity of the phases present. To provide context for this technique, a brief literature review on similar wet-chemistry approaches is provided.

The initial concept of the determination of CO_2 in carbonate minerals using a chemical approach was first introduced in the early 1900s. The first chemical method *via* acid digestion-titration method (DTM), to the best of the authors' knowledge, was devised in 1918 by Van Slyke to determine the carbonate content of bones and to determine bicarbonate content in the blood [37]. The fundamental mechanism of Van Slyke's DTM is that CO_2 from a powder or a solution is rapidly liberated by adding strong acid under reduced pressure. The liberated CO_2 is captured by a prepared barium hydroxide ($Ba(OH)_2$) solution, consequently allowing barium carbonate ($BaCO_3$) to precipitate. An acid-base titration method is then used to calculate the amount of remaining $Ba(OH)_2$ solution, thereby back-calculating the CO_2 that was liberated by the sample. Figure 7- 1a shows the DTM configuration by Van Slyke.

In 1926, Hepburn [38] proposed a DTM technique similar to Van Slyke's method for sodium and calcium carbonate samples. In 1935, Edwards *et al.* [39] modified these methods for food science applications (*e.g.*, baking powder and self-rising flour), and their test configuration is shown in Figure 7- 1b. Another version of the Van Slyke method was proposed by Tinsley *et al.* [40] in 1951 to measure CO_2 content in soil and limestone. Amela *et al.* [41] used a similar method to measure the CO_2 liberated during the reaction of L-tartaric acid with sodium bicarbonate.

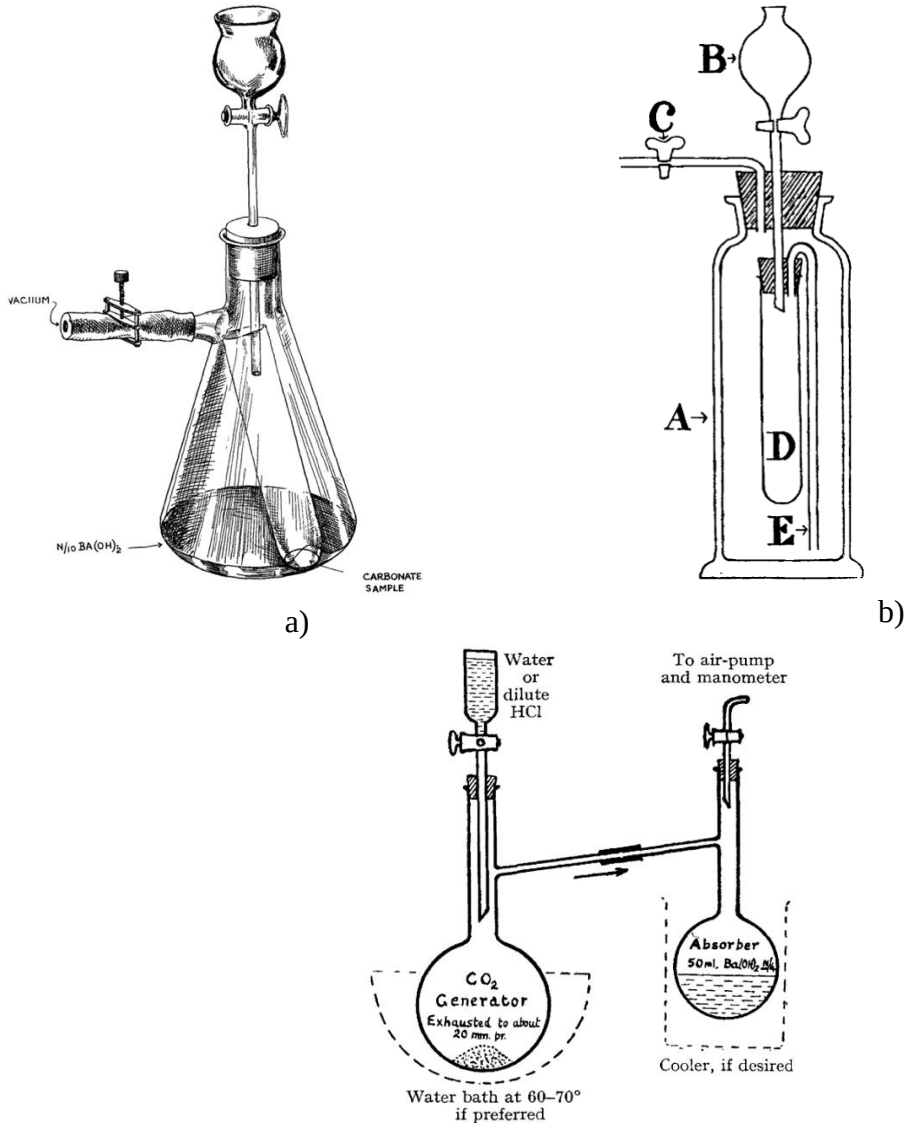

Figure 7- 1. Schematics of the DTM configurations from a) Van Slyke [37] b) Edwards et al. [39], and c) Cornell et al. [42].

The Analytical Investigations Committee of the Australian Chemical Institute [42,43] developed a new system (Figure 7- 1c) for this work based on similar working mechanisms as mentioned earlier but occurring at a reduced boiling point of water. Jones [44] developed a similar system in 1940 but used two separate glass filter tubes instead of distillation flasks. Based on a similar working mechanism, Partridge and Schroeder [45] developed a method that included extra components in an effort to eliminate CO_2 from the ambient air passing into the system during testing.

The different experimental methods discussed for the determination of mineralized CO_2 in different materials are summarized in Table 7- 1. The majority of previous publications utilizing DTM configurations were developed for the food or medical industries, and only one DTM study

[39] was aimed at construction materials, which included quick lime, gypsum plaster, portland cement, white cement, hydrated calcium silicate, and brick mortar. Overall, the published DTM configurations have varied widely in terms of agitation or waiting time, reaction time ranging from 10 minutes (min) to 24 hours (h), and complexity of the test setup.

Table 7- 1. Comparisons between methods for determination of carbon dioxide in different materials.

Categories	Van Slyke [37]	Hepburn [38]	Edwards *et al.* [39]	Tinsley *et al.* [40]	Cornell [42]	Jones [44]	Partridge and Schroeder [45]	TGA
Year found	1918	1926	1935	1951	1936	1940	1932	
Targeted materials	Bones and blood	All carbonates	Baking powders and self-raising flours	Soils and limestone	Baking powders and self-raising flours	Construction materials (e.g., quick lime, gypsum, portland cement)	Carbonates	Powdered materials
Experimental setup	Somewhat simple	Somewhat simple	Somewhat simple	Simple	**Somewhat complicated**	**Somewhat complicated**	**Very complicated**	Simple
Evacuation time	**Not specified**	**Not specified**	**10 min**	**Not specified**	**Not specified**	"a few minutes"	**10 min**	few minutes (taring)
Discomposing/Absorption time (rotating and waiting time)	**7 h**	**12 h to 24 h**	**3.5 h to 4.0 h**	**5.0 h**	15 min to 45 min	**35 min to 40 min**	10 min	**1 h to 2 h**
Calculation Guide	**No**	**No**	**No**	Yes	**No**	**No**	**No**	**No**
Accessibility	Easy	Easy	Easy	Easy	Easy	Easy	**Somewhat difficult**	**Can be difficult**

Note: Disadvantageous properties of each method are bolded.

The novelty of the current study is the configuration and systematic optimization of a DTM test for construction and building materials. This DTM procedure utilizes basic chemistry laboratory supplies and chemicals, allowing for the introduction of an economical and easily accessible test method that can be readily implemented. The DTM procedure was developed in collaboration between researchers at Virginia Tech (VT) and the National Institute of Standards and Technology (NIST). These results are compared to analyses of the same samples by TGA to provide a robust test of the technique.

7.3 Experimental methodology

7.3.1 Test setup

The configuration in this study allows for acid injection directly onto the sample using a 1 mL syringe and needle ensuring contact of the entire sample with all injected solution instead of the separating funnels as previous methods required. As shown in Figure 7- 2, a 15 mL test tube is connected to a 29/42 standard rubber septum Figure 7- 2)[7]. A 2 mm diameter hole was drilled (Figure 7- 2) to liberate the CO_2 from the sample, allowing for the emitted CO_2 to dissolve into the $Ba(OH)_2$ solution. The septum is secured into the top of a 250 mL Erlenmeyer flask with a sidearm to connect a section of tubing with a vacuum stopcock. This arrangement allows the acid to contact the sample under a vacuum environment at the bottom of the tube without the risk of splashing or spraying that could contaminate the $Ba(OH)_2$ solution in the flask. The compact design, along with improvements in pump design and efficiency, minimizes evacuation time to approximately ten seconds compared to upwards of 10 minutes in previous reported configurations. The reduced pumping time and elimination of separating funnels simplifiying each apparatus allows users to run multiple tests the concurrently. Some illustrations of the configuration are presented in Figure 7- 3.

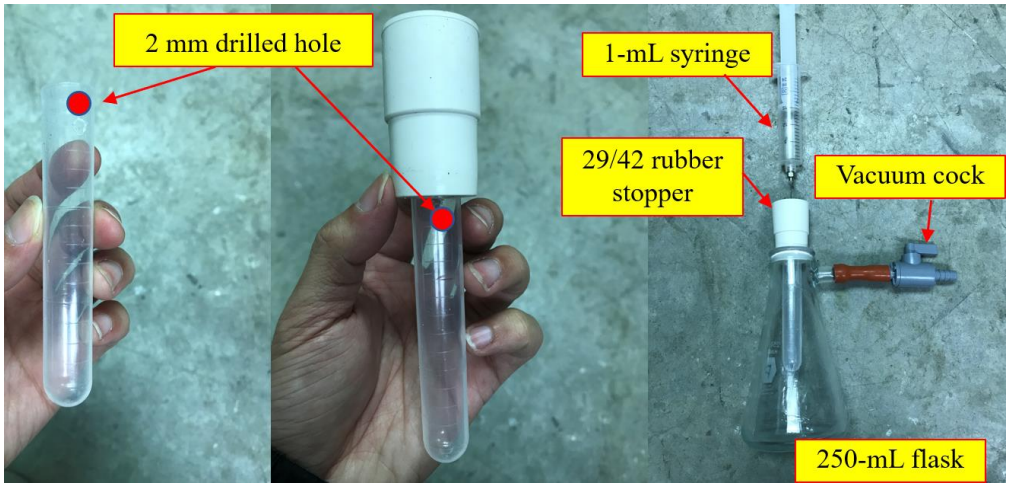

Figure 7- 2. DTM configuration: 1) a 15 mL plastic test tube has a 2 mm diameter hole drilled near the top, 2) a standard 29/42 rubber septum is fit snugly to the test tube, and 3) the septum is secured in a 250 mL Erlenmeyer flask.

[7] The NIST setup used a specially fabricated 30 mL glass test tube.

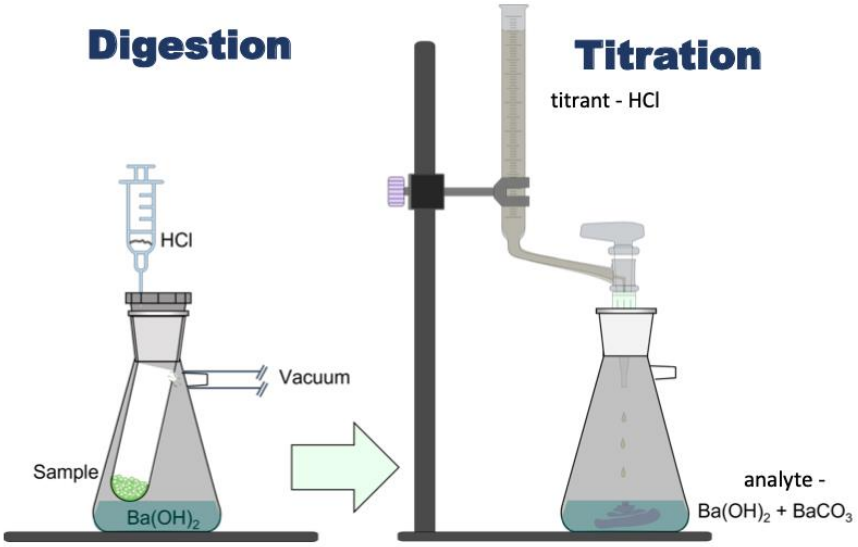

a)

b) c)

Figure 7- 3. A schematic of the DTM test (a) with actual setups at Virginia Tech (b) and NIST (c).

7.3.2 Calculation

When the liberated CO_2 is dissolved in the $Ba(OH)_2$ solution, $BaCO_3$ precipitates according to Equation 1. Titration is then used to determine the remaining hydroxide content, according to Equation 2.

$$Ba(OH)_2\ (aq) + CO_2\ (g) \rightarrow BaCO_3\ (s) + H_2O \quad (1)$$

$$2\ HCl\ (aq) + Ba(OH)_2\ (aq) \rightarrow BaCl_2\ (aq) + 2\ H_2O \quad (2)$$

The total dissolved CO_2 in the $Ba(OH)_2$ solution (M_{CO_2}) is estimated according to Equation 3, where A is the number of mols in the $Ba(OH)_2$ solution at the start of the experiment, b is the number of mols of hydrochloric acid (HCl) titrated ($\frac{b}{2}$ is the number of mols of $Ba(OH)_2$ neutralized

during titration), and b_o is the number of mols of HCl titrated estimated from a baseline titration. The concentration of HCl was kept low (0.1 N) for more accurate titration and to avoid over-neutralizing the remaining barium solution, in which the excessive HCl might dissolve the $BaCO_3$ precipitate and cause misleading in titration reading. A factor of 44 is included to convert from mols of CO_2 to grams, since the molecular weight of CO_2 is 44 g mol^{-1}, and a factor of 1000 is included to convert from liter to milliliter.

$$M_{CO_2} = \frac{44}{1000}\left[\left(A - \frac{b}{2}\right) - \left(A - \frac{b_o}{2}\right)\right] = \frac{44}{1000}\left[\left(\frac{b_o}{2} - \frac{b}{2}\right)\right] = 0.022(b_o - b) \qquad (3)$$

A prepared $Ba(OH)_2$ solution may absorb some atmospheric CO_2 over time. A baseline titration should always be performed before the actual test. Performing a baseline titration is critical to maintain the accuracy of the test method; if this was performed in the DTM configurations presented in the literature it was not explicitly discussed in those publications except for Amela *et al.* [41]. The total $CaCO_3$ amount in a sample (M_{CaCO_3}) will be calculated according to Equation 4, which includes a factor of 44, since the molecular weight of CO_2 is 44 g mol^{-1}, and a factor of 100, since the molecular weight of $CaCO_3$ is 100 g mol^{-1}.

$$M_{CaCO_3} = M_{CO_2}\frac{100}{44} = 0.022(b_o - b)\frac{100}{44} = 0.05(b_o - b) \qquad (4)$$

7.3.3 Design of experiments (DOE)

A DOE approach was used to optimize the experimental configuration. Four factors were considered at three levels, as described in Table 7- 2. The four factors were sample size, absorption time, acid strength for digestion, and $Ba(OH)_2$ solution volume. Since there are three levels and four factors being considered, the full factorial testing would require 81 (= 3^4) experiments. To eliminate the need to perform One Factor at a Time (OFAT) testing, the Orthogonal Arrays (OA) of the Taguchi method was utilized, reducing the required number of experiments. The experimental parameters and their levels are presented in Table 7- 2.

Table 7- 2. Design of Experiment (Phase 1).

Experimental parameters	**Fixed Input**	**Symbol**	**Unit**	**Levels**		
				1	**2**	**3**
Absorption time (shaking time plus a few min of digestion in advance)		A	Minute (min)	5	30	120
Acid concentration (HCl)	3 mL	B	Molarity (M)	1.0	1.5	2.5
Sample size (99% pure $CaCO_3$)		C	Grams (g)	0.05	0.1	0.2
$Ba(OH)_2$	0.3 N	D	Volume (mL)	10	20	40

Based on the OA of the Taguchi method coupled with Qualitek software[8] working with four factors and three levels without interactions, nine trials with three replicates totaling 27 experiments were implemented for this DOE. Finally, the most reliable parameters were the selected to be the ultimate test procedure for the acid DTM.

7.3.4 Method validation

To validate the proposed method, different synthesized materials were made by NIST containing known amounts of calcite (Cal) to be used as validating samples. Three sets of powdered samples were prepared by mass. The first sample set was calcite mixed with calcite-free quartz sand with 0 %, 20 %, 40 %, 60 %, 80 %, and 100 % calcite by mass. The second sample set was beach rock (BR) mix with calcite-free quartz sand with 20 %, 40 %, 60 %, 80 %, and 100 % BR by mass. The third sample set included commercial products including one carbonated cementitious commercial product (CP), NIST SRM 1889b Portland Cement Blended with Limestone [46], and NIST SRM 1884b Portland Cement [47]. Three DTM tests were conducted for each prepared mixture following the proposed procedures. The results obtained by DTM and TGA methods were compared, and sample measurements at NIST and at VT were compared. Approximately 0.1 g of each mixture was subjected to TGA experiments using inert nitrogen at the heating rate of 10 ^{o}C min^{-1} to 1000 ^{o}C. Three TGA replicate tests were conducted at NIST. One TGA test was performed at VT per sample.

While it was assumed that $CaCO_3$ is the only carbonate of concern for cement-based materials, additional experiments were performed using $MgCO_3$ blended with alumina (Al_2O_3) as an inert phase. Samples were prepared with 20 %, 40 %, 60 %, 80 %, and 100 % $MgCO_3$ by mass. It should be noted that the $MgCO_3$ used in this study was 70.4 % purity, as determined using TGA; this is a result of magnesium carbonate typically being present as a hydrous phase (*i.e.*, $MgCO_3 \bullet xH_2O$, where x is 2, 3, or 5).

Since organic content can exist in samples collected in the field and since organic content could interfere with the acid digestion, additional experiments were performed with calcite blended with 10 % of humic acid ($C_9H_9NO_6$) or 10 % tannic acid ($C_{76}H_{52}O_{46}$) by mass. In addition, gypsum ($CaSO_4 \cdot 2H_2O$) containing 20.9 % of $CaCO_3$ was also subjected to the test to check whether the sulfur trioxide formed during decomposition of this material introduces interference in the DTM.

7.4 Results and discussion

7.4.1 DOE results and discussion

Figure 7- 4 plots the results from the nine cases considered in the DOE. The proposed testing configuration worked efficiently absorbing approximately 100 % of the CO_2 liberated from 99 % pure $CaCO_3$ with a maximum standard deviation of 3.4 % regardless of different testing procedures

[8] Certain commercial equipment, instruments, or materials are identified in this paper to foster understanding. Such identification does not imply recommendation or endorsement by the National Institute of Standards and Technology, nor does it imply that the materials or equipment identified are necessarily the best available for the purpose.

such as reacting time. Some cases reported slightly over 100 % of the given $CaCO_3$ (Experiments No. 1, 4, and 9); this may be due to heterogeneity of the sample (from 1 % of its impurity) and/or experimenter error in materials weighting or acid titration. The results indicate that 5 minutes of absorption time is sufficient to obtain quality results. This eliminates shaking and standby hours compared to previous DTM test procedures in the literature. It is important to note that the DOE tests demonstrate that the DTM method is affected by sample size, strength of injected acid, and volume of the $Ba(OH)_2$ solution. For example, No. 5 used only 10 mL of $Ba(OH)_2$ solution, which was insufficient and absorbed roughly 0.088 g of emitted CO_2. No. 7 used the weakest HCl strength (1.0 N) of all concentrations considered, and could not digest the 0.2 g sample, liberating only a small amount of CO_2 captured by the $Ba(OH)_2$ solution.

Table 7- 3. Trials of testing procedures for optimal testing conditions.

Experiment No.	**Testing procedures**				**Measured Values**				
	A	**B**	**C**	**D**	**Y1**	**Y2**	**Y3**	**Average**	**Std Dev**
1	1	1	1	1	97.80	96.82	102.22	102.82	3.30
2	1	2	2	2	101.48	99.46	96.02	98.99	2.76
3	1	3	3	3	100.08	99.35	98.09	99.17	1.01
4	2	1	2	3	105.38	102.58	98.26	102.08	3.59
5	2	2	3	1	72.68	75.25	74.06	**74.00**	1.28
6	2	3	1	2	98.17	100.43	99.12	99.24	1.13
7	3	1	3	2	66.01	65.20	64.82	**65.34**	0.61
8	3	2	1	3	75.57	40.26	23.45	**46.43**	26.60
9	3	3	2	1	102.42	100.48	99.71	100.87	1.40

Note: the bolded numbers are the ones that did not provide expected results

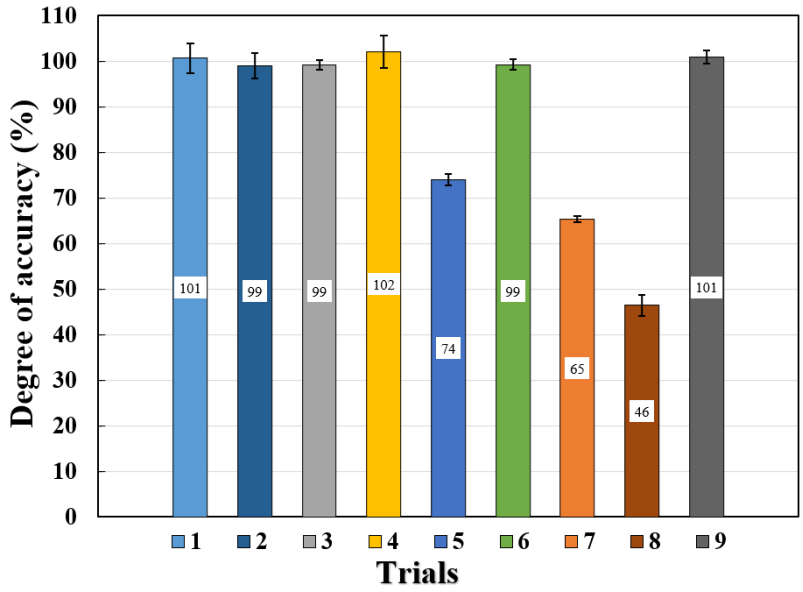

Figure 7- 4. Degree of accuracy of nine DOE trials.

7.4.2 Proposed test procedure

One of the aims of this study was to propose a robust procedure that is capable of managing a wide range of sample types. The above-mentioned issues identified with some of the variants in the DOE tests could be solved by a few chemical calculations and adjusting the testing procedure could case by case. But a most-robust set of parameters were sellected based on the DOE results in Section 7.4.1 and used to devise a final step-by-step DTM procedure.

(1) Weigh 0.2 g of powdered sample into the 15 mL test tube.
(2) Fill the 250 mL Erlenmeyer flask with 15 mL of 0.3 N $Ba(OH)_2$ solution. Connect the vacuum tubing with a vacuum stopcock from the Erlenmeyer flask sidearm to the vacuum pump.
(3) Attach the test tube to the rubber septum, and insert the septum into the top of the Erlenmeyer flask.
(4) Apply vacuum and slowly open the stopcock to subject the Erlenmeyer flask[9] to vacuum until the pressure gauge reaches around 80 kPa. (Approximately 30 seconds or less in our tests).
(5) Use a syringe with a needle to inject 3 mL of 2.5 N HCl through the rubber septum to the powdered sample in the test tube. This should be performed cautiously to avoid violent ebullition that can contaminate the $Ba(OH)_2$ solution.[10] For samples with high $CaCO_3$ contents (> 60 %), it is recommended to inject the acid slowly and in smaller increments (*e.g.*, 0.5 mL at a time). Allow the sample to be digested for a few minutes until no bubbles are visibly generated from the sample.
(6) Allow $Ba(OH)_2$ solution to capture the emitted CO_2 for 5 min with the aid of gentle swirling. In this study, a rotating speed of 180 rpm for an orbital shaker was found to be sufficient to keep

[9] Note that an Erlenmeyer flask may not be rated for vacuum conditions. It is recommended to use vacuum-rated glassware.
[10] The VT researchers discovered this issue when using a 15 mL test tube, but the NIST researchers did not encounter this issue with a 30 mL test tube.

the barium absorbent surface free from precipitates, which can block CO_2 absorption processes. Care should be taken during agitation to prevent HCl from contaminating the $Ba(OH)_2$ solution.
(7) Slowly release the flask from the vacuum by opening the vacuum stopcock and gently take the septum off the flask with the test tube still attached. Add a few drops of phenolphthalein (2 % phenolphthalein in 95 % ethanol) to the $Ba(OH)_2$ solution in the flask as a pH indicator.
(8) Titrate the $Ba(OH)_2$ solution using 0.1 N HCl to determine the remaining $Ba(OH)_2$. A baseline $Ba(OH)_2$ solution should also be titrated at this point to estimate the amount of dissolved atmospheric CO_2. Calculate the CO_2 amount that was dissolved into the solution and precipitated as $BaCO_3$ according to Equation 3.

While the NIST researchers followed the procedure above, the VT researchers used a scaled-down procedure with a smaller sample size to validate the procedure for smaller samples and for samples with a low carbonate content. The VT researchers used the same procedure above, except that the powdered sample amount was 0.05 g, 2 mL of 2.5 N HCl was used for sample digestion, and 5 mL of $Ba(OH)_2$ solution was used to capture the CO_2.

7.4.3 Method validation

Figure 7- 5 shows the comparison of $CaCO_3$ contents obtained by the DTM test and the TGA performed by the NIST researchers. The results achieved by the two methods are in agreement, even though TGA results have less variability. While the maximum standard deviation recorded for TGA is around 1 %, the maximum standard deviation for the DTM test is 2.9 %. The results from the VT researchers also report good agreement between the DTM and TGA results, as shown in Figure 7- 6.

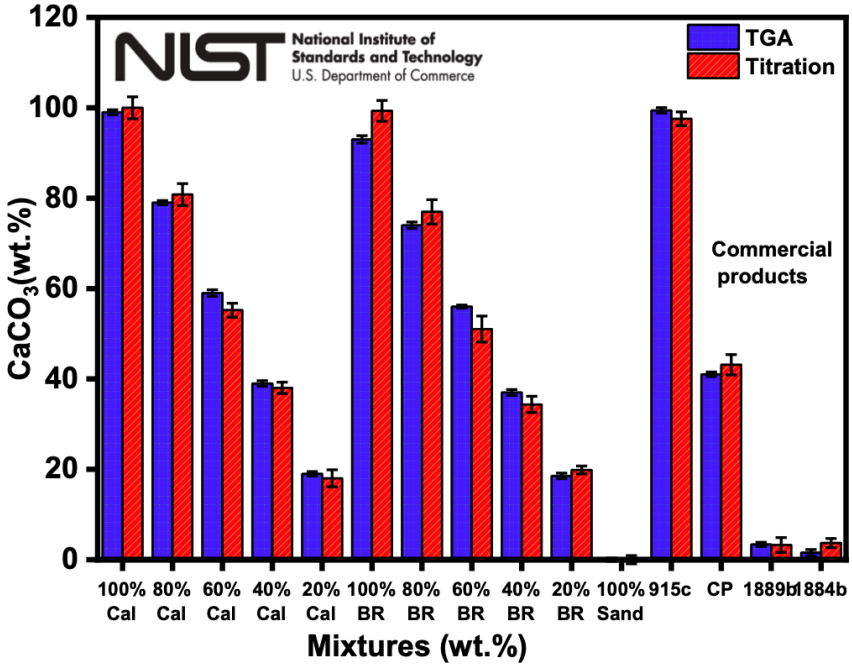

Figure 7- 5. $CaCO_3$ content obtained by NIST researchers using TGA and DTM.

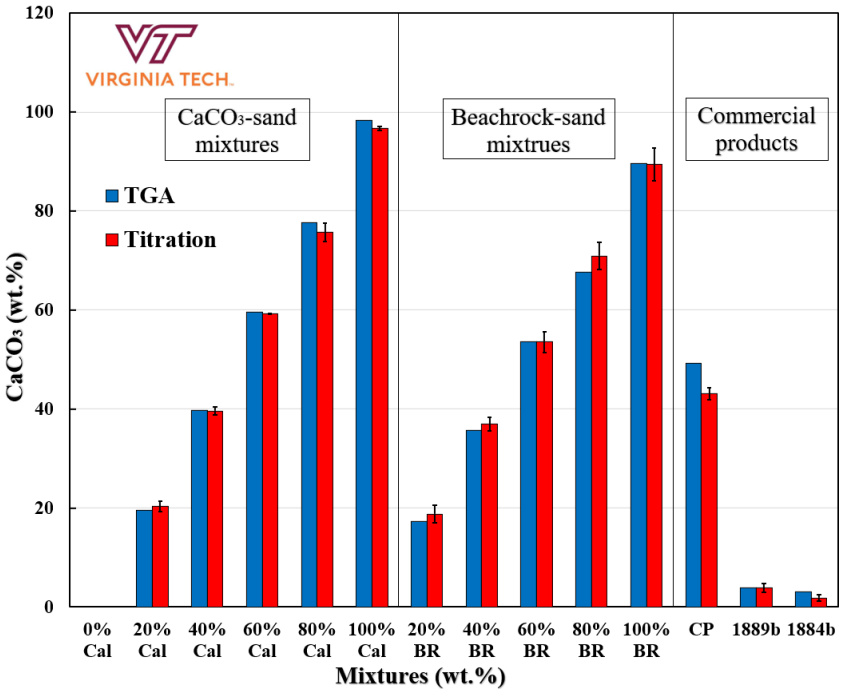

Figure 7- 6. $CaCO_3$ content obtained by VT researchers using TGA and DTM.

Figure 7- 7 compares $CaCO_3$ contents in prepared mixtures using TGA from the NIST and VT researchers. In general, the results show strong agreement, but there was a slight exception for the 80 % BR sample.

Similarly, **Error! Reference source not found.** collates $CaCO_3$ contents in prepared mixtures obtained using DTM from the NIST and VT researchers. In general, there was strong agreement, but there were slight exceptions for the 80 % BR and 100 % BR samples. The results indicate that the down-scaled procedure from VT works as effectively as the NIST procedure. With a smaller amount of sample, this down-scaled procedure is especially recommended for materials containing very high content of $CaCO_3$ (above 60 %) since it can reduce the risk of ebullition, which can contaminate the $Ba(OH)_2$ solution.

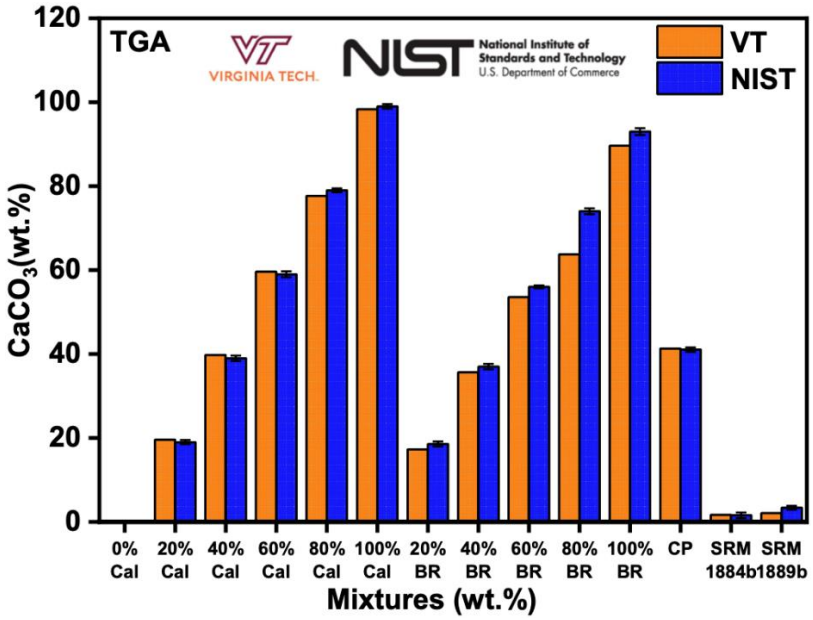

Figure 7- 7. $CaCO_3$ content determined by TGA comparing the NIST and VT results.

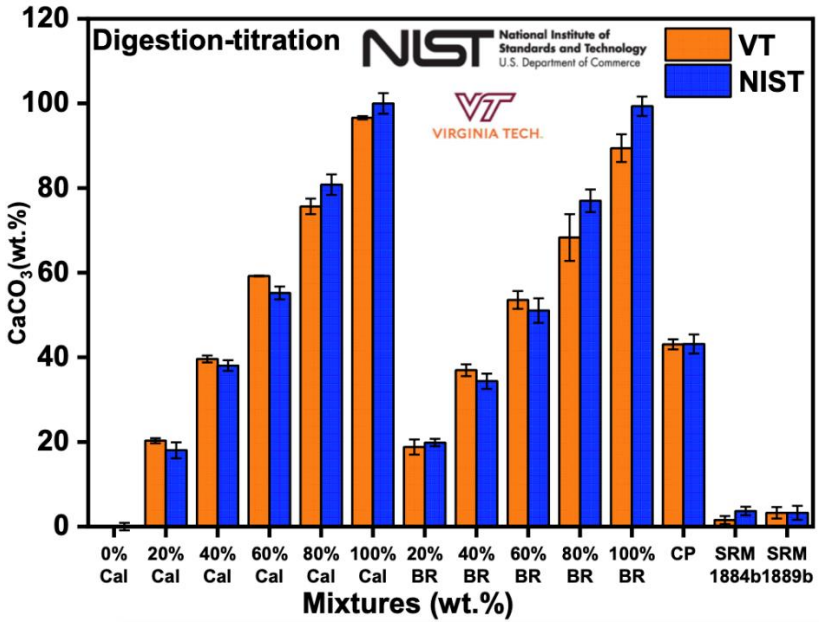

Figure 7- 8. $CaCO_3$ content determined by DTM comparing the NIST and VT results.

For the commercial products, the VT and NIST results yielded similar results for sample CP of around 43 % by DTM but TGA results ranged from 48 % to 49 %. The discrepancy is likely caused by overlapping decomposition temperatures for $CaCO_3$ and other phases. Figure 7- 9 shows the mass loss *vs.* temperature plot corresponding to TGA results for CP, and it can be seen that there is a continuous decreasing mass, which is a strong indication of decomposition of other phases, such as but not limited to calcium silicate hydrate. For TGA analysis, the mass loss associated with $CaCO_3$ may include mass corresponding to the decomposition of other phases, thereby yielding an

overestimated $CaCO_3$ content by TGA, which would explain why TGA yielded a greater estimate of $CaCO_3$ than DTM. The TGA-MS results by Morandeau *et al.* [36] suggests overlapping temperature ranges for loss of mass due to water and CO_2 in carbonated cement pastes, although Lerigoleur [49] showed no water and CO_2 overlap in cement pastes carbonated up to 24 hours. However, regardless of the overlapping decomposition temperature ranges, other authors have reported that TGA typically underestimates $CaCO_3$ contents due to issues buoyancy correction among other errors [35].

When analyzing the portland cement samples, VT and NIST consistently found that SRM 1889b had around 3 % to 4 % $CaCO_3$ using both DTM and TGA. According to the published SRM 1889b Certificate of Analysis [47], the mass loss between 550 ℃ and 950 ℃ is 1.55 % ± 0.12 %, which corresponds to 3.52 % ± 0.27 % $CaCO_3$ if is assumed that this mass loss range is only due to $CaCO_3$ thermal decomposition. Therefore, there is reasonable agreement between the published SRM 1889b and the TGA and DTM results.

However, there was scatter in the result of SRM 1884b, ranging from 1.9 % to 3.7 % reported by DTM method and from 0.9 % to 3.0 % reported by TGA analysis. According to the published SRM 1884b Certificate of Analysis [48], the mass loss between 550 ℃ and 950 ℃ is 0.597 % ± 0.031 %, which corresponds to 1.36 % ± 0.07 % $CaCO_3$ if is assumed that this mass loss range is only due to $CaCO_3$ thermal decomposition. This error could be attributable to the very low $CaCO_3$ content of this sample, making it difficult to determine accurately by DTM and TGA.

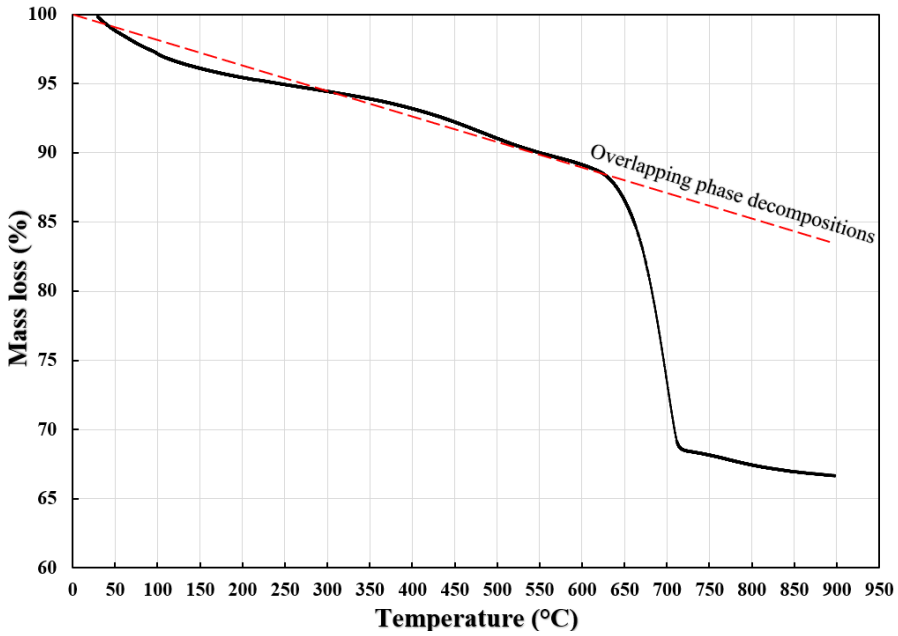

Figure 7- 9. An example of background noise in TGA curve of CP sample.

The results in Figure 7- 10 show that the proposed DTM could measure the $MgCO_3$ content in the mixtures compared to TGA. This is promising when this proposed method can also apply to different types of cements or carbonates, such as a carbonated magnesia-based cement. On the other hand, this can also be a drawback as it could potentially mislead and confuse the DTM results

for the materials containing a mixture carbonate minerals. The $MgCO_3$ amount in a sample will be calculated based on the Equation 5, since the molecular weight of $MgCO_3$ is 84 g mol^{-1}.

$$M_{CaCO_3} = \frac{84}{44} M_{CO_2} \quad (5)$$

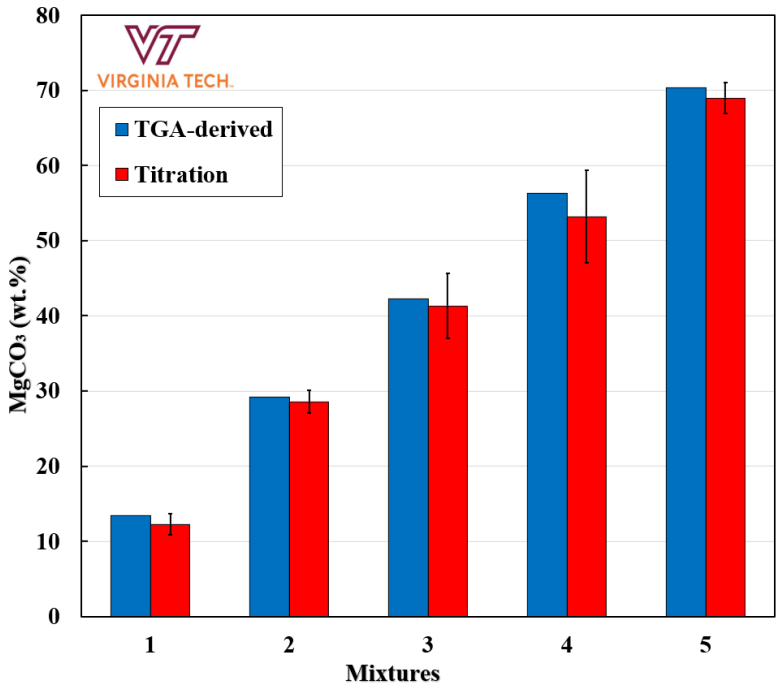

Figure 7- 10. $MgCO_3$ content in $MgCO_3$-Al_2O_3 mixtures obtained by the proposed DTM method at VT.

The authors found that sulfur trioxide, such as formed during decomposition of gypsum ($CaSO_4 \cdot 2H_2O$), did not have interference for the DTM. In addition, humic acid and tannic acid did not appear to interfere with the DTM test. The results are presented in Figure 7- 11, showing similar results with and without the potential interfering compound.

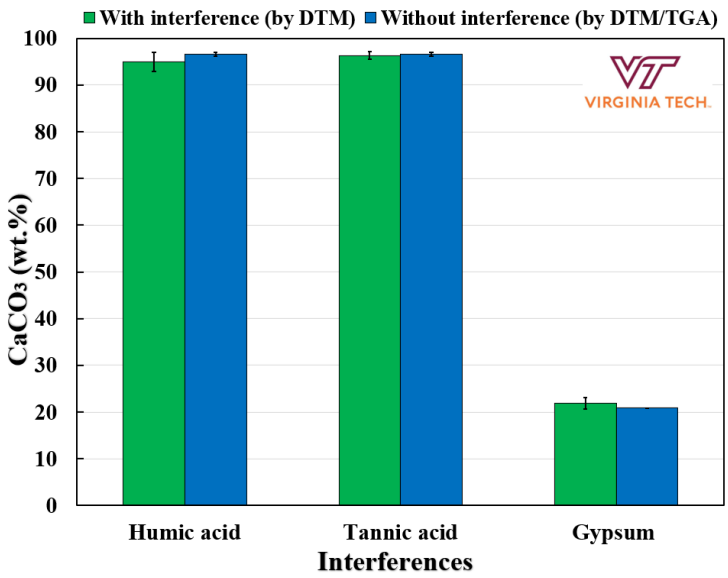

Figure 7- 11. $CaCO_3$ content measured from materials with and without interfering agent.

7.4.4 Statistical analyses

Two-tailed paired t-tests were carried out to compare the mean of DTM results obtained by the two institutions using a significance level of 0.05. Results of the t-test are presented in Table 7- 4. Some results were found to reject the null hypothesis, including 60% Cal, 80% Cal, 100% Cal, 80% BR, 100% BR, and 1884b. The fact that the two institutions had mixed results when comparing the means suggests that there are still procedural questions that need to be answered before the DTM test is considered for standardization. The differences in the means could be due to operator error, which would suggest that the procedure needs more or alternate constraints, or to the fact that the VT researchers used a smaller sample size (0.05 g) for DTM than the NIST researchers (0.2 g), which additionally suggests that the sample size should be further constrained for a standardized test method.

Table 7- 4. t-test results comparing the DTM data from VT and NIST.

Mixture codes	2-tailed t-test (α = 0.05, df = 4, t = 2.1318)							
	DTM by VT		DTM by NIST					
	Cal %	Stdev	Cal %	Stdev	n_1	n_2	Sp^2	T
20% Cal	20.28	1.07	18.01	1.89	3	3	2.37	1.81
40% Cal	39.60	0.81	38.03	1.26	3	3	1.12	1.82
60% Cal	59.21	0.07	55.21	1.53	3	3	1.17	**4.53**
80% Cal	75.65	1.84	80.81	2.41	3	3	4.59	**-2.95**
100% Cal	96.63	0.39	99.99	2.43	3	3	3.03	**-2.37**
20% BR	18.79	1.79	19.85	0.87	3	3	1.97	-0.92
40% BR	36.95	1.40	34.36	1.80	3	3	2.61	1.97
60% BR	53.55	2.09	51.04	2.89	3	3	6.36	1.22
80% BR	70.94	2.74	76.97	2.68	3	3	7.34	**-2.73**
100% BR	89.42	3.28	99.32	2.29	3	3	7.99	**-4.29**
CP	43.05	1.18	43.14	2.25	3	3	3.24	-0.06
1889b	3.86	0.86	3.25	1.64	3	3	1.72	0.56
1884b	1.86	0.68	3.69	1.01	3	3	0.74	**-2.61**

Note: The bolded numbers are the ones that reject the null hypothesis.

Since the NIST researchers were able to perform replicate TGA tests, the same t-test parameters were used to compare the TGA and DTM results from NIST. The t-test results are presented in Table 7- 5. These findings further suggest that additional procedural constraints should be applied to the DTM test prior to standardization. In the case of the CP sample, the fact that the means were different could be due to TGA overestimating the $CaCO_3$ content due overlap with the thermal phenomena of other phases, such as calcium silicate hydrate.

Table 7- 5. T-test results comparing the TGA and DTM data from NIST.

Mixture codes	2-tailed t-test (α = 0.05, df = 4, t = 2.1318)							
	Cal % by TGA		Cal % by DTM					
	Cal %	Stdev	Cal %	Stdev	n_1	n_2	Sp^2	t
20% Cal	18.27	0.11	18.01	1.89	3	3	1.80	0.24
40% Cal	36.97	0.02	38.03	1.26	3	3	0.79	-1.45
60% Cal	55.04	0.02	55.21	1.53	3	3	1.17	-0.20
80% Cal	72.65	0.27	80.81	2.41	3	3	2.95	**-5.82**
100% Cal	91.59	0.11	99.99	2.43	3	3	2.96	**-5.98**
20% BR	19.31	0.12	19.85	0.87	3	3	0.38	-1.08
40% BR	38.32	0.09	34.36	1.80	3	3	1.63	**3.79**
60% BR	57.00	0.67	51.04	2.89	3	3	4.40	**3.48**
80% BR	76.15	0.10	76.97	2.68	3	3	3.58	-0.53
100% BR	95.25	0.07	99.32	2.29	3	3	2.63	**-3.07**
CP	48.43	1.68	43.14	2.25	3	3	3.95	**3.26**
1889b	3.27	0.15	3.25	1.64	3	3	1.36	0.02
1884b	0.93	0.03	3.69	1.01	3	3	0.51	**-4.74**

Note: The bolded numbers are the ones that reject the null hypothesis.

For better visualization of the results, Figure 7- 12 and Figure 7- 13 compare the DTM results from VT and NIST and the NIST results for DTM and TGA, respectively, relative to a 1:1 line. In general, good agreement can be observed between the different test methods and from the two laboratories. However, there does appear to be a trend for reduced accuracy as the expected $CaCO_3$ content increases; this may suggest that the DTM testing parameters should be adjusted based on the expected $CaCO_3$ content.

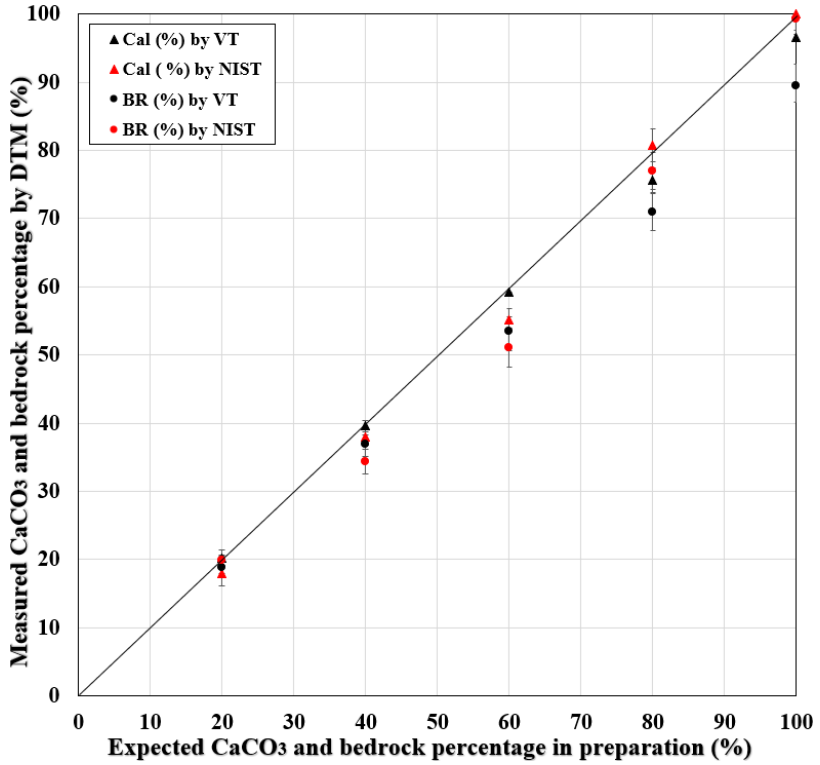

Figure 7- 12. DTM-derived $CaCO_3$ percentage results by VT vs. NIST.

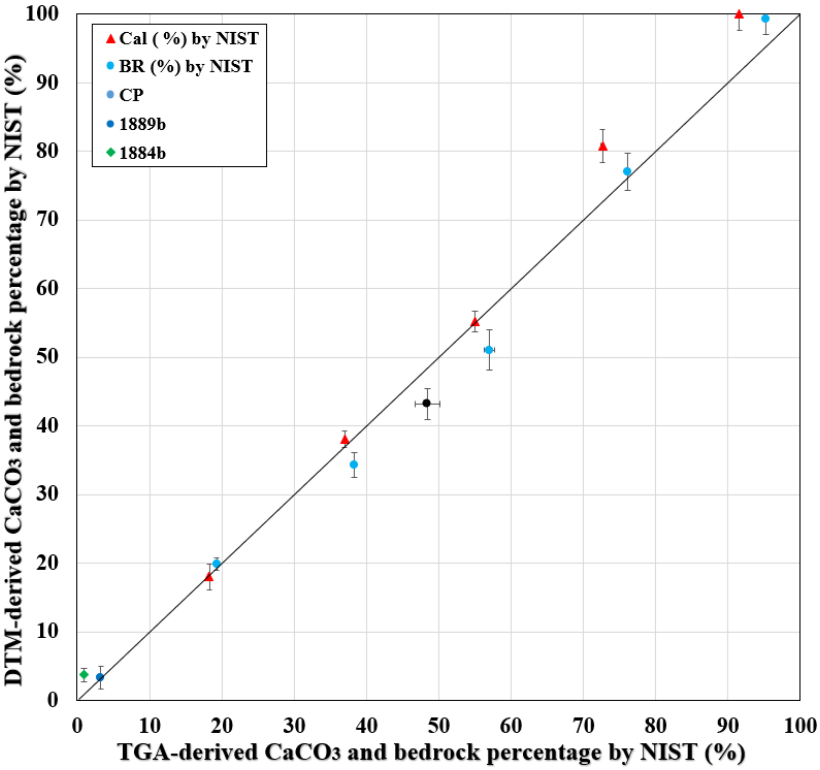

Figure 7- 13. $CaCO_3$ percentage determined by DTM vs. TGA by NIST.

7.4 Conclusions

In this study, an optimized digestion-titration test for the determination of carbonate in construction materials was successfully developed and shown to be comparable to an existing method (TGA) with less variability and without the susceptibility to bias due to overlapping thermal decomposition inherent in the previous method. Comparisons between DTM and TGA in terms of advantages and disadvantages identified in this study are briefly presented in Table 7- 6. Further work to standardize the DTM test would benefit from consideration of the effect of sample sizes used at VT (0.05 g) and NIST (0.2 g). The smaller sample size may be recommended for samples with high carbonate content to avoid violent ebullition during the test. The DTM generally uses much larger sample sizes than TGA, helping experimenters have more reliable sample representation. Overall, this method can serve as a cost-effective and easily accessible alternative method to quantify mineralized CO_2 content.

Table 7- 6. Brief comparisons between DTM and TGA.

Categories	Digestion-titration method (DTM)	Thermogravimetric analysis (TGA)
Targeted materials	Powder	Powder
Sample size	Large (up to 0.2 g and even higher if needed)	Small (around 20 mg)
Experimental setup	Simple	Simple
Evacuation time	10 s	**few minutes (taring)**
Testing time	Around 10 min	**1 h to 2 h**
Calculation Guide	Yes	**No**
Accuracy	High	Very high (cases without overlapping phase decompositions)
Accessibility	Easy	**Can be difficult**
Equipment Cost	A few hundred U.S. dollars	**Ten thousand or more U.S. dollars**

Note: the bolded characters are disadvantage of TGA against DTM.

Acknowledgement

The Virginia Tech researchers acknowledge seed funding from the Economical and Sustainable Materials Stakeholder Committee at Virginia Tech to complete this work. The National Institute of Standards and Technology (NIST) researchers would like to acknowledge funding from the NIST Direct Air Capture (DAC) - Carbon Capture, Utilization, and Storage (CCUS) Working Group and the NIST Professional Research Experience Program (PREP) *via* Johns Hopkins University and Morgan State University.

References

[1] International Energy Agency, Cement Sustainability Initiative, Technology Roadmap: Low-Carbon Transition in the Cement Industry, World Business Council for Sustainable Development, 2018.

[2] B.J. van Ruijven, D.P. van Vuuren, W. Boskaljon, M.L. Neelis, D. Saygin, M.K. Patel, Long-term model-based projections of energy use and CO2 emissions from the global steel and cement industries, Resour. Conserv. Recycl. 112 (2016) 15–36. https://doi.org/10.1016/j.resconrec.2016.04.016.

[3] R.M. Andrew, Global CO2 emissions from cement production, Earth Syst. Sci. Data. 10 (2018) 195–217. https://doi.org/10.5194/essd-10-195-2018.

[4] D. Ravikumar, D. Zhang, G. Keoleian, S. Miller, V. Sick, V. Li, Carbon dioxide utilization in concrete curing or mixing might not produce a net climate benefit, Nat. Commun. 12 (2021) 1–13. https://doi.org/10.1038/s41467-021-21148-w.

[5] M.Á. Sanjuán, C. Andrade, P. Mora, A. Zaragoza, Carbon dioxide uptake by cement-based materials: A spanish case study, Appl. Sci. 10 (2020). https://doi.org/10.3390/app10010339.

[6] S.A. Walling, J.L. Provis, Magnesia-based cements: A journey of 150 years, and cements for the future?, Chem. Rev. 116 (2016) 4170–4204. https://doi.org/10.1021/acs.chemrev.5b00463.

[7] E. Possan, W.A. Thomaz, G.A. Aleandri, E.F. Felix, A.C.P. dos Santos, CO2 uptake potential due to concrete carbonation: A case study, Case Stud. Constr. Mater. 6 (2017) 147–161. https://doi.org/10.1016/j.cscm.2017.01.007.

[8] I. Galan, C. Andrade, P. Mora, M.A. Sanjuan, Sequestration of CO2 by concrete carbonation, Environ. Sci. Technol. 44 (2010) 3181–3186. https://doi.org/10.1021/es903581d.

[9] C.W. Hargis, I.A. Chen, M. Devenney, M.J. Fernandez, R.J. Gilliam, R.P. Thatcher, and Storage (CCUS) Technique, (2021) 1–12.

[10] M. Voldsund, S.O. Gardarsdottir, E. De Lena, J.-F. Pérez-Calvo, A. Jamali, D. Berstad, C. Fu, M. Romano, S. Roussanaly, R. Anantharaman, H. Hoppe, D. Sutter, M. Mazzotti, M. Gazzani, G. Cinti, K. Jordal, Comparison of technologies for CO2 capture from cement production—Part 1: Technical evaluation, Energies. 12 (2019) 559. https://doi.org/10.3390/en12030559.

[11] W.J.J. Huijgen, G.-J. Witkamp, R.N.J. Comans, Mechanisms of aqueous wollastonite carbonation as a possible CO2 sequestration process, Chem. Eng. Sci. 61 (2006) 4242–

4251. https://doi.org/10.1016/j.ces.2006.01.048.
[12] W. Ashraf, J. Olek, Carbonation behavior of hydraulic and non-hydraulic calcium silicates: Potential of utilizing low-lime calcium silicates in cement-based materials, J. Mater. Sci. 51 (2016) 6173–6191. https://doi.org/0.1007/s10853-016-9909-4.
[13] G. Sant, M. Balonis-Sant, N. Neithalath, Reactive limestone as a strategy towards sustainable, low-carbon cements, US20150210592, 2015.
[14] Y.A. Criado, J.C. Abanades, Carbonation rates of dry Ca(OH)2 mortars for CO2 capture applications at ambient temperatures, Ind. Eng. Chem. Res. 61 (2022) 14804–14812. https://doi.org/10.1021/acs.iecr.2c01675.
[15] R. Jenkins, R.L. Snyder, Introduction to X-ray Powder Diffractometry, Wiley, New York, 1996.
[16] P.R. de Matos, J.S. Andrade Neto, D. Jansen, A.G. De la Torre, A.P. Kirchheim, C.E.M. Campos, In-situ laboratory X-ray diffraction applied to assess cement hydration, Cem. Concr. Res. 162 (2022) 106988. https://doi.org/10.1016/j.cemconres.2022.106988.
[17] R. Snellings, A. Salze, K.L. Scrivener, Use of X-ray diffraction to quantify amorphous supplementary cementitious materials in anhydrous and hydrated blended cements, Cem. Concr. Res. 64 (2014) 89–98. https://doi.org/10.1016/j.cemconres.2014.06.011.
[18] L.T. Gibson, Archaeometry and antique analysis | Metallic and ceramic objects, in: P. Worsfold, A. Townshend, C. Poole (Eds.), Encycl. Anal. Sci., 2nd ed., Elsevier, Amsterdam, 2005: pp. 117–123. https://doi.org/10.1016/B0-12-369397-7/00020-0.
[19] K. Scrivener, A. Bazzoni, B.M. Gassó, J.E. Rossen, Electron microscopy, in: K. Scrivener, R. Snellings, B. Lothenbach (Eds.), A Pract. Guid. to Microstruct. Anlysis Cem. Mater., CRC Press, Boca Raton, 2016: pp. 352–417.
[20] J. Skibsted, High-resolution solid-state nuclear magnetic resonance spectroscopy of portland cement-based systems, in: K. Scrivener, R. Snellings, B. Lothenbach (Eds.), A Pract. Guid. to Microstruct. Anal. Cem. Mater., CRC Press, Boca Raton, 2016: pp. 213–286.
[21] D. Jansen, D. Ectors, X. Kong, C. Schmidtke, F. Deschner, J. Pakusch, E. Jahns, J. Neubauer, Synchronous monitoring of cement hydration and polymer film formation using 1H-time-domain-NMR with T2 time-weighted T1 time evaluation: A nondestructive practicable benchtop method, ACS Omega. 6 (2021) 7499–7511. https://doi.org/10.1021/acsomega.0c06010.
[22] S. Joseph, J. Skibsted, Ö. Cizer, A quantitative study of the C3A hydration, Cem. Concr. Res. 115 (2019) 145–159. https://doi.org/10.1016/j.cemconres.2018.10.017.
[23] E. Pustovgar, R.P. Sangodkar, A.S. Andreev, M. Palacios, B.F. Chmelka, R.J. Flatt, J.B. D'Espinose De Lacaillerie, Understanding silicate hydration from quantitative analyses of hydrating tricalcium silicates, Nat. Commun. 7 (2016) 1–9. https://doi.org/10.1038/ncomms10952.
[24] C.E. Hughes, B. Walkley, L.J. Gardner, S.A. Walling, S.A. Bernal, D. Iuga, J.L. Provis, K.D.M. Harris, Exploiting in-situ solid-state NMR spectroscopy to probe the early stages

of hydration of calcium aluminate cement, Solid State Nucl. Magn. Reson. 99 (2019) 1–6. https://doi.org/10.1016/j.ssnmr.2019.01.003.

[25] M. Protić, A. Miltojević, B. Zoraja, M. Raos, I. Krstić, Application of thermogravimetry for determination of carbon content in biomass ash as an indicator of the efficiency of the combustion process, Teh. Vjesn. 28 (2021) 1762–1768. https://doi.org/10.17559/TV-20200508110940.

[26] ASTM C1872, Standard test method for thermogravimetric analysis of hydraulic cement, ASTM international, West Conshohocken, 2018. https://doi.org/10.1520/C1872-18.

[27] B. Lothenbach, P. Durdziński, K. De Weerdt, Thermogravimetric analysis, in: K. Scrivener, R. Snellings, B. Lothenbach (Eds.), A Pract. Guid. to Microstruct. Anal. Cem. Mater., CRC Press, Boca Raton, 2016: pp. 177–211. https://doi.org/10.1201/b19074.

[28] K.S.P. Karunadasa, C.H. Manoratne, H.M.T.G.A. Pitawala, R.M.G. Rajapakse, Thermal decomposition of calcium carbonate (calcite polymorph) as examined by in-situ high-temperature X-ray powder diffraction, J. Phys. Chem. Solids. 134 (2019) 21–28. https://doi.org/10.1016/j.jpcs.2019.05.023.

[29] M. Bilton, A.P. Brown, S.J. Milne, Investigating the optimum conditions for the formation of calcium oxide, used for CO2 sequestration, by thermal decomposition of calcium acetate, J. Phys. Conf. Ser. 371 (2012). https://doi.org/10.1088/1742-6596/371/1/012075.

[30] S. Goto, K. Suenaga, T. Kado, M. Fukuhara, Calcium silicate carbonation products, J. Am. Ceram. Soc. 78 (1995) 2867–2872. https://doi.org/10.1111/j.1151-2916.1995.tb09057.x.

[31] T. Siva, S. Muralidharan, S. Sathiyanarayanan, E. Manikandan, M. Jayachandran, Enhanced polymer induced precipitation of polymorphous in calcium carbonate: Calcite aragonite vaterite phases, J. Inorg. Organomet. Polym. Mater. 27 (2017) 770–778. https://doi.org/10.1007/s10904-017-0520-1.

[32] R. Hay, K. Celik, Accelerated carbonation of reactive magnesium oxide cement (RMC)-based composite with supercritical carbon dioxide (scCO2), J. Clean. Prod. 248 (2020) 119282. https://doi.org/10.1016/j.jclepro.2019.119282.

[33] A. Romero Salvador, E. Garcia Calvo, C. Beneitez Aparicio, Effects of sample weight, particle size, purge gas and crystalline structure on the observed kinetic parameters of calcium carbonate decomposition, Thermochim. Acta. 143 (1989) 339–345. https://doi.org/10.1016/0040-6031(89)85073-7.

[34] J.M. Criado, A. Ortega, A study of the influence of particle size on the thermal decomposition of CaCO3 by means of constant rate thermal analysis, Thermochim. Acta. 195 (1992) 163–167. https://doi.org/10.1016/0040-6031(92)80059-6.

[35] Y.A. Villagrán-Zaccardi, H. Egüez-Alava, K. De Buysser, E. Gruyaert, N. De Belie, Calibrated quantitative thermogravimetric analysis for the determination of portlandite and calcite content in hydrated cementitious systems, Mater. Struct. Constr. 50 (2017). https://doi.org/10.1617/s11527-017-1046-2.

[36] A. Morandeau, M. Thiéry, P. Dangla, Investigation of the carbonation mechanism of CH and C-S-H in terms of kinetics, microstructure changes and moisture properties, Cem.

Concr. Res. 56 (2014) 153–170. https://doi.org/10.1016/j.cemconres.2013.11.015.
[37] D.D. Van Slyke, The Determination of Carbon Dioxide in Carbonates, J. Biol. Chem. 36 (1918) 351–354. https://doi.org/10.1016/S0021-9258(18)86402-X.
[38] J.R.I. Hepburn, A new and simple method for the determination of carbon dioxide in carbonates, Analyst. 51 (1926) 622–624. https://doi.org/10.1039/AN9265100622.
[39] F.W. Edwards, E.B. Parkes, H.R. Nanji, Method for determining “available” and “total” carbon dioxide in baking powders and self-rising flours, Analyst. 60 (1935) 814–816. https://doi.org/10.1039/AN9356000814.
[40] J. Tinsley, T.G. Taylor, J.H. Moore, The determination of carbon dioxide derived from carbonates in agricultural and biological materials, Analyst. 76 (1951) 300–310. https://doi.org/10.1039/an9517600300.
[41] J. Amela, R. Salazar, J. Cemeli, Methods for the Determination of the Carbon Dioxide Evolved from Effervescent Systems, Drug Dev. Ind. Pharm. 19 (1993) 1019–1036. https://doi.org/10.3109/03639049309062998.
[42] G.W. Cornell, Determination of Carbon Dioxide, Analyst. 61 (1936) 756–757. https://doi.org/10.1039/AN9366100756.
[43] G. Ampt, The barium hydroxide vacuum method for the determination of carbon dioxide, Collect. Proc. Soc. Chem. Ind. Victoria. 23 (1923) 1006–1009.
[44] E.F. Jones, A method for the determination of carbonate in small amounts of materials, J. Soc. Chem. Ind. 59 (1940) 21–23. https://doi.org/10.1002/jctb.5000595301.
[45] P.P. Everett, W.C. Schroeder, Development and Testing of Apparatus for Carbonate Determination by Evolution and Absorption in Barium Hydroxide, Ind. Eng. Chem. - Anal. Ed. 4 (1932) 274–278. https://doi.org/10.1021/ac50079a014.
[46] SRM 1889b, Portland cement (blended with limestone), National Institute of Standards and Technology, Gaithersburg, 2019.
[47] SRM 1884b, Portland cement, National Institute of Standards and Technology, Gaithersburg, 2009.
[48] E. Lerigoleur, Effect of early age carbonation curing on the microstructure of cement paste, (2014).
[49] National Institute of Standards and Technology, Standard Reference Material 1889b, (2019).
[50] National Institute of Standards and Technology, NIST Standard Reference Materials® Technical Catalog, (2013).

Chapter 8. Conclusion and recommendation

8.1 Overview

Natural resource depletion and significant carbon footprints are problems for sustainability of cement and concrete industries. With the vision towards the Net Zero Emissions plan by 2050 Scenario, more sustainable technologies and materials should be considered in the production of these materials to achieve the target.

This dissertation presented a comprehensive investigation on the fate of zinc and total organic carbon (TOC) of end-of-life tire (ELT) rubber particles when this material is used in stabilized soil (*via* cation exchange capacity (CEC) of soils), portland cement (PC) concrete (*via* CEC and matrix densification), and asphalt concrete (*via* asphalt binder bonding). The work also examined the capturability of the three materials in immobilizing zinc and TOC within their matrix. In addition, this dissertation investigated the heat of hydration behavior of stabilized soils with different binders. Finally, this dissertation proposed a new chemical test model to determine the CO_2 captured in cementitious materials, which can be an alternative method for thermogravimetric analysis (TGA) with lower experimental cost and easier access.

8.2 Major findings

The major findings are summarized as follows:

1. The strength of rubberized cementitious materials (RCM) tends to decrease with an increase in the ELT rubber content. Some of the treatment methods for ELT rubber can result in a full recovery of strength. The strength recovery index and strength gain can be used as effective metrics to evaluate the efficiency of a treatment method for ELT rubber used in RCM. The significance of strength loss (SL) generally seems to depend on the original material's strength. For high strength cementitious materials, SL is usually smaller than that of normal strength cementitious materials when adding the same amount of ELT rubber when the ELT rubber content no more than 15 %. When the ELT rubber content is ≥ 20 %, the SL becomes similar regardless of the original strength of cementitious material or type of concrete. More interestingly, when the treatment methods are introduced for ELT rubber, the SL of RCM is significantly affected by the type of treatment methods instead of the original strength.
2. The results successfully proved the hypothesis that clays possess a strong ability for zinc immobilization. Kaolin and bentonite clays could effectively immobilize leached zinc and TOC contents in the rubberized stabilized soil (RSS). While the treatment process for zinc recovery from ELT rubber could provide a more environmentally conscious material, it adversely affected the engineering properties of the RSS. ELT rubber enhanced the flowability of stabilized clay mixtures, possibly due to its hydrophobicity. In addition, while adding untreated ELT rubber into stabilized clay could significantly enhance the strength of the mixture by up to roughly 95 % (for kaolin mixture) and 300 % (for bentonite mixture), the zinc-recovery treatment process on ELT rubber negatively affected the significance of

strength improvement in the RSS mixtures. The peak heat of hydration was increased by up to 1.35 times due to the addition of ELT rubber in the stabilized clay mixture.

3. Untreated ELT rubber enhanced the flowability of the rubberized mortars. Meanwhile, a high percentage of treated ELT rubber addition (*i.e.*, 20 % and 30 %) and the presence of silica fume decreased the flowability of the rubberized mortars. The engineering properties of mortars (*i.e.*, unconfirmed compressive strength, flexural strength, and ultrasonic pulse velocity) decreased significantly as higher replacements with ELT rubber were used. The treatment process for zinc recovery from ELT rubber further reduced these properties. Silica fume could effectively recover the lost strength and significantly mitigate the rapid chloride penetrability test value of rubberized mortar. The utilization of ELT rubber generally delayed the hydration peak of the mortar for roughly one hour. The existence of ELT rubber at a high percent (30 %) slightly increased the hydration peak value and accumulated hydration heat. The zinc-recovery treatment process seemed to allow the remaining zinc to leach out from the treated ELT rubber more easily than the untreated one. In addition, silica fume proved to be very efficient in zinc and TOC immobilization since it could capture up to 74 % of leachable zinc and 86 % of TOC contents in the leachate of rubberized mortars after 28 days of soaking.
4. Using ELT rubber in asphalt concrete generally reduced indirect tensile strength (ITS) value and cracking tolerance (CT) index. This happened for both of rubber types. The treated ELT rubber helped improve ITS of the rubberized asphalt concrete (RAC) remarkably, but it did not have significant impact in CT index. ELT rubber effectively improved the rutting resistance of asphalt concrete. ELT rubber improved the dynamic modulus |E*| of asphalt concrete when the material was subjected to higher temperature conditions. Asphalt concretes using ELT rubber tend to release more zinc than conventional asphalt concrete after 7 days of being exposed to normal and extreme environments. While the deicing simulating solution (0.1 M NaCl) did not promote the leachability of zinc, the simulated acid rain solution (pH 4.0) greatly exacerbated the leaching of zinc compared to deionized water. RAC with treated ELT rubber released even more zinc to the leaching environments than the one using untreated ELT rubber. The zinc recovery treatment caused more pores, cracks, and higher specific surface area in ELT rubber particles, and some residual zinc left in the particles have larger contact with surrounding environment, leading to easier leachability. AC is believed to effectively immobilize zinc and especially TOC leaching out from ELT rubber particles.
5. A summary of effects of ELT rubber on the three studied construction materials are presented in Table 8 - 1. Generally, while ELT rubber has a positive impact on the engineering properties of stabilized soil, it has both positive and negative effects on mortar and asphalt concrete materials. The ELT rubber appears to effectively help improve durability of the construction materials. In a return, the three studied materials help immobilize the leachable zinc and TOC from ELT rubber within their matrix. As a result, a

synergy is promoted when using ELT rubber in the three materials, leading to a high possibility to increase the use of ELT rubber for civil engineering purposes.

Table 8 - 1. Effects of ELT rubber on the three studied construction materials.

Categories	Stabilized soil	Mortar	Asphalt concrete
Mixture configurations	Dosage: ELT replaced 10 %, 20 %, and 50% of clay volume. Water content: 2.0xLL for kaolin and 0.5xLL for bentonite. Cement/solid ratio = 0.2.	Dosage: ELT replaced 10%, 20%, and 30% of sand volume. Water/cement ratio = 0.65.	Dosage: ELT replaced 20% of sand volume.
Engineering properties	Increases flowability, compressive strength, and hydration heat	Increases flowability (untreated ELT rubber) and hydration heat. Decreases flowability (treated ELT rubber), compressive strength, tensile strength, and UPV.	Increases dynamic modulus (higher temperatures and lower frequencies). Decreases ITS, CT index, and dynamic modulus (lower temperatures).
Durability		Improves chloride penetration resistance (untreated ELT or with silica fume). Worsens chloride penetration resistance (treated ELT)	Improves rutting resistance
Zinc and TOC leachability	Effectively immobilizes the leached Zinc and TOC from ELT rubber particles		

6. The hydration process of all steel furnace slag (SFS) stabilized mixtures generally occurred faster than that of PC or lime (CaO) because of its high calcium aluminate content. The clay type, particle size, and specific surface area affected the hydration behavior of stabilized clay. The “peak delay” of the thermal power curve strongly depends on the amount of water available in the soil matrix. In addition, at the same condition, the hydration of stabilized kaolin takes place more significantly over that of bentonite during the very early curing time while this trend is opposite after that. In a clay mixture, the hydration of SFS generates more heat than that of cement, but much less heat than that of CaO. Hydration of SFS and PC

keep gradually generating heat as time goes by while it likely generates no heat in the cases of CaO.

7. The Digestion-Titration Method (DTM) test could provide results in agreement with TGA data for samples with controlled carbonate content. The DTM test can be an alternative method to determine CO2 content with lower experimental cost and easier accessibility. The presence of both $MgCO_3$ and $CaCO_3$ in cementitious materials could potentially mislead and confuse the results, since this $MgCO_3$ also gets decomposed under acidic conditions to liberate CO_2. Heterogeneity in the prepared samples and the inconsistency of experimental manipulation should be considered to deal with the scattered test results. Additional procedural constraints should be considered before the DTM test is standardized. The TGA method appeared to have lower variability than the DTM method in controlled samples. However, in samples where the thermal decomposition of $CaCO_3$ overlaps with other phases, the DTM test is more applicable.

8.3 Significance and study importance

Natural resource depletion and CO_2 emissions are widely acknowledged to be serious environmental problems and requires significant consideration when designing and producing a construction material. Hence, understanding the impacts of reusing industrial wastes in a construction material or the significance of reducing CO_2 emissions or CO_2 capturability of a construction material are very important. The methodologies and approaches presented in this dissertation fulfill the need of these considerations. The contribution of this dissertation to science and practice are:

- Chapter 2 proposed effective new metrics for more visible and graphical discussions and comparisons between the treatment methods on ELT rubber before its use in RCM. The readers can understand how to process ELT rubber to achieve greater performance in RCM, thereby reducing the CO_2 footprint over the life cycle.
- Chapter 3 offered a novel approach to immobilize zinc leachate from ELT rubber in stabilized soils while significantly increasing the stabilized mixture's strength. This method can deal with zinc leachability, a heavy metal that is detrimental to aquatic and plant life.
- Chapter 4 proved that strength loss from using ELT rubber can be recovered with the addition of silica fume. In addition, it demonstrated that a cementitious matrix can immobilize zinc and TOC that are leached from ELT rubber, which has not previously been reported in the literature.
- Chapter 5 quantifies the leachability of zinc and TOC in RAC when using ELT rubber under different weather conditions, which has not received significant attention in the literature. It proved that the asphalt binder can effectively mitigate the zinc and TOC leachate from ELT rubber, which poses a significant environmental hazard.
- Chapter 6 applies isothermal calorimetry (IC) for the first time in the literature to understand hydration kinetics during clay stabilization. This demonstrates that IC can be more widely introduced in geotechnical engineering research.

- Chapter 7 establishes a new test method for quantifying mineralized CO_2 in cement-based and other industrial materials. With additional experimental validation and methodology optimization, it is possible that this test method can be standardized.

8.4 Recommendation for future work

This work presents different new approaches towards the sustainable production of cement-based construction materials. Some future work is recommended to further improve and expand the current work:

- Among the multiple treatment methods on ELT rubber, only a few appear to work effectively with proven results. Further studies should focus on these treatments, considering the basic properties of the ELT rubber such as particle size, density, chemical composition, and material sources and how these properties influence the physicochemical interaction with cement paste.
- Based on the large data library reported in literature, relationships between ELT rubber particle size and engineering properties of rubberized concrete are recommended to be established using the aid of machine learning.
- There are usually significant reductions in strength of PC concrete using ELT rubber. Studies on microstructure of this material are recommended to clarify the bonding between cement paste and ELT rubber particles, especially focusing on the interfacial transition zone.
- It is evident that the construction materials explored in this dissertation (*i.e.*, stabilized soil, portland cement concrete, and asphalt concrete) could immobilize the leachable zinc and TOC from ELT rubber effectively. Samples using different ELT rubber types with various particle size as well as chemical composition should be further studied to confirm whether the capturability of zinc and TOC are consistent when working with a variety of input rubber waste materials.
- It is known that the CEC of clay can vary due to the content and types of ions in its structure. Pre-treatments using ion-rich solutions (*e.g.*, Al^{3+}, Ca^{2+}, Na^{+}) can be applied on a clay to enhance its CEC, thus improving the zinc and TOC capturability of this material.
- The findings in this research indicates that asphalt binder in RAC can effectively immobilize the leachability of zinc and TOC from the ELT rubber particles (recorded up to 30 days of leaching). The findings by this study is valuable within dry mixing process, similar studies on wet process are recommended for more comprehensive conclusions.
- The change of thermal power peak and total heat during the hydration can possibly be used to predict the strength development of the stabilized soil mixtures, but it cannot completely reflect the strength development behavior of the mixtures. Further studies should be conducted using IC to clarify the relationship between thermal power during the hydration and strength development behavior.
- The external mixing method in sample preparation could not provide the thermal power data immediately after mixing, resulting in a lack of data in the very early curing time. More in-depth studies should consider how internal mixing should be employed for this issue.

- The TGA method appeared to have lower variability than the DTM method in controlled samples. However, in samples where the thermal decomposition of $CaCO_3$ overlaps with other phases, the DTM test is more applicable. Additional procedural constraints, including interlaboratory variability, should be considered before the DTM test is standardized. In addition, it should be noted that the samples prepared for this study were cement-like form, further studies can be conducted to investigate the effect of sample particle size on ultimate result.